

---

**Resolving the roles of KAI2-mediated signalling  
in root and root hair development in  
*Arabidopsis thaliana***

---

José Antonio Villaécija Aguilar

Dissertation an der Fakultät für Biologie der  
Ludwig-Maximilians-Universität München

München, 2020



Dissertation eingereicht am: 16.06.2020

Tag der mündlichen Prüfung: 25.08.2020

**Erstgutachter:** Prof. Dr. Caroline Gutjahr

**Zweitgutachter:** PD Dr. Cordelia Bolle



### **Eidesstattliche Versicherung**

Ich versichere hiermit an Eides statt, dass die vorgelegte Dissertation von mir selbstständig und ohne unerlaubte Hilfe angefertigt ist.

München, den

José Antonio Villaécija Aguilar

08.06.2020

### **Erklärung**

Hiermit erkläre ich, dass die Dissertation nicht ganz oder in wesentlichen Teilen einer anderen Prüfungskommission vorgelegt worden ist. Ich habe nicht versucht, anderweitig eine Dissertation einzureichen oder mich einer Doktorprüfung zu unterziehen.

München, den

José Antonio Villaécija Aguilar

08.06.2020



## Table of contents

|       |   |     |
|-------|---|-----|
| I.    | List of Abbreviations   | 8   |
| II.   | List of Publications  | 10  |
| III.  | Declarations of contribution as co-author   | 11  |
| IV.   | Summary   | 16  |
| V.    | Zusammenfassung   | 19  |
| VI.   | Introduction  |     |
|       | 1. The karrikin family  | 22  |
|       | 2. KAI2 is the receptor of KARs   | 23  |
|       | 3. KAI2-ligands: putative endogenous hormones   | 25  |
|       | 4. Strigolactones: chemistry and biosynthesis   | 26  |
|       | 5. Proteasome targets of SL/KL signalling pathways  | 28  |
|       | 6. SL and KL signalling cross-talk with signalling pathways of other phytohormones                        | 30  |
|       | 7. Participation of protein phosphatases in plant hormone signalling                                      | 31  |
|       | 8. Arabidopsis root development and behaviour   | 32  |
|       | 9. Regulation of root hair development in Arabidopsis   | 34  |
| VII.  | Aims of the Thesis  | 36  |
| VIII. | Results   |     |
|       | 1. Paper I:   | 37  |
|       | SMAX1/SMXL2 regulate root and root hair development downstream of KAI2-mediated signalling in Arabidopsis |     |
|       | 2. Paper II:  | 74  |
|       | Extensive signal integration by the phytohormone protein network  |     |
|       | 3. Method book chapter I:   | 122 |
|       | Bioassays for the effects of strigolactones and other small molecules on root and root hair development   |     |
|       | 4. Manuscript I:  |     |
|       | KL signalling regulates root hair elongation by promoting accumulation of auxin influx carrier AUX1       | 143 |
| IX.   | General discussion  | 172 |
| X.    | Outlook   | 183 |
| XI.   | References  | 185 |
| XII.  | List of Figures   | 200 |
| XIII. | Acknowledgement   | 201 |
| XIV.  | Copyright Clearance   | 203 |

## I. List of Abbreviations

|       |  |
|-------|--|
| ABA   | Abscisic Acid  |
| ACS   | ACC SYNTHASE   |
| ANOVA | Analysis of Variance   |
| ARF   | AUXIN RESPONSE FACTOR  |
| At    | <i>Arabidopsis thaliana</i>  |
| CCD   | Carotenoid Cleavage Dioxygenases   |
| CK    | Cytokinin  |
| Col-0 | Columbia-0   |
| CPC   | CAPRICE  |
| CYP   | Cytochrome P450  |
| D14   | DWARF 14   |
| D14L  | DWARF 14 Like  |
| D27   | DWARF27  |
| D53   | DWARF 53   |
| DLK2  | DWARF 14 Like 2  |
| EAR   | Ethylene-responsive element binding factor-associated amphiphilic repression |
| EC    | Effective concentration  |
| EGL3  | ENHANCER OF GLABRA3  |
| ETC1  | ENHANCER OF TRY AND CPC1   |
| EXP7  | Expansin 7   |
| GA    | Gibberellin Acid   |
| GL2   | GLABLA2  |
| IAA   | Indole-3-acetic-acid   |
| IPA1  | Ideal Plant Architecture 1   |
| KAI   | KARRIKIN INSENSITIVE   |
| KAR   | Karrikins  |
| KL    | Karrikin Like  |
| Ler   | <i>Landsberg erecta</i>  |
| LRC   | Lateral Root Cap   |
| LRD   | Lateral Root Density   |
| MAX   | MORE AXILLARY GROWTH   |

|      |                             |
|------|-----------------------------|
| PIN  | PIN-FORMED                  |
| PP2A | PROTEIN PHOSPHATASE 2A      |
| RH   | Root hairs                  |
| RHD  | Root hair density           |
| RHD6 | ROOT HAIR DEFECTIVE 6       |
| RHE  | Root hair Element           |
| RHL  | Root hair length            |
| RHS  | Root hair Specific          |
| RSL1 | ROOT HAIR DEFECTIVE 6 LIKE1 |
| RSL2 | ROOT HAIR DEFECTIVE 6 LIKE2 |
| RSL4 | ROOT HAIR DEFECTIVE 6 LIKE4 |
| SCF  | SKP-CULLIN-FBOX complex     |
| SL   | Strigolactone               |
| SMAX | SUPPRESSOR of MAX2          |
| SMXL | SUPPRESSOR of MAX2 Like     |
| TF   | Transcription Factor        |
| TPL  | TOPLESS                     |
| TPR  | TOPLESS RELATED             |
| TRY  | TRIPTYCON                   |
| TTG1 | TRANSPARENT TESTA GLABLA1   |
| WER  | WEREWOLF                    |
| Y2H  | Yeast-2-Hybrid              |

## II. List of Publications

### Research Papers

- **Villaécija-Aguilar, J.A.**; Hamon-Josse, M.; Carbonnel, S.; Kretschmar, A.; Schmidt, C.; Dawid, C.; Bennett, T.; Gutjahr, C. SMAX1/SMXL2 regulate root and root hair development downstream of KAI2-mediated signalling in Arabidopsis. **PLoS Genet.** 2019, 15, e1008327.
- Altmann, M.; Altmann, S.; Rodriguez, P.; Weller, B.; Elorduy Vergara, L.; Palme, J.; Marin-de la Rosa, N.; Sauer, M.; Wenig, M.; **Villaécija-Aguilar, J.A.**; Sales, J.; Lin, Chung-Wen; Pandiarajan, R.; Young, V.; Strobel, A.; Groß, L.; Carbonnel, S.; Kugler, K.; Garcia-Molina A.; Bassel, G.; Falter, C.; Mayer, K.; Gutjahr, C.; Vlot-Schuster, C.; Grill, E.; Falter-Braun, P. Extensive signal integration revealed by a phytohormone protein interactome map. **Nature.** 2020. Accepted.

### Method book chapters

- **Villaécija-Aguilar, J.A.**; Struk S.; Goormachtig S.; Gutjahr, C. Bioassays for the effects of strigolactone and strigolactone-like molecules on root and root hair development. **MIMB.** Accepted and soon to be published in the book “Strigolactones” edited by SpringerNature.
- Torabi S.; Varshney K.; **Villaécija-Aguilar, J.A.**; Gutjahr, C. Quantification of Arbuscular Mycorrhiza Development Under Controlled Conditions. **MIMB.** Accepted and soon to be published in the book “Strigolactones” edited by SpringerNature.

### III. Declaration of contribution

**Paper I:** SMAX1/SMXL2 regulate root and root hair development downstream of KAI2-mediated signalling in Arabidopsis

Reference: **Villaécija-Aguilar, J.A.**; Hamon-Josse, M.; Carbonnel, S.; Kretschmar, A.; Schmidt, C.; Dawid, C.; Bennett, T.; Gutjahr, C. SMAX1/SMXL2 regulate root and root hair development downstream of KAI2-mediated signalling in Arabidopsis. **PLoS Genet.** 2019, 15, e1008327.

José Antonio Villaécija Aguilar designed, performed and analysed most of the experiments, created all the figures, performed statistics and contributed to the conception of this study. Additionally, the following contributed to this work:

- Samy Carbonnel acquired the data for Supplemental Figure 7.
- Annika Kretschmar acquire the data for Supplemental Figure 2D-G.
- Corinna Dawid and Christian Schmidt acquire the data for Supplemental Figure 6.
- Maxime Hamon-Josse performed the primary root length, lateral root density and root skewing (Figure 5G) analysis in Leeds [L].
- Tom Bennet performed the primary root length and lateral root density analysis in Cambridge [C] and contributed to conceive the study, designed experiments and co-wrote the manuscript.
- Caroline Gutjahr contributed to conceive the study, designed experiments and co-wrote the manuscript.

Signature of the Supervisor:

Prof. Dr. Caroline Gutjahr

08.06.2020

Signature of first author:

José Antonio Villaécija Aguilar

08.06.2020

**Paper II:** Extensive signal integration revealed by a phytohormone protein interactome map

Reference: Altmann, M.; Altmann, S.; Rodriguez, P.; Weller, B.; Elorduy Vergara, L.; Palme, J.; Marin-de la Rosa, N.; Sauer, M.; Wenig, M.; **Villaécija-Aguilar, J.A.**; Sales, J.; Lin, Chung-Wen; Pandiarajan, R.; Young, V.; Strobel, A.; Groß, L.; Carbonnel, S.; Kugler, K.; Garcia-Molina A.; Bassel, G.; Falter, C.; Mayer, K.; Gutjahr, C.; Vlot-Schuster, C.; Grill, E.; Falter-Braun, P. Extensive signal integration revealed by a phytohormone protein interactome map. **Nature**. 2020. Accepted.

José Antonio Villaécija Aguilar designed and performed the experiment for Figure 3H and I, analysed the data and created the figure.

Signature of the Supervisor:

Prof. Dr. Caroline Gutjahr

08.06.2020

Signature of co-author:

José Antonio Villaécija Aguilar

08.06.2020

**Method book chapter I:** Bioassays for the effects of strigolactones and other small molecules on root and root hair development

Reference: **Villaécija-Aguilar, J.A.**; Struk S.; Goormachtig S.; Gutjahr, C. Bioassays for the effects of strigolactone and strigolactone-like molecules on root and root hair development. **MIMB**. Accepted and soon to be published in the book “Strigolactones” edited by SpringerNature.

José Antonio Villaécija Aguilar created the script, all the figures and wrote most of the first draft of the chapter. Sylwia Struck wrote the first draft of the lateral root quantification method. All authors contributed to editing and commenting the draft.

Signature of the Supervisor:

Prof. Dr. Caroline Gutjahr  
08.06.2020

Signature of first author:

José Antonio Villaécija Aguilar  
08.06.2020

**Manuscript I:** KL signalling regulates root hair elongation by promoting accumulation of auxin influx carrier AUX1

Reference: Villaecija-Aguilar JA., Magosch S., Hamon-Josse M., Bennett T., Gutjahr C. (2020). KL signalling regulates root hair elongation by promoting accumulation of auxin influx carrier AUX1.

José Antonio Villaécija Aguilar designed, performed and analysed most of the experiments, created all the figures, performed statistics, contributed to the conception of this study and the writing of the manuscript. Additionally, the following contributed to this work:

- Sonja Magosch acquired the data for Figure 1.
- Maxime Hamon-Josse acquired the data for Figure 3 and Figure 4C.
- Tom Bennett contributed to designed and conceive Figure 3 and Figure 4C.
- Caroline Gutjahr contributed to conceive the study, designed experiments, read and comment the manuscript.

Signature of the Supervisor:

Prof. Dr. Caroline Gutjahr  
08.06.2020

Signature of first author:

José Antonio Villaécija Aguilar  
08.06.2020

## IV. Summary

Karrikins (KARs) are small, bicyclic compounds that derive from the combustion of plant material. Initially, karrikins were associated with the promotion of seed germination of fire-following plants. However, karrikins promote the germination of a wide range of flowering plant species, including those that generally do not grow in fire-prone environments, such as *Arabidopsis thaliana*. Karrikin perception requires the  $\alpha/\beta$ -fold hydrolase receptor KAI2. The study of karrikin perception (*kai2*) mutants has increased our understanding of the importance of karrikin signalling in plant development. For instance, KAI2 in *Arabidopsis* regulates hypocotyl elongation, cotyledon expansion and drought resistance. Therefore, karrikins likely mimic endogenous unknown plant hormones, currently denominated as KAI2-ligands (KL).

Recent studies have demonstrated that the perception of karrikins/KL is closely related to that of strigolactones (SLs), a group of plant hormones that are perceived by the related  $\alpha/\beta$ -fold hydrolase DWARF14 (D14). Both signalling pathways converge upon the F-box protein MAX2 for ubiquitylation and subsequent degradation of the members of a group of repressors, belonging to the SMXL family of proteins. SLs have been associated with the regulation of plant development, including shoot branching, leaf senescence or root and root hair development. However, most works focused on understanding the role of SLs controlling root and root hair development in *Arabidopsis* have used *max2* mutants and the unspecific strigolactone analogue *rac*-GR24. Because the non-specific *max2* mutants and *rac*-GR24 do not distinguish between KL and SL signalling, it remained unclear whether SL and/or KL control root and root hair development.

In this doctoral thesis, I dissected the roles of D14- and KAI2-mediated signalling in root and root hair development in *Arabidopsis*. We demonstrate that SL and KL signalling regulate lateral root density and root epidermal cell length. I further describe that KAI2-mediated signalling regulates root skewing, straightness, diameter and root hair density and length. Furthermore, I report that all KAI2 effects in *Arabidopsis* roots can be explained by the activity of the canonical repressor of karrikin signalling, SMAX1/SMXL2. To facilitate the quantification of root skewing and root straightness, I established a script to automate the calculation of skewing to the left or right-slanted and root straightness.

Second, I contributed to finding new interactors of KAI2. A large-scale yeast-2-hybrid screen was conducted for KAI2 interactors and detected several novel *rac-GR24*-dependent KAI2-interactors, among them the phosphatase PP2AA2. To confirm a jointly mediate signalling pathway, I analysed root hair length (RHL) and density (RHD) in *pp2aa2* mutants. I found that both RHL and RHD in *Arabidopsis pp2aa2* mutants are strongly decreased, which perfectly phenocopied the root hair phenotypes of *kai2* mutants. Interestingly, *pp2aa2* mutants did not respond to exogenous karrikin treatment for root hair growth. These results suggest that KAI2 in concert with PP2AA2 mediates the regulation of root hair development in *Arabidopsis* roots.

Finally, I observed that mutations in KL signalling perception attenuate the root hair response to external phosphate deficiency. Upon phosphate starvation, auxin signalling induces the elongation of root hairs, presumably to increase the root surface area and acquire phosphate. Therefore, I hypothesised that KL signalling might regulate root hair development in cross-talk with auxin biosynthesis, signalling and/or transport. To determine this, I first examined the expression of genes involved in auxin signalling and transport. I found that karrikin perception mutants showed significantly reduced expression levels of the AUXIN RESPONSE FACTOR (ARF) genes, *ARF7* and *ARF19*. These results indicate that auxin signalling is perturbed in karrikin signalling mutants. Therefore, we examined auxin signalling in *kai2* mutants by analysing the expression of the auxin reporter *DR5v2:GFP*. We observed that *kai2* mutants show a reduced *DR5v2:GFP* expression in the root meristem. These results suggest that *kai2* mutants may be impaired in auxin sensitivity or distribution. I next demonstrated that external auxin treatment rescued the root hair phenotype of *kai2* to the wild-type level. Therefore, impaired auxin sensitivity is likely not the cause for the alteration in root hair development in karrikin signalling mutants. The auxin influx carrier AUX1 is the principal transporter for auxin uptake in root hairs. Hence to ascertain whether KL signalling regulates root hair development through AUX1, I analysed AUX1-YFP protein accumulation upon activation of karrikin signalling. I observed that exogenous KAR treatment induces accumulation of AUX1-YFP in the epidermal cell layer above the lateral root cap. Furthermore, *aux1* mutants are resistant to the effects of karrikin on root hair development. Thus, I conclude that deficient AUX1

accumulation in the root epidermis of KL signalling mutants disrupts auxin distribution in the root tip region and causes the root hair phenotypes.

## V. Zusammenfassung

Karrikinone sind kleine, bicyclische Signalmoleküle, die bei der Verbrennung von pflanzlichem Material entstehen. Ursprünglich waren Karrikinone mit der Förderung der Samenkeimung feuerfolgender Pflanzen assoziiert. Karrikinone fördern jedoch die Keimung einer Vielzahl von Blütenpflanzen, einschließlich solcher Pflanzen wie beispielsweise *Arabidopsis thaliana*, die im Allgemeinen nicht in feuergefährdeten Umgebungen wachsen. Die Karrikin-Wahrnehmung erfordert den  $\alpha/\beta$ -fachen Hydrolase-Rezeptor KAI2. Die Untersuchung von Karrikin-Wahrnehmungsmutanten (*kai2*) hat unser Verständnis über die Bedeutung der Karrikin-Signalübertragung für die Pflanzenentwicklung verbessert. KAI2 reguliert beispielsweise die Hypokotylelongation, Keimblattausdehnung und Trockenresistenz in *Arabidopsis*. Daher ahmen Karrikinone vermutlich unbekannte endogene Pflanzenhormone nach, die derzeit als KAI2-Liganden (KL) bezeichnet werden.

Jüngste Studien haben gezeigt, dass die Wahrnehmung von Karrikinen/KL eng mit der von Strigolaktonen (SLs), einer Gruppe von Pflanzenhormonen, die von der analogen  $\alpha/\beta$ -fachen Hydrolase DWARF14 (D14) wahrgenommen werden, verwandt ist. Beide Signalwege konvergieren auf dem F-Box-Protein MAX2 zur Ubiquitinierung und anschließendem Abbau der Mitglieder einer Gruppe von Repressoren, die zur SMXL-Proteinfamilie gehören. SLs wurden mit der Regulierung der Pflanzenentwicklung in Verbindung gebracht. Dies beinhaltet unter anderem Sprossverzweigung, Blattalterung oder Wurzel- und Wurzelhaarentwicklung. Die meisten Arbeiten zum Verständnis der Rolle von SLs, die die Wurzel- und Wurzelhaarentwicklung bei *Arabidopsis* steuern, verwendeten jedoch *max2* Mutanten und das unspezifische Strigolakton-Analogon *rac-GR24*. Da die unspezifischen *max2* Mutanten und *rac-GR24* nicht zwischen KL- und SL-Signalen unterscheiden, blieb unklar, ob SL und/oder KL die Wurzel- und Wurzelhaarentwicklung kontrollieren.

In dieser Doktorarbeit habe ich die Rolle der D14- und KAI2-vermittelten Signalübertragung in der Wurzel- und Wurzelhaarentwicklung in *Arabidopsis* untersucht. Wir zeigen, dass SL- und KL-Signale die laterale Wurzeldichte und die Länge der epidermalen Wurzelzellen regulieren. Zudem beschreibe ich, dass die KAI2-vermittelte Signalübertragung die Wurzelkrümmung und -geradlinigkeit, den Durchmesser der Wurzel, sowie die Dichte und Länge der Wurzelhaare reguliert.

Darüber hinaus berichte ich, dass alle KAI2-Effekte in Arabidopsis-Wurzeln durch die Aktivität des kanonischen Repressors der Karrikin-Signalübertragung SMAX1/SMXL2 erklärt werden können. Um die Quantifizierung der Wurzelkrümmung und der Wurzelgeradlinigkeit zu erleichtern, habe ich ein Skript erstellt, um die Berechnung der Krümmung nach links oder rechts und die Geradheit der Wurzel zu automatisieren.

Zusätzlich habe ich dazu beigetragen, neue Interaktoren von KAI2 zu finden. Ein Hefe-2-Hybrid-Screening in großem Maßstab wurde für KAI2-Interaktoren durchgeführt und mehrere neue *rac*-GR24-abhängige KAI2-Interaktoren, darunter die Phosphatase PP2AA2, identifiziert. Um einen gemeinsam vermittelten Signalweg zu bestätigen, wurde die Wurzelhaarlänge (RHL) und -dichte (RHD) in *pp2aa2* Mutanten analysiert. Ich fand heraus, dass sowohl RHL als auch RHD in Arabidopsis *pp2aa2* Mutanten stark verringert sind, was die Wurzelhaar-Phänotypen von *kai2* Mutanten perfekt kopierte. Interessanterweise reagierten *pp2aa2* Mutanten nicht auf eine exogene Karrikin-Behandlung für das Wurzelhaarwachstum. Diese Ergebnisse legen nahe, dass KAI2 zusammen mit PP2AA2 die Regulation der Wurzelhaarentwicklung in Wurzeln von Arabidopsis vermittelt.

Abschließend beobachtete ich, dass Mutationen in der KL-Signalwahrnehmung die Wurzelhaarreaktion auf externen Phosphatmangel abschwächen. Bei Phosphatmangel induziert der Auxin-Signalweg die Verlängerung der Wurzelhaare, vermutlich um die Wurzeloberfläche zu vergrößern und Phosphat aufzunehmen. Daher stellte ich die Hypothese auf, dass die KL-Signalübertragung die Wurzelhaarentwicklung im Nebensprechen mit der Auxin-Biosynthese, der Auxin-Signalübertragung und/oder dem Transport von Auxin regulieren könnte. Um dies festzustellen, untersuchte ich zunächst die Expression von Genen, die an der Signalübertragung und dem Transport von Auxin beteiligt sind. Ich fand heraus, dass Karrikin-Wahrnehmungsmutanten signifikant reduzierte Expressionsniveaus der AUXIN RESPONSE FACTOR (ARF)-Gene ARF7 und ARF19 zeigten. Diese Ergebnisse zeigen, dass die Auxin-Signalweiterleitung in Karrikin-Signalmutanten gestört ist. Daher untersuchten wir die Auxin-Signalweiterleitung in *kai2* Mutanten durch Analyse der Expression des Auxin reporters *DR5v2:GFP*. Wir beobachteten, dass *kai2* Mutanten eine verringerte *DR5v2:GFP*-Expression im Wurzelmeristem zeigen. Diese Ergebnisse legen nahe,

dass *kai2* Mutanten in der Sensitivität gegenüber Auxin oder der Verteilung von Auxin beeinträchtigt sein können. Als nächstes zeigte ich, dass eine externe Behandlung mit Auxin den Wurzelhaar-Phänotyp von *kai2* auf das Wildtyp-Niveau rettete. Daher ist eine beeinträchtigte Auxin-Empfindlichkeit wahrscheinlich nicht die Ursache für die Veränderung der Wurzelhaarentwicklung in Karrikin-Signalmutanten. Der Auxin-Zufluss-Träger AUX1 ist der Haupttransporter für die Auxin-Aufnahme in Wurzelhaaren. Um festzustellen, ob die KL-Signalübertragung die Wurzelhaarentwicklung durch AUX1 reguliert, analysierte ich die AUX1-YFP-Proteinakkumulation bei Aktivierung der Karrikin-Signalübertragung. Ich beobachtete, dass eine exogene Karrikin-Behandlung eine Akkumulation von AUX1-YFP in der epidermalen Zellschicht über der lateralen Wurzelkappe induziert. Darüber hinaus sind *aux1* Mutanten gegen die Auswirkungen von Karrikin auf die Wurzelhaarentwicklung resistent. Daher schliesse ich, dass eine mangelnde AUX1-Akkumulation in der Wurzelepidermis von KL-Signalmutanten die Verteilung von Auxin in der Wurzelspitzenregion stört und die Wurzelhaar-Phänotypen verursacht.

## VI. Introduction

### 1. The karrikin family

Seed germination is a crucial event in the life cycle of higher plants, while seed dormancy is critical to limit germination under disadvantageous environmental conditions. In many regions, wildfires provide an excellent opportunity for different plant species to experience reduced competition for essential resources such as space, light, water, and nutrients (Staden et al., 2000; Dixon et al., 2009). These species, known as fire-following plants, have evolved to break seed dormancy immediately after fire. Heat is not required for seed germination (Roche et al., 1997; Roche et al., 1998), but it is now well known that smoke is an effective stimulant of germination (Dixon et al., 2009).

Attempts to find the bioactive smoke-compound that stimulates seed germination culminated in the isolation of the butenolide 3-methyl-2*H*-furo [2,3-*c*]pyran-2-one, or karrikin 1 (KAR1). This compound defined a new family of butenolide molecules known as karrikins (KARs) (Flematti et al., 2004; Flematti et al., 2009). Until now, almost 50 analogues of KAR have been synthesized (Flematti et al., 2007; Sun et al., 2008) and six KAR molecules have been identified in plant-derived smoke (Figure 1), which differ in their methyl substitutions (Flematti et al., 2009). KARs can stimulate the germination of dormant seeds of plants from numerous families at low concentrations, including species that are not considered as fire-following plants (Chiwocha et al., 2009; Flematti et al., 2009; Nelson et al., 2009; Waters et al., 2012b). Thanks to this breakthrough, a new research area started to move towards the broader biological significance of the KAR signalling pathway.

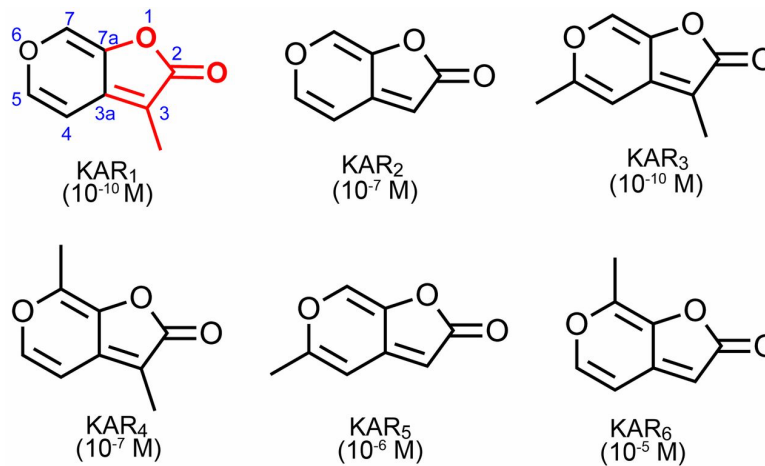


**Figure 1:** Representative structures of the karrikins (KAR<sub>1</sub> to KAR<sub>6</sub>). Germination activity of karrikin half maximal effective concentration (EC<sub>50</sub>) using *Solanum orbiculatum* are shown in parenthesis (Modified from Guo et al., 2013).

## 2. KAI2 is the receptor of KARs

KARs not only induces germination but also increase the response to light in *Arabidopsis thaliana* hypocotyls (Nelson et al., 2010). KAR treatment inhibits hypocotyl elongation and cotyledon expansion (Nelson et al., 2010). Based on these responses to KAR, a forward genetic screen identified the first *karrikin insensitive* (*kai*) mutant in Arabidopsis. Sequencing of two *kai* mutants revealed two frameshift mutations in a gene encoding an F-box protein MAX2 (MORE AXILLARY GROWTH 2) that forms part of the SCF class of E3 ubiquitin ligase complexes and was previously known to act in strigolactone signalling (Nelson et al., 2011). This finding revealed the first F-box protein involved in two plant hormone signalling pathways responsive to KARs and strigolactones (SLs) (Gomez-Roldan et al., 2008; Umehara et al., 2008; Nelson et al., 2011).

For other plant hormones, such as auxin or jasmonate, the F-box proteins directly bind the hormone and selectively target downstream repressor proteins for their degradation (Abd-Hamid et al., 2020). However, the perception of SLs requires the  $\alpha/\beta$  hydrolase DWARF14 (D14) (Arite et al., 2009; Waters et al., 2012a; Yao et al., 2016). This evidence, together with the insensitivity of *max2* mutants to both SLs and KARs and the insensitivity of *d14* to only SL (Waters et al., 2012b), suggested a different KAR receptor. Phylogenetic analysis proposed that the Arabidopsis and rice

*D14* paralogue, *D14-LIKE (D14L)*, serves as the KAR receptor (Waters et al., 2012b). Indeed, genetic dissection demonstrated that *D14L* and *D14* are required for normal KAR and SL responses, respectively, and that both signalling pathways converge upon MAX2 (Waters et al., 2012b). Mutations in *D14L* lead to INSENSITIVITY TO KAR; therefore, *D14L* is now renamed as KAI2 (Waters et al., 2012b).

The identification of the two receptors for KAR and SL provided the molecular basis to separate the regulation of KAR and SL signalling by MAX2. The similarity between KAI2 and D14 signalling pathways raises the intriguing question of how these mechanisms have evolved. D14 can only be found in Angiosperms and Gymnosperms (Delaux et al., 2012; Waters et al., 2015; Waters et al., 2017). However, non-vascular plants, such as the moss *Physcomitrella patens*, produce SLs (Proust et al., 2011). *KAI2* orthologues have been identified in mosses, liverworts and charophytes (Delaux et al., 2012) (Figure 2). Thus, these observations suggest that KAI2 proteins may perceive SLs in non-vascular plants. Phylogenetic studies showed that D14 and KAI2 evolved from a common KAI2-like lineage present in streptophyte algae (Bythell-Douglas et al., 2017) and that gene amplification events from *KAI2* paralogues specifically occurring in parasitic plants within the Orobanchaceae family (Toh et al., 2014; Conn et al., 2015; Tsuchiya et al., 2015). A functional approach demonstrated that *KAI2*-like genes from *Selaginella moellendorffii* (lycophytes) could partially substitute the activity of KAI2 in *Arabidopsis*. However, *KAI2*-like genes from *Marchantia polymorpha* (liverworts) and *Selaginella* could not substitute the activity of D14 (Waters et al., 2015). Taken together, the available evidence indicates that D14 evolved from KAI2 paralogues (Machin et al., 2020).

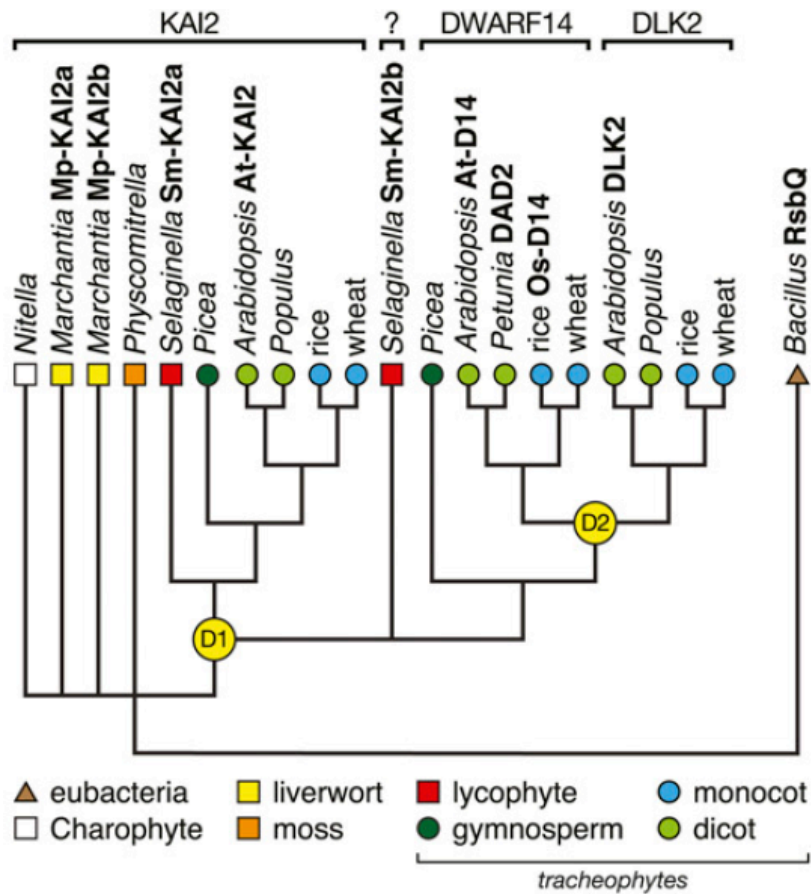


**Figure 2: Phylogeny of the KAI2 and D14 protein family.** Gene duplication events are indicated as D1, before the emergence of tracheophytes, and D2 after the split of angiosperms and gymnosperms (From Waters et al., 2015).

### 3. KAI2-ligands: putative endogenous hormones

The wide evolutionary conservation of KAI2 proteins underlines that the primary function of KAI2 is improbable to be the perception of bioactive molecules from fire (Nelson et al., 2010). Recent studies have promoted the biological significance and role of KAI2 in plant development and interaction with other organisms. KAI2 is required for different developmental traits in Arabidopsis (Li et al., 2006) (Waters et al., 2012b; Waters et al., 2013; Conn and Nelson, 2016; Li et al., 2017; Wang et al., 2018; Swarbreck et al., 2019; Villaécija-Aguilar et al., 2019; Wang et al., 2020). The *kai2* mutant has an elongated hypocotyl and epinastic cotyledons. During vegetative development, *kai2* leaves are elongated with curled margins (Waters et al., 2012b). KAI2 promotes drought resistance (Li et al., 2017) and is also required for arbuscular mycorrhizal symbiosis in rice and petunia (Gutjahr et al., 2015; Liu et al., 2019).

Therefore, KARs are assumed to mimic the action of a yet unknown putative endogenous hormone family, denominated KAI2-ligands (KLs) (Conn and Nelson, 2016).

#### 4. Strigolactones: chemistry and biosynthesis

SLs are a family of terpenoid lactone hormones with a wide range of functions in plants, algae, bryophytes and arbuscular mycorrhizal fungi (Akiyama and Hayashi, 2006; Bouwmeester et al., 2007; Yoneyama et al., 2007; Umehara et al., 2008; Xie et al., 2010; Yoneyama et al., 2010; Proust et al., 2011; Ruyter-Spira et al., 2011; Delaux et al., 2012; Brewer et al., 2013). Their collective name come from the first discovered SL in root exudates of cotton that functions as stimulator of seed germination of the parasitic weed *Striga lutea* (Butler, 1995). Since then, at least 25 characterized naturally SLs occurring have been isolated (Saeed et al., 2017).

Although SL biosynthesis can occur in different parts of the plants, SLs are mainly produced in roots (Koltai and Beveridge, 2013). SLs are carotenoid derivatives defined by the presence of a structure consisting of a butenolide ring (D ring) linked in the stereochemical *R* configuration to a second variable moiety (Matusova et al., 2005; Al-Babili and Bouwmeester, 2015; Jia et al., 2017). Genes involved in the SL biosynthetic pathway have been identified in several plant species (Waters et al., 2017). The production of a central metabolite carlactone from  $\beta$ -carotene involves the all-trans/9-*cis*- $\beta$ -carotene isomerase DWARF27 (D27), followed by the next enzymes in the pathway, the carotenoid cleavage dioxygenases CCD7, and CCD8, which supply the last enzymatic steps of the core pathway. Carlactone is then modified by different enzymes, including the cytochrome P450 (CYP) of the MAX1 sub-family, leading to different types of SLs (Jia et al., 2017). Depending on the structure of their variable moiety, SLs are classified into canonical, if they contain a conserved tricyclic lactone (ABC ring) or non-canonical, if they contain a different structure such as zealactone (Charnikhova et al., 2018), methyl carlactonoate (Abe et al., 2014) or helialactone (Ueno et al., 2014). The differences in the stereochemistry of the BC ring junction divided the canonical SLs into strigol-type or orobanchol-type (Ueno et al., 2011; Xie et al., 2013). Orobanchol-type is synthesized from *ent*-2'-*epi*-5-deoxystrigol (Yokota et al., 1998) and contains the C ring in  $\alpha$  orientation, while strigol-type is derived from 5-

deoxystrigol and contains the C ring in  $\beta$  orientation (Jia et al., 2017) (Figure 3). The two canonical SLs, strigol and orobanchol are named due to their activity in triggering seed germination in *Striga* and *Orobanche* species respectively (Cook et al., 1972; Siame et al., 1993; Yokota et al., 1998). It is common to use strigol and orobanchol as references in the terminology of other structurally related SLs or stereoisomers of the chiral centre at the C2' atom, the BC ring junction, or both. The abbreviations *ent*- and *epi*- is frequently employed to designate two types of stereoisomers, enantiomer, which is a mirror from the reference, and epimer, with an opposite orientation at a single C atom.

The chemical synthesis of natural SLs is an arduous work due to their complex structure and the presence of chiral centres. Besides, it is generally unknown, which SLs are responsible for different biological activity. Therefore, SL research strongly depends on the synthetic analogue *rac*-GR24, which is a racemic mixture of two different enantiomers, GR24<sup>5DS</sup> and GR24<sup>ent-5DS</sup> (Figure 3). Although the synthetic production of GR24 can also generate two other different enantiomers, GR24<sup>4DO</sup> and GR24<sup>ent-4DO</sup>, these compounds are not regularly used in biological experiments (Scaffidi et al., 2014). KAI2 and D14 are capable of detecting synthetic *rac*-GR24. While GR24<sup>ent-5DS</sup> appears to stimulate KAI2 signalling (Scaffidi et al., 2014; Waters et al., 2015), D14 signalling seems to preferentially respond to GR24<sup>5DS</sup> (Nakamura et al., 2013; Scaffidi et al., 2014; Waters et al., 2015; Zhao et al., 2015).

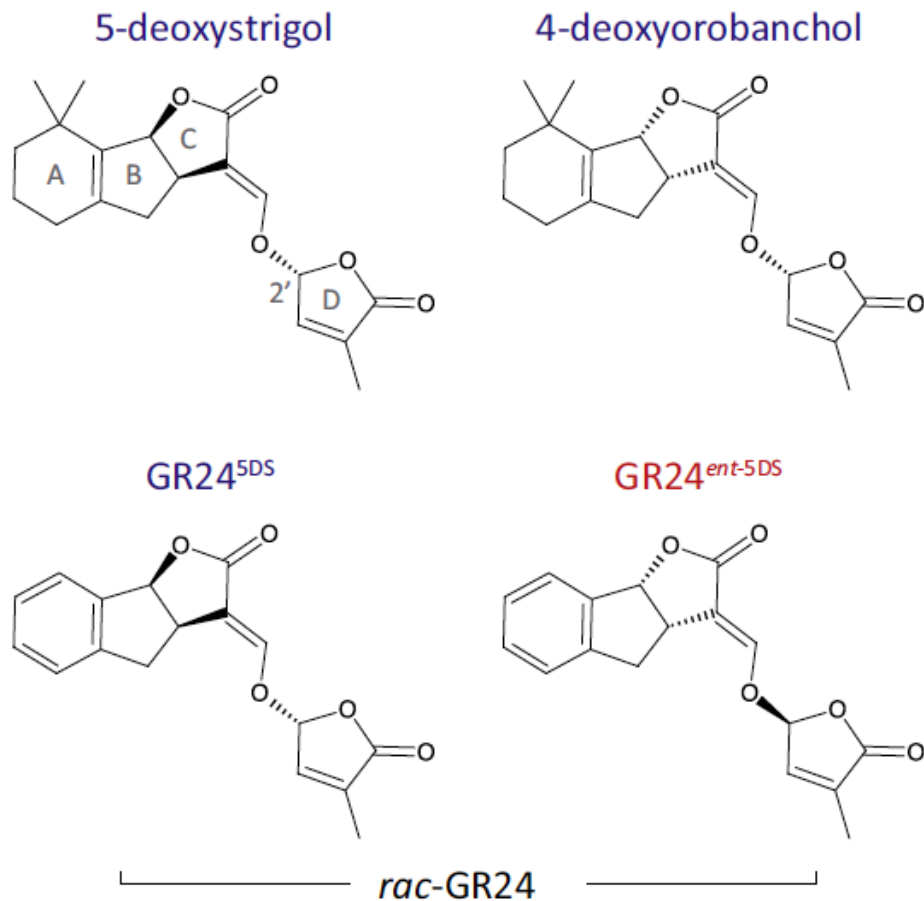


**Figure 3. Structures of Strigolactones (SLs).** Representative structures of the two major classes of natural SLs and the synthetic analogue of SL, GR24. (Morffy et al., 2016).

## 5. Proteasome targets of SL/KL signalling pathways

Previous studies contend that in complex with MAX2, D14 or KAI2 target a group of repressors of the SMXL (SUPPRESSOR OF MAX2 1-LIKE) family of proteins. Eight genes have been identified in Arabidopsis to belong to the SMXL gene family (Stanga et al., 2016). In Arabidopsis, loss-of-function of SMAX1 and/or SMXL2, suppresses KL-signalling related *max2* phenotypes (Stanga et al., 2013; Soundappan et al., 2015; Wang et al., 2015; Swarbreck et al., 2019; Villaécija-Aguilar et al., 2019; Wang et al., 2020), while loss-of-function of the redundant SMXL6, SMXL7 and SMXL8, suppress SL-related *max2* phenotypes (Soundappan et al., 2015; Wang et al., 2015) (Figure 4). Other three genes form a new subclade of the SMXL gene family,

*SMXL3*, *SMXL4* and *SMXL5* which are redundant central regulators of phloem formation, interestingly independent of SL and KL signalling (Wallner et al., 2017).

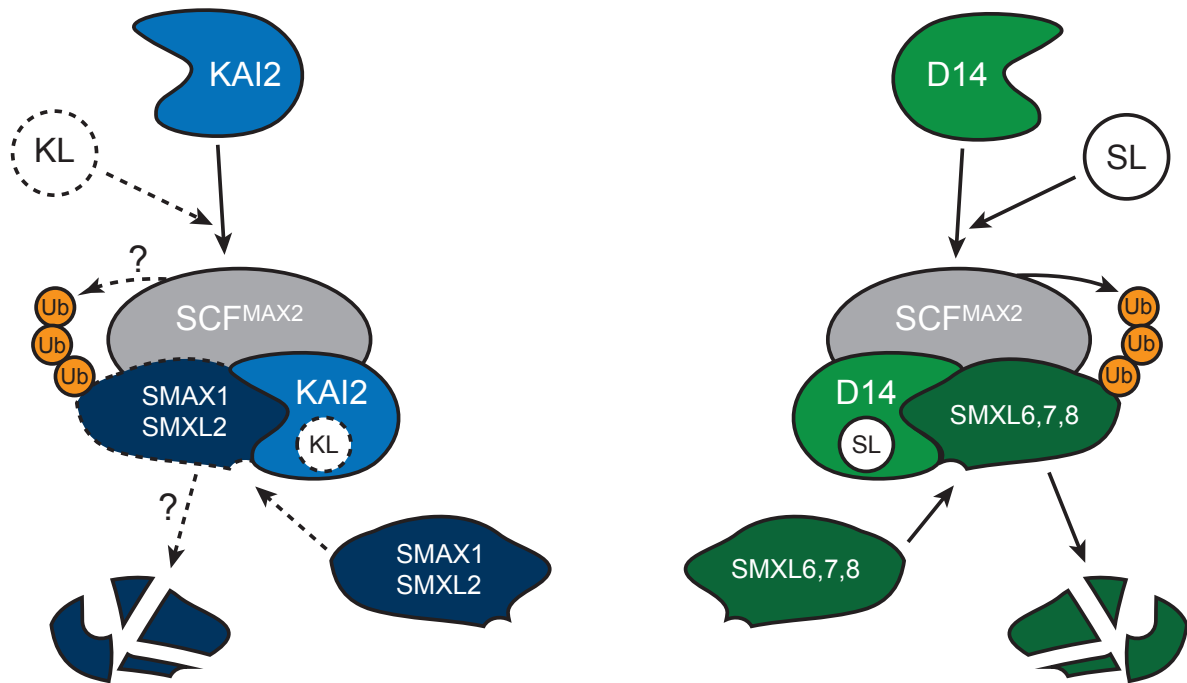


**Figure 4: Model for KAI2 and D14 signalling pathways.** Upon perception of KL or SL, KAI2 and D14 bind to the F-box protein MAX2 to trigger the degradation of SMXLs. (Modified from Villaécija-Aguilar et al., 2019).

SMXL proteins have a weak homology to the Class 1 HsP100/ClpB proteins (Jiang et al., 2013; Stanga et al., 2013; Zhou et al., 2013; Moturu et al., 2018). However, their exact function remains unclear. Previous investigations suggested that SMXLs are associated with transcriptional regulation, due to their interaction with TOPLESS (TPL) and TOPLESSRELATED (TPR) co-repressor proteins (Zhou et al., 2013; Soundappan et al., 2015; Wang et al., 2015). Similar to Aux/IAA proteins in auxin signalling and JAZ proteins in jasmonate signalling, SMXL proteins lack DNA-binding motifs. Aux/IAA interact with TPL/TPR proteins to recruit auxin response factors (ARFs) via an EAR motif (Ethylene-responsive element binding factor-associated amphiphilic repression) (Kagale and Rozwadowski, 2011). Upon auxin perception, the auxin receptor TIR1 F-box protein targets Aux/IAA for its degradation,

which activates auxin signalling. Analogously, jasmonate perception via the F-box protein COI1 targets JAZ for degradation and activation of jasmonate signalling. Although some JAZ has an EAR motif, others associate TPL/TPR by binding NINJA, which has an EAR motif (Szemenyei et al., 2008; Pauwels et al., 2010; Kagale and Rozwadowski, 2011; Causier et al., 2012). Similarly, SMXLs might interact with TPL/TPR via their EAR motif to recruit transcription factors. The EAR motif is conserved among the members of the SMXL protein family (Soundappan et al., 2015). Yeast two-hybrid assays, immunoprecipitation and bimolecular fluorescence complementation assays have proven that TPL/TPR interactions with SMXL proteins are EAR motif-dependent (Jiang et al., 2013; Soundappan et al., 2015; Wang et al., 2015; Liang et al., 2016). Deletion of a phosphate-binding P-loop similar to the EAR motif in SMXL7 leads to degradation resistance of the protein (Liang et al., 2016).

## **6. SL and KL signalling cross-talk with signalling pathways of other phytohormones**

A range of complex interactions of hormone signalling systems regulates crucial aspects of plant development. Auxin, cytokinin (CK), ethylene, gibberellin acid (GA), abscisic acid (ABA), and brassinosteroids exhibit either synergistic or antagonistic interactions (Vanstraelen and Benková, 2012). Previous research has investigated the interaction of SLs with signalling pathways of other hormones (Waters et al., 2012a; Shinohara et al., 2013; Soundappan et al., 2015; Duan et al., 2019; Omoarelojie et al., 2019). In rice roots, prolonged GA treatment suppresses SL exudation (Ito et al., 2017). SL and CK signalling coordinately control bud outgrowth in *Pisum sativum* (Duan et al., 2019). In *Arabidopsis* shoots, SL biosynthesis and signalling mutants display an increase in auxin transport (Bennett et al., 2016), presumably due to over-accumulation of the auxin efflux carrier PIN-FORMED1 (PIN1) at the plasma membrane (Shinohara et al., 2013; Soundappan et al., 2015). Treatments with *rac*-GR24 altered the localization of PIN1 in a *MAX2*-dependent manner. Also, mutations in *pin3 pin4* and *pin7* lead to partial suppression of *max2* phenotype (van Rongen et al., 2019). At the root level, *rac*-GR24 treatment promotes PIN2 endocytosis (Pandya-Kumar et al., 2014) and reduces PIN protein levels in the root meristem (Ruyter-Spira et al., 2011). Nevertheless, whether *rac*-GR24 regulates auxin transport via D14- or KAI2-mediated signalling pathways is unknown. Few pieces of evidence link SL and

ethylene signalling. For example, it was proposed that ethylene signalling is required for the control of root hair elongation by MAX2 (Koltai et al., 2010; Kapulnik et al., 2011b; Kapulnik et al., 2011a; Mayzlish-Gati et al., 2012). However, it remains unclear if ethylene is epistatic to SLs or KL signalling in the context of root-hair development, due to the use of *max2* mutants perturbed in both pathways.

Little research has been conducted to investigate cross-talk between KL and other phytohormone signalling pathways. Recent reports suggest that *Arabidopsis kai2* plants are hyposensitive to ABA in stomatal closure and cotyledon opening, suggesting a link between KL and ABA signalling (Li et al., 2017). Besides, GA biosynthesis and perception are partially required for the induction of seed germination by KARs, indicating that KL signalling acts upstream of GA signalling for seed germination (Nelson et al., 2009). In summary, while the interconnection between SL and auxin signalling has been quite well explored, the interaction between SL and/or KL signalling with other plant hormones is still understudied.

## **7. Participation of protein phosphatases in plant hormone signalling**

Phytohormone regulation of plant development is mediated through a wide range of proteins, including phosphatases. Most of the Ser/Thr phosphatase activities in eukaryotic cells are controlled by the PROTEIN PHOSPHATASE 2A (PP2A) (Millward et al., 1999). PP2A proteins are constituted by a catalytic subunit (PP2Ac), and one or more regulatory subunits, the scaffolding/regulatory (A) subunit and the regulatory (B) (Hendrix et al., 1993; Strack et al., 1998; Janssens and Goris, 2001). Genetics approaches have shown that PP2A and its subunits regulate plant growth (Garbers et al., 1996). In *Arabidopsis*, mutations in *PP2A* genes cause hypocotyl hook formation, root agravitropism and root meristem collapse (Garbers et al., 1996; Zhou et al., 2004; Michniewicz et al., 2007). PP2A plays important roles in stress response and hormone signalling. Under osmotic stress, ABA binds to its receptor PYL to inhibit the activity of PP2A, which leads to the regulation of auxin transport by PIN dephosphorylation (Zhou et al., 2004; Li et al., 2020). PP2A mediates the regulation of ethylene production by controlling the stability of specific 1-aminocyclopropane 1-carboxylate synthase (ACS) enzymes (Skottke et al., 2011). Besides, PP2A positively regulates the transcription factor BZR1 (Tang et al., 2011), which controls

brassinosteroid-responsive gene expression (Gendron and Wang, 2007; Kim et al., 2009; Tang et al., 2010). The fact that most signalling processes involved phosphorylation and dephosphorylation events suggests that PP2A might also be required for KL and/or SL mediate signalling.

## **8. Arabidopsis root development and behaviour**

Root growth and development is essential to ensure efficient uptake of water and nutrients in vascular plants. Because of its relatively simple root structure, *Arabidopsis* roots have been extensively studied (Scheres and Wolkenfelt, 1998; Masson et al., 2002; Benfey et al., 2010). The root system of *Arabidopsis* included a primary root, lateral roots, adventitious roots and root hairs (Smith and De Smet, 2012).

The primary root is developed from embryonic meristematic tissue. A central vascular column consists of xylem and phloem, and a pericycle that constitutes the stele, surrounded by epidermal, cortical and endodermal tissues (Bennett and Scheres, 2010). At the root tip, meristematic cells are the basis for other cells type in the root. In this area is located the root cap and columella cells, involved in the control of root gravitropism (Swarup et al., 2005; Guyomarc'h et al., 2012). Lateral roots (LRs) emerge from the primary root, and they are crucial to increase root surface area and biomass (López-Bucio et al., 2002; Tian et al., 2014; Robbins and Dinneny, 2015; Sun et al., 2017). The formation of LRs begins in the root meristem, and it involves the oscillation of over 3.000 genes (Moreno-Risueno et al., 2010). When the cells move into the differentiation zone, LR originator cells encounter a series of division (Dubrovsky et al., 2009; Dubrovsky and Forde, 2012). LR development has been divided into eight different stages. Stage I from the first asymmetric division, stages II-VII through following rounds of cells division, and stage VIII for LR emergence. LRs development requires the coordinated regulation of multiple phytohormones, such as BR, ABA, ethylene, auxin or SLs (De Smet et al., 2007; Ivanchenko et al., 2008; Negi et al., 2008; Fukaki and Tasaka, 2009; Kapulnik et al., 2011b; Ruyter-Spira et al., 2011; Mayzlish-Gati et al., 2012; Péret et al., 2012; Jiang et al., 2015). However, a role of KL signalling controlling root development remained unknown

Changes in root movements are also essential to maximize plant fitness in a large variety of environmental conditions. The studies of the movement of plants have been in high interest in plant biology for longer than a hundred years. The first studies go back to Charles Darwin in his book, *The Power of Movement in Plants* (Darwin, 1897). Nevertheless, how plants control root behaviour continues being an enigma, and it is difficult to identify a simple model that explains this process (Roy and Bassham, 2014) (Figure 5). When germinating *Arabidopsis* seedlings on a hard agar surface in a petri dish, the root cannot penetrate the agar, causing morphological changes such as root skewing and waving. Skewing was first described in *Arabidopsis* wild type of the ecotype *Landsberg erecta* (Ler) as the deviation of the root growth from the vertical, always as right-slanted (Okada and Shimura, 1990; Vaughn and Masson, 2011). Prior research has highlighted shown that root skewing is likely the result of a touch, rather than the gravity stimulus (Millar et al., 2011; Roy and Bassham, 2014).

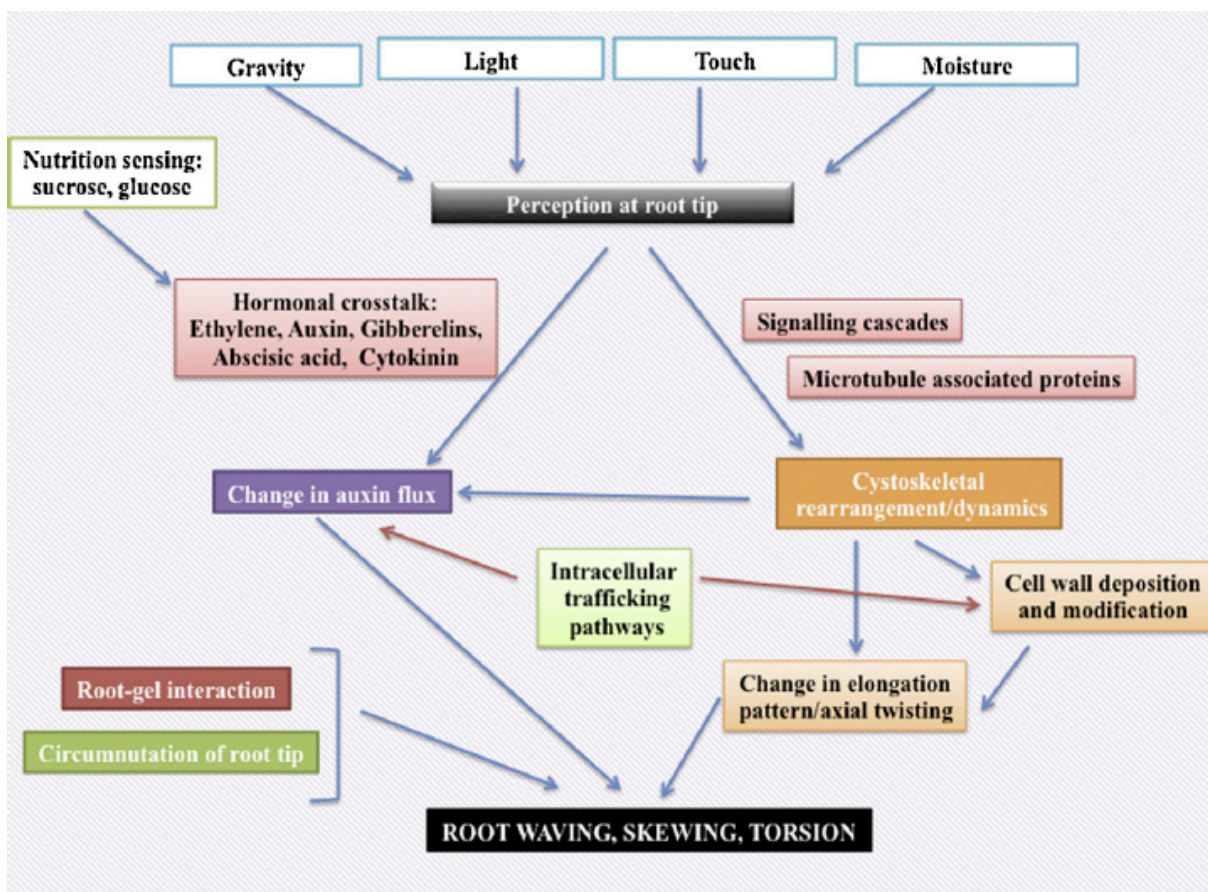


**Figure 5. Control of root skewing and waving** (from Roy and Bassham 2014).

## 9. Regulation of root hair development in Arabidopsis

Root hairs can account for up to 70% of the total root surface area in Arabidopsis seedlings (López-Bucio et al., 2002). Thus, the number and size of root hairs influence the total area/volume ratio of the roots system (López-Bucio et al., 2002; Choi and Cho, 2019). Changes in root hair development are controlled by several essential transcription factors (TFs). R2R3-type MYB transcription factor WER (WEREWOLF) (Lee and Schiefelbein, 1999), GL3 (GLABLA3), a basic helix-loop-helix (bHLH)-type transcription factor or its homologue EGL3 (ENHANCER OF GLABLA3) (Bernhardt et al., 2003), and TTG1 (TRANSPARENT TESTA GLABLA1), a WD repeat protein (Galway et al., 1994), form a complex that enhances the expression of *GL2* (*GLABLA2*). *GL2* is a negative regulator of root hair formation in non-hair cells (Di Cristina et al., 1996; Masucci and Schiefelbein, 1996). Thus, the lack of *GL2* function causes the formation of root hairs from non-hair cell files. In contrast, to promote root hair identity, the WER-GL3-TTG1 complex induces the expression of *CPC* (*CAPRICE*), a mobile R3-Type MYB transcription factor (Wada et al., 1997), in non-root hair cells. *CPC* moves to hair forming cells, where it interacts with TTG1 and GL3 or EGL3. Besides, the *CPC* homologues *ETC1* (ENHANCER OF TRY AND *CPC1*), or *TRY* (*TRIPTYCON*) (Schellmann et al., 2002; Simon et al., 2007) can act in a partially redundant manner (Ishida et al., 2008; Bruex et al., 2012; Grierson et al., 2014; Salazar-Henao et al., 2016). *CPC* or its homologues induce the expression of *RHD6* (*ROOT HAIR DEFECTIVE 6*), a bHLH transcription factor, which determines root hair identity (Masucci and Schiefelbein, 1994; Menand et al., 2007). *RHD6* and its homologue *RSL1* (*ROOT HAIR DEFECTIVE 6 LIKE1*) initiate the root hair polar growth, then promoting the transcription of other bHLH transcription factors, *RSL2* and *RLS4*, during the elongation phase (Menand et al., 2007; Yi et al., 2010). *RSL4* bind to a *cis*-element called *RHE* (Root Hair Element) to promote the expression of *RHS* (*ROOT HAIR SPECIFIC*) genes (Kim et al., 2006; Won et al., 2009; Hwang et al., 2017). Mutations in the *RSL2* or *RSL4* genes cause a reduction in root hair length in Arabidopsis (Yi et al., 2010; Mangano et al., 2018). However, overexpression of *RSL2* does not increase root hair elongation, suggesting that *RSL2* alone is not sufficient to promote root hair growth (Yi et al., 2010).

Several plant hormones, such as auxin and ethylene, regulate *RSL2* and *RSL4* expression to induce root hair growth. Auxin and ethylene are essential for root hair formation (Feng et al., 2017; Bhosale et al., 2018). Exogenous auxin and ethylene treatment increases root hair density and length (Pitts et al., 1998), while defects in auxin and ethylene biosynthesis and/or signalling reduce root hair formation (Velasquez et al., 2016; Feng et al., 2017). Auxin induces the expression of ARFs (AUXIN RESPONSE FACTORS), such as ARF5, ARF7, ARF8 and ARF19 that bind to the promoter of *RSL4* to upregulate its expression (Mangano et al., 2018). Besides, ARF19 activates the expression of *RSL2*. However, it remains unclear whether ARF19 can bind directly to the promoter of *RSL2* (Bhosale et al., 2018). Ethylene increases root hair development by inducing the expression of *RSL4* (Zhang et al., 2016) through the transcription factor EIN3 (ETHYLENE INSENSITIVE 3), which directly binds to the promoter of *RSL4* (Feng et al., 2017). Auxin and ethylene also act systemically to transduce nutrient deficiency signals, such as Pi starvation. Pi deficiency stimulates auxin biosynthesis at the root tip (Bhosale et al., 2018). Auxin is then transported from the root tip to non-root hair cells by the auxin influx carrier AUX1 (AUXIN RESISTANT 1) to promote root hair elongation mediated by ARF19, *RSL2* and *RSL4* (Bhosale et al., 2018). The importance of auxin levels in root hair cells have also been previously surveyed. Expression of six different auxin efflux carriers, PINs (PIN-FORMED), inhibit the formation of root hair, likely by altering the levels of auxin in those cells (Ganguly et al., 2010). In addition, Pi deficiency increases the levels of EIN3, which can promote root hair development by direct binding of root hair specific genes (Song et al., 2016).

## VII. Aims of the thesis

Several studies have investigated the role of SLs in the regulation of root and root hair development in *Arabidopsis thaliana*. However, since *max2* mutants are perturbed in both SL and KL signalling pathway and *rac-GR24* stimulate D14- and KA2-mediated signalling, it remained unclear whether the observed phenotypes were associated with (lack of) SL or KL signalling.

Therefore, the first major goal of my work was to dissect the roles of KL and SL signalling pathways in root and root hair development in *Arabidopsis*, and to understand, whether they are mediated by canonical receptor target interactions. For this purpose, I aimed to study different root parameters, such as root diameter, epidermal cell length, root skewing, root straightness, and root hair density and length. I found that mutations on *KAI2* and *MAX2* strongly reduced root hair development. Thus, the second major aim of my thesis was to understand how KL signalling regulates root hair development. To this end I phenotypically characterized the role of a *KAI2* interactor *PP2AA2* (identified by collaborating with the laboratory of Pascal Falter-Braun). Furthermore, root hair growth is controlled by several hormones, including auxin. Previous reports proposed the interaction between auxin and SL signalling. However, those studies were again based on *max2* mutants and *rac-GR24* treatments. Here my aim was to understand whether there is an interaction between KL signalling and auxin signalling, biosynthesis and/or transport in the control of root hair development.

## VIII. Results

**Paper I:** SMAX1/SMXL2 regulate root and root hair development downstream of KAI2-mediated signalling in Arabidopsis

Reference: **Villaécija-Aguilar, J.A.**; Hamon-Josse, M.; Carbonnel, S.; Kretschmar, A.; Schmidt, C.; Dawid, C.; Bennett, T.; Gutjahr, C. SMAX1/SMXL2 regulate root and root hair development downstream of KAI2-mediated signalling in Arabidopsis. **PLoS Genet.** 2019, 15, e1008327.

RESEARCH ARTICLE

# SMAX1/SMXL2 regulate root and root hair development downstream of KAI2-mediated signalling in Arabidopsis

José Antonio Villaécija-Aguilar <sup>1,2</sup>, Maxime Hamon-Josse <sup>3</sup>, Samy Carbonnel<sup>1,2</sup>, Annika Kretschmar <sup>1</sup>, Christian Schmidt <sup>4</sup>, Corinna Dawid<sup>4</sup>, Tom Bennett <sup>3,5\*</sup>, Caroline Gutjahr <sup>1,2\*</sup>

**1** Faculty of Biology, Genetics, LMU Munich, Biocenter Martinsried, Martinsried, Germany, **2** Plant Genetics, TUM School of Life Sciences Weihenstephan, Technical University of Munich (TUM), Freising, Germany, **3** School of Biology, Faculty of Biological Sciences, University of Leeds, Leeds, United Kingdom, **4** Chair of Food Chemistry and Molecular Sensory Science, TUM School of Life Sciences Weihenstephan, Technical University of Munich (TUM), Freising, Germany, **5** Sainsbury Laboratory Cambridge University, Cambridge, United Kingdom

\* [t.a.bennett@leeds.ac.uk](mailto:t.a.bennett@leeds.ac.uk) (TB); [caroline.gutjahr@tum.de](mailto:caroline.gutjahr@tum.de) (CG)



 OPEN ACCESS

**Citation:** Villaécija-Aguilar JA, Hamon-Josse M, Carbonnel S, Kretschmar A, Schmidt C, Dawid C, et al. (2019) SMAX1/SMXL2 regulate root and root hair development downstream of KAI2-mediated signalling in Arabidopsis. *PLoS Genet* 15(8): e1008327. <https://doi.org/10.1371/journal.pgen.1008327>

**Editor:** Gloria K. Muday, Wake Forest University, UNITED STATES

**Received:** April 29, 2019

**Accepted:** July 22, 2019

**Published:** August 29, 2019

**Copyright:** © 2019 Villaécija-Aguilar et al. This is an open access article distributed under the terms of the [Creative Commons Attribution License](https://creativecommons.org/licenses/by/4.0/), which permits unrestricted use, distribution, and reproduction in any medium, provided the original author and source are credited.

**Data Availability Statement:** All relevant data are within the manuscript and its Supporting Information files.

**Funding:** This work was supported by the SFB924 TP B12 of the Deutsche Forschungsgemeinschaft (DFG, <https://www.dfg.de>) to CD, the BBSRC grant BB/R00398X/1 (<https://bbsrc.ukri.org>) to TB, and by the Emmy Noether program of the Deutsche Forschungsgemeinschaft (DFG, <https://www.dfg.de>) to CG (GU1423/1-1). The funders had no role

## Abstract

Karrikins are smoke-derived compounds presumed to mimic endogenous signalling molecules (KAI2-ligand, KL), whose signalling pathway is closely related to that of strigolactones (SLs), important regulators of plant development. Both karrikins/KLs and SLs are perceived by closely related  $\alpha/\beta$  hydrolase receptors (KAI2 and D14 respectively), and signalling through both receptors requires the F-box protein MAX2. Furthermore, both pathways trigger proteasome-mediated degradation of related SMAX1-LIKE (SMXL) proteins, to influence development. It has previously been suggested in multiple studies that SLs are important regulators of root and root hair development in Arabidopsis, but these conclusions are based on phenotypes observed in the non-specific *max2* mutants and by use of *racemic-GR24*, a mixture of stereoisomers that activates both D14 and KAI2 signalling pathways. Here, we demonstrate that the majority of the effects on Arabidopsis root development previously attributed to SL signalling are actually mediated by the KAI2 signalling pathway. Using mutants defective in SL or KL synthesis and/or perception, we show that KAI2-mediated signalling alone regulates root hair density and root hair length as well as root skewing, straightness and diameter, while both KAI2 and D14 pathways regulate lateral root density and epidermal cell length. We test the key hypothesis that KAI2 signals by a non-canonical receptor-target mechanism in the context of root development. Our results provide no evidence for this, and we instead show that all effects of KAI2 in the root can be explained by canonical SMAX1/SMXL2 activity. However, we do find evidence for non-canonical GR24 ligand-receptor interactions in D14/KAI2-mediated root hair development. Overall, our results demonstrate that the KAI2 signalling pathway is an important new regulator of root hair and root development in Arabidopsis and lay an important basis for research into a molecular understanding of how very similar and partially overlapping hormone signalling pathways regulate different phenotypic outputs.

in study design, data collection and analysis, decision to publish, or preparation of the manuscript.

**Competing interests:** The authors have declared that no competing interests exist.

### Author summary

Karrikins are plant signaling compounds from smoke, which induce germination of fire-following plants. They likely mimic endogenous plant hormones (KAI2-ligand, KL), because Arabidopsis karrikin receptor mutants display shoot developmental phenotypes. Perception of karrikins/KL is very similar to that of another plant hormone class, strigolactones (SLs). Both hormones bind to the related  $\alpha/\beta$ -fold hydrolase receptors KAI2 and D14 respectively, which both interact with the F-box protein MORE AXILLIARY BRANCHES2 (MAX2), for ubiquitylation and subsequent degradation of KL- or SL-signalling specific proteins of the SMXL family. Based on *max2* mutant phenotypes it has been suggested that the development of Arabidopsis root architecture and root hairs is regulated by SL signaling. However, *max2* does not distinguish between the two signalling pathways. We genetically dissected the role of KL and SL signalling in root and root hair development in Arabidopsis seedlings and show that most root traits are regulated by KL and not by SL signaling: lateral root density is controlled by KL and SL signalling together, while root growth direction, root straightness and root hair development are determined by KL signalling alone. Thus, KL signalling regulates vital plant traits for nutrient and water uptake as well as anchorage to the ground.

### Introduction

Plant roots continually integrate environmental information to make decisions about their development, and to optimize their growth for optimal nutrient uptake and anchorage. Increased lateral root formation and root hair growth are necessary to compensate for low nutrient availability in the soil by increasing the root surface area for nutrient uptake, while directional growth is required to avoid stressors such as salt, obstacles or to reach moisture [1–5]. Root development is regulated by a number of phytohormones, low-molecular-weight signalling molecules, which mediate localized developmental responses as well as transmission and integration of information across long distances. Among them, SLs have been suggested to act as important regulators of Arabidopsis seedling root architecture and root hair development [6–9]. However, the exact role of SLs in root development remains uncertain, due to interpretational difficulties inherent in the materials used by those studies, namely *max2* mutants and the synthetic strigolactone *racemic*-GR24 (see below, [10]).

Genes involved in SL biosynthesis have been identified in several plant species [10]. The universal SL precursor carlactone is synthesized from  $\beta$ -carotene by a core pathway of three enzymes; the isomerase DWARF27, and the carotenoid cleavage dioxygenases CCD7 and CCD8 (MAX3 and MAX4 in Arabidopsis) [11]. Carlactone is then modified by a variety of enzymes, including the cytochrome P450s of the MAX1 sub-family, to create a range of active SL molecules [12]. SLs are perceived and hydrolysed by the  $\alpha/\beta$  hydrolase receptor DWARF14 (D14) [13–16]. D14 interacts with the SCF<sup>MAX2</sup> E3 ubiquitin ligase complex to induce ubiquitylation and subsequent degradation of target proteins, essential to trigger SL signal transduction [15, 17].

A second, closely related signalling pathway also acts through the SCF<sup>MAX2</sup> complex [18, 19]. In this pathway MAX2 is thought to interact with KAI2 (KARRIKIN-INSENSITIVE2), an  $\alpha/\beta$  hydrolase receptor protein, which is encoded by an evolutionary older paralog of D14 [20–22]. KAI2 was originally identified as a receptor for karrikins, a family of butenolide compounds found in the smoke of burnt plant material [19, 23]. In fire-following species, karrikins

are used as germination cues, indicating the removal of competing plants. However, karrikins promote germination in a range of flowering plant species, which do not germinate after fire [24–26] and KAI2 is required for a number of developmental traits in Arabidopsis not related to germination as well as for arbuscular mycorrhiza symbiosis in rice [19, 27–30]. Because of these roles of KAI2, karrikins are thought to mimic the action of a yet unknown endogenous plant signalling molecule, which is currently denoted KAI2-ligand (KL) [31–33].

Since KAI2 and D14 act through the same F-box protein MAX2, *max2* mutants are insensitive to both SLs and karrikins, and display the combined phenotypes of *d14* and *kai2* mutants [18, 19, 27, 28]. Most studies aimed at understanding the role of SLs in Arabidopsis root development have used *max2* mutants—likely for historical reasons because they were available prior to *d14* and *kai2*. However, if only *max2* mutants are employed without comparison with the specific receptor mutants, the root phenotypes cannot be reliably attributed to either SL or KL signalling. The second difficulty in interpreting previously published root phenotypes arises from the experimental use of the strigolactone analog GR24, which in standard preparations is a racemic mix of two stereoisomers (*rac*-GR24). While one stereoisomer (GR24<sup>5DS</sup>) is a potent activator of D14 signalling, the non-natural stereoisomer (GR24<sup>ent-5DS</sup>) appears to stimulate KAI2 signalling [31, 34]. As such, the indiscriminate use of *rac*-GR24 has created a legacy of interpretational problems in previous studies, and incorrect attribution of phenotypic effects to SL signalling [10, 34].

Genetic and biochemical evidence indicates that the D14-SCF<sup>MAX2</sup> and the KAI2-SCF<sup>MAX2</sup> complex target a group of regulators—the SMXL (SMAX1-LIKE) family of proteins with weak homology to ClpB type chaperonins—for ubiquitylation and subsequent proteolytic degradation. In Arabidopsis, the genetically defined degradation targets of KL signalling are SMAX1 (SUPPRESSOR OF MAX2 1) and SMXL2, while the targets of SL signalling are SMXL6, SMXL7 and SMXL8 (hereafter SMXL678) [27, 35–37]. In the shoot, the hormone-induced turnover of SMXL678 proteins is key to correctly shaping shoot architecture [38]. The exact molecular function of the SMXL proteins is poorly understood. SMXL678 and their rice ortholog *D53* have been associated with transcriptional regulation, since they physically interact with TOPLESS-RELATED (TPR) co-repressor proteins [27, 39, 40]. Rice *D53* interacts with IPA1, a SQUAMOSA PROMOTER-BINDING FAMILY LIKE (SPL) transcription factor in the regulation of shoot branching and may recruit TPR to repress IPA1-mediated transcription [41]. However, they have also been found to be involved in enhancing PIN1 accumulation at the basal membrane of stem xylem parenchyma cells and auxin transport [38]. The role of SMXL proteins in root and root hair development has not been comprehensively addressed. Initial observations suggested mutations of *SMXL678* suppress the enhanced lateral root density phenotype of *max2* [27], while unexpectedly the increased root skewing phenotype, recently described for *kai2* and *max2* mutants was also suppressed by *smxl678* [29]. These data have been used to propose the existence of non-canonical D14/KAI2 signalling cascades in the context of lateral root development and root skewing [10, 29].

In this study, we dissected the roles of SLs and KLs in the control of root development in Arabidopsis. We aimed to test the important hypothesis that root development might be mediated by non-canonical receptor-target interactions between D14, KAI2 and SMAX1/SMXL2, SMXL678. Our results show that KAI2 is much more important than previously realized in the regulation of root development, and that many effects previously attributed to SL signalling are actually mediated by KAI2 (and therefore KL signalling). We find no evidence for non-canonical receptor-target interactions, but conversely find surprising evidence of non-canonical GR24 ligand-receptor interactions in both KAI2 and D14 signalling.

## Results

### Strigolactones have relatively minor effects on seedling root architecture

SLs have previously been described to regulate primary root length (PRL), lateral root density (LRD) and root hair development [6, 8, 9, 42]. We re-assessed the specific roles of SL signalling in root development in mutants specifically affected in SL biosynthesis, namely the SL biosynthesis mutants *max3-9*, *max4-5* and *max1-1* (here arranged in pathway order). Surprisingly, we found that SLs only have subtle effects on root architecture. We observed decreased primary root length (PRL) and increased lateral root density (LRD) in SL biosynthesis mutants across many experiments, but rarely at the same time (summarized in [S1 Fig](#)). For instance, [Fig 1A](#) shows reduction in PRL relative to Col-0 in all SL biosynthesis mutants, but in the same experiment LRD was not altered ([S1 Fig](#)). Conversely, [Fig 1B](#) shows increased LRD in SL biosynthesis mutants relative to Col-0, but PRL was not altered in the same experiment ([S1 Fig](#)). Thus, consistent with previous reports [8], we found that SL signalling has subtle, and possibly mutually exclusive, effects on PRL and LRD of Arabidopsis, which appear to be sensitive to small differences in growth conditions.

We also examined root hair formation in the suite of SL biosynthesis mutants. Contrary to previous assumptions [7] we found that neither root hair density (RHD) nor root hair length (RHL) are altered in any of the SL biosynthesis mutants ([Fig 2A, 2C and 2D](#)). Thus, the previously observed root hair phenotypes of *max2* mutants must be caused by defects other than SL signalling, for example in KL signalling.

### D14 and KAI2 co-regulate lateral root density

The phenotypes present in SL-specific biosynthesis mutants are insufficient to account for previously described effects of *max2* on root development. We therefore hypothesized that KAI2 signalling may play an important role in the regulation of root and root hair development, and we therefore compared and contrasted root development in *d14* and *kai2* mutants. In the case of LRD, we observed that *d14-1* causes increased LRD and/or reduced PRL, consistent with the phenotypes of SL biosynthesis mutants ([Fig 1A–1D](#)). We also observed that two allelic *kai2* mutants (*kai2-1*, *kai2-2*) in the Col-0 background, showed increased LRD of around the same magnitude as *d14-1* ([Fig 1D, S2A Fig](#)), with no clear effect on PRL ([Fig 1C](#)). This phenotype in *kai2* was particularly evident at 6dpg, and became less evident at later time points. For *d14*, the opposite pattern was seen, and the LRD phenotype only became evident at later time points ([Fig 1D, S2B Fig](#)). Thus, at least some of the confusion about the role of these pathways in regulation of lateral root development may result from the staging of experiments. Taken together, our results suggest that both SL and KL signalling regulate LRD in Arabidopsis. We further tested this idea by examining LRD in *d14 kai2* double mutants. The *d14-1 kai2-2* mutant showed a very strong and consistent increase in LRD in comparison to Col-0, *d14-1* and *kai2-2* ([Fig 1D, S2B Fig](#)). The increase in LRD was always greater in *d14-1 kai2-2* than in the single mutants ([Fig 1D](#)). Thus, both KL and SL signalling regulate LRD in an additive manner, possibly by affecting lateral root development at different developmental stages and time points.

### KAI2 but not D14 regulates root hair development

Given the lack of root hair phenotype in SL biosynthesis mutants, we hypothesized that KAI2 and not D14 signalling would regulate root hair development. Consistent with this hypothesis, we observed no RHD or RHL phenotype in *d14-1* ([Fig 2B–2F](#)). Conversely, RHD and RHL were strongly decreased in two allelic *kai2* mutants in Col-0 as well as Ler, and they perfectly

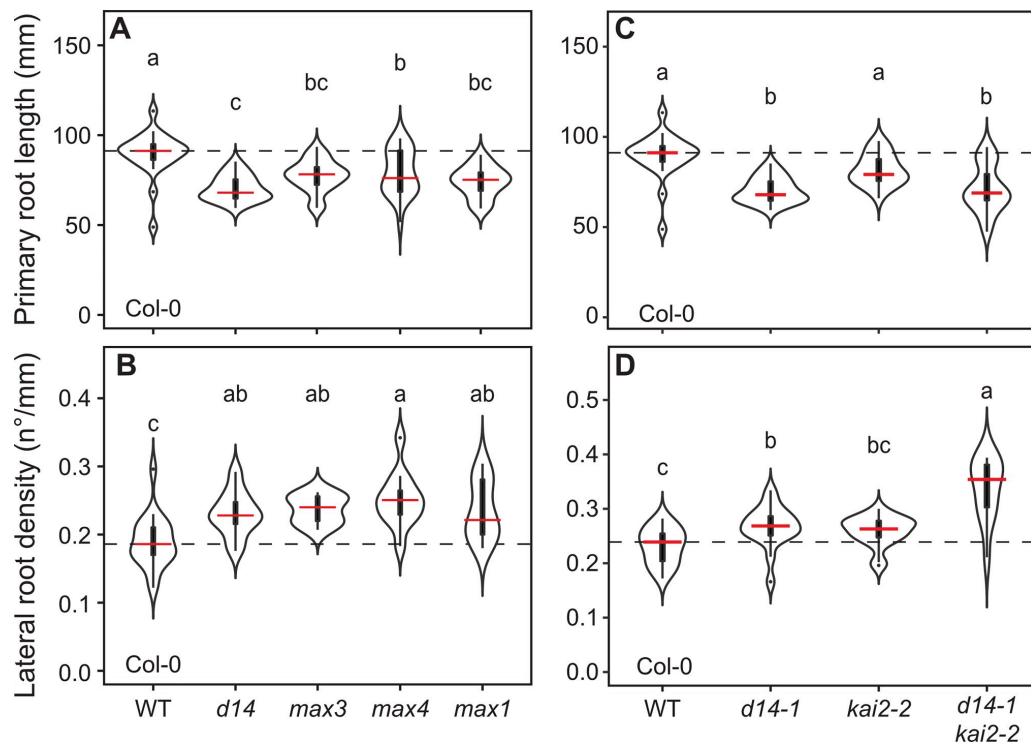


**Fig 1. SL and KL signalling additively regulate lateral root density.** (A) Primary root length (experiment 3 in S1 Fig) and (B) lateral root density (experiment 1 in S1 Fig) of Col-0 wild type, the strigolactone perception mutant *d14-1* and the strigolactone biosynthesis mutants *max3-9*, *max4-5* and *max1-1* (arranged in pathway order). (C) Primary root length and (D) lateral root density in the *d14-1 kai2-2* double mutant and the respective single mutants. Data in (C) form part of the same dataset in (A), and PRL for the Col-0 and *d14-1* genotypes are also shown in (A). LRD was recorded at 10 dpf. The outline of the violin plots represents the probability of the kernel density. Black boxes represent interquartile ranges (IQR), with the red horizontal line representing the median; whiskers extend to the highest and lowest data point but no more than  $\pm 1.5$  times the IQR from the box; outliers are plotted individually. Different letters indicate different statistical groups (ANOVA, posthoc Tukey,  $p \leq 0.001$  (A)  $F_{4,111} = 11.81$ ,  $n = 19-25$  (B)  $F_{4,58} = 5.626$ ,  $n = 8-18$  (C)  $F_{3,88} = 17.83$ ,  $n = 21-26$  (D)  $F_{3,63} = 19.82$ ,  $n = 11-18$ ).

<https://doi.org/10.1371/journal.pgen.1008327.g001>

phenocopied the root hair phenotype of *max2* mutants (Fig 2B, 2E–2H). Thus, the root hair phenotypes previously observed in *max2* mutants and attributed to the lack of SL signalling are actually caused by a lack of KL signalling. To confirm this, we assessed whether root hair development can be influenced by exogenous addition of karrikin. Treatment with  $1 \mu\text{M}$  KAR<sub>2</sub> increased RHD and RHL relative to control treatments in a KAI2 and MAX2-dependent manner (Fig 2G and 2H), corroborating the role of KL-signalling in promoting root hair development.

### KAI2 signalling regulates root skewing and waving

In addition to lateral root and root hair phenotypes, we observed that *kai2* mutants display increased skewing along the surface of vertically-oriented agar plates, in the Col-0 and in the Ler ecotype (Fig 3A–3D, S3 Fig), consistent with a recent report that described this phenotype in *kai2* mutants in Ler [29]. This right-handed skewing is a well-established effect of growing *Arabidopsis* roots on the surface of agar plates, and probably arises from a combination of

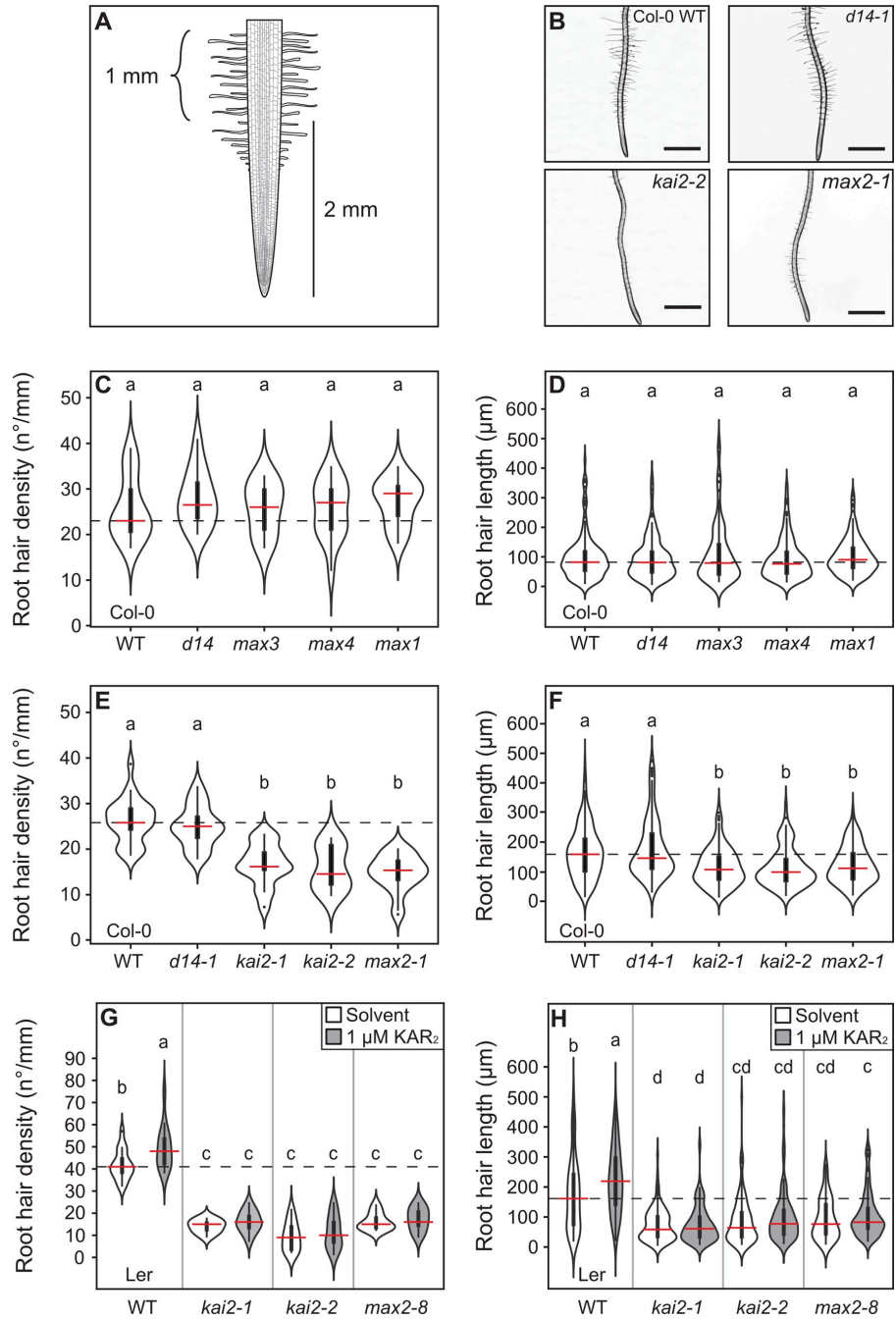


**Fig 2. KL perception mutants are impaired in root hair development.** (A) Diagram showing the primary root zone used for root hair phenotyping (curly bracket). Root hair density and length were quantified in 1 mm primary root length between 2 and 3 mm from the root tip. (B) Representative images of root hair phenotypes of the indicated genotypes. Scale bar, 1 mm. (C,E,G) Root hair density and (D,F,G) root hair length in (C,D) Col-0 wild type, the strigolactone perception mutant *d14-1* and the strigolactone biosynthesis mutants *max3-9*, *max4-5* and *max1-1* (arranged in pathway order), (E,F) the indicated karrikin perception mutants and (G,H) Ler wild type and indicated karrikin perception mutants, treated with solvent (70% Methanol) or 1  $\mu$ M KAR<sub>2</sub>. The outline of the violin plots represents the probability of the kernel density. Black boxes represent interquartile ranges (IQR), with the red horizontal line representing the median; whiskers extend to the highest and lowest data point but no more than  $\pm 1.5$  times the IQR from the box; outliers are plotted individually. Different letters indicate different statistical groups (ANOVA, posthoc Tukey, (C)  $F_{4,65} = 0.242$ ,  $n = 10-18$ ;  $p \leq 0.05$ , (D)  $F_{4,718} = 1.291$ ,  $n = 10-13$ ,  $p \leq 0.05$ , (E)  $F_{4,88} = 28.9$ ,  $n = 11-24$ ,  $p \leq 0.001$ , (F)  $F_{4,825} = 23.43$ ,  $n = 10-13$ ,  $p \leq 0.001$ , (G)  $F_{7,96} = 60.79$ ,  $n = 10-15$ ,  $p \leq 0.001$ , (H)  $F_{7,975} = 45.39$ ,  $n = 10-13$ ,  $p \leq 0.001$ ).

<https://doi.org/10.1371/journal.pgen.1008327.g002>

circumnutation and thigmotropic responses [43, 44]. Increased skewing is also observed for *max2* mutants, but not for SL biosynthesis mutants, nor *d14* (Fig 3B and 3C; S3A Fig). The skewing phenotype of the *d14-1 kai2-2* double mutant in the Col-0 background is equal to *kai2-2* (Col-0), confirming that SL perception is not involved in regulating root growth direction (Fig 3C).

The increased skewing in the *kai2* and *max2* mutants is accompanied by increased root waving, which is displayed as a decrease in root 'straightness' (Fig 3A, 3E and 3F, S3B Fig). Again, this waving phenotype is not observed in *d14-1* or SL biosynthesis mutants (Fig 3E, S3B Fig). The waving phenotype is separable from the skewing phenotype, and growth on plates inclined at 45° generally increases waving relative to plates grown at 90°, while altering skewing only in the Ler but not in the Col-0 wild type (S3C–S3G Fig).

### KAI2 regulates skewing independently of epidermal cell elongation and root diameter

Skewing is often associated with epidermal cell file rotation [44]. To determine whether skewing of *kai2* and *max2* mutants is associated with cell file rotation [45], we inspected epidermal cells between 2 and 3mm above the root tip in *kai2* mutants. Cell length was reduced in *kai2* and *max2* mutants relative to wild-type in both Col-0 and Ler backgrounds (with a concomitant increase in cells/mm) (Fig 4A and 4C, S4A and S4C Fig). However, a careful microscopic inspection of the root surface of *kai2* and *max2* mutants did not show any signs of epidermal cell file rotation, instead they were clearly vertically orientated (Fig 4B, S4B Fig). This is in contrast to the results of [29], who observed increased cell file rotation in *kai2* and *max2* mutants in Ler at a 45° growth angle. Since at a 90° growth angle we observed a skewing phenotype but no cell file rotation, we conclude that there is likely no connection between any cell file rotation phenotype in KL perception mutants and their skewing phenotype. Interestingly, also the SL perception mutant *d14* displayed the short epidermal cell phenotype but had no skewing phenotype, clearly demonstrating that there is no connection between epidermal cell length and skewing in these receptor mutants (Fig 4A and 4C; S4A and S4C Fig).

It has also been speculated that a smaller root cell diameter in *kai2* mutants may cause tissue tensions leading to skewing [29]. We also observed that *kai2* mutants in both the Col-0 and Ler background had thinner primary roots than wild-type. Quantification of root diameter at 2.5 mm above the root tip confirmed that the primary roots of *kai2* and *max2* mutants but not of the *d14* mutant are thinner than those of the wild type (Fig 4D, S4D Fig). This indicates that the regulation of root thickness is specific to KL signalling. However, we could genetically separate the thin root diameter from the skewing and waving phenotypes because the root diameter phenotype of *max2* could be suppressed by *smax1* without altering the waving phenotypes. Conversely, the *max2* root diameter phenotype could not be suppressed by *smxl2* alone, but

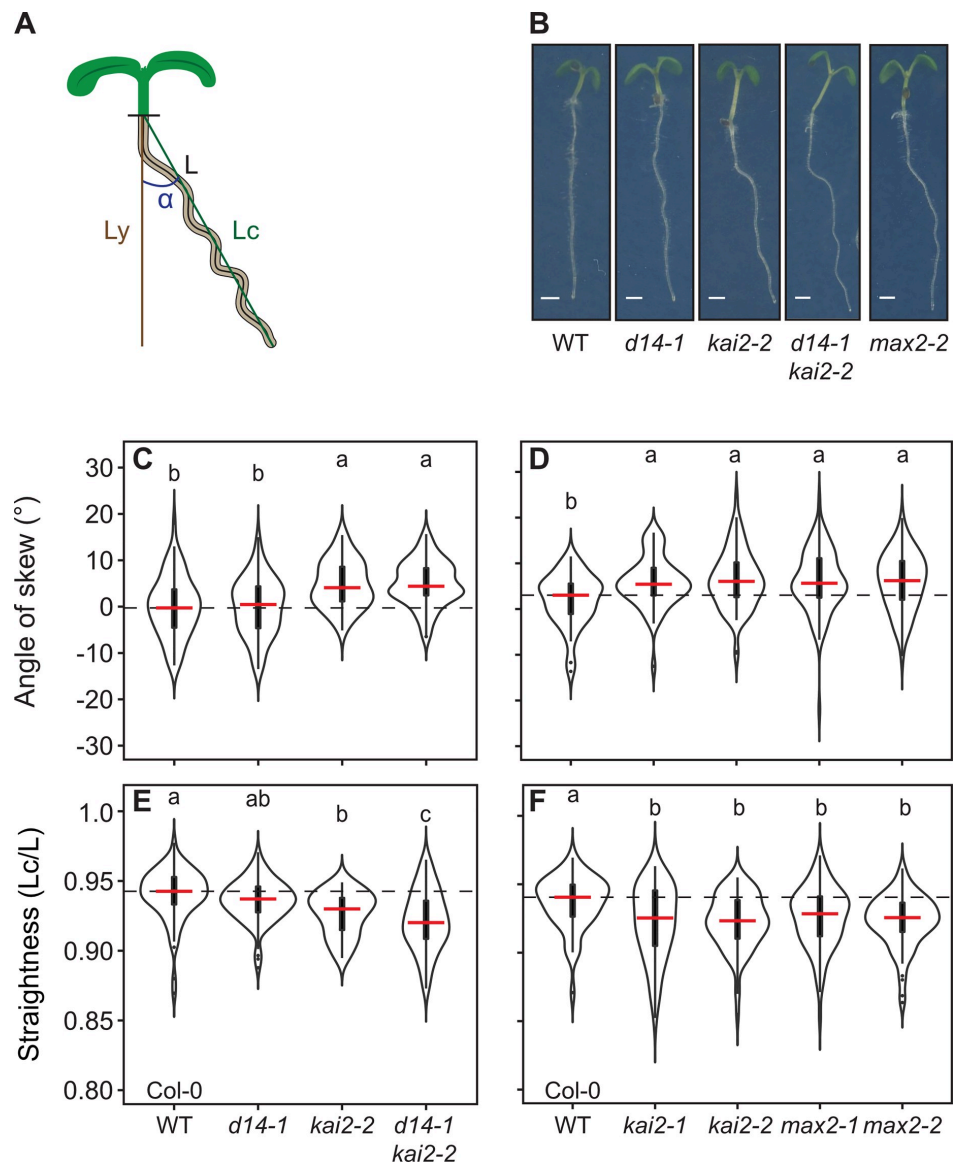


**Fig 3. KL perception mutants display exaggerated skewing and waving.** (A) Diagram showing how skewing-angle and root straightness were determined. Skewing was quantified by measuring the angle between the vertical axis (*Ly*) defined as 0°, and the root tip. Right or left skewing is indicated by positive or negative values, respectively. Straightness was calculated as the ratio of the straight line between the hypocotyl-root junction and the root tip (green line, *Lc*) and the total root length (*L*). (B) Images of representative 5-days-old seedlings of the indicated genotypes. Scale bars, 1 mm. (C, D) Root skewing and (E and F) root straightness of the indicated genotypes. The outline of the violin plot represents the probability of the kernel density. Black boxes represent interquartile ranges (IQR), the red horizontal line representing the median; whiskers extend to the highest and lowest data point but no more than  $\pm 1.5$  times the IQR from the box; outliers are plotted individually. Different letters indicate different statistical groups (ANOVA, posthoc Tukey,  $p \leq 0.001$ , (C)  $F_{3,315} = 16.08$ ,  $n > 60$  (D)  $F_{4,347} = 4.762$ ,  $n > 50$  (E)  $F_{3,315} = 13.62$ ,  $n > 60$  (F)  $F_{4,347} = 4.28$ ,  $n > 50$ ).

<https://doi.org/10.1371/journal.pgen.1008327.g003>

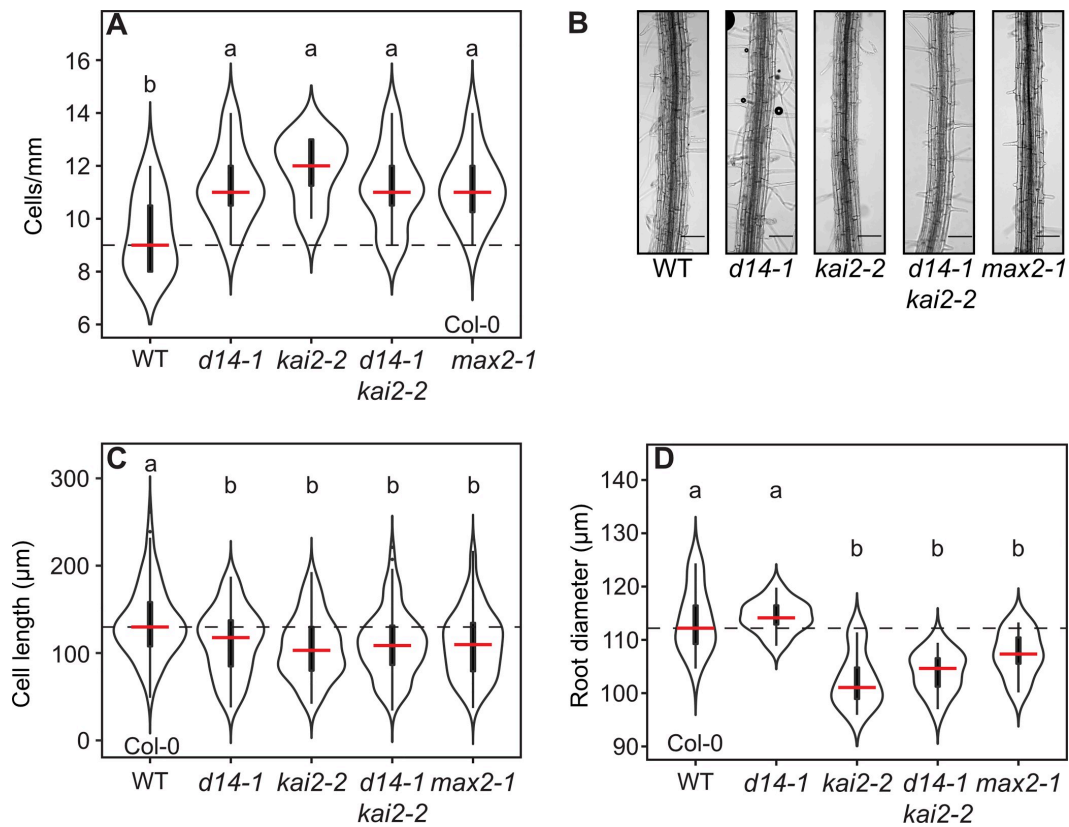


**Fig 4. KL perception mutants exhibit decreased epidermal cell lengths and root diameter.** (A) Number of root epidermal cells per mm of the indicated genotypes. (B) Images of representative roots between 2 and 3 mm from the root tip of 5-days-old seedlings of the indicated genotypes. Scale bars, 0.1 mm. (C) Root cell length and (D) root diameter of the indicated genotypes. The outline of the violin plots represents the probability of the kernel density. Black boxes represent interquartile ranges (IQR), the red horizontal line representing the median; whiskers extend to the highest and lowest data point but no more than  $\pm 1.5$  times the IQR from the box; outliers are plotted individually. Different letters indicate different statistical groups (ANOVA, posthoc Tukey, (A)  $F_{4,52} = 4.715$ ,  $n = 9-13$ ,  $p \leq 0.01$ , (C)  $F_{3,392} = 10.64$ ,  $n = 10-11$ ,  $p \leq 0.001$ , (D)  $F_{4,50} = 15.95$ ,  $n = 10-12$ ,  $p \leq 0.001$ ).

<https://doi.org/10.1371/journal.pgen.1008327.g004>

*smxl2* was sufficient to suppress the skewing phenotype (Fig 5A and 5C; S5A and S5C Fig).

Thus, decreased root diameter is unlikely to cause the skewing and waving phenotypes in *kai2* and *max2* as previously suggested [29].

### KAI2 regulates skewing and waving through SMAX1/SMXL2

The mechanism by which KAI2 regulates root skewing has been proposed to include the non-canonical degradation of SMXL678 [29]. We tested this important hypothesis in more detail, by using different combinations of *smxl* alleles. We observed that, for skewing, *smxl1* or *smxl2* were both independently sufficient to suppress the *max2* phenotype (Fig 5A and 5B, S1 Table), indicating that skewing may be very sensitive to the stoichiometry of SMXL proteins or that SMAX1 and SMXL2 act in different cells. *smxl1* and *smxl2* could not suppress the *max2* waving phenotype individually, but in combination they were able to completely suppress this

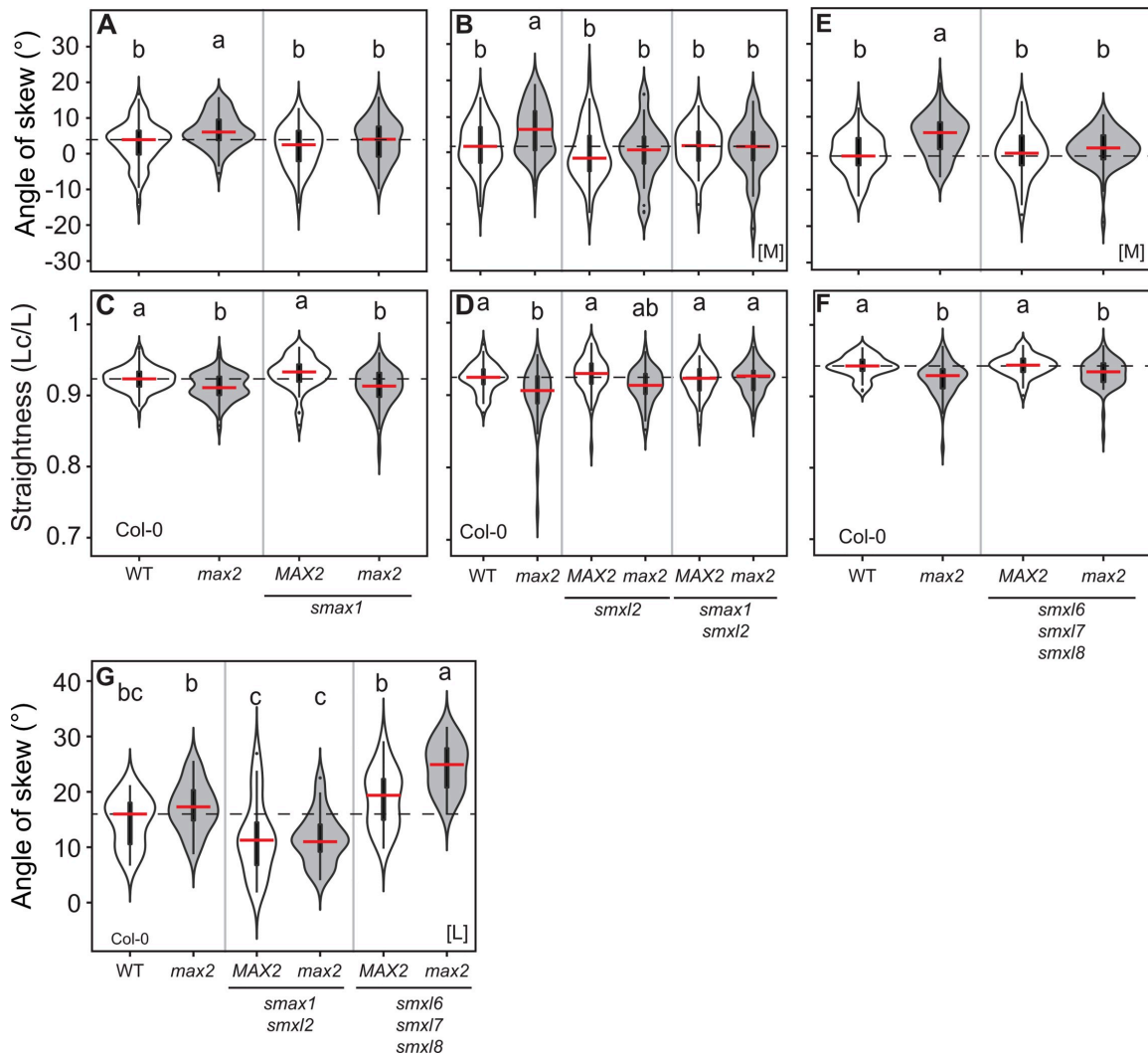


**Fig 5. SMXL1 and SMXL2 regulate skewing and root straightness.** (A, B, E, F) Root skewing and (C, D, G) root straightness in Col-0 wild type and the indicated genotypes (the mutant alleles are *max2-1*, *smxl1-2*, *smxl2-1*, *smxl6-4*, *smxl7-3* and *smxl8-1*). The outline of the violin plot represents the probability of the kernel density. Black boxes represent interquartile ranges (IQR), with the red horizontal line representing the median; whiskers extend to the highest and lowest data point but no more than  $\pm 1.5$  times the IQR from the box; outliers are plotted individually. Different letters indicate different statistical groups (ANOVA, posthoc Tukey,  $p \leq 0.001$ ) (A)  $F_{3,345} = 7.612$ ,  $n > 60$ ; (B)  $F_{5,259} = 5.051$ ,  $n > 30$ ; (C)  $F_{3,440} = 16.32$ ,  $n > 60$ ; (D)  $F_{5,261} = 6.57$ ,  $n > 30$  (E)  $F_{3,209} = 8.784$ ,  $n > 45$  (F)  $F_{3,209} = 10.22$ ,  $n > 45$ ; (G)  $F_{5,127} = 21.07$ ,  $n = 21$ ). [M] = experiment performed in Munich, [L] = experiment performed in Leeds.

<https://doi.org/10.1371/journal.pgen.1008327.g005>

phenotype (Fig 5C and 5D, S1 Table), indicating that SMXL1 and SMXL2 act redundantly to promote waving. These results are thus consistent with SMXL1 and SMXL2 acting genetically downstream of KAI2 and MAX2 to regulate root growth patterns. Notably, the effect of *kai2*,

*smx1* and *smx2* on skewing was consistent between plants grown in Munich [M] and Leeds [L].

Consistent with the results of [29], we observed a reduction in skewing in *smxl678 max2-1* relative to *max2-1* in plants grown in Munich [M] (Fig 5E). However, this was not the case in Leeds [L], where root skewing was often increased in *smxl678* relative to wild-type, and in which there was an additive increase in skewing in *smxl678 max2-1* (Fig 5G). We also did not observe any suppression of the *max2-1* waving phenotype in *smxl678* (Fig 5F). Thus, our analysis of *smxl678* mutants indicates that SMXL678 proteins likely do not act downstream of KAI2/MAX2 in the regulation of root growth patterns, but rather, that SMXL678 regulates skewing in parallel to the KAI2-SMAX1/SMXL2 pathway.

### SMAX1, SMXL2 as well as SMXL678 regulate lateral root density

Previous results showed that the *max2* LRD phenotype was suppressed in a *smxl678* background but not in a *max1* background [27], suggesting that the *max2* LRD phenotype arises solely from excess SMXL678 protein accumulation. Since our results show that both D14 and KAI2 regulate LRD, this would again imply non-canonical regulation of SMXL678 by KAI2. To again test this hypothesis, we re-examined the regulation of LRD using more recently-available *smx1 smx2* double mutants [35]. We found that *smx1 smx2* was as efficient in reducing LRD of *max2* as *smxl678* (Fig 6). However, consistent with a role of both SL and KL signalling in regulating LRD neither *smx1 smx2* nor *smxl678* appeared to be completely epistatic to *max2* (Fig 6). The most parsimonious explanation for these results is that the *max2* LRD phenotype arises from the accumulation of both SMAX1/SMXL2 and SMXL678, and that SL and KL signalling act together in the regulation of LR development by their canonical pathways: SL signalling by promoting SMXL678 turnover, and KL signalling by promoting SMAX1 SMXL2 turnover.

### SMAX1 and SMXL2 but not SMXL678 regulate root hair development

We also assessed, whether regulation of RHD and RHL by KAI2 occurs through canonical or non-canonical signalling. For both RHD and RHL, we found that *smx1 smx2* have increased RHD and RHL, and are epistatic to *max2-1* in both of these phenotypes. *smx2* but not *smx1* single mutants display an increased RHL with respect to the wild type, suggesting that SMXL2 may be more important in regulating RHL than SMAX1. Conversely, *smxl678* mutants have no RHD or RHL phenotype, and no effect on the *max2* phenotype (Fig 7A–7F). This is consistent with our observation that *kai2* and not *d14* phenocopies the root hair phenotype of *max2* and that root hair development is regulated by KL signalling under standard conditions.

### The stereoisomers GR24<sup>5DS</sup> and GR24<sup>ent-5DS</sup> non-specifically enhance root hair development through both D14 and KAI2

As a final test for non-canonical signalling in root development, we examined ligand-receptor interactions, using the easily scorable, karrikin-responsive root hair phenotypes as a system. Exogenous application of *rac*-GR24 was previously shown to promote root hair elongation [7, 42]. In light of the effects of KAI2 mutations on root hair development, we hypothesized that *rac*-GR24, and in particular the GR24<sup>ent-5DS</sup> stereoisomer, would modulate RHD and RHL, in a manner dependent on KAI2 [34]. Similar to KAR<sub>2</sub>, *rac*-GR24 treatment increased both RHD and RHL in Col-0 (Fig 8A and 8B), and this effect was dependent on MAX2 as previously reported [7, 42]. However, unexpectedly, it was independent of KAI2, suggesting that *rac*-GR24 might promote RHD and RHL via D14 (Fig 8A and 8B). We assessed this in detail and quantified RHD and RHL after treatment with the pure stereoisomers GR24<sup>5DS</sup> and

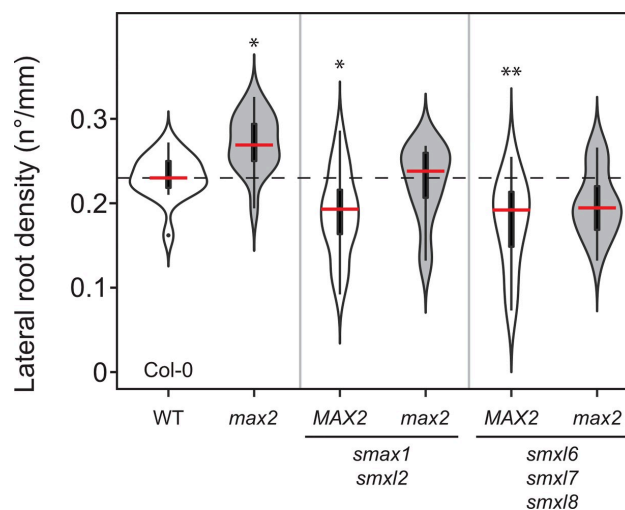


**Fig 6. Lateral root density is regulated by both SMAX1/SMXL2 and SMXL678.** Lateral root density in Col-0 wild type and the indicated genotypes (the mutant alleles are *max2-1*, *smax1-2*, *smxl2-1*, *smxl6-4*, *smxl7-3* and *smxl8-1*). The outline of the violin plots represents the probability of the kernel density. Black boxes represent interquartile ranges (IQR), with the red horizontal line representing the median; whiskers extend to the highest and lowest data point but no more than  $\pm 1.5$  times the IQR from the box; outliers are plotted individually. Asterisks indicate a significant difference with wild type (ANOVA, posthoc Dunnett's test comparing to wild-type,  $F_{5,90} = 10.62$ ,  $n = 10-17$ ; \*  $p \leq 0.05$ , \*\*  $p \leq 0.01$ , \*\*\*  $p \leq 0.001$ ).

<https://doi.org/10.1371/journal.pgen.1008327.g006>

GR24<sup>ent-5DS</sup>, which are thought to specifically activate D14 and KAI2, respectively [34]. We observed that both GR24<sup>5DS</sup> and GR24<sup>ent-5DS</sup> promote RHD and RHL in the wild-type, but their effects in *d14* and *kai2* mutants were intriguingly divergent from expectations. In *d14-1*, only GR24<sup>ent-5DS</sup> promotes RHD (as expected), but both GR24<sup>5DS</sup> and GR24<sup>ent-5DS</sup> promote RHL to a similar degree in *kai2*, suggesting that both can be perceived by KAI2 to promote RHL (Fig 3A and 3B). Furthermore, both stereoisomers cause increased RHD and RHL in *kai2-2*, although the 'canonical' D14 ligand GR24<sup>5DS</sup> has a significantly stronger effect than GR24<sup>ent-5DS</sup> (Fig 8A and 8B). Neither stereoisomer promoted RHD and RHL in the *d14-1 kai2-2* double and *max2-1* mutants (Fig 8), confirming that no additional unknown receptor is involved in the response to *rac*-GR24. The first major implication of these results is that D14 can act to promote root hair development, when stimulated with ligand, even if that is not the standard function of D14 (Fig 2). The second major implication is that in roots, contrary to previous suggestions for the regulation of Arabidopsis hypocotyl elongation [34], D14 can perceive GR24<sup>ent-5DS</sup> ligands when KAI2 is absent, and KAI2 can perceive GR24<sup>5DS</sup> ligands when D14 is absent.

Since these results are unexpected we wondered whether the GR24 stereoisomers we used are really pure and determined their purity by nuclear magnetic resonance (NMR), circular dichroism (CD) spectroscopy and polarimetry (S6 Fig). Both <sup>1</sup>H-NMR, <sup>13</sup>C-NMR and CD as well as rotation values determined by means of polarimetric measurements confirmed the purity of the compounds and recapitulated previously published NMR- and CD-spectra for (+)-5-Desoxystrigol and (-)-ent-5-Desoxystrigol [46, 47]. Since the stereoisomers are pure, we conclude that they do not specifically act through KAI2 or D14 but that both molecules can bind to and trigger both receptors in the context of root hair development.

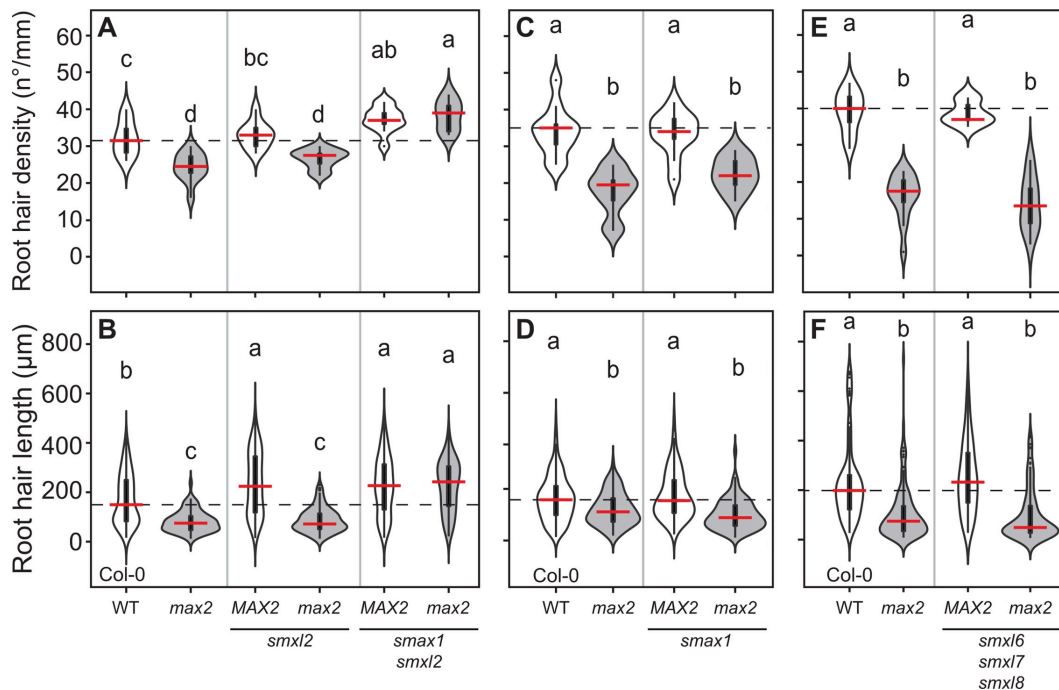


**Fig 7. SMAX1 and SMXL2 regulate root hair development.** (A, C, E) Root hair density and (B, D, F) root hair length in Col-0 wild type and the indicated genotypes (the mutant alleles are *max2-1*, *smax1-2*, *smxl2-1*, *smxl6-4*, *smxl7-3* and *smxl8-1*). The outline of the violin plot represents the probability of the kernel density. Black boxes represent interquartile ranges (IQR), with the red horizontal line representing the median; whiskers extend to the highest and lowest data point but no more than  $\pm 1.5$  times the IQR from the box; outliers are plotted individually. Different letters indicate different statistical groups (ANOVA, posthoc Tukey,  $p \leq 0.001$ ) (A)  $F_{17,385} = 79.17$ ,  $n = 9-13$  (B)  $F_{3,44} = 67.45$ ,  $n = 9-11$  (C)  $F_{3,39} = 20.33$ ,  $n = 9-11$  (D)  $F_{3,615} = 30.02$ ,  $n = 9-11$  (E)  $F_{3,44} = 67.45$ ,  $n = 9-15$  (F)  $F_{3,410} = 38.66$ ,  $n = 8-11$ ).

<https://doi.org/10.1371/journal.pgen.1008327.g007>

Previous Arabidopsis hypocotyl elongation assays suggested specific roles of GR24<sup>5DS</sup> and GR24<sup>ent-5DS</sup> in triggering D14- vs KAI2-mediated signalling respectively because GR24<sup>5DS</sup> suppressed hypocotyl elongation specifically in *kai2* mutants and GR24<sup>ent-5DS</sup> in *d14* mutants [34]. We re-examined the effects of the GR24 stereoisomers on hypocotyl elongation (S7 Fig). Similar to root hair elongation and contrary to a previous report [34] the *d14-1* mutant responds equally to GR24<sup>5DS</sup> and GR24<sup>ent-5DS</sup> with a decrease in hypocotyl growth, showing that in the hypocotyl KAI2 can mediate responses to both molecules. The *kai2-1* mutant also responds to both molecules but to a lesser extent to GR24<sup>ent-5DS</sup>, suggesting together with the above results that D14 is more effective in mediating responses to its previously suggested ligand GR24<sup>5DS</sup> than to GR24<sup>ent-5DS</sup> [34]. Similar to root hair development, the *d14-1 kai2-2* double mutant and the *max2-1* mutant do not respond to any molecule in this assay, confirming that in the hypocotyl response to the GR24 stereoisomers no additional receptor is involved. In summary, we show that GR24<sup>5DS</sup> and GR24<sup>ent-5DS</sup> can activate both signalling through KAI2 and through D14 in the regulation of RHL as well as hypocotyl elongation.

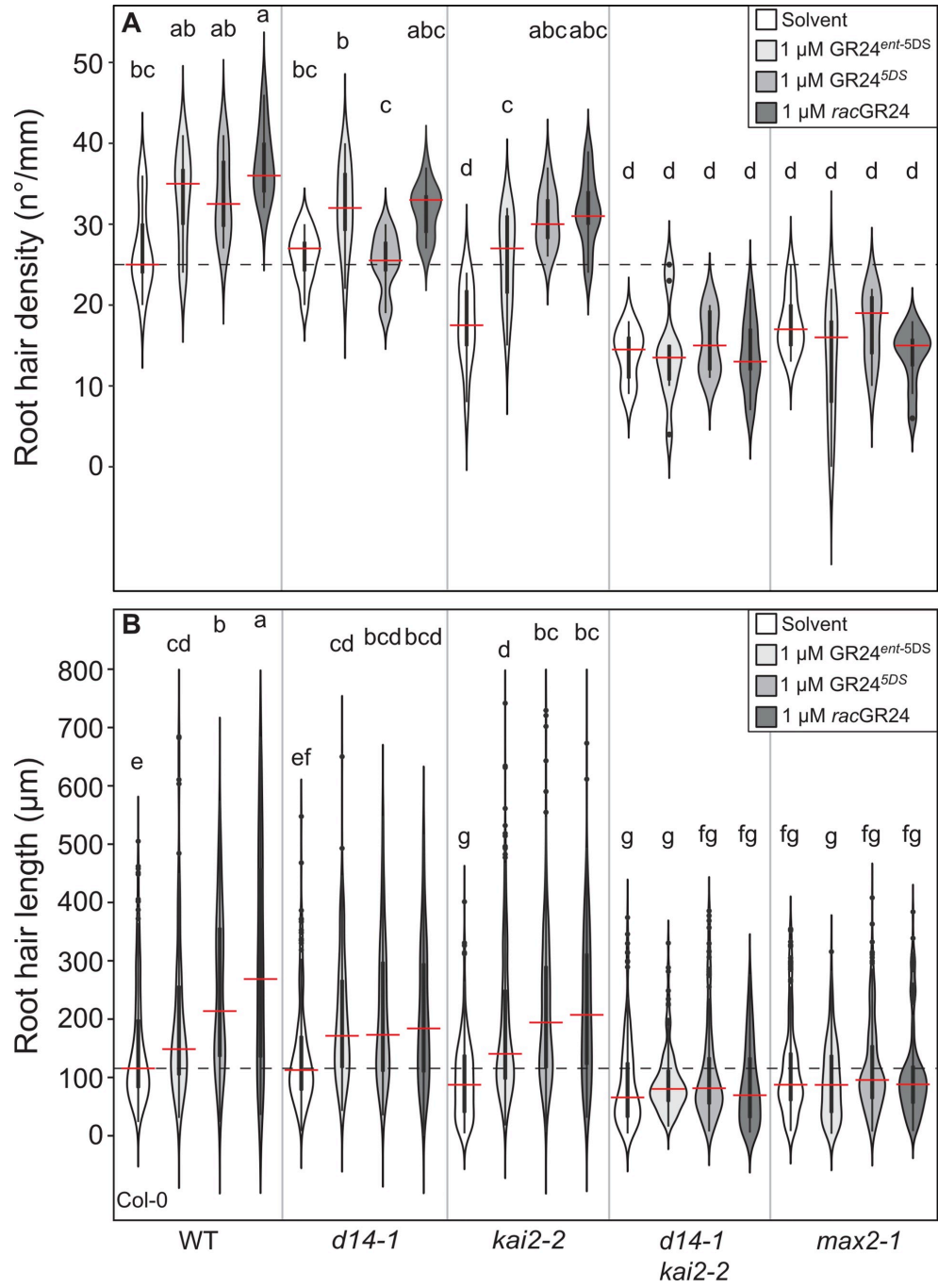


**Fig 8. The two GR24 stereoisomers regulate root hair development through both D14 and KAI2.** (A) Root hair density and (B) root hair length of the indicated genotypes treated with solvent (acetone), 1  $\mu$ M GR24<sup>ent-5DS</sup>, 1  $\mu$ M GR24<sup>5DS</sup> or 1  $\mu$ M rac-GR24. The outline of the violin plot represents the probability of the kernel density. Black boxes represent interquartile ranges (IQR), with the red horizontal line representing the median; whiskers extend to the highest and lowest data point but no more than  $\pm 1.5$  times the IQR from the box; outliers are plotted individually. Different letters indicate different statistical groups (ANOVA, posthoc Tukey,  $n = 8-11$  (A)  $F_{19,3740} = 1.983$ ;  $p \leq 0.01$  (B)  $F_{19,3740} = 57.83$ ,  $p \leq 0.001$ ).

<https://doi.org/10.1371/journal.pgen.1008327.g008>

## Discussion

Root systems flexibly adapt their architecture and morphology to heterogeneous soil environments and to the physiological needs of the plant. A network of plant hormone signalling pathways is essential for translating environmental signals and physiological states into developmental outputs [48]. Strigolactones (SLs) have been assumed to play an important role in modulating root development [7–9]. Here we demonstrate that under standard growth conditions KL signalling plays a much larger role than SL signaling in shaping root and root hair development (Fig 9).

### KL signalling regulates lateral root density together with SL signalling

Previous reports showed increased LRD in *max2* and suppression of lateral root emergence by *rac-GR24* [8, 9]. Our study indicates that these effects are mediated through both the KAI2 and D14 signalling pathways, in an additive manner. We observed that lateral root density (LRD) is consistently higher in *kai2* mutants than wild type (particularly at earlier time points). We found SL biosynthesis and perception mutants also displayed subtle changes in root architectural parameters, such as primary root length (PRL) and LRD. In a range of experiments with SL mutants, we either observed strongly decreased PRL or strongly increased LRD, but not both phenotypes together. This suggests that the effects of SL signalling on PRL or LRD are to some extent mutually exclusive, and that expression of one phenotype reduces expression of the other, which may explain some of the previous contradictory reports regarding effects of SLs on root development [8, 9]. We also found that the time after germination matters for the LRD phenotypes. Thus, confusion about the role of SLs in LR development may also reflect differences in the physiological timing of observations within experiments. The *d14 kai2* double mutant showed a much larger increase in LRD compared to the single mutants, indicating that both signalling pathways contribute additively to modulating LRD, and that previously reported *max2* phenotypes reflect a lack of both signalling pathways. This is further supported by suppression of the *max2* LRD phenotype by mutants in both the targets of KL signalling (SMAX1/SMXL2) and SL signalling (SMXL678).

### KL signalling is a key regulator of root hair development

A major finding of our work is the important role of KL signalling in root hair development. Root hair density (RHD) and root hair length (RHL) are strongly reduced in *kai2* and *max2* mutants and increased in *smx1 smxl2* mutants, as well as by karrikin treatment of wild type roots. Our results thus present compelling evidence that KL signalling is a key regulator of root hair development. KAI2 being a major regulator of root hair development rather than D14 seems to make sense from an evolutionary point of view. Root hair development and tip growth in *Arabidopsis* rely on conserved functions and genes that also operate in the development of rhizoids of *Marchantia polymorpha* gametophytes, which appear to be homologous to root hairs [49–51]. *D14* occurs only in genomes of seed plants while *KAI2* is already present in algae [19, 20, 22]. Thus, it is possible that KAI2-SMAX1 module is part of an ancient and conserved pathway regulating tip growth of epidermal cells.



ethylene, are among the candidates [55, 56]. Here we demonstrate that KL signalling is a novel regulator of root skewing and root straightness. The increased skewing and waving phenotypes of KL perception mutants were found in both the Col-0 and Ler background although Ler shows an intrinsically higher tendency to skew than Col-0. Our results are broadly consistent with the recent report of [29], but our interpretation of the cause of the phenotype differs. Swarbreck et al. [29], speculated that skewing may be caused by increased epidermal cell file rotation and/or smaller root diameter of *kai2* mutants. Under our conditions, we did not observe epidermal cell file rotation in *kai2* and *max2*, but rather shorter epidermal cells. Since both *kai2* and *d14* have a reduced epidermal cell length, but skewing only occurs in *kai2*, we conclude that epidermal cell length is not related to skewing. Interestingly, in the experiments in which epidermal cell length was inspected, PRL was not significantly altered. This implies that a compensatory increase in epidermal cell division must occur in both the KL and SL perception mutants, which would be consistent with increased cell division in the primary root meristem. Alternatively, the epidermal cell length may differ among different root zones thus compensating for the shorter epidermal cell length in the zone 2–3 mm above the root tip. We also show that the reduced root diameter of KL perception mutants does not cause either skewing or waving since *smx1* alone suppresses the root diameter but not the waving phenotype of *max2*, and *smx2* suppresses the *max2* skewing but not the root diameter phenotype.

### KL and SL signalling in the root employ the canonical receptor-target pairs

We have previously highlighted some phenotypic characteristics suggesting that KL and SL signalling in the root might not act through the canonical KAI2-SMAX1 and D14-SMXL678 receptor-target pairs [10]. The main reason for this suggestion was that *max2* mutants had stronger LRD phenotypes than SL biosynthesis mutants [7–9], which suggested that KAI2 regulates lateral root emergence rather than or in addition to D14, while mutations of the genes encoding the canonical SL signalling targets SMXL678 were able to completely suppress the *max2* LRD phenotype with *smx1* being unable to do so [10, 27]. Similarly, Swarbreck et al. [29] suggested that non-canonical signalling may occur in skewing responses, since *smx678* mutants can completely suppress the *max2* skewing phenotype, which arises solely through lack of KAI2 signalling.

We have now robustly tested this hypothesis, and find no evidence for non-canonical KL and SL signalling in roots under our growth conditions. Using *smx1 smx2* double mutants, we show that every effect of loss of KAI2 activity can be suppressed by loss of SMAX1 and SMXL2 (or only one of the two), and that similarly, all effects of loss of D14 activity can be suppressed by loss of SMXL678. In the case of LRD, we show that *smx1 smx2* mutants can suppress the phenotype of *max2*, demonstrating that the canonical KL signalling targets are involved in regulating lateral root emergence and that SMXL2 compensates for the absence of functional SMAX1 in lateral root development [27]. The suppression of the *max2* LRD phenotype by *smx678* as well as *smx1 smx2* is consistent with our observation that both D14 and KAI2 regulate LRD. Thus, the accumulation of both SMAX1/SMXL2 and SMXL678 contributes to *max2* LRD phenotypes and there is no need to invoke non-canonical receptor-target pairs to explain the effects of KAI2 and D14 on LRD.

We also reject the idea that KL signalling regulates skewing through SMXL678 [29]. We find that *smx2* mutations are sufficient to suppress skewing in *max2*, consistent with canonical KAI2-SMAX1/SMXL2 signalling acting in this response. It is certainly interesting that *smx678* mutants suppress skewing of *max2* under some conditions, which does not reflect any known effect of D14 signalling. However, we show that this phenotype is highly variable, and under our growth conditions in Leeds, *smx678* mutants actually increased root skewing additively with *max2*. Thus, although SMXL678 can certainly regulate skewing, this appears to be

unrelated to the clearly defined and consistent effect of KL signalling on skewing. In fact, it appears consistent with the observation that *rac*-GR24 treatment—which stimulates SMXL678 degradation—causes an increase in root skewing in the wild type [29]. The location-dependent skewing behaviour of *smxl678* mutants suggests that the role of SMXL678 in skewing may strongly depend on environmental conditions, and it will be interesting to identify the mechanisms underlying this phenomenon in the future.

The case is even more clear-cut for RHL, RHD, root straightness and root diameter, for which only *kai2* and *max2* mutants show a phenotypic difference to wild type, and which can only be suppressed by mutating *SMAX1* and *SMXL2*. Interestingly, the *smxl2* mutant alone has longer root hairs than wild-type showing for the first time a phenotype in which SMXL2 plays a more important role than SMAX1, although it is alone not sufficient to suppress the *max2* phenotype. In the case of root diameter, mutation of *SMAX1* is sufficient to suppress the *max2* phenotypes (S2 Table). This partial redundancy of SMAX1 and SMXL2 is also seen in seed germination, hypocotyl growth and leaf shape [27, 35]. This likely arises from different expression patterns of the two genes: in tissues where only one of the two proteins is expressed, removing this one is sufficient to suppress the phenotype. Conversely, in the case of skewing, removing either *SMAX1* or *SMXL2* alone suffices to suppress the *max2* phenotype (S1 Table), suggesting that skewing is particularly sensitive to SMAX1/SMXL2 levels or stoichiometry or that SMAX1 or SMXL2 regulate skewing in different tissues.

### D14 and KAI2 are not completely ligand stereo-specific

In contrast to the lack of evidence for non-canonical receptor-target interactions, we uncovered unexpected evidence for non-canonical receptor ligand interactions in the context of root development. The two stereoisomers of *rac*-GR24, GR24<sup>5DS</sup> and GR24<sup>ent5DS</sup> have been suggested to specifically activate D14 and KAI2 respectively in the regulation of hypocotyl growth [34]; and GR24<sup>ent5DS</sup> showed only a very low efficiency in inhibiting shoot branching in Arabidopsis and rice [34, 57]. However, our study shows that there is very little specificity of the two receptors for the two stereoisomers, as both *d14* and *kai2* mutants respond to both with increased RHL and even with decreased hypocotyl elongation. This result is strengthened by confirming the purity of the employed compounds via NMR and CD. It has been shown by differential scanning fluorimetry (DSF) *in vitro* that D14 can bind both GR24<sup>5DS</sup> and GR24<sup>ent5DS</sup> but KAI2 only bound GR24<sup>ent5DS</sup> [31]. However, the situation *in vivo* may be different and binding of both ligands to both  $\alpha/\beta$  hydrolase receptors D14 and KAI2 may be stabilized through receptor protein complexes. Although binding of the 'wrong' stereoisomer to the  $\alpha/\beta$  hydrolase receptor may be less efficient than binding of the 'correct' one, it may suffice to trigger developmental responses, which are very sensitive to removal of SMXL proteins, or which may require additional interaction partners in the receptor complex that stabilize the complex in presence of the hypo-specific ligand. Independent of the mechanism, our results show that GR24<sup>5DS</sup> and GR24<sup>ent5DS</sup> cannot safely be used to specifically trigger D14 and KAI2-mediated signalling, respectively. This also implies that the community urgently needs an affordable synthetic SL that triggers D14 in a highly specific manner.

### Regulation of root development by KAI2 and D14 signalling

Overall our results show that KL signaling and therefore SMAX1 and SMXL2 play an important role in controlling root architecture and root hair development (Fig 9). However, some traits such as LRD and epidermal cell length are regulated by both SMAX1/SMXL2 and SMXL678. Key challenges for future studies will be to understand how exactly SMXL proteins regulate root architecture. Ruyter-Spira et al. [8] previously suggested that the impact of SLs on root development might be best understood as a reflection of their effect on the auxin

landscape, and we hypothesize that this may also be the case for KAI2 signalling. Most of the traits we have examined are known to be regulated by auxin, and SL signalling in the shoot is known to modulate auxin transport by regulating PIN protein abundance [27, 58]. Thus, it is very possible that the KAI2-SMAX1/SMXL2 and D14-SMXL678 pairs regulate the auxin landscape of the root, for example by controlling the abundance of auxin transport proteins. Such a scenario might underlie the variability in phenotypes observed in the mutants in our study (for instance, the strong variation in *smxl678* skewing phenotype), since environmental parameters such as light or temperature are known to affect endogenous auxin levels [59, 60].

We do not currently know enough about the upstream inputs into the KL signalling pathway to understand the aetiology of KAI2-induced root development, but undoubtedly the phenotypes described here will provide important clues and tools in this regard. SL production increases in several plant species upon phosphate starvation [12, 61–63] and the effect of SL biosynthesis on root architecture was suggested to depend on the sucrose level in the medium and thus on the carbon-status of the plants [8], but it is yet unknown whether KL signalling is also influenced by mineral nutrient levels. However, expression of KAI2 does respond to light conditions, and thus KL signalling could potentially integrate light cues into root development [64]. Indeed, it is likely that both signalling pathways are influenced by multiple abiotic and perhaps biotic stimuli, and it will be exciting to learn how SL and KL signalling tune root development to environmental conditions.

## Materials and methods

### Plant material

*Arabidopsis thaliana* genotypes were in Columbia-0 (Col-0) or Landsberg *erecta* (Ler) parental backgrounds. The following mutants were used: Ler: *max2-8* [18], *kai2-1*, *kai2-2* [18], Col-0: *kai2-2* [28], *max3-9* [65], *max4-5*, *d14-1 kai2-2* [66], *d14-1* [19], *max1-1*, *max2-1*, *max2-2* [67], *smax1-2*, *max2-1 smax1-2* [37], *smax1-2 smxl2-1*, *max2-1 smax1-2 smxl2-1* [35], *smxl6-4 smxl7-3 smxl8-1*, *max2-1 smxl6-4 smxl7-3 smxl8-1* [27].

### Plant growth conditions

For analysis of root growth, *Arabidopsis thaliana* seeds were grown in axenic conditions on 12x12cm square plates containing 60 ml agar-solidified medium. Seed were surface sterilized either by vapour sterilization, or by washing with 1 ml of 70% (v/v) ethanol and 0.05% (v/v) Triton X-100 with gentle mixing by inversion for 6 minutes at room temperature, followed by 1 wash with 96% ethanol and 5 washes with sterile distilled water. For primary root length and lateral root density plants were grown in Cambridge and Leeds on plates containing ATS medium [68] supplemented with 1% sucrose (w/v) and solidified with 0.8% ATS. For measurements of skewing, waving, cell length, root diameter, root hair density and root hair length, seedlings were grown in Munich on plates containing 0.5X Murashige & Skoog medium, pH5.8 (½ MS) (Duchefa, Netherlands), supplemented with 1% sucrose and solidified with 1.5% agar. Plates were stratified at 4°C for 2–3 days in the dark, and then transferred to a growth cabinet under controlled conditions at 22°C, 16-h/8-h light/dark cycle (intensity ~120 μmol m<sup>-2</sup> s<sup>-1</sup>). Unless otherwise indicated, the plates were placed vertically.

### Phytohormone treatments

*rac*-GR24 was purchased from Chiralix (Nijmegen, The Netherlands), GR24<sup>ent5DS</sup> and GR24<sup>5DS</sup> from Strigolab (Turin, Italy), and KAR<sub>2</sub> from Olchemim (Olomouc, Czech Republic). For treatment with *rac*-GR24, GR24<sup>ent5DS</sup> or GR24<sup>5DS</sup>, 1 mM stock solutions were

prepared in 100% acetone. KAR<sub>2</sub> was dissolved in 70% methanol for the preparation of 1 mM stock. The volume required to reach the final concentration of these different stock solutions was added to molten media prior to pouring Petri dishes. In each experiment, an equivalent volume of solvent was added to Petri dishes for untreated controls.

### Primary and lateral root quantification

For quantification of primary root length and lateral root number, seedlings were grown as described above in Cambridge and Leeds for 10 days post germination (dpg). This allowed for the emergence of lateral roots sufficient for quantification in wild-type seedlings. A dissecting microscope was used to count emerged lateral roots in each root system, and images of the plates were then taken using a flatbed scanner. Primary root length was quantified using Image J. Separate experiments were primarily used to assess root skewing (see below), but root skewing angles were also measured from these images generated in these experiments.

### Root skewing and straightness assay

The root slanting assay was modified from the method described by [69]. *Arabidopsis* seedlings were grown in Munich under the conditions described above (except for Fig 8G for which plants were grown in Leeds). Images were taken 5 days post germination (dpg) using an Epson Perfection V800 Pro Scanner. Images were analysed using the Simple Neurite Tracer plug-in of Fiji (<https://imagej.net/Fiji/Downloads>) to determine the following parameters as illustrated in Fig 4; root length (L), ratio of the straight line between the hypocotyl-root junction and the root tip (Lc), and vertical axis (Ly). These measurements were taken from at least 60 individual roots per genotype and used to calculate the root skewing angle ( $\alpha$ ) and root straightness (Lc/L) as previously described [70, 71].

### Determination of root hair density, length and position

Root hair growth was examined in Munich on the same *Arabidopsis* roots, which were used for determining root skewing and straightness. Images were taken at 2 mm from the root tip of a minimum of 8 roots per genotype and treatment with a Leica DM6 B microscope equipped with a Leica DFC9000 GT camera. The number of root hairs was determined by counting the root hairs between 2 and 3 mm from the root tip on each root, and root hair length was measured for 10–18 different root hairs per root using Fiji. The root hair position was determined following the method described by [72] for 5–15 root hairs per root and a minimum of 8 roots per genotype.

### Root diameter and cell length analysis

Using the same images as for root hair quantification, root diameter, root cell length and number of cells were analysed in Munich using Fiji. Root diameter was measured at 2.5 mm from the root tip. The number of cells was defined as the number of epidermal cells that crossed a 1-mm-long straight line drawn between 2 to 3 mm from the root tip. Root cell length was measured for at least 10 different epidermal cells per individual root in a minimum of 10 roots per genotype, between 2 to 3 mm from the root tip.

### Determination of purity of GR24 stereoisomers

**Chemicals.** The following compounds were obtained commercially from the sources given in parentheses: formic acid, chloroform (HPLC grade) (Merck, Darmstadt, Germany); acetonitrile (MS grade, J. T. Baker, Deventer, Netherlands); (CD<sub>3</sub>)<sub>2</sub>CO was obtained from

Euriso-Top (Gif-Sur-Yvette, France). Water for UHPLC separation was purified by means of a Milli-Q water advantage A 10 water system (Millipore, Molsheim, France).

**General experimental procedures.**  $^1\text{H}$  NMR experiments were performed on an Avance III 400 MHz spectrometer with a BBI probe (Bruker, Rheinstetten, Germany) at 298 K.  $(\text{CD}_3)_2\text{CO}$  was used as solvent and chemical shifts are reported in parts per million, relative to solvent signal:  $^1\text{H}$  NMR: 2.05 ppm and  $^{13}\text{C}$  NMR: 29.84 ppm. Data processing was performed by using Topspin software (version 2.1; Bruker) as well as MestReNova software (version 5.2.3; Mestrelab Research, Santiago de Compostella, Spain). For circular dichroism (CD) spectroscopy, sample solutions of compounds were analysed by means of a Jasco J-810 spectropolarimeter (Hachioji, Japan). High-resolution mass spectra were measured on a TripleTOF 6600 mass spectrometer (Sciex, Darmstadt, Germany) equipped with a DuoSpray source (Sciex), running in ESI positive mode, connected to a Nexera X2 UHPLC (Shimadzu, Duisburg, Germany), consisting of two LC pump systems 30AD, a DGU-20A5 degasser, a SIL-30AC autosampler, a CTO-30A column oven and a CBM-20A controller. Calibration of the mass spectrometer was performed after every 5 samples using a Calibrant Delivery System (Sciex) linked to the APCI probe of the DuoSpray source and either positive or negative APCI Calibration solution (Sciex). Rotation values were determined by means of a P3000 polarimeter (Krüss, Hamburg, Germany). The structures of compound of GR24<sup>5DS</sup> and GR24<sup>ent-5DS</sup> were characterized, by means of UHPLC-TOF-MS,  $^1\text{H}$  NMR, CD spectroscopy and polarimetric experiments.

**GR24<sup>5DS</sup>:** LC-TOF-MS:  $m/z$  299.0915 (measured),  $m/z$  299.0919 (calcd. for  $[\text{C}_{17}\text{H}_{14}\text{O}_5 + \text{H}^+]^+$ );  $^1\text{H}$  NMR (400 MHz,  $(\text{CD}_3)_2\text{CO}$ ):  $\delta$ /ppm: 7.56 (d,  $J = 2.6$  Hz, 1H, H-C(6')), 7.44 (d,  $J = 7.4$  Hz, 1H, H-C(8)), 7.36–7.21 (m, 3H, H-C(5–7)), 6.55 (t,  $J = 1.4$  Hz, 1H, H-C(2')), 5.94 (d,  $J = 7.9$  Hz, 1H, H-C(3')), 4.02–3.93 (m, 1H, H-(3a)), 3.40 (dd,  $J = 16.9, 9.3$  Hz, 1H, H-C(4 $\alpha$ )), 3.08 (dd,  $J = 16.9, 3.3$  Hz, 1H, H-C(4 $\beta$ )), 1.95 (t,  $J = 1.5$  Hz, 3H, H-C(7')).  $^{13}\text{C}$  NMR (100 MHz,  $(\text{CD}_3)_2\text{CO}$ ):  $\delta$ /ppm: 171.29 (C = O), 171.28 (C = O), 152.73 C(6'), 143.85 C(8a), 143.24 C(3'), 140.55 C(4a), 135.56 C(4'), 130.59 C(5), 128.09 C(7), 127.04 C(8), 126.09 C(6), 113.45 C(3), 102.24 C(2'), 86.25 C(8b), 39.60 C(3a), 37.85 C(4), 10.60 C(7'). CD(20°C; ACN;  $c = 0.01$  mM)  $\lambda_{\text{max}}(\Delta\epsilon)$  262 (–1.7), 230 (25.5) nm.  $[\alpha]_{\text{D}}^{15} +420^\circ$  ( $\text{CDCl}_3$ ,  $c$  0.25 mM) [+436°, [46]].

**GR24<sup>ent-5DS</sup>:** LC-TOF-MS:  $m/z$  299.0920 (measured),  $m/z$  299.0919 (calcd. for  $[\text{C}_{17}\text{H}_{14}\text{O}_5 + \text{H}^+]^+$ );  $^1\text{H}$  NMR (400 MHz,  $(\text{CD}_3)_2\text{CO}$ ):  $\delta$ /ppm: 7.56 (d,  $J = 2.6$  Hz, 1H, H-C(6')), 7.44 (d,  $J = 7.4$  Hz, 1H, H-C(8)), 7.36–7.19 (m, 3H, H-C(5–7)), 6.55 (t,  $J = 1.4$  Hz, 1H, H-C(2')), 5.94 (d,  $J = 7.9$  Hz, 1H, H-C(3')), 4.07–3.92 (m, 1H, H-(3a)), 3.40 (dd,  $J = 16.9, 9.3$  Hz, 1H, H-C(4 $\alpha$ )), 3.08 (dd,  $J = 16.9, 3.3$  Hz, 1H, H-C(4 $\beta$ )), 1.95 (t,  $J = 1.5$  Hz, 3H, H-C(7')).  $^{13}\text{C}$  NMR (100 MHz,  $(\text{CD}_3)_2\text{CO}$ ):  $\delta$ /ppm: 171.29 (C = O), 171.28 (C = O), 152.73 C(6'), 143.85 C(8a), 143.24 C(3'), 140.55 C(4a), 135.56 C(4'), 130.59 C(5), 128.09 C(7), 127.04 C(8), 126.09 C(6), 113.45 C(3), 102.24 C(2'), 86.25 C(8b), 39.60 C(3a), 37.85 C(4), 10.60 C(7'). CD (20°C; ACN;  $c = 0.01$  mM)  $\lambda_{\text{max}}(\Delta\epsilon)$  262 (1.7), 230 (–26.9) nm.  $[\alpha]_{\text{D}}^{15} -427^\circ$  ( $\text{CDCl}_3$ ,  $c$  0.25 mM) [–446°, [46]].

**Purity of both isomers.** 93–95% ( $^1\text{H}$  NMR).

### Statistical analysis

Statistical analyses were performed in R-studio, using one-way Analysis of Variance (ANOVA), followed by Tukey HSD or Dunnett's post hoc test.

### Accession numbers

Sequence data for the genes mentioned in this article can be found in The Arabidopsis Information Resource (TAIR; <https://www.arabidopsis.org>) under the following accession numbers: MAX3, AT2G44990; MAX4, AT4G32810; MAX1, AT2G26170; D14, AT3G03990; KAI2,

AT4G37470; *MAX2*, AT2G42620; *SMAX1*, AT5G57710; *SMXL2* AT4G30350; *SMXL6*, AT1G07200; *SMXL7*, AT2G29970; *SMXL8*, AT2G40130.

## Supporting information

**S1 Fig. Variation in root growth parameters in strigolactone synthesis and perception mutants.** Mean primary root lengths (PRL) and mean lateral root densities (LRD) for strigolactone synthesis mutants (*max1-1*, *max3-9*, *max4-5*) and perception mutants (*d14-1*) across 5 different experiments. Values shown are quoted as a percentage, relative to the mean value for the Col-0 wild-type control in the same experiment (set to 100). Shading of cells represents percent below or above the mean of the wild type. Strong reductions in PRL are never accompanied by strong increase in LRD, and strong increases in LRD are never accompanied by strong reductions in PRL.

(TIFF)

**S2 Fig. KL signaling regulates lateral root density.** (A) Lateral root density of the indicated genotypes. (B) Lateral root density at 6, 8 or 10 days post germination (dpg). The outline of the violin plot represents the probability of the kernel density. Black boxes represent interquartile ranges (IQR), with the red horizontal line representing the median; whiskers extend to the highest and lowest data point but no more than  $\pm 1.5$  times the IQR from the box; outliers are plotted individually. Percentage numbers indicate the percent significant difference between the median of each indicated genotype and the median of the wild type at the same time point. Different letters indicate different statistical groups (A) ANOVA, posthoc Tukey,  $F_{2,79} = 5.29$ ,  $n = 24-30$ ,  $p < 0.01$ . Asterisks indicate a significant difference compared to wild type for each time point. (B) ANOVA, post-hoc Dunnett's tests comparing to wild-type, at each time-point,  $F_{11,239} = 47.87$ ,  $n = 14-24$ ; \* $p \leq 0.05$ , \*\* $p \leq 0.01$ , \*\*\* $p \leq 0.001$ .

(TIFF)

**S3 Fig. KAR perception mutants respond to tilted agar surface.** (A, D, E) Root skewing and (B, F, G) root straightness of the indicated genotypes. In (A, B) plants were grown at a  $90^\circ$  angle. (D-E) Plants were grown either at a  $90^\circ$  angle (white violins) or a  $45^\circ$  angle (grey violins) as shown in the diagram in (C). The outline of the violin plots represents the probability of the kernel density. Black boxes represent interquartile ranges (IQR), with the red horizontal line representing the median; whiskers extend to the highest and lowest data point but no more than  $\pm 1.5$  times the IQR from the box; outliers are plotted individually. Different letters indicate different statistical groups (ANOVA, posthoc Tukey,  $p \leq 0.001$ ,  $n > 40$ ) (A)  $F_{5,333} = 5.057$  (B)  $F_{4,290} = 7.168$  (D)  $F_{7,383} = 5.788$  (E)  $F_{7,472} = 12.54$  (F)  $F_{7,430} = 25.89$  (G)  $F_{7,497} = 18.36$ .

(TIFF)

**S4 Fig. KL perception mutants in the Ler background exhibit decreased epidermal cell lengths and root diameter.** (A) Number of root epidermal cells per mm of the indicated genotypes. (B) Images of representative roots between 2 and 3 mm from the root tip from 5-days-old seedlings of the indicated genotypes. Scale bars, 0.1 mm. (C) Root cell length and (D) and root diameter of the indicated genotypes. The outline of the violin plots represent the probability of the kernel density. Black boxes represent interquartile ranges (IQR), with the red horizontal line representing the median; whiskers extend to the highest and lowest data point but no more than  $\pm 1.5$  times the IQR from the box; outliers are plotted individually. Different letters indicate different statistical groups (ANOVA, posthoc Tukey,  $p \leq 0.001$ ) (A)  $F_{2,43} = 9.58$ ,  $n = 13-18$  (C)  $F_{2,191} = 43.1$ ,  $n = 10-11$  (D)  $F_{2,64} = 77.45$ ,  $n = 21$ .

(TIFF)

**S5 Fig. Regulation of root skewing by KAI2 can be genetically separated from root diameter.** (A, B, C) Root diameter of Col-0 wild type and the indicated genotypes (the mutant alleles are *max2-1*, *smax1-2*, *smxl2-1*, *smxl6-4*, *smxl7-3* and *smxl8-1*). The outline of the violin plot represents the probability of the kernel density. Black boxes represent interquartile ranges (IQR), with the red horizontal line representing the median; whiskers extend to the highest and lowest data point but no more than  $\pm 1.5$  times the IQR from the box; outliers are plotted individually. Different letters indicate different statistical groups (ANOVA, posthoc Tukey,  $p \leq 0.001$ , (A)  $F_{3,38} = 15.04$ ,  $n = 10-11$  (B)  $F_{3,38} = 15.04$ ,  $n = 8-21$  (C)  $F_{3,47} = 8.221$ ,  $n = 10-11$ ). (TIFF)

**S6 Fig. Purity evaluation of SL stereoisomers.** (A) Chemical structures of GR24<sup>5DS</sup> and GR24<sup>ent-5DS</sup>. (B) CD spectra of GR24<sup>5DS</sup> and GR24<sup>ent-5DS</sup>. (C) <sup>1</sup>H-NMR (400 MHz, 298 K, (CD<sub>3</sub>)<sub>2</sub>CO) of GR24<sup>5DS</sup>. (D) <sup>13</sup>C-NMR (100 MHz, 298 K, (CD<sub>3</sub>)<sub>2</sub>CO) of GR24<sup>5DS</sup>. (E) <sup>1</sup>H-NMR (400 MHz, 298 K, (CD<sub>3</sub>)<sub>2</sub>CO) of GR24<sup>ent-5DS</sup>. (F) <sup>13</sup>C-NMR (100 MHz, 298 K, (CD<sub>3</sub>)<sub>2</sub>CO) of GR24<sup>ent-5DS</sup>. For more information see [Materials and Methods](#). (TIFF)

**S7 Fig. GR24 stereoisomers regulate hypocotyl length through D14 and KAI2.** Hypocotyl length of the indicated genotypes treated with solvent (acetone), 1  $\mu$ M GR24<sup>ent-5DS</sup>, 1  $\mu$ M GR24<sup>5DS</sup> or 1  $\mu$ M *rac*-GR24. The outline of the violin plot represents the probability of the kernel density. Black boxes represent interquartile ranges (IQR), with the red horizontal line representing the median; whiskers extend to the highest and lowest data point but no more than  $\pm 1.5$  times the IQR from the box; outliers are plotted individually. Different letters indicate different statistical groups (ANOVA, posthoc Tukey,  $F_{2,43} = 9.58$ ,  $n = 32-42$ ,  $p \leq 0.001$ ). (TIFF)

**S1 Table. Summary of effects of SMXL mutations on *max2* root phenotypes.** (PDF)

**S2 Table. Raw data for all figures.** (XLSX)

## Acknowledgments

We thank David Nelson (UC Riverside, USA) and Mark Waters (University of Western Australia) for providing mutant seeds. The Gutjahr group is grateful to Jürgen Soll (LMU Munich, Germany) for generously providing space in his *Arabidopsis* growth chamber.

## Author Contributions

**Conceptualization:** José Antonio Villaécija-Aguilar, Tom Bennett, Caroline Gutjahr.

**Formal analysis:** José Antonio Villaécija-Aguilar, Corinna Dawid, Tom Bennett, Caroline Gutjahr.

**Funding acquisition:** Corinna Dawid, Tom Bennett, Caroline Gutjahr.

**Investigation:** José Antonio Villaécija-Aguilar, Maxime Hamon-Josse, Samy Carbonnel, Annika Kretschmar, Christian Schmidt, Tom Bennett.

**Methodology:** José Antonio Villaécija-Aguilar, Maxime Hamon-Josse, Christian Schmidt.

**Project administration:** Tom Bennett, Caroline Gutjahr.

**Supervision:** Corinna Dawid, Tom Bennett, Caroline Gutjahr.

**Visualization:** José Antonio Villaécija-Aguilar.

**Writing – original draft:** José Antonio Villaécija-Aguilar, Tom Bennett, Caroline Gutjahr.

**Writing – review & editing:** Maxime Hamon-Josse, Tom Bennett, Caroline Gutjahr.

## References

- Zhang H, Forde BG. Regulation of Arabidopsis root development by nitrate availability. *Journal of Experimental Botany*. 2000; 51:51–9. PMID: [10938795](#)
- Ma Z, Bielenberg D, Brown K, Lynch J. Regulation of root hair density by phosphorus availability in *Arabidopsis thaliana*. *Plant, Cell & Environment*. 2001; 24:459–67.
- Gruber BD, Giehl RFH, Friedel S, von Wirén N. Plasticity of the Arabidopsis root system under nutrient deficiencies. *Plant Physiology*. 2013; 163:161–79. <https://doi.org/10.1104/pp.113.218453> PMID: [23852440](#)
- Pierik R, Testerink C. The art of being flexible: how to escape from shade, salt, and drought. *Plant Physiology*. 2014; 166:5–22. <https://doi.org/10.1104/pp.114.239160> PMID: [24972713](#)
- Dietrich D. Hydrotropism: how roots search for water. *Journal of Experimental Botany*. 2018; 69:2759–71. <https://doi.org/10.1093/jxb/ery034> PMID: [29529239](#)
- Koltai H, Dor E, Hershenhorn J, Joel DM, Weininger S, Lekalla S, et al. Strigolactones' Effect on root growth and root-hair elongation may be mediated by auxin-efflux carriers. *Journal of Plant Growth Regulation*. 2010; 29:129–36.
- Kapulnik Y, Delaux P-M, Resnick N, Mayzlish-Gati E, Wininger S, Bhattacharya C, et al. Strigolactones affect lateral root formation and root-hair elongation in Arabidopsis. *Planta*. 2011; 233:209–16. <https://doi.org/10.1007/s00425-010-1310-y> PMID: [21080198](#)
- Ruyter-Spira C, Kohlen W, Charnikhova T, van Zeijl A, van Bezouwen L, de Ruijter N, et al. Physiological effects of the synthetic strigolactone analog GR24 on root system architecture in Arabidopsis: another below-ground role for strigolactones? *Plant Physiology*. 2011; 155:721–34. <https://doi.org/10.1104/pp.110.166645> PMID: [21119044](#)
- Jiang L, Matthys C, Marquez-Garcia B, De Cuyper C, Smet L, De Keyser A, et al. Strigolactones spatially influence lateral root development through the cytokinin signaling network. *Journal of Experimental Botany*. 2015; 67:379–89. <https://doi.org/10.1093/jxb/erv478> PMID: [26519957](#)
- Waters MT, Gutjahr C, Bennett T, Nelson DC. Strigolactone signaling and evolution. *Annual Review of Plant Biology*. 2017; 68:291–322. <https://doi.org/10.1146/annurev-arplant-042916-040925> PMID: [28125281](#)
- Jia K-P, Baz L, Al-Babili S. From carotenoids to strigolactones. *Journal of Experimental Botany*. 2017; 69:2189–204.
- Yoneyama K, Mori N, Sato T, Yoda A, Xie X, Okamoto M, et al. Conversion of carlactone to carlactonoic acid is a conserved function of MAX1 homologs in strigolactone biosynthesis. *New Phytologist*. 2018; 218:1522–33. <https://doi.org/10.1111/nph.15055> PMID: [29479714](#)
- Hamiaux C, Drummond RS, Janssen BJ, Ledger SE, Cooney JM, Newcomb RD, et al. DAD2 is an  $\alpha/\beta$  hydrolase likely to be involved in the perception of the plant branching hormone, strigolactone. *Current Biology*. 2012; 22:2032–6. <https://doi.org/10.1016/j.cub.2012.08.007> PMID: [22959345](#)
- de Saint Germain A, Clavé G, Badet-Denisot M-A, Pillot J-P, Comu D, Le Caer J-P, et al. An histidine covalent receptor and butenolide complex mediates strigolactone perception. *Nature Chemical Biology*. 2016; 12:787–94. <https://doi.org/10.1038/nchembio.2147> PMID: [27479744](#)
- Yao R, Ming Z, Yan L, Li S, Wang F, Ma S, et al. DWARF14 is a non-canonical hormone receptor for strigolactone. *Nature*. 2016; 536:469–73. <https://doi.org/10.1038/nature19073> PMID: [27479325](#)
- Seto Y, Yasui R, Kameoka H, Tamiru M, Cao M, Terauchi R, et al. Strigolactone perception and deactivation by a hydrolase receptor DWARF14. *Nature Communications*. 2019; 10:191. <https://doi.org/10.1038/s41467-018-08124-7> PMID: [30643123](#)
- Shabek N, Ticchiarelli F, Mao H, Hinds TR, Leyser O, Zheng N. Structural plasticity of D3–D14 ubiquitin ligase in strigolactone signalling. *Nature*. 2018; 563:652–6. <https://doi.org/10.1038/s41586-018-0743-5> PMID: [30464344](#)
- Nelson DC, Scaffidi A, Dun EA, Waters MT, Flematti GR, Dixon KW, et al. F-box protein MAX2 has dual roles in karrikin and strigolactone signaling in *Arabidopsis thaliana*. *Proceedings of the National Academy of Sciences*. 2011; 108:8897–902.
- Waters MT, Nelson DC, Scaffidi A, Flematti GR, Sun YK, Dixon KW, et al. Specialisation within the DWARF14 protein family confers distinct responses to karrikins and strigolactones in Arabidopsis. *Development*. 2012; 139:1285–95. <https://doi.org/10.1242/dev.074567> PMID: [22357928](#)

20. Delaux P-M, Xie X, Timme RE, Puech-Pages V, Dunand C, Lecompte E, et al. Origin of strigolactones in the green lineage. *New Phytologist*. 2012; 195:857–71. <https://doi.org/10.1111/j.1469-8137.2012.04209.x> PMID: 22738134
21. Toh S, Holbrook-Smith D, Stokes Michael E, Tsuchiya Y, McCourt P. Detection of parasitic plant suicide germination compounds using a high-throughput Arabidopsis HTL/KAI2 strigolactone perception system. *Chemistry & Biology*. 2014; 21:988–98.
22. Bythell-Douglas R, Rothfels CJ, Stevenson DWD, Graham SW, Wong GK-S, Nelson DC, et al. Evolution of strigolactone receptors by gradual neo-functionalization of KAI2 paralogs. *BMC Biology*. 2017; 15:52. <https://doi.org/10.1186/s12915-017-0397-z> PMID: 28662667
23. Guo Y, Zheng Z, La Clair JJ, Chory J, Noel JP. Smoke-derived karrikin perception by the  $\alpha/\beta$ -hydrolase KAI2 from Arabidopsis. *Proceedings of the National Academy of Sciences*. 2013; 20:8284–9.
24. Nelson DC, Riseborough J-A, Flematti GR, Stevens J, Ghisalberti EL, Dixon KW, et al. Karrikins discovered in smoke trigger Arabidopsis seed germination by a mechanism requiring gibberellic acid synthesis and light. *Plant Physiology*. 2009; 149:863–73. <https://doi.org/10.1104/pp.108.131516> PMID: 19074625
25. Soós V, Sebestyén E, Juhász A, Light ME, Kohout L, Szalai G, et al. Transcriptome analysis of germinating maize kernels exposed to smoke-water and the active compound KAR1. *BMC Plant Biology*. 2010; 10:236. <https://doi.org/10.1186/1471-2229-10-236> PMID: 21044315
26. Ruduś I, Cembrowska-Lech D, Jaworska A, Kepczyński J. Involvement of ethylene biosynthesis and perception during germination of dormant *Avena fatua* L. caryopses induced by KAR1 or GA3. *Planta*. 2019; 249:719–38. <https://doi.org/10.1007/s00425-018-3032-5> PMID: 30370496
27. Soundappan I, Bennett T, Morffy N, Liang Y, Stanga JP, Abbas A, et al. SMAX1-LIKE/D53 family members enable distinct MAX2-dependent responses to strigolactones and karrikins in Arabidopsis. *Plant Cell*. 2015; 27:3143–59. <https://doi.org/10.1105/tpc.15.00562> PMID: 26546447
28. Bennett T, Hines G, van Rongen M, Waldie T, Sawchuk MG, Scarpella E, et al. Connective auxin transport in the shoot facilitates communication between shoot apices. *PLoS Biology*. 2016; 14:e1002446. <https://doi.org/10.1371/journal.pbio.1002446> PMID: 27119525
29. Swarbreck SM, Guerringue Y, Matthus E, Jamieson FJC, Davies JM. Impairment in karrikin but not strigolactone sensing enhances root skewing in *Arabidopsis thaliana*. *Plant Journal*. 2019; 98:607–21. <https://doi.org/10.1111/tpj.14233> PMID: 30659713
30. Gutjahr C, Gobatto E, Choi J, Riemann M, Johnston MG, Summers W, et al. Rice perception of symbiotic arbuscular mycorrhizal fungi requires the karrikin receptor complex. *Science*. 2015; 350:1521–4. <https://doi.org/10.1126/science.aac9715> PMID: 26680197
31. Waters MT, Scaffidi A, Flematti G, Smith SM. Substrate-induced degradation of the  $\alpha/\beta$ -fold hydrolase KARRIKIN INSENSITIVE2 requires a functional catalytic triad but is independent of MAX2. *Molecular Plant*. 2015; 8:814–7. <https://doi.org/10.1016/j.molp.2014.12.020> PMID: 25698586
32. Conn CE, Nelson DC. Evidence that KARRIKIN-INSENSITIVE2 (KAP2) receptors may perceive an unknown signal that is not karrikin or strigolactone. *Frontiers in Plant Science*. 2016; 6:1219. <https://doi.org/10.3389/fpls.2015.01219> PMID: 26779242
33. Sun H, Tao J, Gu P, Xu G, Zhang Y. The role of strigolactones in root development. *Plant Signaling & Behavior*. 2016; 11:e1110662-e.
34. Scaffidi A, Waters M, Sun YK, Skelton BW, Dixon KW, Ghisalberti EL, et al. Strigolactone hormones and their stereoisomers signal through two related receptor proteins to induce different physiological responses in Arabidopsis. *Plant Physiology*. 2014; 165:1221–32. <https://doi.org/10.1104/pp.114.240036> PMID: 24808100
35. Stanga JP, Morffy N, Nelson DC. Functional redundancy in the control of seedling growth by the karrikin signaling pathway. *Planta*. 2016; 243:1397–406. <https://doi.org/10.1007/s00425-015-2458-2> PMID: 26754282
36. Wang L, Wang B, Jiang L, Liu X, Li X, Lu Z, et al. Strigolactone signaling in Arabidopsis regulates shoot development by targeting D53-like SMXL repressor proteins for ubiquitination and degradation. *Plant Cell*. 2015; 27:3128–42. <https://doi.org/10.1105/tpc.15.00605> PMID: 26546446
37. Stanga JP, Smith SM, Briggs WR, Nelson DC. *SUPPRESSOR OF MAX2 1* controls seed germination and seedling development in *Arabidopsis thaliana*. *Plant Physiology*. 2013; 163:318–30. <https://doi.org/10.1104/pp.113.221259> PMID: 23893171
38. Liang Y, Ward S, Li P, Bennett T, Leyser O. SMAX1-LIKE7 signals from the nucleus to regulate shoot development in Arabidopsis via partially EAR motif-independent mechanisms. *Plant Cell*. 2016; 28:1581–601. <https://doi.org/10.1105/tpc.16.00286> PMID: 27317673
39. Jiang L, Liu X, Xiong G, Liu H, Chen F, Wang L, et al. DWARF 53 acts as a repressor of strigolactone signalling in rice. *Nature*. 2013; 504:401. <https://doi.org/10.1038/nature12870> PMID: 24336200

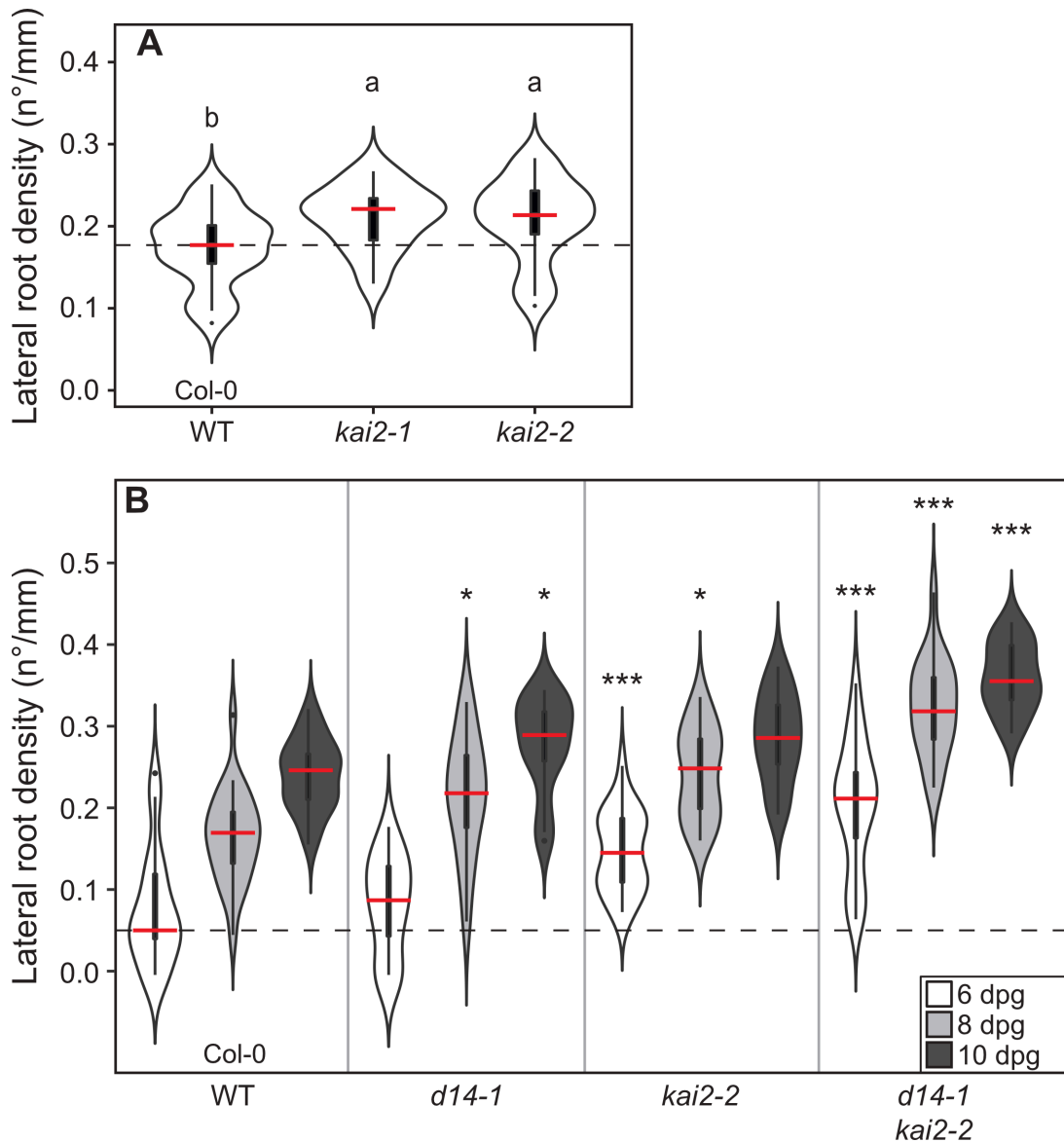
40. Zhou F, Lin Q, Zhu L, Ren Y, Zhou K, Shabek N, et al. D14–SCFD3-dependent degradation of D53 regulates strigolactone signalling. *Nature*. 2013; 504:406. <https://doi.org/10.1038/nature12878> PMID: 24336215
41. Song X, Lu Z, Yu H, Shao G, Xiong J, Meng X, et al. IPA1 functions as a downstream transcription factor repressed by D53 in strigolactone signaling in rice. *Cell Research*. 2017; 27:1128–41. <https://doi.org/10.1038/cr.2017.102> PMID: 28809396
42. Kapulnik Y, Resnick N, Mayzlish-Gati E, Kaplan Y, Winer S, Hershenhorn J, et al. Strigolactones interact with ethylene and auxin in regulating root-hair elongation in Arabidopsis. *Journal of Experimental Botany*. 2011; 62:2915–24. <https://doi.org/10.1093/jxb/erq464> PMID: 21307387
43. Oliva M, Dunand C. Waving and skewing: how gravity and the surface of growth media affect root development in Arabidopsis. *New Phytologist*. 2007; 176:37–43. <https://doi.org/10.1111/j.1469-8137.2007.02184.x> PMID: 17692076
44. Roy R, Bassham DC. Root growth movements: waving and skewing. *Plant Science*. 2014; 221:42–7. <https://doi.org/10.1016/j.plantsci.2014.01.007> PMID: 24656334
45. Wang Y, Wang B, Gilroy S, Chehab EW, Braam J. CML24 is involved in root mechanoresponses and cortical microtubule orientation in Arabidopsis. *Journal of Plant Growth Regulation*. 2011; 30:467–79.
46. Willem J. F. Thuring J, Keltjens R, H. L. Nefkens G, Zwanenburg B. Synthesis and biological evaluation of potential substrates for the isolation of the strigol receptor. *Journal of the Chemical Society, Perkin Transactions 1*. 1997:759–66.
47. Akiyama K, Ogasawara S, Ito S, Hayashi H. Structural requirements of strigolactones for hyphal branching in AM fungi. *Plant and Cell Physiology*. 2010; 51:1104–17. <https://doi.org/10.1093/pcp/pcq058> PMID: 20418334
48. Osmont KS, Sibout R, Hardtke CS. Hidden branches: developments in root system architecture. *Annual Review of Plant Biology* 2007; 58:93–113. <https://doi.org/10.1146/annurev.arplant.58.032806.104006> PMID: 17177637
49. Tam THY, Catarino B, Dolan L. Conserved regulatory mechanism controls the development of cells with rooting functions in land plants. *Proceedings of the National Academy of Sciences*. 2015; 112: E3959–E68.
50. Honkanen S, Dolan L. Growth regulation in tip-growing cells that develop on the epidermis. *Current Opinion in Plant Biology*. 2016; 34:77–83. <https://doi.org/10.1016/j.cup.2016.10.006> PMID: 27816817
51. Honkanen S, Jones VA, Morieri G, Champion C, Hetherington AJ, Kelly S, et al. The mechanism forming the cell surface of tip-growing rooting cells is conserved among land plants. *Current Biology*. 2016; 26:3238–44. <https://doi.org/10.1016/j.cub.2016.09.062> PMID: 27866889
52. Ito S, Nozoye T, Sasaki E, Imai M, Shiwa Y, Shibata-Hatta M, et al. Strigolactone regulates anthocyanin accumulation, acid phosphatases production and plant growth under low phosphate condition in Arabidopsis. *PLoS One*. 2015; 10:e0119724. <https://doi.org/10.1371/journal.pone.0119724> PMID: 25793732
53. Mayzlish-Gati E, De Cuyper C, Goormachtig S, Beeckman T, Vuylsteke M, Brewer P, et al. Strigolactones are involved in root response to low phosphate conditions in Arabidopsis. *Plant Physiology*. 2012; 160:1329–41. <https://doi.org/10.1104/pp.112.202358> PMID: 22968830
54. Madmon O, Mazuz M, Kumari P, Dam A, Ion A, Mayzlish-Gati E, et al. Expression of MAX2 under SCARECROW promoter enhances the strigolactone/MAX2 dependent response of Arabidopsis roots to low-phosphate conditions. *Planta*. 2016; 243:1419–27. <https://doi.org/10.1007/s00425-016-2477-7> PMID: 26919985
55. Buer CS, Wasteneys GO, Masle J. Ethylene modulates root-wave responses in Arabidopsis. *Plant Physiology*. 2003; 132:1085–96. <https://doi.org/10.1104/pp.102.019182> PMID: 12805636
56. Qi B, Zheng H. Modulation of root-skewing responses by *KNAT1* in *Arabidopsis thaliana*. *Plant Journal*. 2013; 76:380–92. <https://doi.org/10.1111/tpj.12295> PMID: 23889705
57. Umehara M, Cao M, Akiyama K, Akatsu T, Seto Y, Hanada A, et al. Structural requirements of strigolactones for shoot branching inhibition in rice and Arabidopsis. *Plant and Cell Physiology*. 2015; 56:1059–72. <https://doi.org/10.1093/pcp/pcv028> PMID: 25713176
58. Shinohara N, Taylor C, Leyser O. Strigolactone can promote or inhibit shoot branching by triggering rapid depletion of the auxin efflux protein PIN1 from the plasma membrane. *PLoS Biology*. 2013; 11: e1001474. <https://doi.org/10.1371/journal.pbio.1001474> PMID: 23382651
59. Gray WM, Östin A, Sandberg G, Romano CP, Estelle M. High temperature promotes auxin-mediated hypocotyl elongation in Arabidopsis. *Proceedings of the National Academy of Sciences*. 1998; 95:7197–202.
60. Ljung K. Auxin metabolism and homeostasis during plant development. *Development*. 2013; 140:943–50. <https://doi.org/10.1242/dev.086363> PMID: 23404103

61. López-Ráez JA, Charnikhova T, Gómez-Roldán V, Matusova R, Kohlen W, De Vos R, et al. Tomato strigolactones are derived from carotenoids and their biosynthesis is promoted by phosphate starvation. *New Phytologist*. 2008; 178:863–74. <https://doi.org/10.1111/j.1469-8137.2008.02406.x> PMID: 18346111
62. Decker EL, Alder A, Hunn S, Ferguson J, Lehtonen MT, Scheler B, et al. Strigolactone biosynthesis is evolutionarily conserved, regulated by phosphate starvation and contributes to resistance against phytopathogenic fungi in a moss, *Physcomitrella patens*. *New Phytologist*. 2017; 216:455–68. <https://doi.org/10.1111/nph.14506> PMID: 28262967
63. Sun H, Tao J, Liu S, Huang S, Chen S, Xie X, et al. Strigolactones are involved in phosphate- and nitrate-deficiency-induced root development and auxin transport in rice. *Journal of Experimental Botany*. 2014; 65:6735–46. <https://doi.org/10.1093/jxb/eru029> PMID: 24596173
64. Sun X-D, Ni M. HYPOSENSITIVE TO LIGHT, an alpha/beta fold protein, acts downstream of ELONGATED HYPOCOTYL 5 to regulate seedling de-etiolation. *Molecular Plant*. 2011; 4:116–26. <https://doi.org/10.1093/mp/ssf055> PMID: 20864454
65. Booker J, Sieberer T, Wright W, Williamson L, Willett B, Stirnberg P, et al. MAX1 encodes a cytochrome P450 family member that acts downstream of MAX3/4 to produce a carotenoid-derived branch-inhibiting hormone. *Developmental Cell*. 2005; 8:443–9. <https://doi.org/10.1016/j.devcel.2005.01.009> PMID: 15737939
66. Bennett T, Liang Y, Seale M, Ward S, Müller D, Leyser O. Strigolactone regulates shoot development through a core signalling pathway. *Biology Open*. 2016; 5:1806–20. <https://doi.org/10.1242/bio.021402> PMID: 27793831
67. Stirnberg P, van De Sande K, Leyser HO. MAX1 and MAX2 control shoot lateral branching in *Arabidopsis*. *Development*. 2002; 129:1131–41. PMID: 11874909
68. Wilson AK, Pickett FB, Turner JC, Estelle M. A dominant mutation in *Arabidopsis* confers resistance to auxin, ethylene and abscisic acid. *Molecular and General Genetics MGG*. 1990; 222:377–83. <https://doi.org/10.1007/bf00633843> PMID: 2148800
69. Rutherford R, Masson PH. *Arabidopsis thaliana sku* mutant seedlings show exaggerated surface-dependent alteration in root growth vector. *Plant Physiology*. 1996; 111:987–98. <https://doi.org/10.1104/pp.111.4.987> PMID: 8756492
70. Grabov A, Ashley M, Rigas S, Hatzopoulos P, Dolan L, Vicente-Agullo F. Morphometric analysis of root shape. *New Phytologist*. 2005; 165:641–52. <https://doi.org/10.1111/j.1469-8137.2004.01258.x> PMID: 15720674
71. Vaughn LM, Masson PH. A QTL study for regions contributing to *Arabidopsis thaliana* root skewing on tilted surfaces. *G3: Genes, Genomes, Genetics*. 2011; 1:105–15.
72. Masucci JD, Schiefelbein JW. The *rhd6* mutation of *Arabidopsis thaliana* alters root-hair initiation through an auxin- and ethylene-associated process. *Plant Physiology*. 1994; 106:1335–46. <https://doi.org/10.1104/pp.106.4.1335> PMID: 12232412

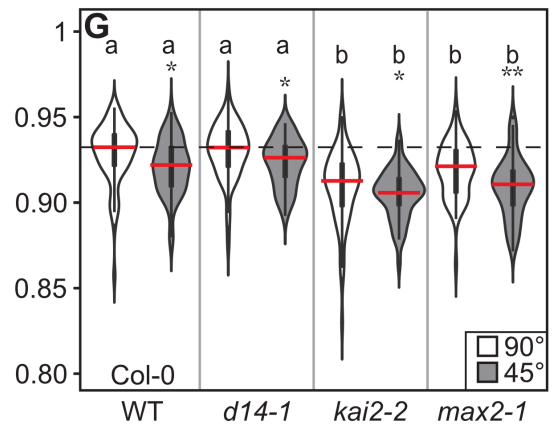
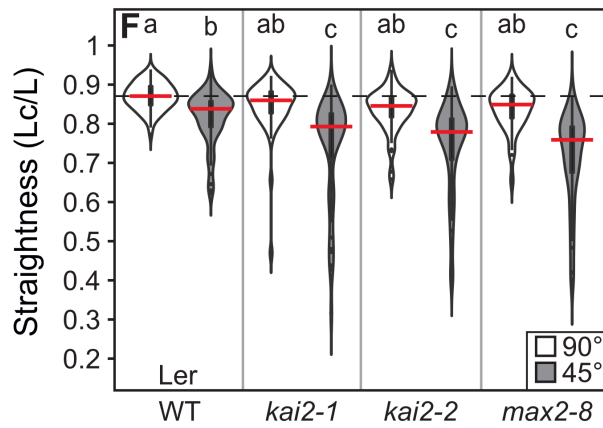
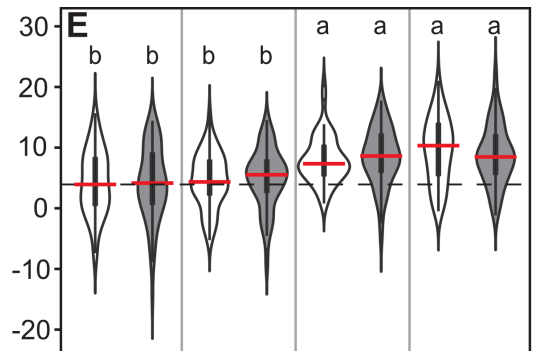
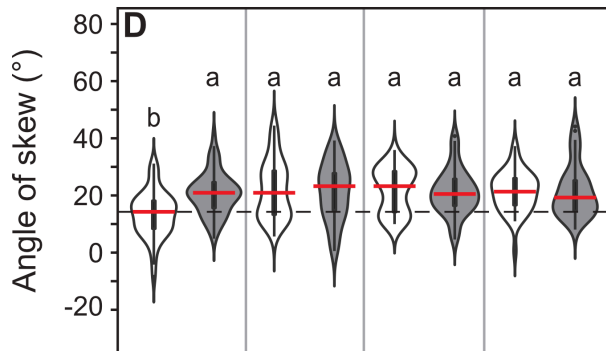
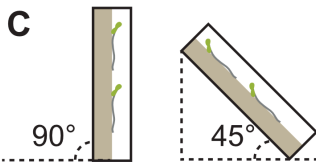
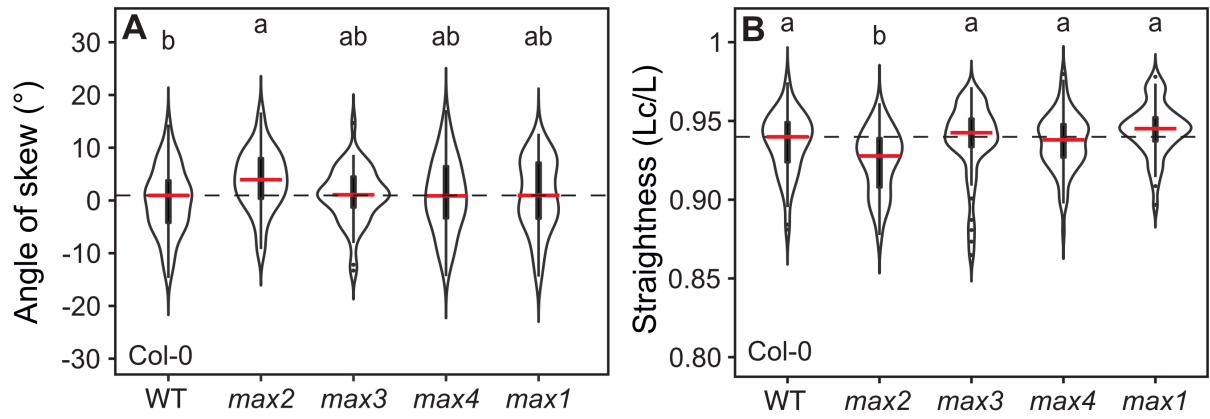
| Experiment    |     | 1   | 2   | 3   | 4   | 5   |
|---------------|-----|-----|-----|-----|-----|-----|
| <i>max3-9</i> | PRL | 89  | 75  | 86  | 87  | 97  |
|               | LRD | 125 | 105 | 98  | 105 | 108 |
| <i>max4-5</i> | PRL | 89  | 95  | 88  | 85  | 81  |
|               | LRD | 128 | 105 | 106 | 101 | 108 |
| <i>max1-1</i> | PRL | 95  | 80  | 83  | 82  | 88  |
|               | LRD | 124 | 89  | 107 | 92  | 116 |
| <i>d14-1</i>  | PRL | 110 | 108 | 79  | 87  | 92  |
|               | LRD | 125 | 115 | 86  | 86  | 116 |

|             |
|-------------|
| < -15%      |
| -15% to -5% |
| ±5%         |
| 5% to 15%   |
| >15%        |

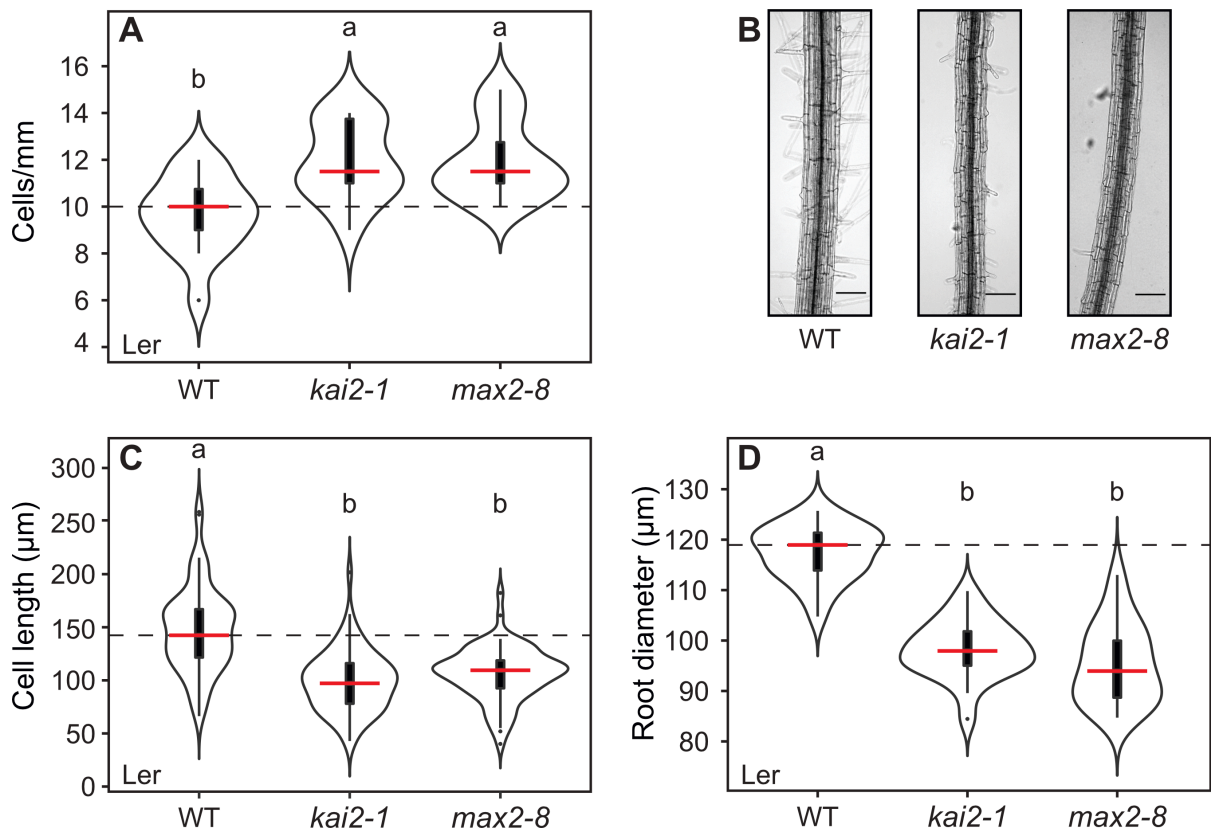
**S1 Fig. Variation in root growth parameters in strigolactone synthesis and perception mutants.** Mean primary root lengths (PRL) and mean lateral root densities (LRD) for strigolactone synthesis mutants (*max1-1*, *max3-9*, *max4-5*) and perception mutants (*d14-1*) across 5 different experiments. Values shown are quoted as a percentage, relative to the mean value for the Col-0 wild-type control in the same experiment (set to 100). Shading of cells represents percent below or above the mean of the wild type. Strong reductions in PRL are never accompanied by strong increase in LRD, and strong increases in LRD are never accompanied by strong reductions in PRL.



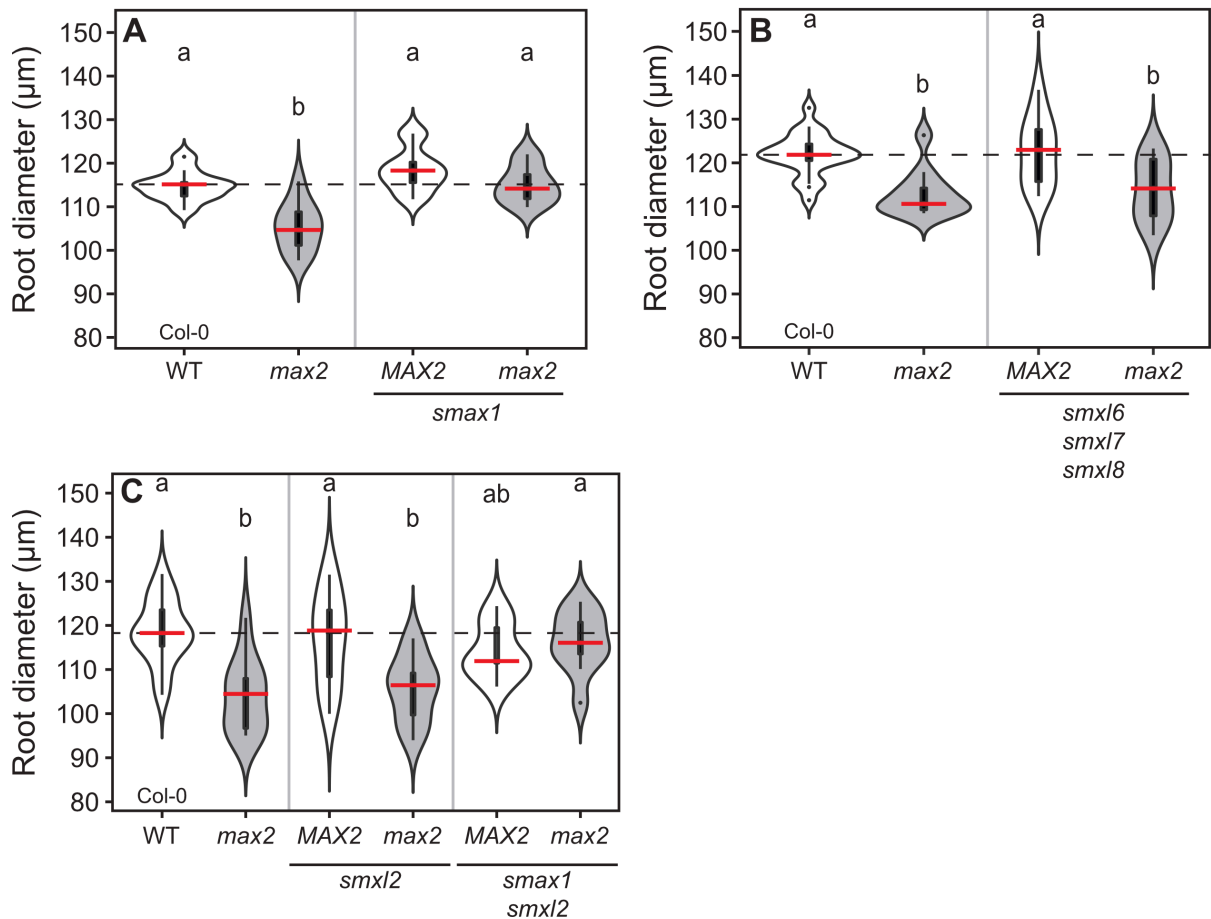
**S2 Fig. KL signaling regulates lateral root density.** (A) Lateral root density of the indicated genotypes. (B) Lateral root density at 6, 8 or 10 days post germination (dpg). The outline of the violin plot represents the probability of the kernel density. Black boxes represent interquartile ranges (IQR), with the red horizontal line representing the median; whiskers extend to the highest and lowest data point but no more than  $\pm 1.5$  times the IQR from the box; outliers are plotted individually. Percentage numbers indicate the percent significant difference between the median of each indicated genotype and the median of the wild type at the same time point. Different letters indicate different statistical groups (A) ANOVA, posthoc Tukey,  $F_{2,79} = 5.29$ ,  $n = 24-30$ ,  $p < 0.01$ . Asterisks indicate a significant difference compared to wild type for each time point. (B) ANOVA, post-hoc Dunnett's tests comparing to wild-type, at each time-point,  $F_{11,239} = 47.87$ ,  $n = 14-24$ ; \* $p \leq 0.05$ , \*\* $p \leq 0.01$ , \*\*\* $p \leq 0.001$ ).



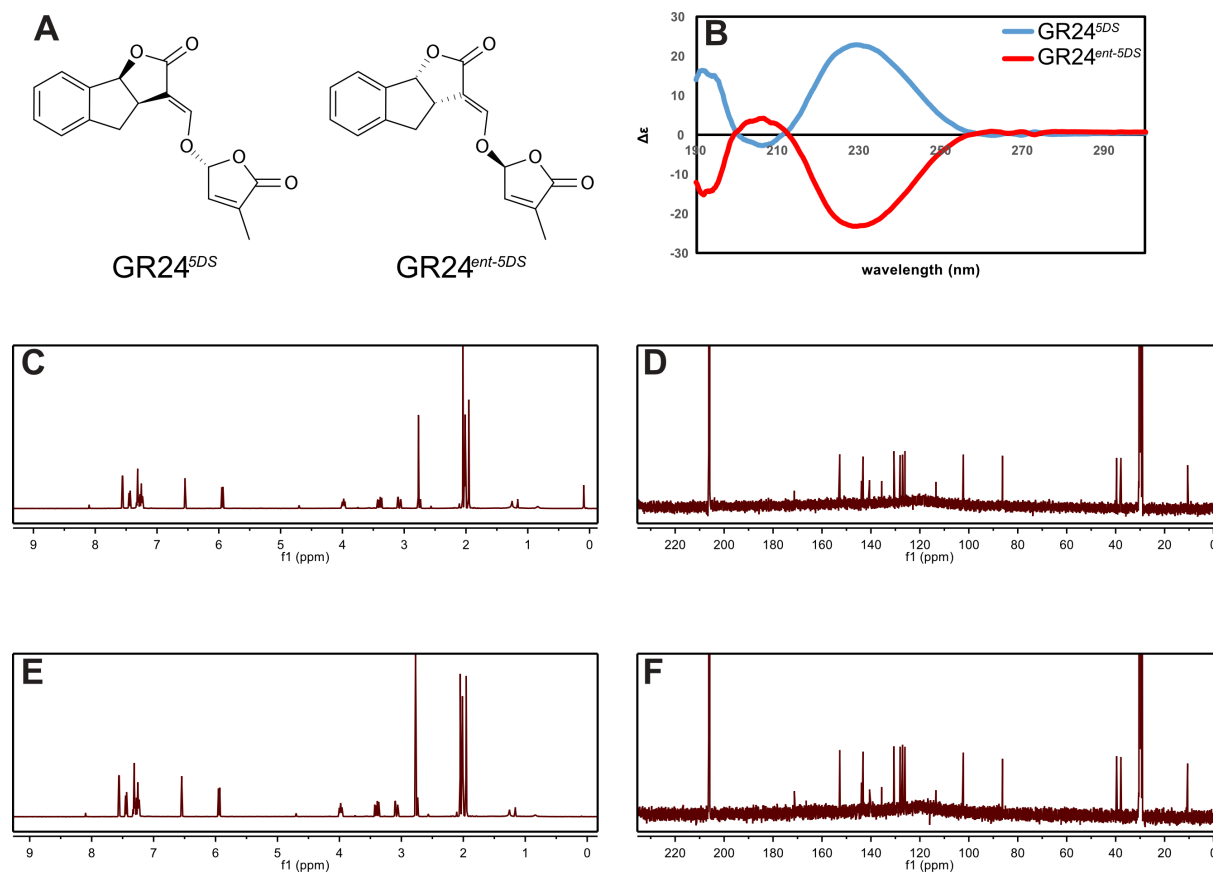
**S3 Fig. KAR perception mutants respond to tilted agar surface.** (A, D, E) Root skewing and (B, F, G) root straightness of the indicated genotypes. In (A, B) plants were grown at a 90° angle. (D-E) Plants were grown either at a 90° angle (white violins) or a 45° angle (grey violins) as shown in the diagram in (C). The outline of the violin plots represents the probability of the kernel density. Black boxes represent interquartile ranges (IQR), with the red horizontal line representing the median; whiskers extend to the highest and lowest data point but no more than  $\pm 1.5$  times the IQR from the box; outliers are plotted individually. Different letters indicate different statistical groups (ANOVA, posthoc Tukey,  $p \leq 0.001$ ,  $n > 40$  (A)  $F_{5,333} = 5.057$  (B)  $F_{4,290} = 7.168$  (D)  $F_{7,383} = 5.788$  (E)  $F_{7,472} = 12.54$  (F)  $F_{7,430} = 25.89$  (G)  $F_{7,497} = 18.36$ ).



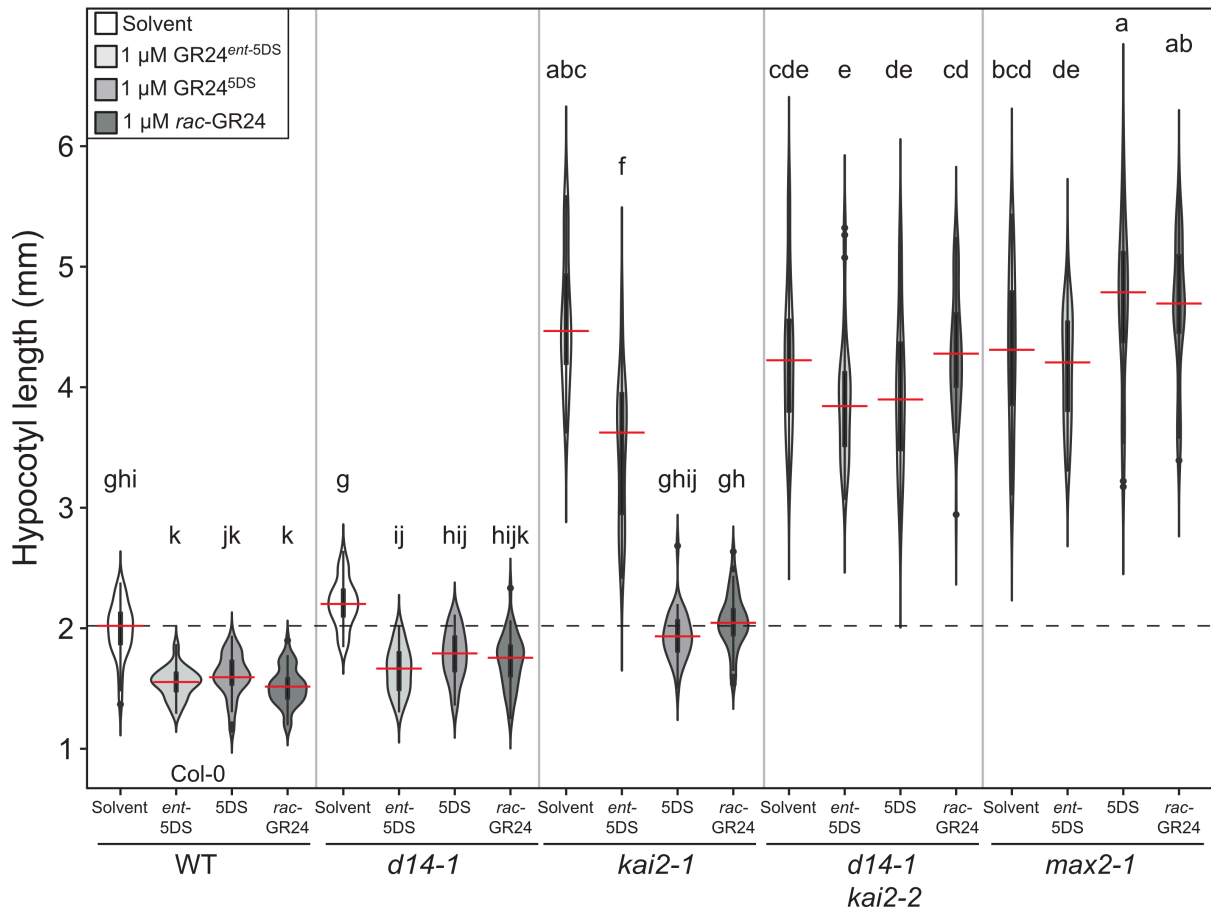
**S4 Fig. KL perception mutants in the Ler background exhibit decreased epidermal cell lengths and root diameter.** (A) Number of root epidermal cells per mm of the indicated genotypes. (B) Images of representative roots between 2 and 3 mm from the root tip from 5-daysold seedlings of the indicated genotypes. Scale bars, 0.1 mm. (C) Root cell length and (D) and root diameter of the indicated genotypes. The outline of the violin plots represent the probability of the kernel density. Black boxes represent interquartile ranges (IQR), with the red horizontal line representing the median; whiskers extend to the highest and lowest data point but no more than  $\pm 1.5$  times the IQR from the box; outliers are plotted individually. Different letters indicate different statistical groups (ANOVA, posthoc Tukey,  $p \leq 0.001$ ) (A)  $F_{2,43} = 9.58$ ,  $n = 13-18$  (C)  $F_{2,191} = 43.1$ ,  $n = 10-11$  (D)  $F_{2,64} = 77.45$ ,  $n = 21$ ).



**S5 Fig. Regulation of root skewing by KAI2 can be genetically separated from root diameter.** (A, B, C) Root diameter of Col-0 wild type and the indicated genotypes (the mutant alleles are *max2-1*, *smax1-2*, *smxl2-1*, *smxl6-4*, *smxl7-3* and *smxl8-1*). The outline of the violin plot represents the probability of the kernel density. Black boxes represent interquartile ranges (IQR), with the red horizontal line representing the median; whiskers extend to the highest and lowest data point but no more than  $\pm 1.5$  times the IQR from the box; outliers are plotted individually. Different letters indicate different statistical groups (ANOVA, posthoc Tukey,  $p \leq 0.001$ , (A)  $F_{3,38} = 15.04$ ,  $n = 10-11$  (B)  $F_{3,38} = 15.04$ ,  $n = 8-21$  (C)  $F_{3,47} = 8.221$ ,  $n = 10-11$ ).



**S6 Fig. Purity evaluation of SL stereoisomers.** (A) Chemical structures of GR24<sup>5DS</sup> and GR24<sup>ent-5DS</sup>. (B) CD spectra of GR24<sup>5DS</sup> and GR24<sup>ent-5DS</sup>. (C) <sup>1</sup>H-NMR (400 MHz, 298 K, (CD<sub>3</sub>)<sub>2</sub>CO) of GR24<sup>5DS</sup>. (D) <sup>13</sup>C-NMR (100 MHz, 298 K, (CD<sub>3</sub>)<sub>2</sub>CO) of GR24<sup>5DS</sup>. (E) <sup>1</sup>H-NMR (400 MHz, 298 K, (CD<sub>3</sub>)<sub>2</sub>CO) of GR24<sup>ent-5DS</sup>. (F) <sup>13</sup>C-NMR (100 MHz, 298 K, (CD<sub>3</sub>)<sub>2</sub>CO) of GR24<sup>ent-5DS</sup>. For more information see [Materials and Methods](#).



**S7 Fig. GR24 stereoisomers regulate hypocotyl length through D14 and KAI2.** Hypocotyl length of the indicated genotypes treated with solvent (acetone), 1 μM GR24<sup>ent-5DS</sup>, 1 μM GR24<sup>5DS</sup> or 1 μM *rac*-GR24. The outline of the violin plot represents the probability of the kernel density. Black boxes represent interquartile ranges (IQR), with the red horizontal line representing the median; whiskers extend to the highest and lowest data point but no more than ±1.5 times the IQR from the box; outliers are plotted individually. Different letters indicate different statistical groups (ANOVA, posthoc Tukey,  $F_{2,43} = 9.58$ ,  $n = 32-42$ ,  $p \leq 0.001$ ).

**Supplemental Table S1.** Summary of effects of *SMXL* mutations on *max2* root phenotypes.

|                      | <i>max2</i>  |              |                    |                  |
|----------------------|--------------|--------------|--------------------|------------------|
|                      | <i>smax1</i> | <i>smxl2</i> | <i>smax1 smxl2</i> | <i>smxl6,7,8</i> |
| Lateral root density |              |              | +                  | +                |
| Root hair density    | -            | -            | +                  | -                |
| Root hair length     | -            | -            | +                  | -                |
| Root skewing         | +            | +            | +                  | +/-              |
| Root straightness    | -            | -            | +                  | -                |
| Root diameter        | +            | -            | +                  | -                |

+ Suppression of *max2* phenotypes

- No suppression of *max2* phenotypes

+/- Opposite effects in Munich (+) and Leeds (-)

**Paper II:** Extensive signal integration by the phytohormone protein network

Reference: Altmann, M.; Altmann, S.; Rodriguez, P.; Weller, B.; Elorduy Vergara, L.; Palme, J.; Marin-de la Rosa, N.; Sauer, M.; Wenig, M.; **Villaécija-Aguilar, J.A.**; Sales, J.; Lin, Chung-Wen; Pandiarajan, R.; Young, V.; Strobel, A.; Groß, L.; Carbonnel, S.; Kugler, K.; Garcia-Molina A.; Bassel, G.; Falter, C.; Mayer, K.; Gutjahr, C.; Vlot-Schuster, C.; Grill, E.; Falter-Braun, P. Extensive signal integration revealed by a phytohormone protein interactome map. **Nature**. 2020.

*Nature* <https://doi.org/10.1038/s41586-020-2460-0> Published online 1 July 2020

## TITLE

**Extensive signal integration by the phytohormone protein network**

## AUTHORS

**Melina Altmann<sup>1\*</sup>, Stefan Altmann<sup>1\*</sup>, Patricia A. Rodriguez<sup>1</sup>, Benjamin Weller<sup>1</sup>, Lena Elorduy Vergara<sup>1</sup>, Julius Palme<sup>1,2</sup>, Nora Marín-de la Rosa<sup>1</sup>, Mayra Sauer<sup>1</sup>, Marion Wenig<sup>3</sup>, José Antonio Villaécija-Aguilar<sup>4</sup>, Jennifer Sales<sup>3</sup>, Chung-Wen Lin<sup>1</sup>, Ramakrishnan Pandiarajan<sup>1</sup>, Veronika Young<sup>1</sup>, Alexandra Strobel<sup>1</sup>, Lisa Gross<sup>5</sup>, Samy Carbonnel<sup>6</sup>, Karl G. Kugler<sup>7</sup>, Antoni Garcia-Molina<sup>1,8</sup>, George W. Bassel<sup>9</sup>, Claudia Falter<sup>1</sup>, Klaus F. X. Mayer<sup>7,10</sup>, Caroline Gutjahr<sup>4,6</sup>, A. Corina Vlot<sup>3</sup>, Erwin Grill<sup>5</sup> & Pascal Falter-Braun<sup>1,11</sup>**

<sup>1</sup>*Institute of Network Biology (INET), Helmholtz Center Munich, German Research Center for Environmental Health, Munich-Neuherberg, Germany*

<sup>2</sup>*current address: Department of Genetics, Harvard Medical School, Boston, MA, USA*

<sup>3</sup>*Inducible Resistance Signaling Group, Institute of Biochemical Plant Pathology (BIOP), Helmholtz Center Munich, German Research Center for Environmental Health, Munich-Neuherberg, Germany*

<sup>4</sup>*Plant Genetics, School of Life Sciences Weihenstephan, Technical University of Munich (TUM), Freising, Germany*

<sup>5</sup>*Botany, School of Life Sciences Weihenstephan, Technical University of Munich (TUM), Freising, Germany*

<sup>6</sup>*Genetics, Faculty of Biology, Ludwig-Maximilians-Universität (LMU) München, Planegg-Martinsried, Germany.*

<sup>7</sup>*Plant Genome and Systems Biology (PGSB), Helmholtz Center Munich, German Research Center for Environmental Health, Munich-Neuherberg, Germany*

<sup>8</sup>*current address: Plant Molecular Biology, Faculty of Biology, Ludwig-Maximilians-Universität (LMU) München, Planegg-Martinsried, Germany*

<sup>9</sup>*School of Biosciences, University of Birmingham, Birmingham B15 2TT, UK*

<sup>10</sup>*School of Life Sciences Weihenstephan, Technical University of Munich (TUM), Freising, Germany*

<sup>11</sup>*Microbe-Host Interactions, Faculty of Biology, Ludwig-Maximilians-Universität (LMU) München, Planegg-Martinsried, Germany.*

**Running title:** Arabidopsis phytohormone interactome map

**Corresponding author:** Pascal Falter-Braun, [pascal.falter-braun@helmholtz-muenchen.de](mailto:pascal.falter-braun@helmholtz-muenchen.de)

**Keywords:** Arabidopsis, hormone signaling, systems biology, crosstalk, network, interactome

\*These authors contributed equally to this work.

**Plant hormones orchestrate responses to environmental cues with developmental programs<sup>1</sup>, and are fundamental for stress resilience and agronomic yield<sup>2</sup>. The core signaling pathways have been elucidated by genetic screens and hypothesis-driven approaches, and extended by interactome studies for select pathways<sup>3</sup>. However, fundamental questions remain about how information from different pathways is integrated. Genetically most phenotypes are regulated by multiple hormones, whereas transcriptional profiling suggests that hormones trigger largely exclusive transcriptional programs<sup>4</sup>. We hypothesized that protein-protein interactions play an important role in phytohormone signal integration. Therefore, we generated experimentally a systems-level map of the Arabidopsis phytohormone signaling network consisting of more than 2,000 binary protein-protein interactions. In the highly interconnected network, pathway communities and hundreds of novel pathway contact points can be identified that represent potential points of crosstalk. Functional validation of candidates in seven hormone pathways demonstrate novel functions for 74% of tested proteins in 84% of candidate interactions, and indicate that a large majority of signaling proteins function pleiotropically in multiple pathways. Moreover, we identify several hundred largely small-molecule-dependent interactions of hormone receptors. Comparison with previous reports suggests that non-canonical and non-transcription mediated receptor-signaling is more common than currently appreciated.**

**Phytohormone network mapping and analysis**

To examine phytohormone signal integration by the plant protein network we first identified 1,252 genes with likely or genetically demonstrated functions in phytohormone signaling (**Fig. 1a, Supplementary Table 1**). The corresponding network of literature curated binary interactions (LCI) from the IntAct database<sup>5</sup> (LCI<sub>IntA</sub>) shows extensive intra-pathway but sparse inter-pathway connectivity (**Extended Data Fig. 1**), which could reflect an insulated organization of hormone signaling or be an artifact of inspection biases<sup>6</sup>. We therefore experimentally generated a systematic (unbiased design) map of the phytohormone signaling network. After cloning open reading frames (ORFs) for 1,226 (98%) of the selected genes (PhyHormORFeome), five-fold interrogation of the pairwise matrix using a high-quality yeast-2-hybrid (Y2H)-based mapping pipeline<sup>7</sup> yielded the phytohormone interactome main (PhI<sub>MAIN</sub>) network. To find links into the broader Arabidopsis network, PhyHormORFeome was screened against ~13,000 Arabidopsis ORFs<sup>8</sup> resulting in an asymmetric PhI<sub>EXT</sub> dataset. Moreover, we conducted focused screens for pathway-specific repressors with transcription factors<sup>9</sup> (TFs), and for hormone-dependent interactions of phytohormone receptors. In the stringent final step of the common Y2H pipeline all candidate pairs were four-fold verified (**Fig. 1b**). The combined PhI network contains 2,072 interactions, of which 1,572 are novel (**Fig. 1c, Extended Data Fig. 1, Supplementary Table 2**). The interaction-density in the symmetrically interrogated PhI<sub>MAIN</sub> (0.4‰) is higher than in the proteome-scale Arabidopsis Interactome-1 (AI-1, 0.1‰)<sup>10</sup>, but lower than in the ABA-focused interactome (7.5‰)<sup>3</sup>. Likely, the increasing focus on functionally coherent proteins is underlying this trend, but also system differences<sup>11</sup> and screening parameters<sup>12</sup> affect overall sensitivity. We implemented our interactome mapping framework<sup>6,12</sup> to compare PhI to literature-based network maps from IntAct and BioGrid<sup>13</sup> (LCI<sub>BioG</sub>). Sampling sensitivity of PhI<sub>MAIN</sub> after five repeat screens was 86% ± 5% (**Fig. 1d**). For benchmarking, we re curated<sup>12</sup> a positive

and a random reference set ( $PRS_{\text{PhI}}/RRS_{\text{PhI}}$ ) of 92 and 95 protein pairs (**Supplementary Table 2**), respectively. Benchmarking our Y2H system yielded an unconditional assay sensitivity of 20.4% (**Fig. 1e**); excluding hormone-dependent  $PRS_{\text{PhI}}$  interactions increased this to 23%. The resulting overall completion of  $16.0\% \pm 6.8\%$  matches the overlap with LCI datasets (**Fig. 1g**). Thus, missed interactions explain the incomplete overlap between  $\text{PhI}_{\text{MAIN}}$  and  $\text{LCI}_{\text{PhI}}$  suggesting a low false-discovery rate. This is substantiated by the observation that no  $RRS_{\text{PhI}}$  pair scored positive (**Fig. 1e**). To further assess PhI quality, we used a pull-down assay in which protein pairs are expressed in wheat-germ lysate and, following an anti-FLAG immunoprecipitation, interactions are detected via activity of renilla luciferase-fused second protein. Benchmarking this assay with  $PRS_{\text{PhI}}/RRS_{\text{PhI}}$  revealed an assay performance similar to previous implementations<sup>10,11</sup>; the slightly increased background likely results from the functionally relative coherent search space from which RRS was sampled. Subsequent testing of 285 interactions from the unconditional  $\text{PhI}_{\text{MAIN}}$ ,  $\text{PhI}_{\text{EXT}}$ , and  $\text{PhI}_{\text{REP}}$  subsets yielded a PhI validation rate of 22.5%, which is indistinguishable from  $PRS_{\text{PhI}}$  (23.5%, **Fig. 1f**) and similar for the individual subsets (**Extended Data Fig. 1**). These data demonstrate that PhI is a high-quality map of the Arabidopsis phytohormone signaling network on par with high-quality literature data.

For hypothesis generation and local network analyses the full PhI will be most useful. For topological and systems-level questions the symmetrically mapped  $\text{PhI}_{\text{MAIN}}$  should be employed to avoid biases<sup>6</sup>.  $\text{PhI}_{\text{MAIN}}$  has a scale-free degree-distribution and, in contrast to  $\text{LCI}_{\text{PhI}}$  networks, a hierarchical modularity as expected for unbiased network maps (**Fig. 1h, Extended Data Fig. 1**)<sup>14</sup>. We used  $\text{PhI}_{\text{MAIN}}$  to investigate the topological organization of phytohormone signaling pathways.

Important features of hierarchical networks are highly connected hubs and interconnected communities<sup>14</sup>. Using an edge-betweenness-based detection algorithm<sup>15</sup>, we identified 21 network communities in  $\text{PhI}_{\text{MAIN}}$ , of which nine were significantly enriched in different phytohormone pathways (**Fig. 1i**, **Extended Data Fig. 2**, **Supplementary Tables 3, 4**). Thus, the topology of  $\text{PhI}_{\text{MAIN}}$  recapitulates biological knowledge and confirms that at least some pathway proteins are highly interconnected. Additionally, most communities encompass proteins from different pathways that possibly mediate crosstalk. In the JA community, e.g., the canonical JA TF MYC2 is physically linked to ABA signaling via interaction with the protein kinase CIPK14 (**Fig. 1j**), validated by *in vitro* pull-down and bimolecular fluorescence complementation (BiFC) (**Extended Data Fig. 2**). Additional pathway contacts occur between different communities (**Fig. 1j**). However, on average only 27% of pathway proteins reside within the corresponding communities indicating that phytohormone signaling may not be predominantly organized in topological communities (**Supplementary Table 3**).

We next analyzed inter-pathway connectivity. The distances between the phytohormone pathways are considerably shorter in  $\text{PhI}_{\text{MAIN}}$  than in  $\text{LCI}_{\text{PhI}}$  (**Fig. 1k, I**). This is mirrored by significantly more pathway contact points (PCPs) in  $\text{PhI}_{\text{MAIN}}$  than  $\text{LCI}_{\text{PhI}}$ , *i.e.* protein interaction-mediated contacts between different pathways. As some proteins operate in multiple pathways, we distinguished 192 Type I PCPs ( $\text{PCP}_{\text{I}}$ ) of proteins with strictly different annotations from 248 Type II PCPs ( $\text{PCP}_{\text{II}}$ ), where the interactors share annotations, but at least one has additional functions (**Fig. 1m**). Bootstrap subsampling confirmed that  $\text{PhI}_{\text{MAIN}}$  contains significantly more  $\text{PCP}_{\text{I}}$  (**Fig. 1n**), but not  $\text{PCP}_{\text{II}}$  (not shown), than  $\text{LCI}_{\text{IntA}}$  or  $\text{LCI}_{\text{BioG}}$ , and this is valid for essentially all pathway-pairs (**Extended Data Fig. 3**). Each PCP supports a specific crosstalk hypothesis and the abundance of PCPs suggests extensive protein-interaction mediated information exchange among pathways.

## Validation of pathway contact points

We experimentally tested if PCPs reflect yet unknown functions of the interacting partners. Assays for most hormones are established in seedlings. Therefore, and for standardization, we focused on seedling-expressed PCP interaction pairs. Validated homozygous T-DNA lines for 19 pairs were evaluated in response-assays for six different phytohormones to establish whether the candidates function in the pathway of their respective partner (**Fig. 2a - f, Extended Data Figs. 4 - 7, Supplementary Table 5**).

ABA regulates seed germination and desiccation stress responses including root growth<sup>16</sup>. In the presence of 0.3  $\mu$ M ABA, germination of *WT* seeds was ~40% decreased. In contrast, the candidate lines *ddl*<sub>Lit\_ET</sub> and *eds1*<sub>Lit\_SA</sub> displayed a similar ABA-hypersensitivity as the *rcar1* control. Root growth was significantly less affected in five candidate lines resulting in altogether six lines (66%) with a novel ABA phenotype (**Fig. 2a, b, Extended Data Fig. 4**).

Anthocyanin production is a widely used assay for CK signaling<sup>17</sup>. At low concentrations CK-induced anthocyanin accumulation was impaired in the candidate lines similar to the *spy* control. At higher concentrations *myc2*<sub>Lit\_JA/ABA</sub> remained similar to *spy* whereas *jaz1*<sub>Lit\_JA/ABA</sub> over-accumulated anthocyanin indicating complexity in CK signaling (**Fig. 2c, d**).

For ET we assayed the triple response, *i.e.* formation of exaggerated apical hooks (loops) and development of shorter and thicker roots and hypocotyls in dark-grown seedlings<sup>18</sup>. Ten of our twelve candidates (83%) displayed an apical loop phenotype; seven of these additionally displayed a root growth phenotype, and *tfl* also had a hypocotyl growth defect following ACC treatment (**Fig. 2e, Extended Data Fig. 5**). To ensure specificity we tested six mutant lines for proteins in PhI that showed no interaction with ET annotated proteins. Of these controls only one displayed a weak

root growth phenotype and none exhibited a hypocotyl or loop formation defect (**Fig. 2e, Extended Data Fig. 6**).

Salicylic acid (SA) mediates defense responses to (hemi-) biotrophic pathogens<sup>19</sup>. Following inoculation with *Pseudomonas syringae* pv. tomato (*Pst*), titers in the *gi*<sub>Lit\_GA</sub> mutant were significantly elevated indicating enhanced disease susceptibility and impaired SA signaling. Similarly, leaves of mature *rcar1*<sub>Lit\_ABA</sub> and *pp2ca*<sub>Lit\_ABA</sub> plants supported enhanced *Pst* growth (**Fig. 2f**). Assays for root growth inhibition by brassinosteroids, gibberellins, and jasmonates revealed new phenotypes for two or one candidates, respectively (**Extended Data Fig. 4**).

Altogether, interactome-guided phenotyping revealed a function in new pathways for 74% of tested proteins (20/27) involved in 84% of interactions in the validation set (**Fig. 2g; Extended Data Fig. 7**). Notably, for all PCP<sub>I</sub> pairs a novel function was revealed for at least one partner, such that all interactions are substantiated by phenotypes in at least one common pathway (**Fig. 2g**). For three of the six PCP<sub>II</sub> pairs an additional common pathway was identified, such that more than half (11/19) of all PCP pairs genetically operate in two common pathways (**Fig. 2g**). To support these functional data we demonstrate for nine pairs *in planta* interactions by BiFC (**Fig. 2h, Extended Data Fig 7**). Intriguingly, prior to our experiments a large majority of signaling proteins in the literature and in our validation set were considered pathway-specific (**Fig. 2i**). After the interactome-guided phenotyping however, 82% of proteins in the validation set are known to function in multiple pathways, whereas only one-fifth is single-pathway specific (**Fig. 2g, i**). The new annotations are distributed across different pathways (**Extended Data Fig. 7**) and the network degree is not correlated to the number of phenotypes (not shown). As the validation set is not obviously biased, the observation of widespread pleiotropy may extrapolate to most of the phytohormone signaling network. Thus, our data point to a highly integrated central signal-processing

network that channels different inputs into a balanced multifactorial output. To facilitate further studies, we provide an expression-based ‘edge-score’ indicating the possibility of each PhI interaction occurring in different plant tissues (**Supplementary Table 6**).

### **Hormone-receptor interactions**

Input into the central processing unit is provided by hormone receptors, which often initiate signaling via small molecule-regulated protein-interactions<sup>20</sup>. To better understand initial phytohormone-signaling, we conducted interaction screens with soluble hormone receptors in the presence and absence of their cognate hormone. For ABA, GA, IAA, KAR, SA, and SL-receptors 241 interactions were identified, of which 101 are hormone-dependent. Re-identified pairs include interactions of GA-receptors with DELLA proteins, and of RCAR/PYR/PYL ABA-receptors with type 2C protein phosphatases (PP2Cs) (**Fig. 3a, Extended Data Fig. 8**), which display known patterns of hormone dependence<sup>21</sup>. Notably, several ABA-receptors interacted also with TFs and other non-PP2C proteins (**Fig. 3a**). As some of these additionally link to PP2Cs, we wondered if interactions are combinatorially modulated and investigated by yeast-3-hybrid the effect of different PP2Cs on RCAR1/PYL9 interactions with MYB-family TFs. The RCAR1-MYB73 interaction was blocked by several PP2Cs, whereas the RCAR1-MYB77 interaction was enabled by ABI1/2, together demonstrating dynamic modulation of complex formation (**Fig. 3b, c**). In addition, PP2C-independent RCAR-functions have been described for RCAR9/PYL6 via MYC2<sup>22</sup> and for RCAR3/PYL8 via MYB77<sup>23</sup>. Our data suggest that such core-pathway-independent functions may be more widespread. The independently validated interaction of DELAY-OF-GERMINATION 1 (DOG1) with PP2Cs<sup>24</sup> similarly points to non-canonical PP2C-signaling mechanisms. Thus, core-pathway independent signaling and complex

multimeric interaction-regulation are important mechanisms underlying the functional diversification in the ABA signaling system.

Receptors for the defense hormone SA are the NON-EXPRESSOR OF PATHOGEN RELATED PROTEIN 1 (NPR1) and its orthologues NPR3 and NPR4<sup>25</sup>. While NPR1 is a well-studied positive regulator of defense-gene transcription, NPR3 and NPR4 are emerging as alternative negative or complementary transcriptional regulators<sup>25,26</sup>. The pattern of SA-regulated NPR3 interactions (**Fig. 3d; Extended Data Fig. 9**), especially with NIMIN proteins, differs from the described NPR1 pattern<sup>27</sup>, suggesting dynamic complexity of this signaling system. EMB1968/RFC4, a member of the replication factor C (RFC) complex, is a new interactor common to NPR1 and NPR3 possibly integrating defense with DNA repair or replication. Most novel NPR3/NPR4 interactors can be linked to immunity via mutant phenotypes or known interactions with virulence effectors and immune receptors<sup>8</sup> (**Fig. 3d; Extended Data Fig. 9**). These data support the biological validity of the interactions and indicate that SA-receptors also act via non-transcriptional signaling.

The karrikin (KAR) and strigolactone (SL) pathways have been discovered most recently and mediate germination (KAR) and diverse aspects of development and organismal interactions<sup>28</sup>. We screened the KAR-receptor KAI2 and SL-receptor D14 together with the F-box protein MAX2 in the absence and presence of a stereoisomer-mix of two synthetic strigolactones, which bind to D14 and KAI2, respectively<sup>29</sup>. For KAI2 we found the previously described interaction with MAX2 and 21 novel interactors of which fifteen were hormone-dependent (**Fig. 3f, g; Extended Data Fig. 9**). Recently we described that *KAI2* regulates root hair length (RHL) and density (RHD)<sup>30</sup>. As both phenotypes are also regulated by auxin, and the hormone-dependent KAI2-interactor PP2AA2 regulates PIN auxin exporters we wondered whether PP2AA2 mediates the KAR effect on these phenotypes. Similar to *kai2-2*, *pp2aa2-2* displayed a lower RHL

and RHD than Col-0 (**Fig. 3h, i**) (**Supplementary Table 5**). Strikingly, in both *kai2-2* and *pp2aa2-2* the response to exogenous karrikin treatment was abolished, indicating that they jointly mediate signaling by the karrikin pathway.

Transcriptional changes are common outcomes of phytohormone signaling. Investigating PhI<sub>REP</sub> we found no evidence of significant hormone crosstalk at the level of transcriptional regulators from different pathways converging on TFs (not shown). Nonetheless, only a quarter of TFs interacting with regulators were previously implicated in hormone signaling (**Extended Data Fig. 10**). While most pathways converge on TCP-family TFs, which are known for their high connectivity<sup>10</sup> the vast majority of TFs interacts with repressors from one to three pathways suggesting more specific signal integration at this level.

Taken together, we present a systematic map of the Arabidopsis phytohormone signaling network, which reveals an unexpectedly high interconnectivity of the signaling pathways. If the observed level of functional pleiotropy extends into the larger hormone signaling network, the concept of dedicated signal transduction pathways may need to be revised in favor of network based models. The small-molecule dependent interactions of hormone-receptors point towards prominent roles for non-canonical signaling mechanisms. We expect that our findings and the PhI resource will stimulate important mechanistic and systems-level analysis in Arabidopsis with a significant outreach into crops.

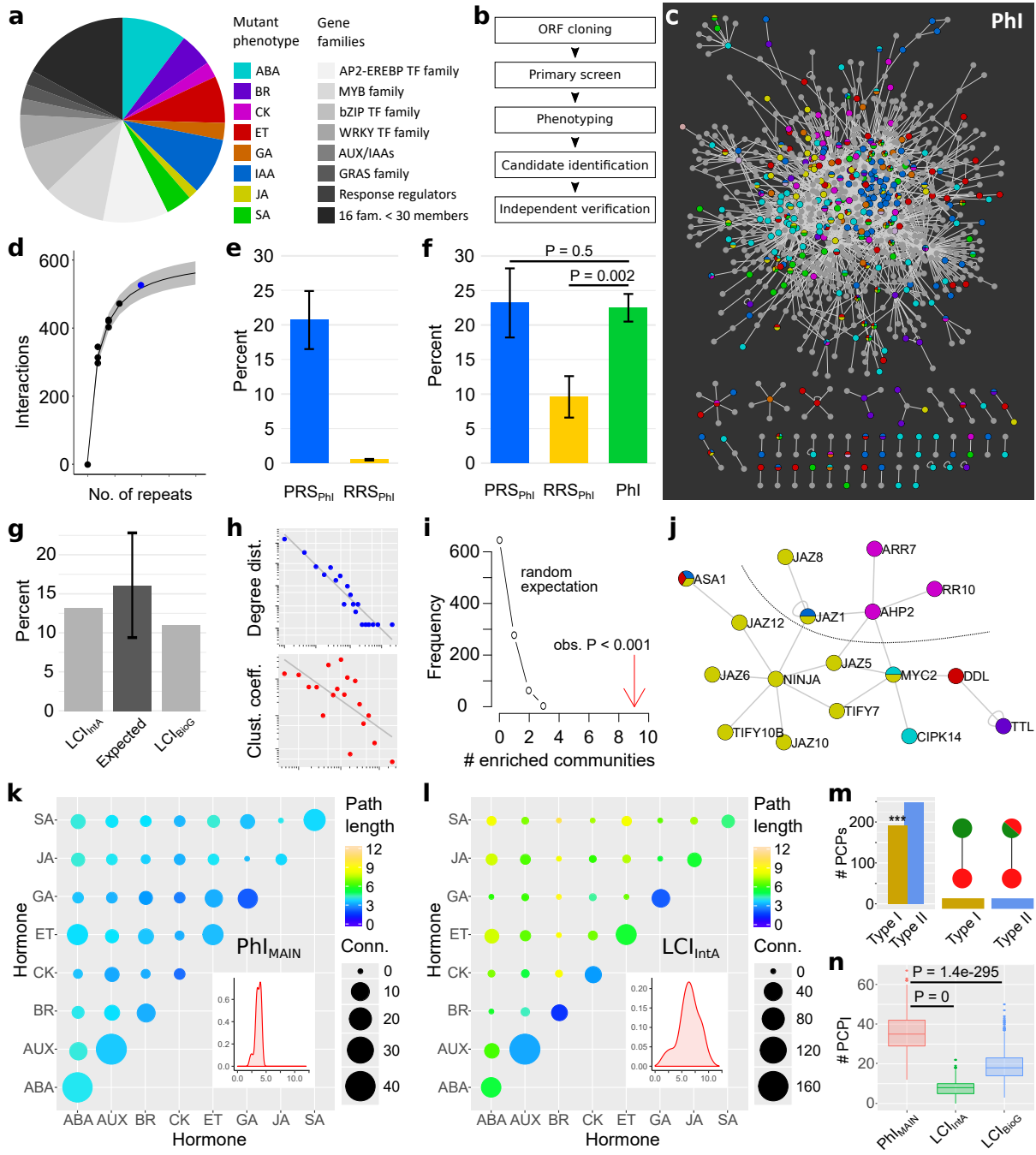


**Fig. 1 | Phytohormone network mapping and analysis.** **a**, Mutant phenotypes and overrepresented families in PhyHormORFeome candidates. **b**, Protein interaction mapping pipeline **c**, Phytohormone interactome (PhI) network. Node colors: hormone annotations (legend in a). **d**, PhI<sub>MAIN</sub> sampling sensitivity: verified interactions of first three primary-screen repeats (black dots;  $n = 3$ ); screen saturation model based on three repeats (black line, grey corridor: standard error); identified interactions after five repeats (blue dot). **e**, Y2H assay sensitivity: positive fractions of PRS<sub>PhI</sub> ( $n = 92$ ) and RRS<sub>PhI</sub> ( $n = 95$ ). Error bars: standard error. **f**, Validation results: positive fractions of PRS<sub>PhI</sub> ( $n = 69$ ), RRS<sub>PhI</sub> ( $n = 83$ ) and PhI ( $n = 285$ ). One-sided Fisher-exact, error bars: standard error of proportion. Overlap of PhI<sub>MAIN</sub> with LCI<sub>IntA</sub> ( $n = 109$ ) and LCI<sub>BioG</sub> ( $n = 150$  interactions). Error bars: propagated standard error. **h**, PhI<sub>MAIN</sub> degree and clustering coefficient distribution **i**, Number of hormone-signaling-function enriched communities in PhI<sub>MAIN</sub> (red arrow) compared to  $n = 1,000$  randomized control networks (experimental  $P < 0.001$ ). **j**, JA- and CK-enriched community links (node colors: legend in a). **k, l**, Distances between pathway combinations in PhI<sub>MAIN</sub> (**k**) and LCI<sub>IntA</sub> (**l**). Color: average shortest distance, circle size: connection count. Insets: shortest distance distributions. **m**, Count of type I ( $n = 192$ ) and type II PCPs ( $n = 248$ ) in PhI<sub>MAIN</sub> –  $P$  from analysis in **n**. **n**, Proportion of PCP<sub>I</sub> in PhI<sub>MAIN</sub> and LCI networks from bootstrap subsampling ( $n = 1,000$ ) of 100 interactions (two-sided Welch two sample t-test). Boxes: interquartile range (IQR) and median; whiskers: highest and lowest data point within 1.5 IQR; outliers plotted individually. Pathway abbreviations throughout manuscript: ABA - abscisic acid, AUX - auxin, BR - brassinosteroids, CK - cytokinins, ET - ethylene, GA - gibberellic acid, JA - jasmonic acid, KAR - karrikin, SA - salicylic acid, SL - strigolactone.

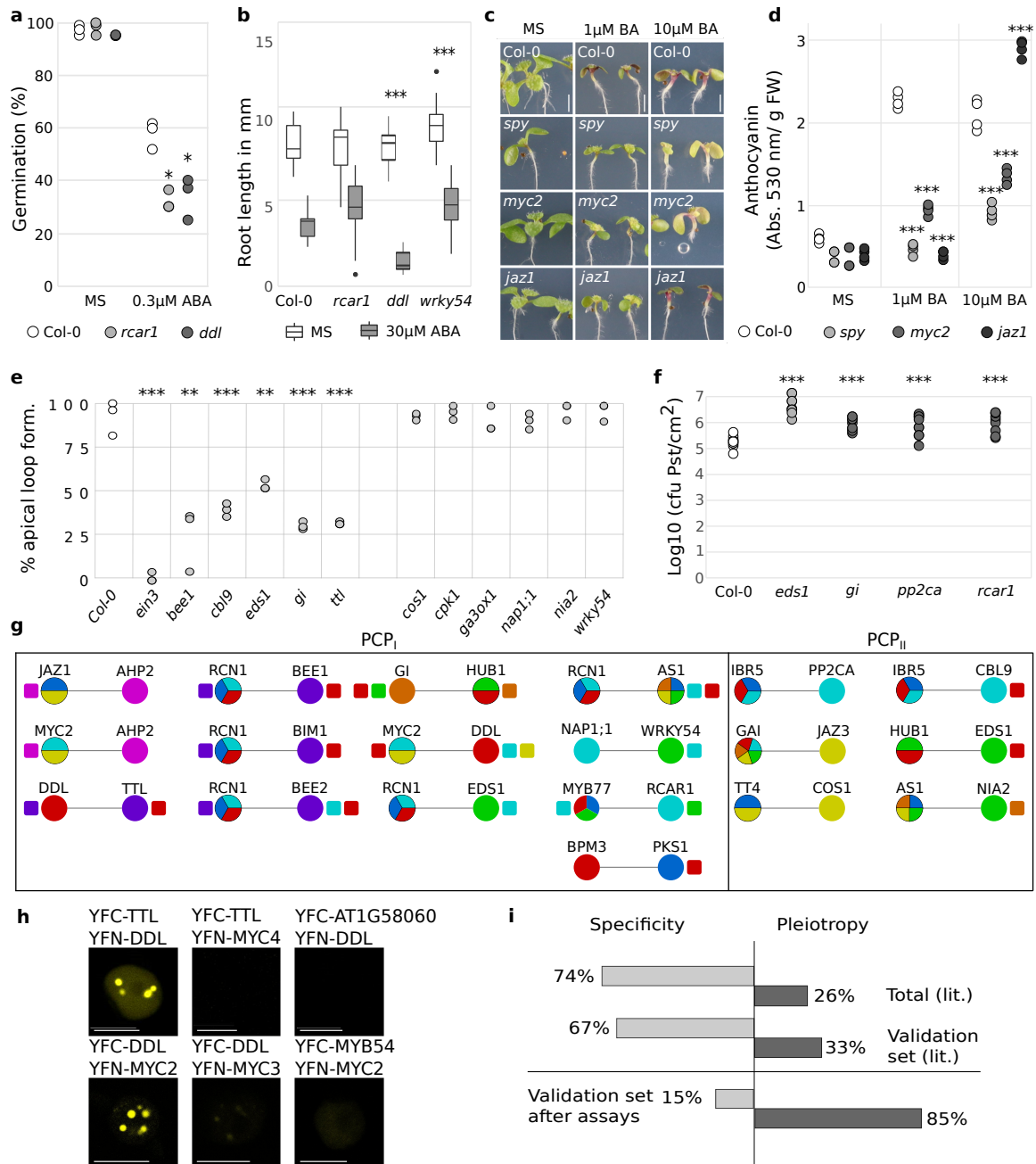


**Figure 2 | Validation of pathway contact points.** **a**, Proportion of germinating seeds in absence (MS) or presence of 0.3  $\mu\text{M}$  ABA ( $n \geq 20$ , three repeats). **b**, Root elongation in absence (MS) or presence of 30  $\mu\text{M}$  ABA. Boxes represent the interquartile range (IQR), with the bold black line representing the median; whiskers indicate highest and lowest data point within 1.5 IQR; outliers are plotted individually ( $n \geq 8$ ; two repeats). **c**, **d**, CK-dependent anthocyanin accumulation in response to indicated concentrations of 6-benzylamino purine (BA). **c**, Seedlings at 10 d after stratification following the indicated treatment. **d**, Quantified anthocyanin content per g fresh weight for lines in **c** ( $n = 15$ ; four repeats). **e**, ET induced apical loop formation in response to 10  $\mu\text{M}$  1-aminocyclopropane-carboxylic acid (ACC) ( $n \geq 10$ ; three repeats). **f**, SA-associated phenotypes in response to inoculation with *Pseudomonas syringae* pv. tomato (*Pst*). *In planta* *Pst* titers ( $n = 9$ ). **g**, Summary of hormone validation assays for 19 PCP. Node colors indicate known pathway annotations. Square colors indicate new phenotypes. Colors according to legend in 1a. **h**, Bimolecular fluorescent complementation assay of indicated PCP<sub>1</sub> candidate pairs and matched negative controls. Scale-bar: 10  $\mu\text{m}$ . Assay was performed in duplicate for all constructs. **i**, Literature reported specificity (single pathway annotation) and pleiotropy (multiple pathway annotations) of genes encoding 1,252 target proteins (total) and 27 proteins in validation set (above line), updated specificity and pleiotropy after hormone validation assay (below line). In **a**, **b**, **d** – **f**, Two sided t-test \*  $P \leq 0.05$ , \*\*  $P \leq 0.01$ , \*\*\*  $P \leq 0.001$ . **a** – **f**, Precise P values, biological repeats, and n for each test are shown in **Extended Table 5**.

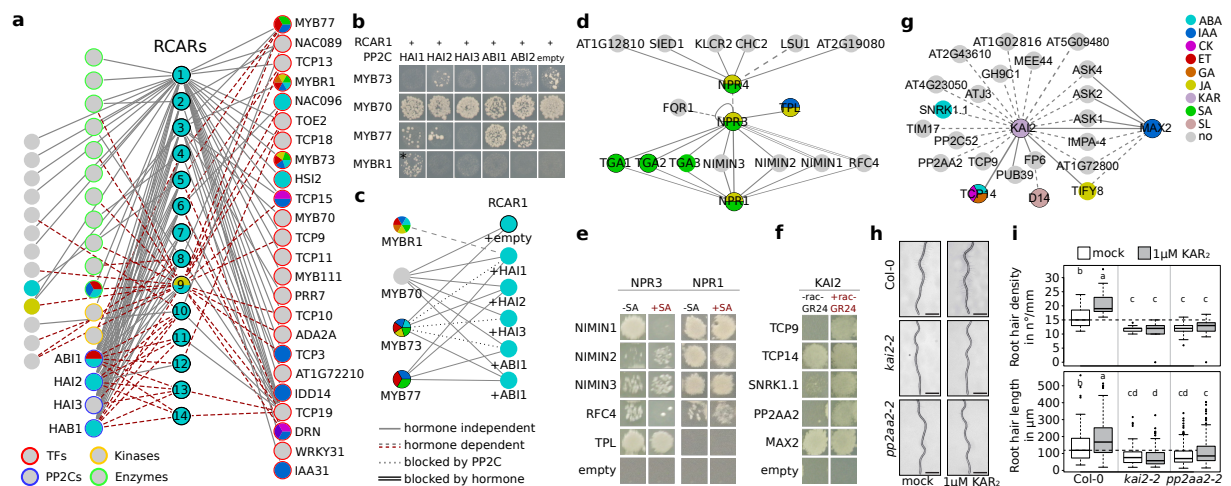


**Fig. 3 | Hormone receptor interactions.** **a**, ABA-dependent Y2H interactions. All identified interactors were systematically tested against all receptors in presence and absence of ABA. **b**, **c**, Y3H assays for indicated protein triplets. In all sets DB-RCAR1 is tested for interactions with AD-MYB proteins in the presence of the indicated PP2Cs and in presence and absence of ABA. **b**, One of four representative Y3H results. \* indicates ABA-dependent interaction. **c**, Y3H subnetwork of data in **b**. **d**, SA-dependent interactors of NPR1,3,4. **e**, One representative yeast colony of four repeats in presence and absence of 100 μM SA for identified NPR interactors. **f**, Hormone-dependent and -independent interactions of KAI2, D14 and MAX2. **g**, One representative of four yeast spots for selected KAI2 interactors in presence and absence of *rac*-GR24. **h**, Representative images for analysis in **i** show root hair phenotypes of the indicated genotypes. Scale bar: 1 mm. **i**, Quantification of RHD (right top) and RHL (right bottom) after indicated treatment. Letters indicate statistical groups (ANOVA, post-hoc Tukey,  $P \leq 0.05$ ). Boxes represent interquartile range (IQR) and bold line median; whiskers indicate highest and lowest data point within 1.5 IQR; outliers plotted individually. Precise *n* and *P* values for all group comparisons in **Supplementary Table 5**. **a**, **c**, **d**, **g**, Modulated interactions are represented by line shape as in legend **c**. Node colors represent hormone annotations as in legend **g**.

## References

- 1 Krouk, G. *et al.* A framework integrating plant growth with hormones and nutrients. *Trends Plant Sci* **16**, 178-182, doi:10.1016/j.tplants.2011.02.004 (2011).
- 2 Peleg, Z. & Blumwald, E. Hormone balance and abiotic stress tolerance in crop plants. *Current Opinion in Plant Biology* **14**, 290-295, doi:10.1016/j.pbi.2011.02.001 (2011).
- 3 Lumba, S. *et al.* A mesoscale abscisic acid hormone interactome reveals a dynamic signaling landscape in Arabidopsis. *Dev Cell* **29**, 360-372, doi:10.1016/j.devcel.2014.04.004 (2014).
- 4 Nemhauser, J. L., Hong, F. & Chory, J. Different plant hormones regulate similar processes through largely nonoverlapping transcriptional responses. *Cell* **126**, 467-475, doi:10.1016/j.cell.2006.05.050 (2006).
- 5 Orchard, S. *et al.* The MIntAct project--IntAct as a common curation platform for 11 molecular interaction databases. *Nucleic Acids Res* **42**, D358-363, doi:10.1093/nar/gkt1115 (2014).
- 6 Yu, H. *et al.* High-quality binary protein interaction map of the yeast interactome network. *Science* **322**, 104-110 (2008).
- 7 Altmann, M., Altmann, S., Falter, C. & Falter-Braun, P. High-Quality Yeast-2-Hybrid Interaction Network Mapping. *Curr Protoc Plant Biol* **3**, e20067, doi:10.1002/cppb.20067 (2018).
- 8 Wessling, R. *et al.* Convergent targeting of a common host protein-network by pathogen effectors from three kingdoms of life. *Cell host & microbe* **16**, 364-375, doi:10.1016/j.chom.2014.08.004 (2014).
- 9 Pruneda-Paz, J. L. *et al.* A Genome-Scale Resource for the Functional Characterization of Arabidopsis Transcription Factors. *Cell reports* **8**, 621-631, doi:10.1016/j.celrep.2014.06.033 (2014).
- 10 Consortium, A. I. M. Evidence for network evolution in an Arabidopsis interactome map. *Science* **333**, 601-607, doi:10.1126/science.1203877 (2011).
- 11 Braun, P. *et al.* An experimentally derived confidence score for binary protein-protein interactions. *Nat Methods* **6**, 91-97 (2009).
- 12 Braun, P. Interactome mapping for analysis of complex phenotypes: insights from benchmarking binary interaction assays. *Proteomics* **12**, 1499-1518, doi:10.1002/pmic.201100598 (2012).

- 13 Oughtred, R. *et al.* The BioGRID interaction database: 2019 update. *Nucleic Acids Res* **47**, D529-D541, doi:10.1093/nar/gky1079 (2019).
- 14 Barabasi, A.-L., Gulbahce, N. & Loscalzo, J. Network medicine: a network-based approach to human disease. *Nature Reviews Genetics* **12**, 56-68, doi:10.1038/nrg2918 (2011).
- 15 Girvan, M. & Newman, M. E. Community structure in social and biological networks. *Proc Natl Acad Sci U S A* **99**, 7821-7826, doi:10.1073/pnas.122653799 (2002).
- 16 Cutler, S. R., Rodriguez, P. L., Finkelstein, R. R. & Abrams, S. R. in *Annual Review of Plant Biology, Vol 61* Vol. 61 *Annual Review of Plant Biology* (eds S. Merchant, W. R. Briggs, & D. Ort) 651-679 (Annual Reviews, 2010).
- 17 Deikman, J. & Hammer, P. E. Induction of Anthocyanin Accumulation by Cytokinins in *Arabidopsis thaliana*. *Plant Physiol* **108**, 47-57, doi:10.1104/pp.108.1.47 (1995).
- 18 Guzman, P. & Ecker, J. R. Exploiting the triple response of *Arabidopsis* to identify ethylene-related mutants. *Plant Cell* **2**, 513-523, doi:10.1105/tpc.2.6.513 (1990).
- 19 Vlot, A. C., Dempsey, D. A. & Klessig, D. F. Salicylic Acid, a multifaceted hormone to combat disease. *Annu Rev Phytopathol* **47**, 177-206, doi:10.1146/annurev.phyto.050908.135202 (2009).
- 20 Lumba, S., Cutler, S. & McCourt, P. in *Annual Review of Cell and Developmental Biology, Vol 26* Vol. 26 *Annual Review of Cell and Developmental Biology* (eds R. Schekman, L. Goldstein, & R. Lehmann) 445-469 (Annual Reviews, 2010).
- 21 Tischer, S. V. *et al.* Combinatorial interaction network of abscisic acid receptors and coreceptors from *Arabidopsis thaliana*. *Proc Natl Acad Sci U S A* **114**, 10280-10285, doi:10.1073/pnas.1706593114 (2017).
- 22 Aleman, F. *et al.* An ABA-increased interaction of the PYL6 ABA receptor with MYC2 Transcription Factor: A putative link of ABA and JA signaling. *Scientific reports* **6**, 28941, doi:10.1038/srep28941 (2016).
- 23 Zhao, Y. *et al.* The ABA receptor PYL8 promotes lateral root growth by enhancing MYB77-dependent transcription of auxin-responsive genes. *Sci Signal* **7**, ra53, doi:10.1126/scisignal.2005051 (2014).

- 24 Nee, G. *et al.* DELAY OF GERMINATION1 requires PP2C phosphatases of the ABA signalling pathway to control seed dormancy. *Nat Commun* **8**, 72, doi:10.1038/s41467-017-00113-6 (2017).
- 25 Kuai, X., MacLeod, B. J. & Despres, C. Integrating data on the Arabidopsis NPR1/NPR3/NPR4 salicylic acid receptors; a differentiating argument. *Front Plant Sci* **6**, 235, doi:10.3389/fpls.2015.00235 (2015).
- 26 Ding, Y. *et al.* Opposite Roles of Salicylic Acid Receptors NPR1 and NPR3/NPR4 in Transcriptional Regulation of Plant Immunity. *Cell* **173**, 1454-1467 e1415, doi:10.1016/j.cell.2018.03.044 (2018).
- 27 Hermann, M. *et al.* The Arabidopsis NIMIN proteins affect NPR1 differentially. *Front Plant Sci* **4**, 88, doi:10.3389/fpls.2013.00088 (2013).
- 28 Waters, M. T., Gutjahr, C., Bennett, T. & Nelson, D. C. Strigolactone Signaling and Evolution. *Annu Rev Plant Biol* **68**, 291-322, doi:10.1146/annurev-arplant-042916-040925 (2017).
- 29 Scaffidi, A. *et al.* Strigolactone Hormones and Their Stereoisomers Signal through Two Related Receptor Proteins to Induce Different Physiological Responses in Arabidopsis. *Plant Physiol* **165**, 1221-1232, doi:10.1104/pp.114.240036 (2014).
- 30 Villaecija-Aguilar, J. A. *et al.* SMAX1/SMXL2 regulate root and root hair development downstream of KAI2-mediated signalling in Arabidopsis. *PLoS Genet* **15**, e1008327, doi:10.1371/journal.pgen.1008327 (2019).

## Material and Methods

**PhyHormORFeome selection and cloning.** We selected target genes with i) a known mutant phenotype in phytohormone signaling based on AHD2.0<sup>31</sup> annotations, ii) all members of gene families were enriched in (ii) and iii) input from colleagues. In total 1,252 genes were selected, for which 1,226 full-length Open Reading Frames (ORFs) could be obtained. To physically assemble the PhyHormORFeome, 688 ORFs were picked from our published AtORFeome collection<sup>8</sup>, 276 ORFs were obtained from ABRC, 11 ORFs were obtained from colleagues and 277 ORFs were amplified from Col-0 cDNA-mix from different tissues. For RNA extraction, 6-10 d old *Arabidopsis thaliana* Col-0 seedlings, separated organs and plant organs from mature plants were used (flower and silique - all developmental stages, node, internode, rosette leaves, cauline leaves, root from 15 d old plants grown on solid MS agar plates in vertical orientation, imbibed seeds). From all plant organs, tissue types, and seedlings, specific total RNA was extracted using the NucleoSpin RNA kit from Macherey and Nagel, following the manufacturer's recommendations. For cDNA synthesis, Superscript III (Thermo Fisher 18080044) protocol was modified using 25 ng random primers and 250 ng oligo d(T) 16 per 1 µg total RNA. Mixture was heated to 70 °C/5 min and incubated at 21°C/10 minutes. A mixture of 2.5 µl (0.1 µM) DTT, 10 U RNase OUT (40 U/µl), 250 U SSIII (200 U/µl), 4 µl SSIII 5x buffer, 2.5 µL 2 µM dNTPs was added and incubated at 21 °C for 10 minutes followed by 42 °C for 120 min incubation. To generate cDNA longer than 5 KB an additional 250 U of SSIII (200 U/µl) were added to the mixture followed by 55 °C for 30 minutes incubation for elongation and 70 °C for 15 minutes inactivation. All generated cDNAs from different organs, tissues and seedlings were mixed in equal amounts and 2 µl non diluted cDNA mixture (~100 ng) was used to amplify the ORFs of interest. ORF amplification was conducted as nested PCR to attach attB cloning-sites for further Gateway cloning. The specific primers

consist of 18 bp specific and 12 bp of a partial attB site (for attB overhang - GCAGGCTCAGGA, rev attB overhang – GAAAGCTGGGTC). All ORFs were generated with a stop codon. In the second PCR, full attB sites were added to the ORFs (attB for – GGGACAAGTTTGTACAAAAAAGCAGGCTCAGGAATG, attB rev – GGGGACCACTTTGTACAAGAAAGCTGGGTC). Gateway cloning and yeast transformation were performed as described<sup>7</sup>. ORFs cloned in this project are available from stock centers.

**Y2H interaction mapping pipeline.** Network mapping was performed according to Altmann et al., 2018<sup>7</sup>. Briefly, bait ORFs were expressed as genetic fusions to the GAL4 DNA binding domain (**pDEST-DB**), prey ORFs were expressed as genetic fusions to the minimal GAL4 activation domain. Both constructs were maintained on low copy centromeric (*cen*) plasmids (**pAD-DEST**) and expressed from weak *adh2* promoters. Primary screening was done by mating individual DB plasmid-containing haploid yeast strains (Y8930, MAT $\alpha$ ) with a mini-pool of haploid Y8800 (MATa) AD-plasmid containing strains. Following 3 day selection on selective plates containing 1mM 3-Amino-1,2,4-triazole to repress background HIS3 activity, positive single colonies were picked and retested on selective media and cycloheximide control plates. Colonies showing specific selective growth were lysed, the respective ORFs amplified with generic primers that include position-specific barcodes and subsequently identified using the kiloSeq service by seqWell (Beverly, MA, US). All primary Y2H screens were performed once, except for the PhI<sub>MAIN</sub> screen, which was performed with five repeats. The receptor screens and the PhI<sub>REP</sub> screen were verified systematically, i.e. in the final verification all identified interaction candidates were tested against all receptors or repressors/regulators, respectively. The receptor screens were performed in the absence and presence of the respective phytohormones applied to the selective media. For the ABA receptor screen, 30  $\mu$ M

abscisic acid was used, for the IAA receptor screen 100  $\mu$ M indol-3-acetic acid, for the GA receptor screen 100  $\mu$ M GA3 and for the SA receptor screen 100  $\mu$ M salicylic acid was used. The receptors of strigolactone (D14) and karrikin (KAI2) signaling pathways were both screened with 5  $\mu$ M *rac*-GR24.

**Y3H assay.** RCAR1 was genetically fused to the GAL4 DNA binding domain using **pDEST DB**, the MYB proteins were genetically fused to the minimal GAL4 activation domain using **pAD-DEST**. To test for modulation of these interactions, the indicated PP2Cs were expressed from the helper plasmid **pVTU-DEST** maintained via the URA3 selection marker. All combinations RCAR1 and PP2Cs were transformed into the haploid yeast strain Y8930 and mated against Y8800 transformed with the AD-MYB constructs. The Y3H assays were performed in four independent repeats in presence and absence of 30  $\mu$ M ABA treatment on selective plates (Sc-W-L-U-H) containing 1 mM 3-Amino-1,2,4-triazole to repress activity of background HIS3 reporter activity. Interactions that were verified in three repeats were counted as Y3H interactions.

**Protein-protein interaction reference set.** Candidate interactions for the positive reference set (PRS) were compiled from protein-protein interactions from IntAct (downloaded august 2014)<sup>5</sup> and BioGRID (Version 3.2.115)<sup>32</sup>. At this time, the IntAct dataset contained 17,574 interactions and the BioGRID dataset contained 21,474 interactions among *Arabidopsis thaliana* molecules. In both datasets protein-DNA interactions, interactions derived from papers that reported more than 100 interactions, and non-binary interactions in protein complexes were removed. Subsequently, both datasets were filtered for interactions described in at least two publications or identified in at least two binary interaction detection methods. This resulted in 233 interactions from which 140 interactions described in 247 publications were randomly picked for re-curation. This re-curation yielded a selection of 92 highly reliable binary protein-protein interactions, which constitute the PRS<sub>PhI</sub>. 10 of these 92 interactions were

phytohormone dependent interactions. To assemble the random reference set (RRS<sub>PHI</sub>) we sampled randomly 95 protein pairs from proteins in our PhyHormORFeome, excluding already described protein-protein interaction pairs.

**Implementation of interaction mapping framework parameters.** To assess the quality of PhI map, i.e. false positive and false negative interactions, the interactome mapping framework was implemented as described<sup>33</sup> and the assay sensitivity, sampling sensitivity, precision and completeness were estimated.

Completeness of the PhI<sub>MAIN</sub> screening space, i.e. the proportion of tested protein pairs in comparison to the theoretical number in the full search space was based on the number of available ORFs in PhyHormORFeome. The initially defined search space comprised 1,252 loci and thus 1,567,504 possible protein pairs. For the screen of PhI<sub>MAIN</sub> 1,254 ORFs corresponding to 1,199 gene loci were tested, of which 1,179 were present as AD- and DB-hybrid constructs, 15 only as AD-hybrid constructs, and 5 only as DB-hybrid constructs. Together, AD- and DB-hybrid constructs for 90.2% of locus combinations were tested for interactions, corresponding to the completeness.

The assay sensitivity of our Y2H system for detection of phytohormone signaling related proteins was estimated by benchmarking the system using PRS<sub>PHI</sub>/RRS<sub>PHI</sub>. Of the 92 tested PRS<sub>PHI</sub> pairs 19 pairs were detected, whereas no RRS<sub>PHI</sub> scored positive, thus yielding an assay sensitivity of 20.7% ± 4.2%. Excluding the 9 interactions from PRS<sub>PHI</sub> that are dependent on presence of a phytohormone, none of which was detected by the unconditional Y2H, resulted in an unconditional assay sensitivity of 22.8% ± 4.6%.

Sampling sensitivity was estimated as described<sup>10</sup>. Briefly, a modified Michaelis-Menten function was fitted to the number of identified interactions with increasing number of iterations of the experiment using the R-package drc (3.0-1). Using the first three repeats of the PhI<sub>MAIN</sub> screen for developing the saturation model we estimated

saturation to occur at  $616 \pm 38$  interactions. The model was then challenged by two additional repeats of the primary screen. These resulted in a dataset of 529 interactions, which matches the model prediction of  $519 \pm 31$  interactions after 5 repeats.

Overall sensitivity is the product of assay sensitivity and sampling sensitivity. With an assay sensitivity of  $20.7\% \pm 4.2\%$  and sampling sensitivity of  $85.9\% \pm 5.3\%$ , the overall sensitivity is  $17.8\% \pm 6.8\%$  including conditional interactions in PRS<sub>PHI</sub>. The unconditional overall sensitivity of  $19.4\% \pm 7.0\%$  is the product of the unconditional assay sensitivity of  $22.8\% \pm 4.6\%$  and sampling sensitivity of  $85.9\% \pm 5.3\%$ . Overall completion of the screen was estimated as the product of overall sensitivity and completeness of the screen; overall completion of PHI<sub>MAIN</sub> is thus  $16.0\% \pm 6.8\%$ .

**Luciferase validation assay.** Protein expression: Proteins constituting PRS<sub>PHI</sub>/RRS<sub>PHI</sub> pairs and the interaction pairs from the different subsets were expressed in cell-free coupled transcription translation wheat-germ lysate (Promega, L3260) using SP6 promoters. Of each protein pair, one partner was expressed as an N-terminal FLAG-fusion protein, the second protein carried an N-terminal renilla luciferase fusion. Protein pairs were co-expressed according to the manufacturer's protocol, except that the amounts were proportionally adjusted to 20  $\mu$ l final reaction volume. Input DNA plasmids were isolated from 1.5 ml bacterial cultures grown in Terrific Broth for 20 h on a vibration platform shaker (Union Scientific) using a Qiagen Biorobot3000 and Turbo Prep 96-well plasmid isolation kits. These yielded approximately 20-40 ng  $\mu$ l<sup>-1</sup> DNA of which 4  $\mu$ l were used in a 20  $\mu$ l fv. TnT reaction. Protein expression was done by incubating the reaction mixture containing both plasmids for 2 h at 30 °C. Immunoprecipitation (IP) plate preparation: anti-FLAG antibody coated plates were made in-house by incubating white 96-well Lumitrac high binding plates (Greiner) over night at 4 °C with 75  $\mu$ l PBS (pH 7.4) per well containing 8  $\mu$ g ml<sup>-1</sup> M2 anti-Flag antibody

(Sigma). 2 h before use, the antibody solution was replaced with 100  $\mu$ l blocking buffer containing 10  $\mu$ g  $\mu$ l<sup>-1</sup> bovine serum albumin (BSA) followed by 2 h shaking at room temperature. Following protein expression 2  $\mu$ l lysate were diluted in 28  $\mu$ l PBS (pH7.4) to quantify expression of the prey protein by addition of 10  $\mu$ l Renilla glow luciferase substrate. The remaining expression lysate was diluted in 42  $\mu$ l blocking buffer and added to the empty wells of the IP plates. The plates were incubated with gentle shaking for 2 h at 4 °C, washed 3 times with 100  $\mu$ l blocking buffer. Co-IP efficiency was determined by addition of 10  $\mu$ l Renilla glow luciferase substrate (Promega) diluted in 30  $\mu$ l PBS (pH7.4). Interaction pairs were scored as positive when the expression level was at least 10% of the median of the respective plate (expression positive), the immunoprecipitation (IP) exceeded the median IP of the plate (min IP signal) and the Z-test on the IP efficiency gave a score greater than 0.4 (IP ratio of sample relative to those of the plate). For determination of dataset precision a total of 446 pairs were tested from PRS<sub>PHI</sub> (78), PRS<sub>unc</sub> (69), RRS<sub>PHI</sub> (83), PHl<sub>MAIN</sub> (115), PHl<sub>EXT</sub> (110), PHl<sub>REP</sub> (60). Dataset differences were statistically compared using one-sided Fisher exact test.

**Network topology.** To determine network topology of PHl<sub>MAIN</sub> the distributions of degree and clustering coefficients were calculated for the indicated networks using the igraph package. The distributions were used to determine the underlying network topology<sup>34</sup>.

**Network visualization and annotation.** Networks were visualized with Cytoscape<sup>35</sup> (v. 3.7.2) using protein annotations from Araport11<sup>36</sup>. Hormone annotations were downloaded from AHD2.0, and extracted from TAIR10 GO annotations (03/08/2018). Hormone annotations were inferred from GO annotations when a gene has a GO term that contains one of these key words: "auxin", "abscisic acid", "brassinosteroid", "cytokinin", "ethylene", "gibberellin", "jasmonic acid", "salicylic acid", "strigolactone", "karrikin". GO annotations with evidence code IEP were excluded from all analyses.

**Community detection.** Communities in  $PhI_{MAIN}$  were determined using the edge betweenness algorithm<sup>15</sup> implemented in R-package igraph (v. 1.2.4)<sup>37</sup>.

**Hormone enrichment.** Communities were tested for enrichment with proteins functioning in the hormone signaling pathways using the hormone annotations from AHD2.0 and TAIR10. For each community the number of proteins with a given pathway annotation was compared to the total in the full  $PhI_{MAIN}$  network using two-sided Fisher's exact test and multiple hypothesis corrected with Benjamini-Hochberg algorithm.

**GO enrichment.** All communities were tested for GO enrichment using R package GOstats (2.50.0)<sup>38</sup>. GO annotation data were derived from R package GO.db (3.7.0). Communities were tested for overrepresentation of GO terms using a hypergeometric test function hyperGTest invoked with parameter conditional = TRUE. *P* values of each community were corrected for testing multiple GO terms using the Benjamini-Hochberg method.

**Pathway distance calculation.** To determine the distance between different hormone pathways, all shortest paths between proteins of the respective hormone signaling pathways were determined. Only shortest paths were considered that do not contain proteins in the same pathways as those under consideration. The mean path length was calculated from all shortest paths between the two pathways.

**Pathway contact point determination and network comparison.** Hormone pathway annotations from AHD2.0 and GO were used for this analysis. From the  $PhI_{MAIN}$  network we extracted interactions between two proteins annotated with distinct hormone signaling pathways (Type I) and for interactions between two proteins involved in distinct but also common pathways (Type II). To compare the number of PCPs in  $PhI_{MAIN}$  with LCI networks, we used a subsampling bootstrapping approach. From each network we conducted 1,000 iterations of sampling 100 interactions without

replacement. For each sampling the total number of PCPs of type I and type II and the number of PCPs for each specific hormone combination were determined. The derived distributions for total PCPs from PhI<sub>MAIN</sub> were compared to the distributions obtained from LCI networks using a two-sided Welch Two-Sample t-test. The distributions of hormone combination-specific PCPs were compared using a two-sided Wilcoxon test and multiple testing corrected by the number of hormone combinations tested (45).

**Literature curated interactions.** Interactions curated from literature were downloaded from IntAct<sup>5</sup> and BioGRID<sup>39</sup>. Arabidopsis protein-protein interactions were extracted from IntAct database downloaded in June 2016 and from BioGRID database version 3.4.142 (downloaded November 2016).

**Phytohormone sources.** 1-aminocyclopropane-carboxylic acid (ACC) from SIGMA (A-3903), 6-benzylamino purine (BA) from SIGMA (B3408), brassinolide (BL) from SIGMA (B1439), karrikin2 (KAR2) from Olchemim (025 682), karrikin2 (KAR2) from Toronto Research Chemicals (F864800) for Y2H experiments, gibberellic acid 3 (GA) from Duchefa (G0907), *rac*-GR24 from Chiralix (CX23880), indol-3-acetic acid (IAA) from SIGMA (I2886), paclobutrazol (Pac) from Duchefa (P0922), salicylic acid from SIGMA (S5922), abscisic acid (ABA) from SIGMA (A1049), and methyl-jasmonate (Me-JA) from SIGMA (392707).

**Plant material and growth conditions.** All *Arabidopsis thaliana* lines, i.e. WT, *ahp2*, *as1*, *bee1*, *bee2*, *bim1*, *bpm3*, *cbl9*, *cos1*, *cpk1*, *ddl*, *eds1*, *ga3ox1*, *gai*, *gi*, *hub1*, *ibr5*, *jaz1*, *jaz3*, *kai2-2*, *myb77*, *myc2*, *nap1;1*, *nia2*, *pks1*, *pp2aa2-2*, *pp2ca*, *rcar1*, *rcn1*, *rgl1*, *tt4*, *tll*, *wrky54*, *rga*, *rga-28*, *spy*, and *ein3* are in the Col genetic background. Seeds were obtained from NASC and propagated for three generations in a greenhouse environment at 21 °C and LD light (16 h / 8 h). For genotyping, one leaf of a 12 - 14 days old plant was frozen in liquid nitrogen and genomic DNA was extracted in 1.5 ml tubes using Edwards DNA extraction buffer<sup>40</sup>. For expression level analysis

of the mutant lines, RNA was extracted using NucleoSpin RNA kit from Macherey-Nagel and the M-MuLV Reverse Transcriptase (Biozym 350400201) according to the manufacturer's recommendations. All seeds were surface sterilized and stratified for 3 d at 4 °C in the dark on MS plates or plates containing the indicated additives. LD light conditions were 75-85  $\mu\text{M m}^{-2} \text{s}^{-1}$  measured with LI-250A light sensor (LI-COR). *Nicotiana benthamiana* seeds were spread on soil and grown in a greenhouse environment with 23 °C and LD light (16 h / 8 h). For all assays, measurements were done with distinct samples (no repeat measurements on the same sample). For statistical tests of significance a normal distribution of the measured variable (e.g. root length) was assumed; hormone treatments and genotype were tested as covariates.

**ET triple response measurement.** Sterile seeds were placed directly on standard MS or 10  $\mu\text{M}$  ACC containing plates, stratified for 3 d at 4 °C in the dark, transferred into light for 1 h to induce germination, and then incubated for 3 d at 23 °C in the dark. Apical hook vs loop formation was scored visually, image analysis for hypocotyl and root length determination was performed using the Fiji imaging software<sup>41</sup> and herein the Simple Neurite Tracer<sup>42</sup> plugin (v 3.1.3).

**Root elongation measurements.** Seedlings were grown on MS plates to 5 DAG and then transferred to MS mock plates or MS containing the appropriate phytohormone additive as indicated in the figures (Pac 0.5  $\mu\text{M}$ , 1.0  $\mu\text{M}$ ; BL 0.1  $\mu\text{M}$ , 0.5  $\mu\text{M}$ ; 25  $\mu\text{M}$  Me-JA). Transferred seedlings grew in vertical position for another 4 days at 23 °C in LD light conditions (16 h / 8 h). Root lengths were determined as described above.

**Anthocyanin accumulation.** Anthocyanin content in response to the indicated treatments was determined as described by Nakata et al, 2014<sup>43</sup> and expressed per g fresh weight.

**Root hair growth.** Analysis was performed according to Villaécija-Aguilar et al., 2019<sup>44</sup> using 1  $\mu\text{M}$  KAR2. Arabidopsis seeds were stratified in the dark for 3 d at 4 °C and

then transferred to a growth cabinet at 22 °C, 16 h / 8 h light/dark cycle (intensity ~100  $\mu\text{M m}^{-2} \text{s}^{-1}$ ). Images were taken with a Zeiss SteREO Discovery.V8 microscope (Carl Zeiss, Germany) equipped with a Zeiss Axiocam 503 color camera (Carl Zeiss, Germany). The number of root hairs was determined by counting the root hairs between 2 and 3 mm from the root tip on each root, and root hair length was measured for 10 - 12 different root hairs per root as described above. For karrikin treatments, KAR2 (Olchemim, Olomouc) was dissolved in 75% methanol for the preparation of a 10 mM stock solution. Analysis and data are based on two repeats.

**Infection assay.** To measure bacterial proliferation in 4 - 5 week old plants, assays were conducted as described<sup>18</sup> using *Pseudomonas syringae* pv. tomato DC3000. To prepare the inoculum, bacteria were grown overnight on NYGA medium (5 g/l bactopectone, 3 g/l yeast extract and 20 ml glycerol) and resuspended and diluted to  $5 \times 10^5$  colony forming units  $\text{ml}^{-1}$  in 10 mM  $\text{MgCl}_2$ . Bacteria were inoculated by syringe infiltration of two leaves per plant, and harvested at 4 days post inoculation as described<sup>45</sup>. In short, 3 leaf discs per sample were incubated for 1 hour in 10 mM  $\text{MgCl}_2$  containing 0.01% Silwett. The resulting suspension was then serially diluted, 20  $\mu\text{l}$  of each dilution were plated, and colonies were counted after two days.

**Bimolecular fluorescent complementation assay (BiFC).** For BiFC the vectors pMDC43-YFC, pMDC43-YFN<sup>46</sup>, and pDEST-VYNE(R), pDEST-VYCE(R)<sup>47</sup> were used. After Gateway recombination, the ORF-containing destination clones were introduced into *Agrobacterium tumefaciens* GV3101 strain. Transformed *A. tumefaciens* cells were grown overnight and resuspended in infiltration buffer (10 mM  $\text{MgCl}_2$ , 10 mM MES pH 5.6, and 150  $\mu\text{M}$  acetosyringone) with a final  $\text{OD}_{600}$  of 0.3 for each expression vector. The abaxial leaf surface of *N. benthamiana* plants was transiently transformed by *A. tumefaciens*, harboring the constructs and the p19 silencing inhibitor protein, by infiltration using a needleless syringe. Two days after infiltration, two leaves from two

independently transformed plants were used for fluorescence detection. Reconstitution of fluorescence was observed under an epifluorescence microscope (Olympus BX61) using YFP and RFP band-pass filters for the YFC-MYC2 and YFN-CIPK14 interaction, and either a TCS SP8 (Leica) or a LSM880 laser scanning confocal microscope (Carl Zeiss) was used for the remaining BiFC assays. Laser excitation wavelength for both microscopes was 488 nm and the detection band was set to 493-545 for Venus protein. The objectives were a PL APO 40x/1.10 and a Plan-Apochromat 20x/0.8 M27 for the TCS SP8 and LSM880, respectively. Image analysis was performed using the Fiji imaging software<sup>41</sup>. Analyses were performed in duplicate for all constructs.

***In vitro* pull-down assays.** For *in vitro* pull down assays, Amylose Resin (New England Biolabs) coated with MBP-MYC2 was incubated for 2 hours at 4 °C with equimolar amount of purified GST-CIPK14. Wash and elution steps were performed following manufacturer's instructions. Pull-downs were analyzed by western blot using  $\alpha$ -GST (Amersham Biosciences) and  $\alpha$ -MBP (New England Biolabs) antibodies.

**Estimation of the protein-protein interaction likely scores** We developed the Edge-score model to determine the protein-protein interaction likely score in different plant tissues and development states. The Edge-score modelling was designed to exploit transcript abundance to estimate possibility and to some extent likelihood of an interaction taking place in a given tissue and condition. It is based on using transcript abundance as a proxy for protein concentration and modeling binary complex formation by the law of mass action. Tissue specific transcriptome data were collected from Kleptikova<sup>48</sup>. FastQC (v0.11.7) was used for read quality control before and after trimming. Adaptor sequences and low quality reads were trimmed with Trimmomatic v0.36<sup>49</sup>, using the ILLUMINACLIP:TruSeq3-SE.fa:2:30:10, LEADING:3, TRAILING:3, SLIDING WINDOW:4:15 and MINLEN:36 options. High quality reads were mapped to the *Arabidopsis thaliana* (TAIR10) reference genome. The estimation of gene

abundance was performed with Kallisto v0.45<sup>50</sup>. To estimate the chance of two proteins  $i$  and  $j$  to interact in a given condition, the law of mass action was used to obtain a quantitative estimate of their interaction feasibility. The amount of protein  $i$  and  $j$  was estimated using their respective transcript levels as proxy  $t_i$  and  $t_j$ . Edge-scores were calculated using the following scheme: The score of the interaction between protein  $i$  and protein  $j$  in tissue  $t_k$  sets as  $S_{ij}^{t_k}$  (Equation 1). In each tissue, let  $t_i^{t_k}$  and  $t_j^{t_k}$  denote the abundance of genes  $i$  and  $j$  in tissue  $t_k$ .

$$S_{ij}^{t_k} = t_i^{t_k} * t_j^{t_k} \quad (1)$$

After obtaining a score for each interaction in each tissue, the Edge-score of a specific interaction in tissue  $t_k$  was computed with Z-transformation (Equation 2).

$$es_{ij}^{t_k} = \frac{S_{ij}^{t_k} - \overline{S_{ij}^{t_k}}}{\sqrt{\frac{1}{N-1} \sum_{i=1}^N (S_{ij}^{t_k} - \overline{S_{ij}^{t_k}})^2}} \quad (2)$$

Finally, we normalized this score to fit the range of [0, 1] (Equation 3).

$$es_{ij}^{t_k} = \frac{es_{ij}^{t_k} - \min(es_{ij}^{t_k})}{\max(es_{ij}^{t_k}) - \min(es_{ij}^{t_k})} \quad (3)$$

A higher Edge-score indicates that an interaction in this tissue is more likely as both proteins are expressed jointly. A higher Z-score indicates that an interaction in this tissue is more likely as both proteins are expressed jointly.

## Data Availability

All functional, genetic, and interaction data generated in this study are available as supplementary information. The genes selected for interactome mapping (search space) are presented in **Supplementary Information Table 1**. All protein-protein interaction data acquired in this study can be found in **Supplementary Information**

**Table 2.** The data for genetic validation assays can be found in **Supplementary Information Table 5**. The preliminary edge-scores for all interactions identified in this study are presented in **Supplementary Information Table 6**. Additionally, all protein interactions from this work have been submitted to the IMEx (<http://www.imexconsortium.org>) consortium through IntAct<sup>5</sup> and assigned the identifier IM-27834.

### Code Availability

Custom scripts used in this manuscript are available at <https://github.com/INET-HMGU/PhyHormInteractome>

### Method References

- 31 Jiang, Z. *et al.* AHD2.0: an update version of Arabidopsis Hormone Database for plant systematic studies. *Nucleic Acids Res* **39**, D1123-1129, doi:10.1093/nar/gkq1066 (2011).
- 32 Stark, C. *et al.* BioGRID: a general repository for interaction datasets. *Nucleic Acids Research* **34**, D535-D539, doi:10.1093/nar/gkj109 (2006).
- 33 Venkatesan, K. *et al.* An empirical framework for binary interactome mapping. *Nat Methods* **6**, 83-90 (2009).
- 34 Barabasi, A. L. & Oltvai, Z. N. Network biology: understanding the cell's functional organization. *Nat Rev Genet* **5**, 101-113 (2004).
- 35 Shannon, P. *et al.* Cytoscape: A software environment for integrated models of biomolecular interaction networks. *Genome Research* **13**, 2498-2504, doi:10.1101/gr.1239303 (2003).
- 36 Cheng, C. Y. *et al.* Araport11: a complete reannotation of the Arabidopsis thaliana reference genome. *Plant J* **89**, 789-804, doi:10.1111/tpj.13415 (2017).
- 37 Csardi, G. & Nepusz, T. The igraph software package for complex network research. *InterJournal Complex Systems* (2006).
- 38 Falcon, S. & Gentleman, R. Using GOstats to test gene lists for GO term association. *Bioinformatics* **23**, 257-258, doi:10.1093/bioinformatics/btl567 (2007).

- 39 Chatr-Aryamontri, A. *et al.* The BioGRID interaction database: 2017 update. *Nucleic Acids Res* **45**, D369-D379, doi:10.1093/nar/gkw1102 (2017).
- 40 Edwards, K., Johnstone, C. & Thompson, C. A simple and rapid method for the preparation of plant genomic DNA for PCR analysis. *Nucleic Acids Res* **19**, 1349, doi:10.1093/nar/19.6.1349 (1991).
- 41 Schindelin, J. *et al.* Fiji: an open-source platform for biological-image analysis. *Nat Methods* **9**, 676-682, doi:10.1038/nmeth.2019 (2012).
- 42 Longair, M. H., Baker, D. A. & Armstrong, J. D. Simple Neurite Tracer: open source software for reconstruction, visualization and analysis of neuronal processes. *Bioinformatics* **27**, 2453-2454, doi:10.1093/bioinformatics/btr390 (2011).
- 43 Nakata, M. & Ohme-Takagi, M. Quantification of Anthocyanin Content. *Bio-protocol* **4**, e1098, doi:10.21769/BioProtoc.1098 (2014).
- 44 Villaecija Aguilar, J. A. *et al.* KAI2 regulates root and root hair development by modulating auxin distribution. *bioRxiv*, 539734, doi:10.1101/539734 (2019).
- 45 Wenig, M. *et al.* Systemic acquired resistance networks amplify airborne defense cues. *Nat Commun* **10**, 3813, doi:10.1038/s41467-019-11798-2 (2019).
- 46 Belda-Palazon, B. *et al.* Aminopropyltransferases involved in polyamine biosynthesis localize preferentially in the nucleus of plant cells. *PLoS One* **7**, e46907, doi:10.1371/journal.pone.0046907 (2012).
- 47 Gehl, C. *et al.* Quantitative analysis of dynamic protein-protein interactions in planta by a floated-leaf luciferase complementation imaging (FLuCI) assay using binary Gateway vectors. *Plant Journal* **67**, 542-553, doi:10.1111/j.1365-313X.2011.04607.x (2011).
- 48 Klepikova, A. V., Kasianov, A. S., Gerasimov, E. S., Logacheva, M. D. & Penin, A. A. A high resolution map of the Arabidopsis thaliana developmental transcriptome based on RNA-seq profiling. *Plant J* **88**, 1058-1070, doi:10.1111/tpj.13312 (2016).
- 49 Bolger, A. M., Lohse, M. & Usadel, B. Trimmomatic: a flexible trimmer for Illumina sequence data. *Bioinformatics* **30**, 2114-2120, doi:10.1093/bioinformatics/btu170 (2014).

- 50 Bray, N. L., Pimentel, H., Melsted, P. & Pachter, L. Near-optimal probabilistic RNA-seq quantification. *Nat Biotechnol* **34**, 525-527, doi:10.1038/nbt.3519 (2016).

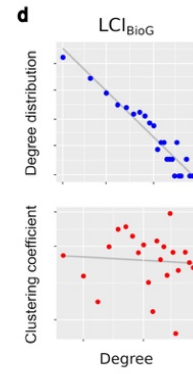
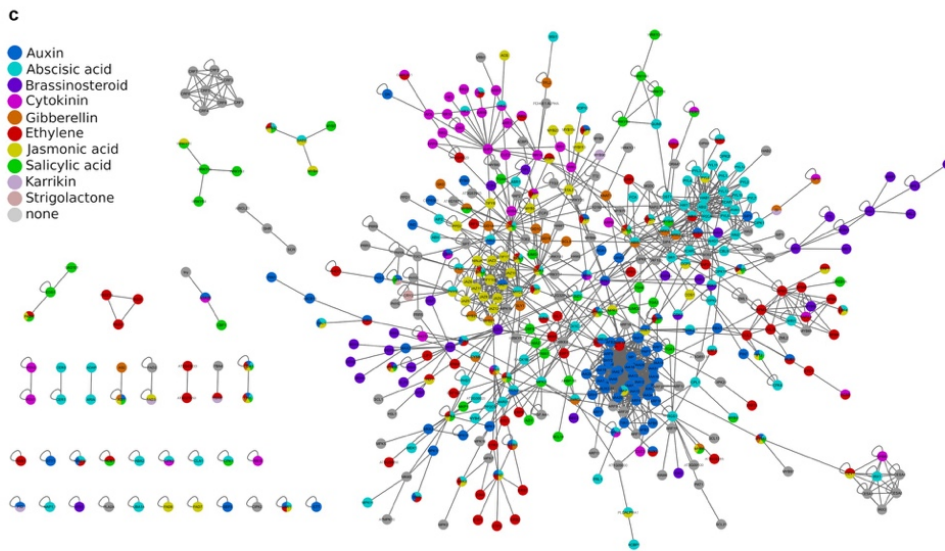
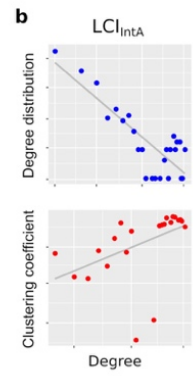
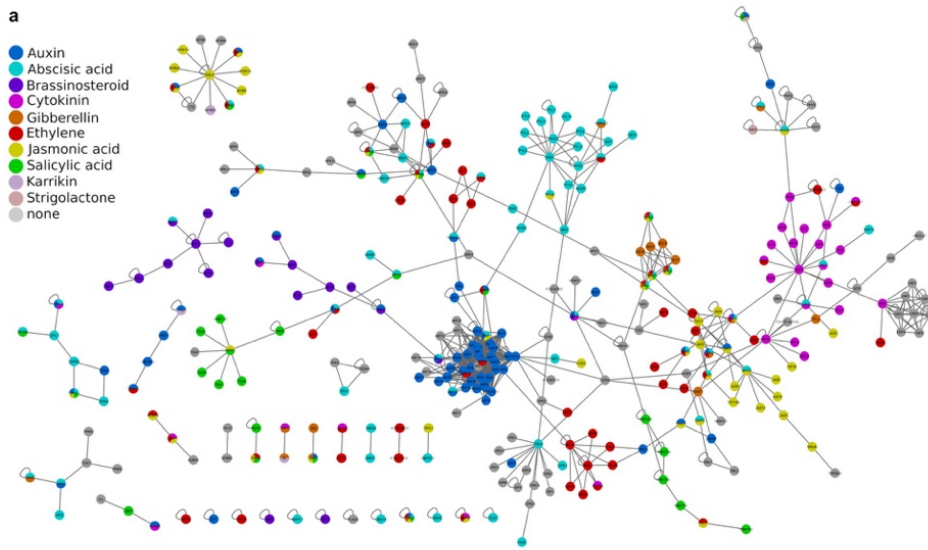
### **Acknowledgements**

We thank all INET members for helpful discussions and the reviewers for very constructive suggestions. This work was supported by DFG Emmy Noether program (GU1423/1-1) to CG, by DFG SFB924 to ACV, CG, EG, and PFB; by BMBF: 031L0141 e:Bio-Modul III: ChlamyInt/Bundesministerium für Bildung, Wissenschaft, Forschung und Technologie (Federal Ministry for Education, Science, Research and Technology) to PFB, and the European Research Council's Horizon 2020 Research and Innovation Programme (Grant Agreement 648420) grant to PFB.

### **Author contributions**

Project conception: PFB; ORF selection and cloning: MA, SA, PFB, GWB, SC, CG; Y2H screening: MA, PAR, LEV, MS, VY, RP; NMR; Hormone-dependent Y2H screens: MA, JP; PRS<sub>PhI</sub>/RRS<sub>PhI</sub> curation: MA, SA, NMR, AGM, PFB; network analyses: SA, PFB, MA, KK, KFXM,; Edge-score calculation: CWL, SA, PFB; pulldown experiment: JP, NMR; Systematic validation assay: BW, PAR, MS, MA, AS, VY, PFB; BiFC validations and figure panel: PAR, MA, NMR, JP; genetic validation assays: ABA: MA, EG, LG, SA, PFB; CK: MA, LEV; ET: MA, LEV; SA: ACV, MW, JS, MA; JA: NMR, MA, PAR; GA: MA; Karrikin/GR24 vignette and figure panel: JAVA, CG; Figures: MA; SA, CF, PFB; manuscript writing: PFB, CF, MA, SA, CG, ACV.

**Competing interests** The authors declare no competing interests

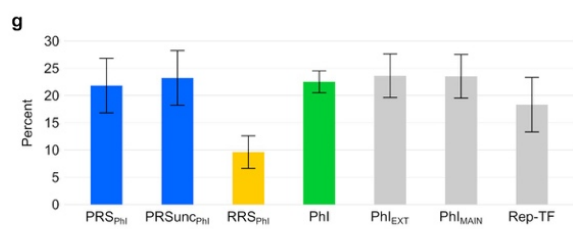


**e**

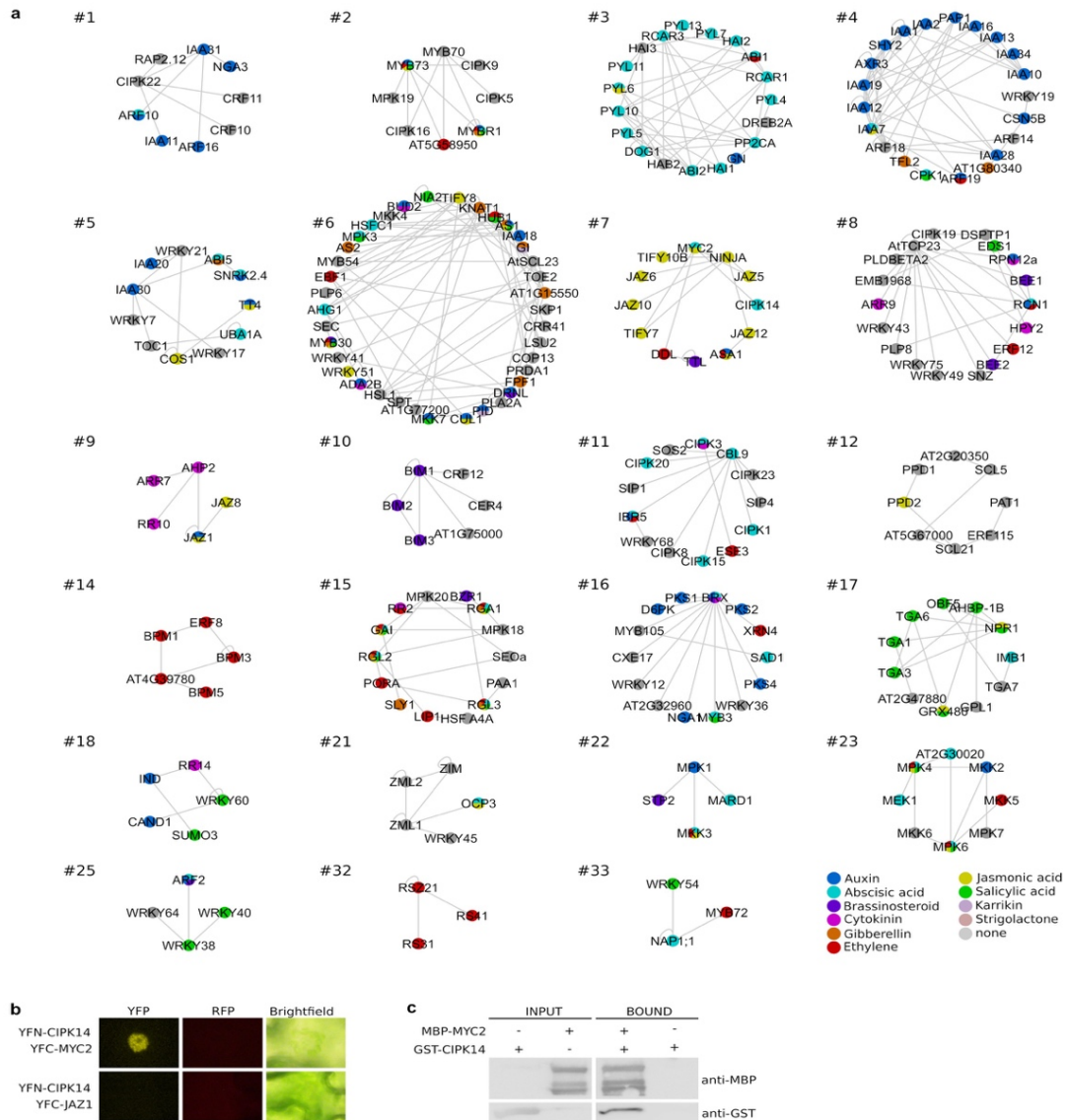
| Network             | Proteins | Interactions |
|---------------------|----------|--------------|
| PhI <sub>MAIN</sub> | 273      | 529          |
| PhI <sub>EXT</sub>  | 658      | 789          |
| Rep-TF              | 141      | 690          |
| Receptors           | 138      | 241          |
| PhI                 | 924      | 2072         |

**f**

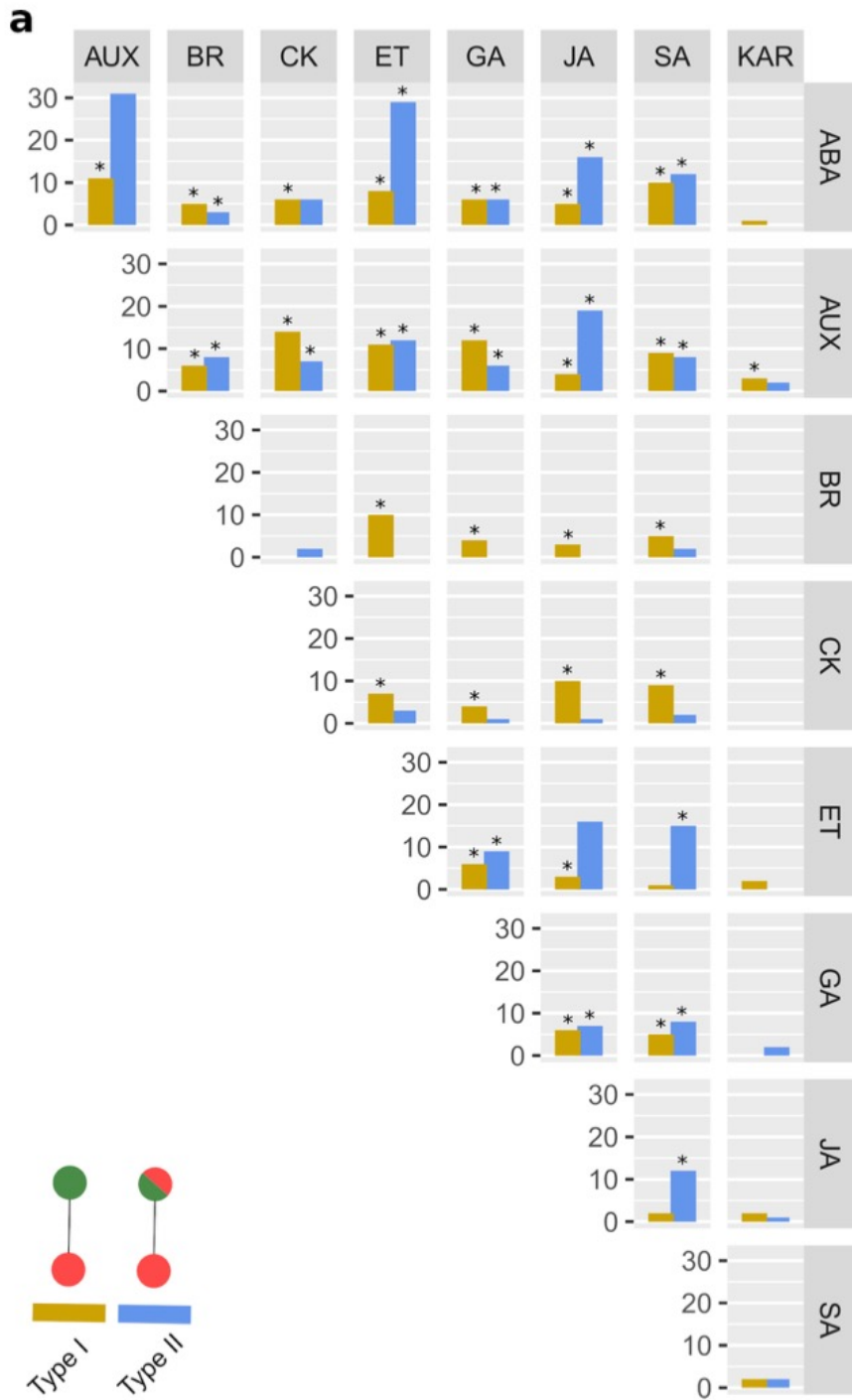
| Hormone | Interactions |      |
|---------|--------------|------|
|         | total        | new  |
| ABA     | 731          | 581  |
| AUX     | 981          | 705  |
| BR      | 180          | 155  |
| CK      | 233          | 204  |
| ET      | 521          | 435  |
| GA      | 239          | 201  |
| JA      | 594          | 475  |
| KAR     | 35           | 34   |
| SA      | 410          | 328  |
| SL      | 1            | 1    |
| PhI     | 2072         | 1572 |



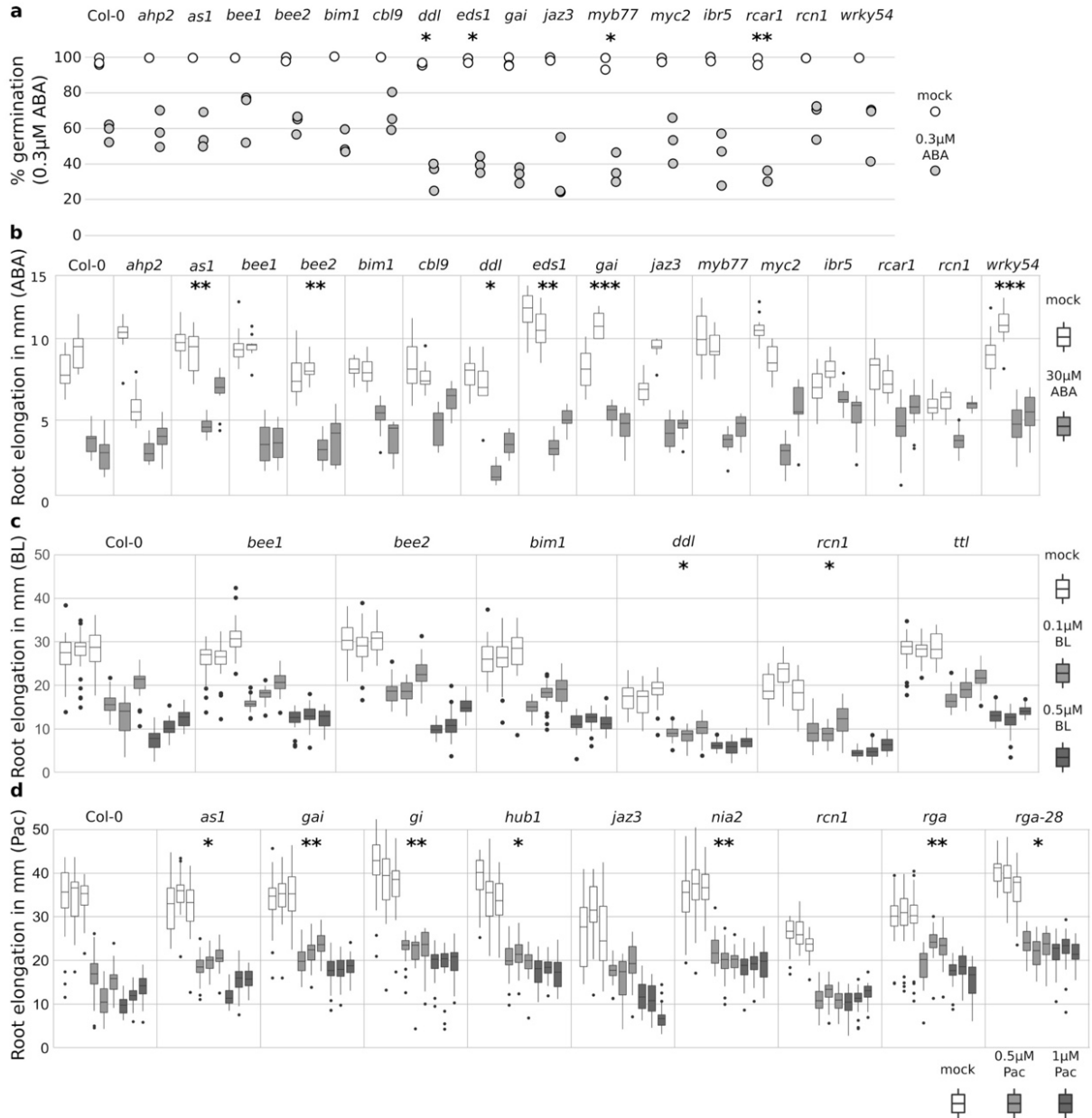
**Extended Data Fig. 1 | Network analyses.** **a**, Network map of binary protein-protein interactions among search space proteins derived from IntAct ( $LCI_{IntA}$ ). Color code indicates hormone pathway annotations as indicated in legend. **b**, Degree distribution and clustering coefficient distribution on log-log scale of network in **a**. **c**, Network map of binary protein-protein interactions among search space proteins derived from BioGRID ( $LCI_{BioG}$ ). Color code indicates hormone pathway annotations as indicated in the legend. **d**, as in **b**, but for network shown in **c**. **e**, number of proteins and interactions in the PhI interactome subsets. **f**, number of total and new interactions in PhI for all proteins belonging to each pathway and the non-redundant total for PhI. **g**, Fraction of positive scoring pairs of  $PRS_{PhI}$  (78),  $PRS_{unc}$  (hormone-independent PRS interactions) (69),  $RRS_{PhI}$  (85), combined PhI subsets (green) (285) and the individual subsets from the single Y2H screens:  $PhI_{EXT}$  (110),  $PhI_{MAIN}$  (115), and Rep-TF (60). Error bars indicate standard error of proportion. Individual results for all pairs are provided in **Supplementary Table 2**.



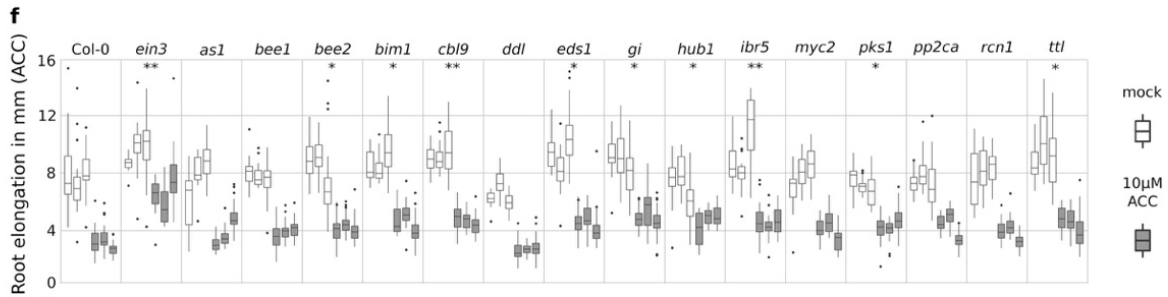
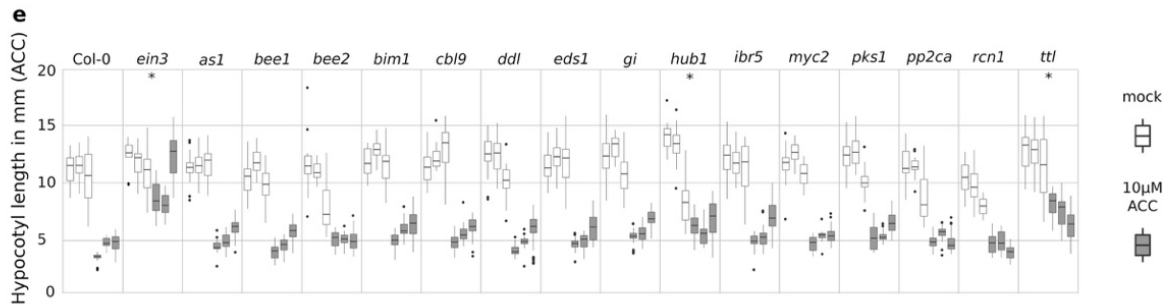
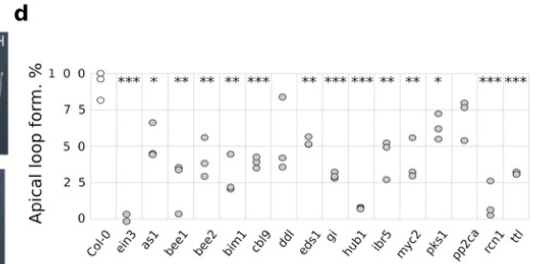
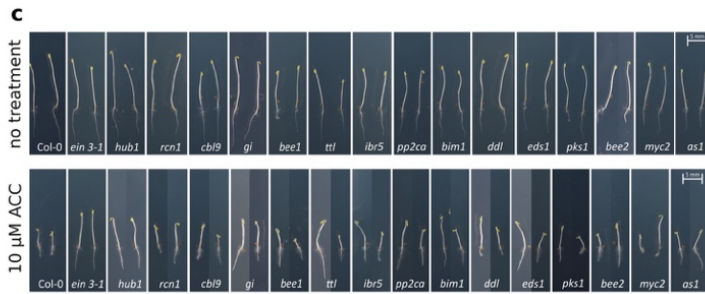
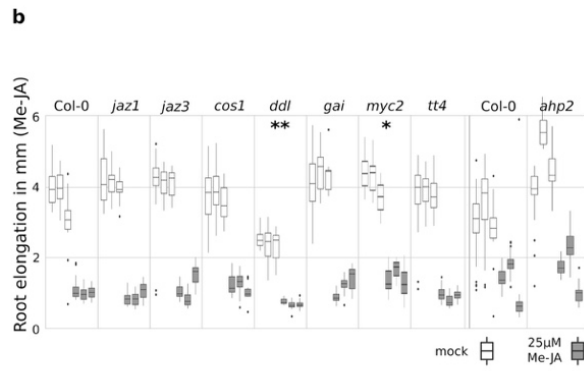
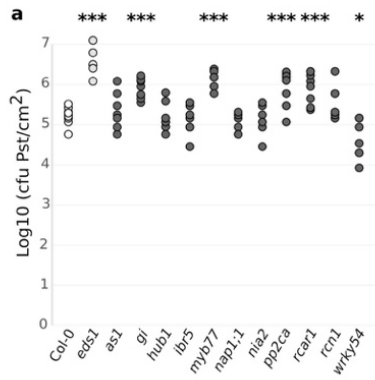
**Extended Data Fig. 2 | Communities and validation.** **a**, Communities with three or more nodes identified in  $PhI_{MAIN}$ . Community numbers correspond to the numbering in Supplementary Table 3. Color code indicates hormone pathway annotations as indicated in legend. Node labels are gene symbols when available, otherwise Locus IDs. **b**, Bimolecular fluorescence complementation (BiFC) for CIPK14-MYC2. *Nicotiana benthamiana* epidermal leaves transiently co-expressing cYFP-MYC2 and nYFP-CIPK14 restore YFP fluorescence, whereas co-expression of the non-interacting cYFP-JAZ1 and nYFP-CIPK14 does not. **c**, maltose-binding-protein (MBP) pull-down of MBP-MYC2 and glutathione-S-reductase (GST) tagged CIPK14 shows specific co-purification of the latter. **b**, **c** Shown are representative results of two experiments with similar results.



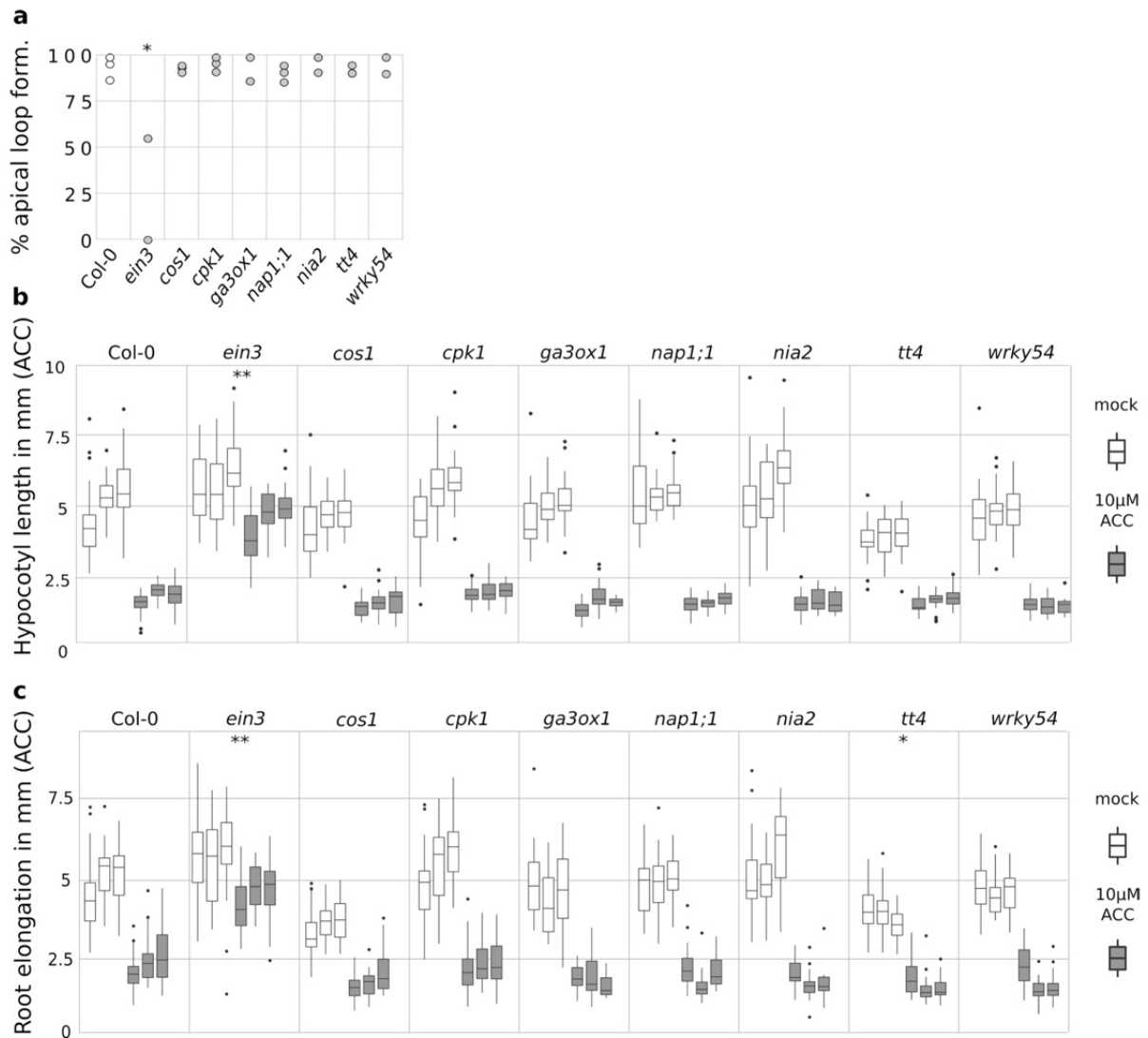
**Extended Data Fig. 3 | Pathway contact points enrichment. a**, Number of pathway contact points (PCPs) per hormone combination for type I and type II are shown. \* indicates a significantly higher number of PCPs compared to  $LCI_{IntA}$  as obtained by bootstrap subsampling analysis ( $n = 1,000$ ) of 100 interactions followed by two-sided Welch two sample t-test. Precise  $P$  Values for  $PCP_I$  and  $PCP_{II}$  and pathway combinations are listed in **Supplementary Table 2**.



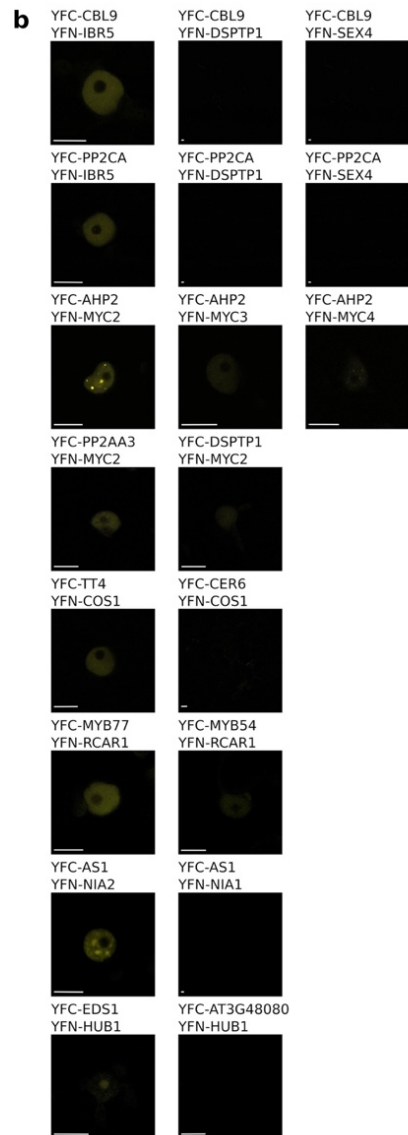
**Extended Data Fig. 4 | Hormone response assays I. a**, ABA germination rate for Col-0 (*WT* background), *cbi9*, *gai*, *myc2*, *ibr5*, *rcar1* and *rcn1* (positive controls), *ahp2*, *as1*, *bee1*, *bee2*, *bim1*, *ddl*, *eds1*, *jaz3*, *myb77* and *wrky54* in absence (MS) or presence of 0.3 μM ABA. **b**, Root elongation in absence (MS) or presence of 30 μM ABA for the same lines as in a. **c**, BR root length inhibition in absence (mock) or presence of indicated concentrations of BL for Col-0 (*WT* background), *bee1*, *bee2*, *bim2* (controls), and *ddl*, *rcn1*, and *ttl* (candidates) lines. **d**, GA root length inhibition in the presence of indicated concentrations of Paclobutrazol (Pac) for Col-0 (*WT* background), *as1*, *gai*, *gi*, *rga* and *rga-28* (controls) and *hub1*, *jaz3*, *nia2*, and *rcn1* (candidate) lines. **b – d**, Boxes represent IQR, bold black line represents median; whiskers indicate highest and lowest data point within 1.5 IQR; outliers are plotted individually. **a – d**, Two sided t-test \*  $P \leq 0.05$ , \*\*  $P \leq 0.01$ , \*\*\*  $P \leq 0.001$ . Precise n for each repeat and precise  $P$  values are provided in **Supplementary Table 5**.



**Extended Data Fig. 5 | Hormone response assays II.** **a**, SA-associated phenotypes: *Pst* titers following 3 dpi with *Pseudomonas syringae* pv. tomato (*Pst*) by syringe infiltration. In planta *Pst* titers were elevated in mature plants of indicated genotypes relative to *WT* Col-0 plants. **b**, JA root growth in absence (MS) or presence of 25  $\mu$ M Me-JA. **c – f**, ET triple response in control conditions compared to Col-0. Apical hook formation graph indicates hook or loop formation following 10  $\mu$ M ACC treatment. The hypocotyl and root length values are shown with and without 10  $\mu$ M 1-aminocyclopropane-carboxylic acid (ACC) treatment. **c**, Apical hook formation in absence or presence of 10  $\mu$ M ACC. Representative results underlying quantitation in **d**. **d**, Proportion of apical loop formation in presence of ACC treatment for same lines as in **c**. **e**, Hypocotyl length in absence or presence of 10  $\mu$ M ACC for same lines as in **d**. **f**, Root elongation in absence or presence of 10  $\mu$ M ACC for same lines as in **d**. Two sided t-test \*  $P \leq 0.05$ , \*\*  $P \leq 0.01$ , \*\*\*  $P \leq 0.001$ . **b**, **e**, **f**, Boxes represent IQR, black line represents median; whiskers indicate highest and lowest data point within 1.5 IQR; outliers are plotted individually. **a**, **b**, **d – f**, Two sided t-test \*  $P \leq 0.05$ , \*\*  $P \leq 0.01$ , \*\*\*  $P \leq 0.001$ . Precise *n* for each repeat and exact *P* values are provided in **Supplementary Table 5**.

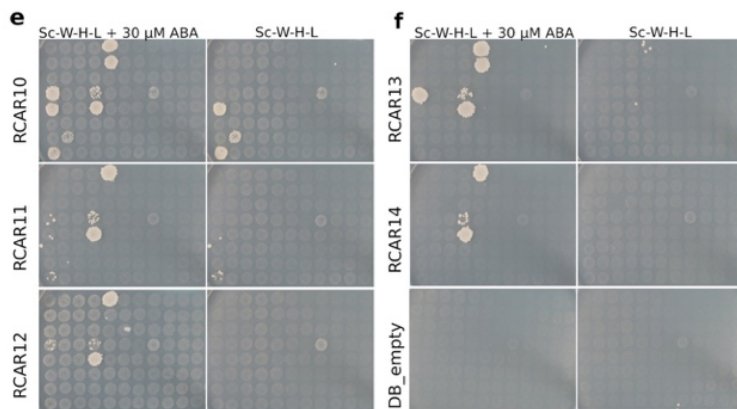
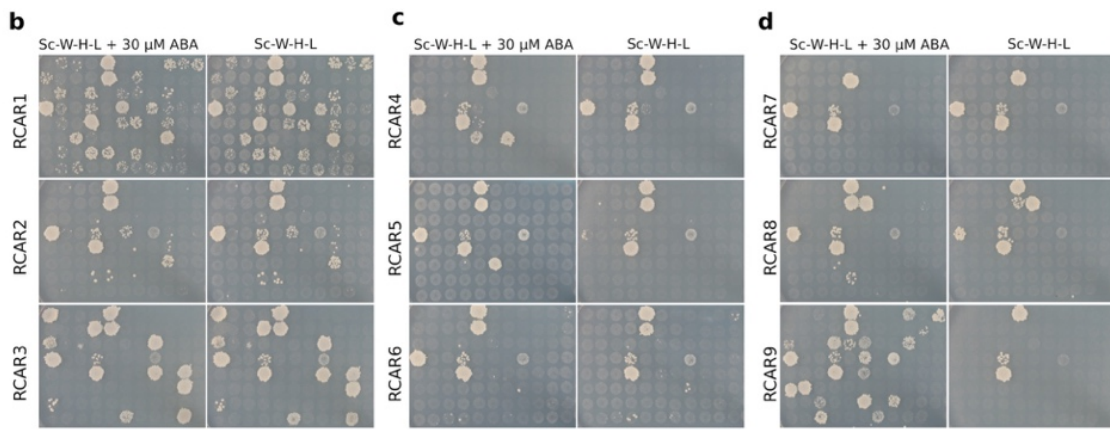
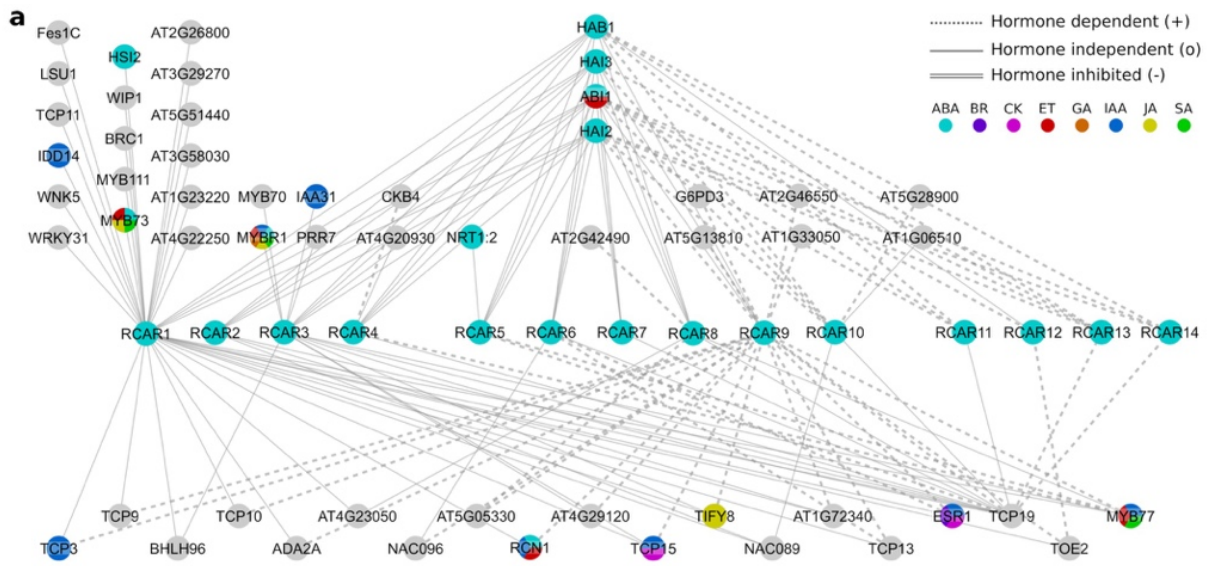


**Extended Data Fig. 6 | ET triple response assays (negative controls).** ET triple response in negative control lines compared to Col-0 and *ein3*. **a**, proportion of apical loop formation in response to 10  $\mu$ M ACC. **b**, Hypocotyl length in absence or presence of 10  $\mu$ M ACC. **d**, Root elongation in absence or presence of 10  $\mu$ M ACC. Two sided t-test \*  $P \leq 0.05$ , \*\*  $P \leq 0.01$ . **b**, **c**, Boxes represent IQR, black line represents median; whiskers indicate highest and lowest data point within 1.5 IQR; outliers are plotted individually. Precise n for each repeat and precise  $P$  values are provided in **Supplementary Table 5**.



**Extended Data Fig. 7 | PCP validation.** **a**, Summary of hormone-assay results for 27 candidate genes. Light colors indicate known hormone pathway annotations. Bright colors indicate significant new phenotypes observed in validation assays. **b**, Bimolecular fluorescent complementation assay (BiFC) in *N. benthamiana* of two PCP<sub>I</sub> pairs (AHP2-MYC2, MYB77-RCAR1) and five PCP<sub>II</sub> pairs (CBL9-IBR5, PP2CA-IBR5, TT4-COS1, AS1-NIA2, EDS1-HUB1). PCP pairs are additionally tested with one or two negative controls in the BiFC assay. Each construct was tested in duplicate and in two independent assays and one representative result is shown. Scale-bar = 10  $\mu$ m.

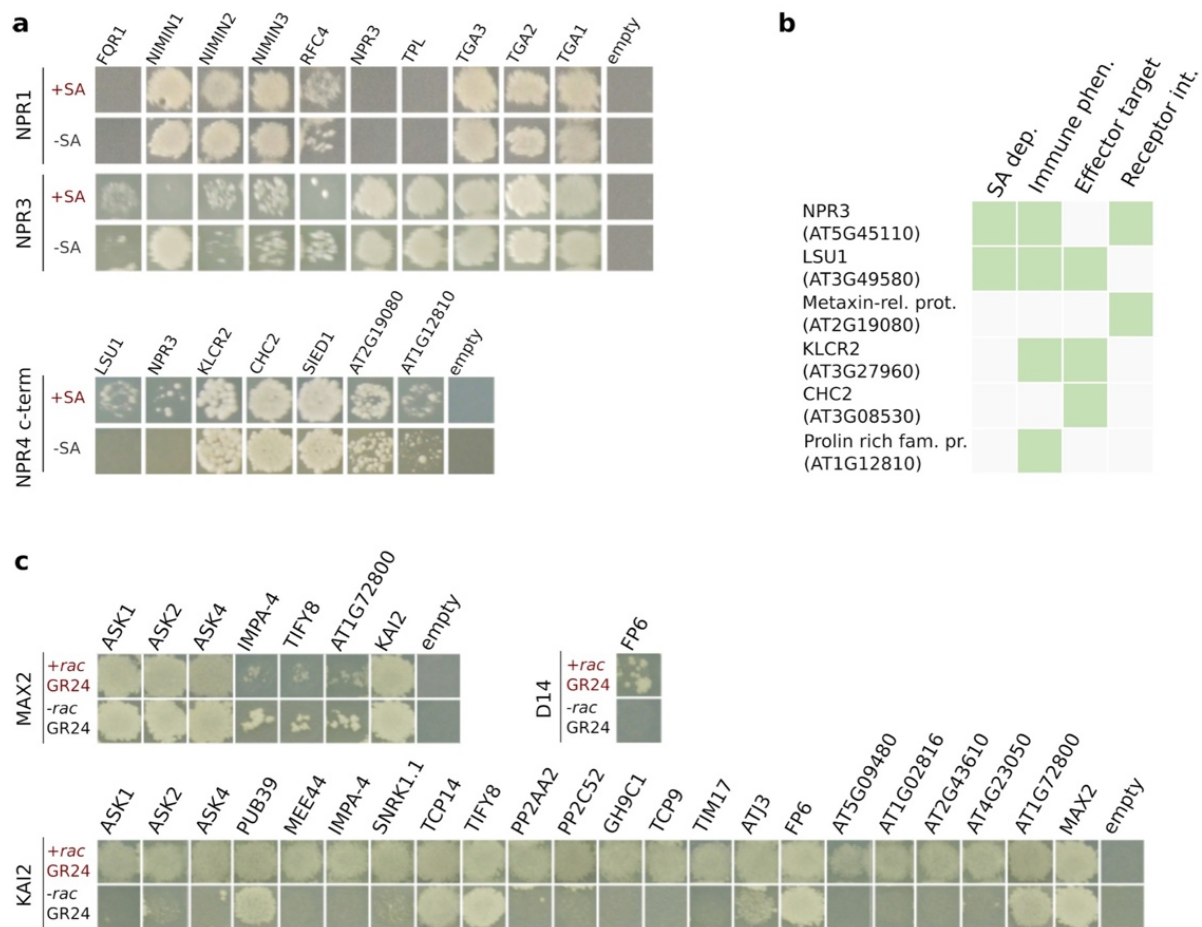
**Extended Data Fig. 8 ABA Y2H interactions.** **a**, ABA-dependent and -independent interactions of RCAR1-14 ABA receptors. All identified interactors were systematically tested against all receptors in presence and absence of 30  $\mu$ M ABA. Except for PP2Cs, single RCAR-specific interactors are displayed above, interactors common to multiple RCARs are displayed below receptors. Color of nodes represent hormone annotations. Solid lines indicate ABA independent interactions, dashed lines indicate ABA-dependent interactions as indicated in legend. **b – f**, one representative set of Y2H results, out of four repeats, showing yeast growth on selective media in presence and absence of 30  $\mu$ M ABA as indicated. All candidate interactors identified in primary screens were tested systematically against all receptors in the shown representative verification experiments. **g**, plate layout of candidate-interactors tested with the indicated RCARs in b-f.



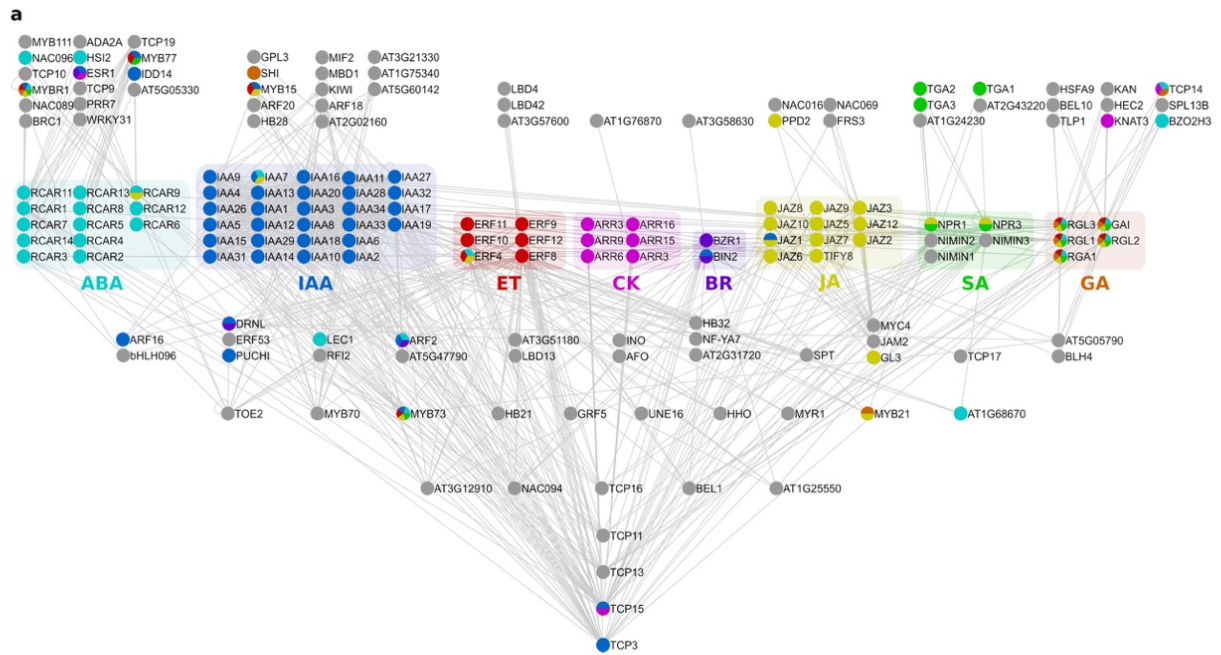
**g**

|   | 1         | 2         | 3         | 4         | 5         | 6         |
|---|-----------|-----------|-----------|-----------|-----------|-----------|
| A | MYB1      | AT3G29270 | TCP15     | AT1G01360 | HAB1      | AT2G26800 |
| B | AT2G26800 | LSU1      | PYL4      | MYB70     | HAI3      | CUAO Zeta |
| C | AT4G29120 | Fes1C     | MYB77     | TCP13     | NAC096    | RCN1      |
| D | HAI2      | AT4G22250 | 4CL1      | TCP19     | HDH1      | AT1G72340 |
| E | AT5G28900 | WNK5      | RCAR3     | ABI1      | CKB4      | TCP10     |
| F | AT1G33050 | AT5G13810 | WIP1      | TOE2      | CKB4      | NRT1-2    |
| G | PRR7      | NAC089    | G6PD3     | AT5G51440 | AT4G23050 | AT2G46550 |
| H | AT1G06510 | TCP11     | TIFY8     | IAA31     | TCP3      | AT1G72210 |
|   | 7         | 8         | 9         | 10        | 11        |           |
| A | AT1G17140 | BRC1      | TCP9      | TCP3      | ESR1      |           |
| B | IDD14     | MYB1      | PTF1      | AT5G05330 | ETC2      |           |
| C | ADA2A     | TCP15     | TOE2      | MYB105    | TCP11     |           |
| D | AT3G11410 | MYB77     | IDD14     | MYB73     | HSI2      |           |
| E | AT1G23220 | IAA31     | MYB111    | MYB70     | ELF4-L2   |           |
| F | CKB4      | NAC096    | NAC089    | TCP19     |           |           |
| G | MUSE-1    | ADA2A     | AT1G72210 | WRKY31    | AD empty  |           |
| H | TCP9      | TCP10     | BRC1      | TIFY8     | AD empty  |           |

**Extended Data Fig. 8 ABA Y2H interactions.** **a**, ABA-dependent and -independent interactions of RCAR1-14 ABA receptors. All identified interactors were systematically tested against all receptors in presence and absence of 30  $\mu$ M ABA. Except for PP2Cs, single RCAR-specific interactors are displayed above, interactors common to multiple RCARs are displayed below receptors. Color of nodes represent hormone annotations. Solid lines indicate ABA independent interactions, dashed lines indicate ABA-dependent interactions as indicated in legend. **b – f**, one representative set of Y2H results, out of four repeats, showing yeast growth on selective media in presence and absence of 30  $\mu$ M ABA as indicated. All candidate interactors identified in primary screens were tested systematically against all receptors in the shown representative verification experiments. **g**, plate layout of candidate-interactors tested with the indicated RCARs in b-f.



**Extended Data Fig. 9 Hormone dependent Y2H interactions.** **a**, SA-dependent interactors of NPR1,3,4. in presence and absence of 100  $\mu$ M SA. **b**, Evidence for NPR4 interactor functions in defense. **c**, MAX2, D14 and KAI2 interactions in presence and absence of 5  $\mu$ M *rac*-GR24. **a**, **c** One representative set of Y2H results, out of four, showing yeast growth in presence and absence of hormone. All candidate interactors identified in primary screen were tested against all receptors in the shown representative verification experiments.



**Extended Data Fig. 10 | Pathway convergence on transcription factors. a**, Y2H-derived interaction map of repressor and non-DNA binding transcriptional regulators (boxed and color coded for the respective main pathway involvement) with Arabidopsis TFs. Above repressors are TFs interacting specifically with regulators from one pathway. Lower layers show the TFs interacting with regulators from multiple number of pathways. Node annotations are represented by color-code as indicated.

**Method book chapter I** Bioassays for the effects of strigolactones and other small molecules on root and root hair development

**Reference: Villaécija-Aguilar, J.A.;** Struk S.; Goormachtig S.; Gutjahr, C. Bioassays for the effects of strigolactone and strigolactone-like molecules on root and root hair development. **MIMB**. Accepted and soon to be published in the book “Strigolactones” edited by SpringerNature.

# Bioassays for the effects of strigolactones and other small molecules on root and root hair development

José Antonio Villaécija-Aguilar<sup>1</sup>, Sylwia Struk<sup>2,3</sup>, Sofie Goormachtig<sup>2,3</sup>, Caroline Gutjahr<sup>1</sup>

**1** Plant Genetics, TUM School of Life Sciences Weihenstephan, Technical University of Munich (TUM), Freising, Germany, **2** Department of Plant Biotechnology and Bioinformatics, Ghent University, Ghent, Belgium, **3** Center for Plant Systems Biology, VIB, Ghent, Belgium.

## Abstract

Growth and development of plant roots are highly dynamic and adaptable to environmental conditions. They are under the control of several plant hormone signalling pathways, and therefore root developmental responses can be used as bioassays to study the action of plant hormones and other small molecules. In this chapter, we present different procedures to measure root traits of the model plant *Arabidopsis thaliana*. We explain methods for phenotypic analysis of lateral root development, primary root length, root skewing, straightness and root hair density and length. We describe optimal growth conditions for *Arabidopsis* seedlings for reproducible root and root hair developmental outputs; and how to acquire images and measure the different traits using image analysis with relatively low-tech equipment. We provide guidelines for a semi-automatic image analysis of primary root length, root skewing and straightness in Fiji and a script to automate the calculation of root angle deviation from the vertical and root straightness. By including mutants defective in strigolactones (SL) or KAI2 ligand (KL) synthesis and/or signalling, these methods can be used as bioassays for different SLs or SL-like molecules. In addition, the techniques described here can be used for studying seedling root system architecture, root skewing, and root hair development in any context.

**Key words** *Arabidopsis* root, lateral root, root hair, root skewing, ImageJ

## 1 Introduction

Growth of vascular plants depends to a great extent on root growth and development, as roots are essential for the uptake of water and nutrients, anchorage and interaction with soil organisms. Roots are subjected to continuous changes and patchy variations in their soil environment. Therefore, for optimal function, root systems dynamically

adapt their morphology to the local soil environment. In developmental studies, trait-based phenotyping is important to investigate the actions of different proteins and molecules. However, this is challenging due to the belowground location of roots. For this reason, root development, especially for the model plant *Arabidopsis thaliana* is commonly analyzed on agar surface in Petri dishes. In these conditions, several traits, such as root hair length and density, lateral root density, root straightness or skewing, are easily assessed.

Lateral roots contribute to the increase of root surface area and biomass, probably to ensure a higher water and nutrient uptake **(1-3)**. Hence, the variability of lateral root growth is considered as an important factor for root system efficiency **(4-5)**. There are different methods to measure the impact of environmental or genetic factors on lateral root development. Because the number of lateral roots increases with the length of the main root, often the lateral root density, calculated as a ratio between the number of lateral roots and the total length of the primary root, is reported instead of the number **(6)**. This easy measurement is then the start for more detailed methods to investigate at which stage the lateral root development is affected, for example at lateral root priming, lateral root outgrowth or others **(7-8)**.

*Arabidopsis* roots growing on hard agar surface cannot penetrate the agar, causing morphological changes such as root skewing and waving **(9-12)**. Skewing was initially described in *Arabidopsis* wild type roots of the ecotype *Landsberg erecta* (Ler) as the tendency of the root to deviate their growth progressively away from the vertical, always as right-slanted **(13-14)**. Although less well studied than other architectural root parameters, recent studies have highlighted the importance of root skewing in understanding root growth behavior and demonstrated that it is likely the result of a touch, rather than the gravity stimulus **(12,15-16)**. Thus far, most of the studies used laborious image analysis and calculations to quantify skewing in *Arabidopsis* roots **(10-11)**. In this chapter, we describe an easy method for semi-automatic image analysis in Fiji to determine the angle of deviation from the gravity vector as well as root straightness and a script to automate the calculation of root skewing to the left or right and of root straightness.

Root hair length and density are highly responsive to environmental conditions and represent another trait that is often used as a read-out for root responses to external

cues or to small molecules. In *Arabidopsis* seedlings, root hairs greatly expand the total root surface area, increasing nutrient and water absorption (17). The knowledge on root hair development is rapidly increasing (18). Thus, several manual and semi-automatic methods have been described for root hair quantification (19-24). However, some of these methods include machine learning approaches and manual analysis of images to train an algorithm for automated detection. Hence, here we describe a simple and easily accessible manual method to measure root hair density and length of *Arabidopsis* roots using microscopy images in Fiji.

All traits described above are regulated by plant hormones that can act both as systemic integrators as well as locally (25). Among them, strigolactones (SLs), have been suggested to play a role in different aspects of plant and root development (26-28). The perception of SLs is closely related to that of karrikins (KARs), molecules released from burning vegetation considered to mimic unknown endogenous plant hormones, called KAI2-ligands (KLs) (29,27,30). Lateral root density is controlled by both SL and KL signalling, while KL signalling regulates root hair development and root skewing (31-33,7).

SLs and KARs/KLs are perceived by the  $\alpha/\beta$ -hydrolase receptor DWARF14 (D14) (34-37) and its homolog KARRIKIN INSENSITIVE 2 (KAI2) (38-41), respectively. SL and KL signalling share the F-box protein MORE AXILLARY GROWTH 2 (MAX2) (42-43,39,44-49). Hence, phenotypes resulting from the loss-of-function of *MAX2* are the consequence of the combination of the phenotypes of *d14* and *kai2* mutants (43,39,32,50-51). Therefore, to understand the specific roles of SL and SL-like molecules in root and root hair development and to assign their function to the correct signalling pathway, it is necessary to use *d14* and *kai2* single mutants specific for SL and KL perception, respectively. Furthermore, pharmacological treatments with SL currently largely depend on the use of synthetic SL analogue, *rac*-GR24 (52-53). However, *rac*-GR24 consists of two stereoisomers, GR24<sup>5DS</sup> and GR24<sup>ent5DS</sup>, that stimulate both D14 and KAI2 (52,54,32,55). Furthermore, a contaminant 'contalactone', which also acts as an SL mimic through D14 and KAI2 has been detected in several preparations of *rac*-GR24 (56). Therefore, the use of single and pure stereoisomers in combination with pathway-specific mutants is warranted.

Here we present methods for genetic and phenotypic analysis of lateral root development, root skewing, root straightness and root hair density and length in *Arabidopsis thaliana*. These methods allow dissection of SL and KL signalling pathways and can be used as bioassays for SLs and SL-like molecules or any other signalling compounds.

## **2 Material**

### **2.1 Seed sterilization**

1. Arabidopsis seeds.
2. Sterilizing solution: 70% (v/v) ethanol and 0.05% (v/v) Triton X-100 or 0.05% (w/v) dodecyl sulfate sodium salt (SDS). Store at room temperature.
3. 96% (v/v) ethanol.
4. Sterile water.
5. Pipette for 1000 µl.
6. Sterile tips for 1000 µl.
7. Eppendorf tube.
8. Eppendorf tube rotator or shaker.
9. Laminar air flow cabinet.

### **2.2 Growth conditions**

1. Murashige and Skoog (MS) medium.
2. Sucrose.
3. Bactoagar.
4. Agar, plant tissue culture.
5. MES monohydrate.
6. Myo-inositol.
7. Distilled water (dH<sub>2</sub>O).
8. Sterile toothpicks.
9. Milligram scale.
10. KOH.
11. pH meter.
12. Autoclave.
13. 500 mL or 1 L glass bottle.
14. Square Petri dishes: 120 x 120 mm.

15. Autoclaved graduated cylinder.
16. Pipette for 200  $\mu$ l.
17. Sterile tips for 200  $\mu$ l.
18. Laminar air flow cabinet.
19. Parafilm.
20. Microtape.
21. Aluminium foil or dark box to keep Petri dishes containing seeds in dark during the stratification period.
22. Cold room at 4°C.
23. Rack or other support to maintain the square Petri dishes in vertical position.
24. Growth cabinet: 21°C, 16-h light /8-h dark photoperiod. Humidity at 50-60%. Light intensity 120  $\mu$ mol m<sup>-2</sup> s<sup>-1</sup>.

## 2.4 Phytohormones treatments

1. *rac*-GR24 (Chiralix, Nijmegen, The Netherlands; Strigolab, Turin, Italy; or Olchemim, Olomouc, Czech Republic).
2. GR24<sup>ent5DS</sup> (Strigolab, Turin, Italy).
3. GR24<sup>5DS</sup> (Strigolab, Turin, Italy).
4. KAR<sub>1</sub> or KAR<sub>2</sub> (Olchemim, Olomouc, Czech Republic).
5. 100% acetone.
6. 70% (v/v) methanol.

## 2.3 Image and data acquisition

1. High resolution scanner with a minimum of 800 dpi (dots per inch).
2. Root hairs: stereo microscope equipped with a camera.
3. Lateral roots: binocular S4E microscope.
4. Computer with Fiji software.

## 3 Methods

### 3.1 Seed sterilization

1. Place 1 ml of sterilization solution in an Eppendorf tube containing a maximum of approximately 200 Arabidopsis seeds per tube and wash with

gentle mixing by inversion on a tube rotator or shaker for 6 minutes at room temperature.

2. Remove sterilization solution and briefly wash seeds once with 96% (v/v) ethanol under sterile conditions. For primary and lateral root analysis go directly to step 5.
3. Wash four times with sterile water under sterile conditions.
4. Suspend the seeds in 100-200  $\mu$ L of sterile water. The volume varies depending on the number of seeds. Work under sterile conditions.
5. Discard the solution and leave the Eppendorf tube open in the laminar air flow cabinet until the seeds are completely dry.

### 3.2 Growth conditions

#### 3.2.1. Primary and lateral root analysis

Plants are grown in Petri dishes (120 x 120 mm) on solid half MS medium supplemented with sucrose. For one biological repeat at least 30 seedlings are tested for each genotype and treatment.

1. Solid half-strength MS medium: 2.151 g/L MS, 1% (w/v) sucrose, 0.5 g/L MES, 0.1 g/L Myo-inositol, and 800 ml of dH<sub>2</sub>O. Adjust the pH to 5.8 (with KOH), top up to 1 L with dH<sub>2</sub>O and add 8 g/L plant tissue culture agar. Autoclave the medium at 121 °C for 20 min.
2. When testing phytohormone effect see point 3.3.
3. Use an autoclaved graduated cylinder to pour 60 mL of medium in each square Petri dish, to ensure equal medium thickness among Petri dishes.
4. Use sterile toothpick to equally distribute 12 seeds on the surface of solidified medium (see **Note 1**).
5. Seal the plate with micropore tape.
6. Place the plates at 4°C for 2-3 days for stratification in the dark.
7. Transfer the plates to suitable growth chambers, 21°C with a photoperiod of 16-h light/8-h dark; 120  $\mu$ E light intensity, and place them vertically with a distance of approx. 4 cm between plates.
8. Grow the seedlings vertically for 10 days.

#### 3.2.2. Analysis of root skewing, straightness and root hair development

Plants are grown in Petri dishes (120 x 120 mm) on solid half MS medium supplemented with sucrose. For one biological repeat at least 50 seedlings are for each genotype and treatment for root skewing and straightness analysis, or at least 10 seedlings are tested for each genotype and treatment for root hair analysis.

1. Solid half-strength MS medium: add into distilled water 2.151 g/L MS and 1% (w/v) sucrose. Adjust the pH to 5.8 (with KOH) and add 15 g/L Bactoagar. Autoclave the medium at 121 °C for 20 min.
2. Use an autoclaved graduated cylinder to pour 60 mL of medium in each square Petri dish, to ensure equal medium thickness among Petri dishes.
3. Pipette seeds resuspended in water with 200 µL sterile tips.
4. Remove sterile tip from the pipette and position the pipette tip over the surface of the agar. Dispense single seeds with a maximum of 20 seeds per row (see **Note 2-4**).
5. Seal  $\frac{3}{4}$  of the Petri dish with parafilm and  $\frac{1}{4}$  with micropore tape to increase transpiration and avoid an accumulation of water in the dish (see **Note 5**).
6. Place the Petri dishes at 4°C for 2-3 days for stratification in the dark.
7. Transfer the plates to suitable growth chambers, 21°C with a photoperiod of 16-h light/8-h dark; 120 µE light intensity, and place them vertically with a distance of approx. 4 cm between plates.
8. Grow the seedlings vertically for 5 days
9. Image acquisition using a scanner for root skewing or stereo microscope for root hair analysis are described below.

### 3.3 Phytohormone treatments

1. Prepare 1 mM stock solutions in 100% acetone for *rac*-GR24 (Chiralix, Nijmegen, The Netherlands), GR24<sup>ent5DS</sup> (Strigolab, Turin, Italy) or GR24<sup>5DS</sup> (Strigolab, Turin, Italy) or in 70% (v/v) methanol for KAR<sub>1</sub> or KAR<sub>2</sub> (Olchemim, Olomouc, Czech Republic).
2. Add the required volume of stock solution to reach your desired final concentration (for example 1 µM) to molten, slightly cooled (approx. 60°C) media prior to pouring it into Petri dishes.

3. For untreated controls, add an equivalent volume of solvent to molten media prior to pouring it into Petri dishes.

### 3.4 Data acquisition and analysis

Image analysis for primary root length, root skewing, root straightness, root hair density and root hair length quantification are implemented in the open-source package Fiji of ImageJ (<https://doi.org/10.1038/nmeth.2019>). Fiji is freely available for different operating systems from <https://imagej.net/Fiji/Downloads>

#### 3.4.1 Analysis of lateral roots

1. Count the number of all visible emerged lateral roots in 10-day-old seedlings under a binocular S4E microscope (see **Note 6**).
2. Take images of Petri dishes containing 10-day-old seedlings next to a ruler using a high-resolution scanner with a minimum of 400 dpi (dots per inch).
3. To measure main root length, follow 6-19 points described in 3.4.2
4. Lateral root density is calculated by dividing the number of lateral roots by the corresponding primary root length.

#### 3.4.2 Analysis of primary root length, root skewing and root straightness using Fiji

1. Take images of Petri dishes containing 5-day-old seedlings next to a ruler using a high-resolution scanner with a minimum of 800 dpi (dots per inch) (see **Note 6 and 7**).
2. Open your image in Fiji.
3. To calculate the angle of the deviation from the vertical and root straightness, we provide the following script:

```
IJ.renameResults("Branch information", "Results");
```

```
for(i=0; i<nResults; i++) {  
    x1 = getResult("V1 x", i);  
    y1 = getResult("V1 y", i);
```

```

x2 = getResult("V2 x", i);
y2 = getResult("V2 y", i);
rootlength = getResult("Branch length", i);

opposite = abs(x1-x2);
adjacent = abs(y1-y2);
normalize = (y2-y1);
hypotenuse = sqrt(((y2-y1)*(y2-y1))+((x2-x1)*(x2-x1)));
straightness = (hypotenuse/rootlength);

angle = atan2(opposite, adjacent)*(180/PI);
if (normalize<0) {
    angle = atan2(opposite, adjacent)*(-180/PI);
}

getResult("Primary root length", i, rootlength);
getResult("Angle", i, angle);
getResult("Straightness", i, straightness);
}

```

4. To insert the script into Fiji go to File -> New -> Script... and select Language -> IJ1 Macro.
5. Copy the script provided above and paste it inside the new Macro. Save the script using Edit -> Save as.
6. Open images using Fiji.
7. Using the segmented line tool of Fiji, draw a line of 1 cm on the ruler picture.
8. Go to Analyze -> Set Scale. Change "Known distance" to 10 and "Unit of length" to mm (millimeter).
9. After setting the scale go to Plugins -> Segmentation -> Simple Neurite Tracer.
10. Convert RGB image to an 8-bit luminance image first.
11. To start the quantification, click at the beginning and at the end of the root. Tracing will automatically trace a line between these two points (Fig. 1a)
12. If the trace is correct, click "Y" (Yes) followed by clicking "F" (Finish Path).
13. If the trace is not correct, we can improve the segmentation using "Pick Sigma Manually" or "Pick Sigma Visually" in the Simple Neurite Tracer plugin.

14. Go to the next seedling and proceed again from point 11 to 13.
15. If two roots are in contact, the trace will be segmented, and therefore it will not be useful for either root length or root skewing quantification (see **Note 7**).
16. After completing the paths for all the roots, in the Simple Neurite Tracer plugin, go to Analysis -> Render/Analyze Skeletonized Path and select Run "Analyze Skeleton" plugin.
17. In the next window of Analyze Skeleton do not use any Prune cycle method. Only select "Show detailed info".
18. Two new windows containing the Branch information and Results will appear.
19. Branch length provides the root length results for each of the roots analyzed.
20. Open the script saved in 5 and run it. Three new columns will appear in the table "Results", called "Primary root length", "Angle" and "Straightness". For Angle, negative or positive values will indicate left or right skewing, respectively (Fig. 1b).
21. Save the table "Results" as a text file.
22. Open the text file in Excel for further statistical analysis.

### 3.4.3 Analysis of root hair density and length

We suggest to analyse the root hair density and length in a specific part of the root between 2 and 3 mm from the root tip.

1. Take images of a minimum of 10 roots per genotype and treatment with a stereo microscope equipped with a camera. The pictures should cover at least 3 mm from the root tip (see **Note 6 and 7**).
2. Open images using Fiji.
3. Using segmented line tool of Fiji, draw a line from root tip to 2 mm (Fig. 2a). Use Edit -> Draw to permanently keep the line on the image.
4. Using arrow tool of Fiji, draw an arrow to 2 mm from the root tip (Fig. 2b). Use Edit -> Draw to permanently keep the arrow on the image.
5. Using segmented line tool of Fiji, draw a line between 2 to 3 mm (Fig. 2b). Use Edit -> Draw to permanently keep the line on the image.
6. Using arrow tool of Fiji, draw another arrow to 3 mm from the root tip (Fig. 2b). Use Edit -> Draw to permanently keep the arrow on the image.

7. **For quantification of root hair density** count all the root hairs between the 2 arrows (2 to 3 mm from the root tip) and write the number of root hairs in an excel file for further statistical analysis.
8. **For quantification of root hair length** use segmented line tool of Fiji to draw a line from the base of a root hair to the end of the root hair (yellow line in Fig. 2c). Click “M” to measure the length.
9. Measure a minimum of 10 root hairs length per root.
10. After finishing all measurements from one root, select and copy the table in the “Results” windows of Fiji and paste it into an excel file. The root hair length will appear in the column “Length” which can be used for further statistical analysis.

#### 4 Notes

1. Equal distribution of seeds can be facilitated by use of a paper template with indicated seed position below the Petri dish.
2. For root skewing and root straightness, it is possible to use 3 rows of seeds, at 3 cm, 5.5 cm and 8 cm from the top of the Petri dish.
3. Root hair development is very sensitive to light conditions. To avoid influences on root hair development by different light conditions among seedlings, place the 20 seeds as described above in only one row, 3 cm from the top of the Petri dish for root hair density and length analysis. Avoid multiple rows below as light intensity increases further down.
4. If using different genotypes, it is recommendable to divide the plate in 2, with seedlings of genotype “A” in the left and genotype “B” in the right. In that case, differences between plates are easily observable.
5. Hermetic sealing of Petri dishes using parafilm can reduce gas exchange and subsequently increase ethylene accumulation in the Petri dish. Ethylene modulates root skewing, root hair density and length (**57-58,24**). Therefore, a complete sealing of the plate or different sealing between plates might alter the outcome of the experiment. The same is true for the number of seedlings per plate: too many seedlings may increase the amount of ethylene. Therefore, we recommend only 20 seedlings per plate for the particularly sensitive root hair assays.

6. For all the root parameters described in this chapter, roots that are growing not on the surface but inside the agar should be excluded from the analysis.
7. Root hair development, root skewing and root straightness will be altered if different roots touch each other. Therefore, a minimum space between seedlings is necessary. Thus, roots in contact with each other should be excluded from the analysis of these root parameters.

### **Acknowledgments**

This work was supported by the Emmy Noether program (GU1423/1-1) of the Deutsche Forschungsgemeinschaft (DFG) to CG

### **References**

1. Robbins NE, 2nd, Dinneny JR (2015) The divining root: moisture-driven responses of roots at the micro- and macro-scale. *J Exp Bot* 66 (8):2145-2154
2. Sun C-H, Yu J-Q, Hu D-G (2017) Nitrate: A Crucial Signal during Lateral Roots Development. *Front Plant Sci* 8:485-485
3. Tian H, De Smet I, Ding Z (2014) Shaping a root system: regulating lateral versus primary root growth. *Trends Plant Sci* 19 (7):426-431
4. Forde BG (2009) Is it good noise? The role of developmental instability in the shaping of a root system. *J Exp Bot* 60 (14):3989-4002
5. Freixes S, Thibaud M-C, Tardieu F, Muller B (2002) Root elongation and branching is related to local hexose concentration in *Arabidopsis thaliana* seedlings. *Plant Cell Environ* 25 (10):1357-1366
6. De Smet I, White PJ, Bengough AG, Dupuy L, Parizot B, Casimiro I, Heidstra R, Laskowski M, Lepetit M, Hochholdinger F, Draye X, Zhang H, Broadley MR, Péret B, Hammond JP, Fukaki H, Mooney S, Lynch JP, Nacry P, Schurr U, Laplaze L, Benfey P, Beeckman T, Bennett M (2012) Analyzing Lateral Root Development: How to Move Forward. *Plant Cell* 24 (1):15-20
7. Jiang L, Matthys C, Marquez-Garcia B, De Cuyper C, Smet L, De Keyser A, Boyer F-D, Beeckman T, Depuydt S, Goormachtig S (2016) Strigolactones spatially influence

lateral root development through the cytokinin signaling network. *J Exp Bot* 67 (1):379-389

8. Malamy JE, Benfey PN (1997) Organization and cell differentiation in lateral roots of *Arabidopsis thaliana*. *Development* 124 (1):33-44

9. Okada K, Shimura Y (1990) Reversible Root Tip Rotation in *Arabidopsis* Seedlings Induced by Obstacle-Touching Stimulus. *Science* 250 (4978):274-276

10. Grabov A, Ashley M, Rigas S, Hatzopoulos P, Dolan L, Vicente-Agullo F (2005) Morphometric analysis of root shape. *New Phytol* 165 (2):641-652

11. Vaughn LM, Masson PH (2011) A QTL study for regions contributing to *Arabidopsis thaliana* root skewing on tilted surfaces. *G3* 1 (2):105-115

12. Roy R, Bassham DC (2014) Root growth movements: waving and skewing. *Plant Science* 221:42-47

13. Simmons C, Migliaccio F, Masson P, Caspar T, Söll D (1995) A novel root gravitropism mutant of *Arabidopsis thaliana* exhibiting altered auxin physiology. *Physiol Plant* 93 (4):790-798

14. Rutherford R, Masson PH (1996) *Arabidopsis thaliana sku* mutant seedlings show exaggerated surface-dependent alteration in root growth vector. *Plant Physiol* 111 (4):987-998

15. Millar KDL, Johnson CM, Edelmann RE, Kiss JZ (2011) An Endogenous Growth Pattern of Roots Is Revealed in Seedlings Grown in Microgravity. *Astrobiology* 11 (8):787-797

16. Paul A-L, Amalfitano CE, Ferl RJ (2012) Plant growth strategies are remodeled by spaceflight. *BMC Plant Biol* 12 (1):232

17. López-Bucio J, Cruz-Ramírez A, Herrera-Estrella L (2003) The role of nutrient availability in regulating root architecture. *Curr Opin Plant Biol* 6 (3):280-287

18. Kwasniewski M, Nowakowska U, Szumera J, Chwialkowska K, Szarejko I (2013) iRootHair: A Comprehensive Root Hair Genomics Database. *Plant Physiol* 161 (1):28-35

19. Guichard M, Allain J-M, Bianchi MW, Frachisse J-M (2019) Root Hair Sizer: an algorithm for high throughput recovery of different root hair and root developmental parameters. *Plant Methods* 15 (1):104
20. Vincent C, Rowland D, Na C, Schaffer B (2017) A high-throughput method to quantify root hair area in digital images taken *in situ*. *Plant and Soil* 412 (1):61-80
21. Pečenková T, Janda M, Ortmannová J, Hajná V, Stehlíková Z, Žárský V (2017) Early *Arabidopsis* root hair growth stimulation by pathogenic strains of *Pseudomonas syringae*. *Ann Bot* 120 (3):437-446
22. Narukawa M, Kanbara K, Tominaga Y, Aitani Y, Fukuda K, Kodama T, Murayama N, Nara Y, Arai T, Konno M, Kamisuki S, Sugawara F, Iwai M, Inoue Y (2009) Chlorogenic Acid Facilitates Root Hair Formation in Lettuce Seedlings. *Plant Cell Physiol* 50 (3):504-514
23. Liu C-Y, Zhang F, Zhang D-J, Srivastava AK, Wu Q-S, Zou Y-N (2018) Mycorrhiza stimulates root-hair growth and IAA synthesis and transport in trifoliate orange under drought stress. *Sci Rep* 8 (1):1978
24. Feng Y, Xu P, Li B, Li P, Wen X, An F, Gong Y, Xin Y, Zhu Z, Wang Y, Guo H (2017) Ethylene promotes root hair growth through coordinated EIN3/EIL1 and RHD6/RSL1 activity in *Arabidopsis*. *Proc Natl Acad Sci U S A* 114 (52):13834-13839
25. Vanstraelen M, Benková E (2012) Hormonal Interactions in the Regulation of Plant Development. *Annu Rev Cell Dev Biol* 28 (1):463-487
26. Matthys C, Walton A, Struk S, Stes E, Boyer F-D, Gevaert K, Goormachtig S (2016) The Whats, the Wheres and the Hows of strigolactone action in the roots. *Planta* 243 (6):1327-1337
27. Waters MT, Gutjahr C, Bennett T, Nelson DC (2017) Strigolactone signaling and evolution. *Annu Rev Plant Biol* 68:291-322
28. Waldie T, McCulloch H, Leyser O (2014) Strigolactones and the control of plant development: lessons from shoot branching. *Plant J* 79 (4):607-622
29. De Cuyper C, Struk S, Braem L, Gevaert K, De Jaeger G, Goormachtig S (2017) Strigolactones, karrikins and beyond. *Plant Cell Environ* 40 (9):1691-1703

30. Machin DC, Hamon-Josse M, Bennett T (2020) Fellowship of the rings: a saga of strigolactones and other small signals. *New Phytol* 225 (2):621-636
31. Kapulnik Y, Delaux P-M, Resnick N, Mayzlish-Gati E, Winer S, Bhattacharya C, Séjalon-Delmas N, Combier J-P, Bécard G, Belausov E, Beeckman T, Dor E, Hershenhorn J, Koltai H (2011) Strigolactones affect lateral root formation and root-hair elongation in *Arabidopsis*. *Planta* 233 (1):209-216
32. Villaécija-Aguilar JA, Hamon-Josse M, Carbonnel S, Kretschmar A, Schmid C, Dawid C, Bennett T, Gutjahr C (2019) SMAX1/SMXL2 regulate root and root hair development downstream of KAI2-mediated signalling in *Arabidopsis*. *PLoS Genet* 15 (8):e1008327
33. Swarbreck SM, Guerringue Y, Matthus E, Jamieson FJC, Davies JM (2019) Impairment in karrikin but not strigolactone sensing enhances root skewing in *Arabidopsis thaliana*. *Plant J*
34. Hamiaux C, Drummond RS, Janssen BJ, Ledger SE, Cooney JM, Newcomb RD, Snowden KCJ (2012) DAD2 is an  $\alpha/\beta$  hydrolase likely to be involved in the perception of the plant branching hormone, strigolactone. *Curr Biol* 22 (21):2032-2036
35. de Saint Germain A, Clavé G, Badet-Denisot M-A, Pillot J-P, Cornu D, Le Caer J-P, Burger M, Pelissier F, Retailleau P, Turnbull C, Sandrine B, Joanne C, Catherine R, François-Didier B (2016) An histidine covalent receptor and butenolide complex mediates strigolactone perception. *Nat Chem Biol* 12 (10):787-794
36. Yao R, Ming Z, Yan L, Li S, Wang F, Ma S, Yu C, Yang M, Chen L, Chen L, Li Y, Yan C, Miao D, Sun Z, Yan J, Sun Y, Wang L, Chu J, Fan S, He W, Deng H, Nan F, Li J, Rao Z, Lou Z, Xie D (2016) DWARF14 is a non-canonical hormone receptor for strigolactone. *Nature* 536 (7617):469-473
37. Seto Y, Yasui R, Kameoka H, Tamiru M, Cao M, Terauchi R, Sakurada A, Hirano R, Kisugi T, Hanada A, Umehara M, Seo E, Akiyama K, Burke J, Noriko T-K, Li W, Hirano Y, Hakoshima T, Mashiguchi K, Noel JP, Kyojuka J, Yamaguchi S (2019) Strigolactone perception and deactivation by a hydrolase receptor DWARF14. *Nat Commun* 10 (1):191

38. Guo Y, Zheng Z, La Clair JJ, Chory J, Noel JP (2013) Smoke-derived karrikin perception by the  $\alpha/\beta$ -hydrolase KAI2 from *Arabidopsis*. *Proc Natl Acad Sci U S A* 20:8284-8289
39. Waters MT, Nelson DC, Scaffidi A, Flematti GR, Sun YK, Dixon KW, Smith SM (2012) Specialisation within the DWARF14 protein family confers distinct responses to karrikins and strigolactones in *Arabidopsis*. *Development* 139 (7):1285-1295
40. Sun H, Tao J, Gu P, Xu G, Zhang Y (2016) The role of strigolactones in root development. *Plant Signal Behav* 11 (1):e11110662-e11110662
41. Kagiya M, Hirano Y, Mori T, Kim SY, Kyojuka J, Seto Y, Yamaguchi S, Hakoshima T (2013) Structures of D14 and D14L in the strigolactone and karrikin signaling pathways. *Genes to Cells* 18 (2):147-160
42. Stanga JP, Smith SM, Briggs WR, Nelson DC (2013) *SUPPRESSOR OF MAX2 1* controls seed germination and seedling development in *Arabidopsis thaliana*. *Plant Physiol* 163:318-330
43. Nelson DC, Scaffidi A, Dun EA, Waters MT, Flematti GR, Dixon KW, Beveridge CA, Ghisalberti EL, Smith SM (2011) F-box protein MAX2 has dual roles in karrikin and strigolactone signaling in *Arabidopsis thaliana*. *Proc Natl Acad Sci U S A* 108 (21):8897-8902
44. Soós V, Sebestyén E, Juhász A, Light ME, Kohout L, Szalai G, Tandori J, Van Staden J, Balázs E (2010) Transcriptome analysis of germinating maize kernels exposed to smoke-water and the active compound KAR1. *BMC Plant Biol* 10 (1):236
45. Wang L, Wang B, Jiang L, Liu X, Li X, Lu Z, Meng X, Wang Y, Smith SM, Li J (2015) Strigolactone signaling in *Arabidopsis* regulates shoot development by targeting D53-like SMXL repressor proteins for ubiquitination and degradation. *Plant Cell* 27:3128-3142
46. Liang Y, Ward S, Li P, Bennett T, Leyser O (2016) SMAX1-LIKE7 signals from the nucleus to regulate shoot development in *Arabidopsis* via partially EAR motif-independent mechanisms. *Plant Cell* 28:1581-1601

47. Jiang L, Liu X, Xiong G, Liu H, Chen F, Wang L, Meng X, Liu G, Yu H, Yuan Y, Yi W, Zhao L, Ma H, He Y, Wu Z, Melcher K, Qian Q, Xu HE, Wang Y, Li J (2013) DWARF 53 acts as a repressor of strigolactone signalling in rice. *Nature* 504:401
48. Zhou F, Lin Q, Zhu L, Ren Y, Zhou K, Shabek N, Wu F, Mao H, Dong W, Gan L, Ma W, Gao H, Chen J, Yang C, Wang D, Tan J, Zhang X, Guo X, Wang J, Jiang L, Liu X, Chen W, Chu J, Yan C, Ueno K, Ito S, Asami T, Cheng Z, Wang J, Lei C, Zhai H, Wu C, Wang H, Zheng N, Wan J (2013) D14–SCFD3-dependent degradation of D53 regulates strigolactone signalling. *Nature* 504:406
49. Stanga JP, Morffy N, Nelson DC (2016) Functional redundancy in the control of seedling growth by the karrikin signaling pathway. *Planta* 243 (6):1397-1406
50. Soundappan I, Bennett T, Morffy N, Liang Y, Stanga JP, Abbas A, Leyser O, Nelson DC (2015) SMAX1-LIKE/D53 family members enable distinct MAX2-dependent responses to strigolactones and karrikins in Arabidopsis. *Plant Cell* 27:3143-3159
51. Bennett T, Hines G, van Rongen M, Waldie T, Sawchuk MG, Scarpella E, Ljung K, Leyser O (2016) Connective auxin transport in the shoot facilitates communication between shoot apices. *PLoS Biology* 14 (4):e1002446
52. Scaffidi A, Waters M, Sun YK, Skelton BW, Dixon KW, Ghisalberti EL, Flematti G, Smith S (2014) Strigolactone hormones and their stereoisomers signal through two related receptor proteins to induce different physiological responses in Arabidopsis. *Plant Physiol* 165:1221-1232
53. Mangnus EM, Dommerholt FJ, De Jong RL, Zwanenburg B (1992) Improved synthesis of strigol analog GR24 and evaluation of the biological activity of its diastereomers. *J Agric Food Chem* 40 (7):1230-1235
54. Waters MT, Scaffidi A, Flematti G, Smith SM (2015) Substrate-induced degradation of the  $\alpha/\beta$ -fold hydrolase KARRIKIN INSENSITIVE2 requires a functional catalytic triad but is independent of MAX2. *Mol Plant* 8 (5):814-817
55. Nakamura H, Xue Y-L, Miyakawa T, Hou F, Qin H-M, Fukui K, Shi X, Ito E, Ito S, Park S-H, Miyauchi Y, Asano A, Totsuka N, Ueda T, Tanokura M, Asami T (2013)

Molecular mechanism of strigolactone perception by DWARF14. Nat Commun 4 (1):2613

56. de Saint Germain A, Retailleau P, Norsikian S, Servajean V, Pelissier F, Steinmetz V, Pillot J-P, Rochange S, Pouvreau J-B, Boyer F-D (2019) Contalactone, a contaminant formed during chemical synthesis of the strigolactone reference GR24 is also a strigolactone mimic. Phytochemistry 168:112112

57. Pitts RJ, Cernac A, Estelle M (1998) Auxin and ethylene promote root hair elongation in *Arabidopsis*. Plant J 16 (5):553-560

58. Buer CS, Wasteneys GO, Masle J (2003) Ethylene modulates root-wave responses in *Arabidopsis*. Plant Physiol 132 (2):1085-1096

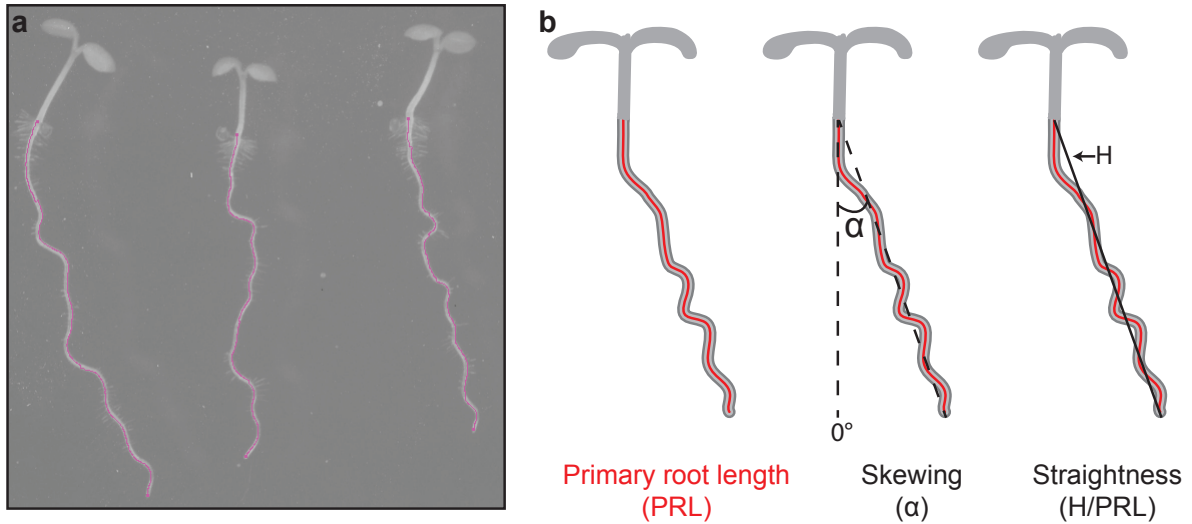


**Figure 1.** (a) Visualization of the path using Simple Neurite Tracer plugin for primary root length, root skewing and root straightness quantification. (b) Schematic diagram showing how primary root length, skewing-angle and root straightness are determined. Skewing is calculated as the angle between the vertical, defined as  $0^\circ$  and the root tip. Straightness is measured as the ratio of the chord line between the hypocotyl-root junction and the root tip (H) and the primary root length (PRL).

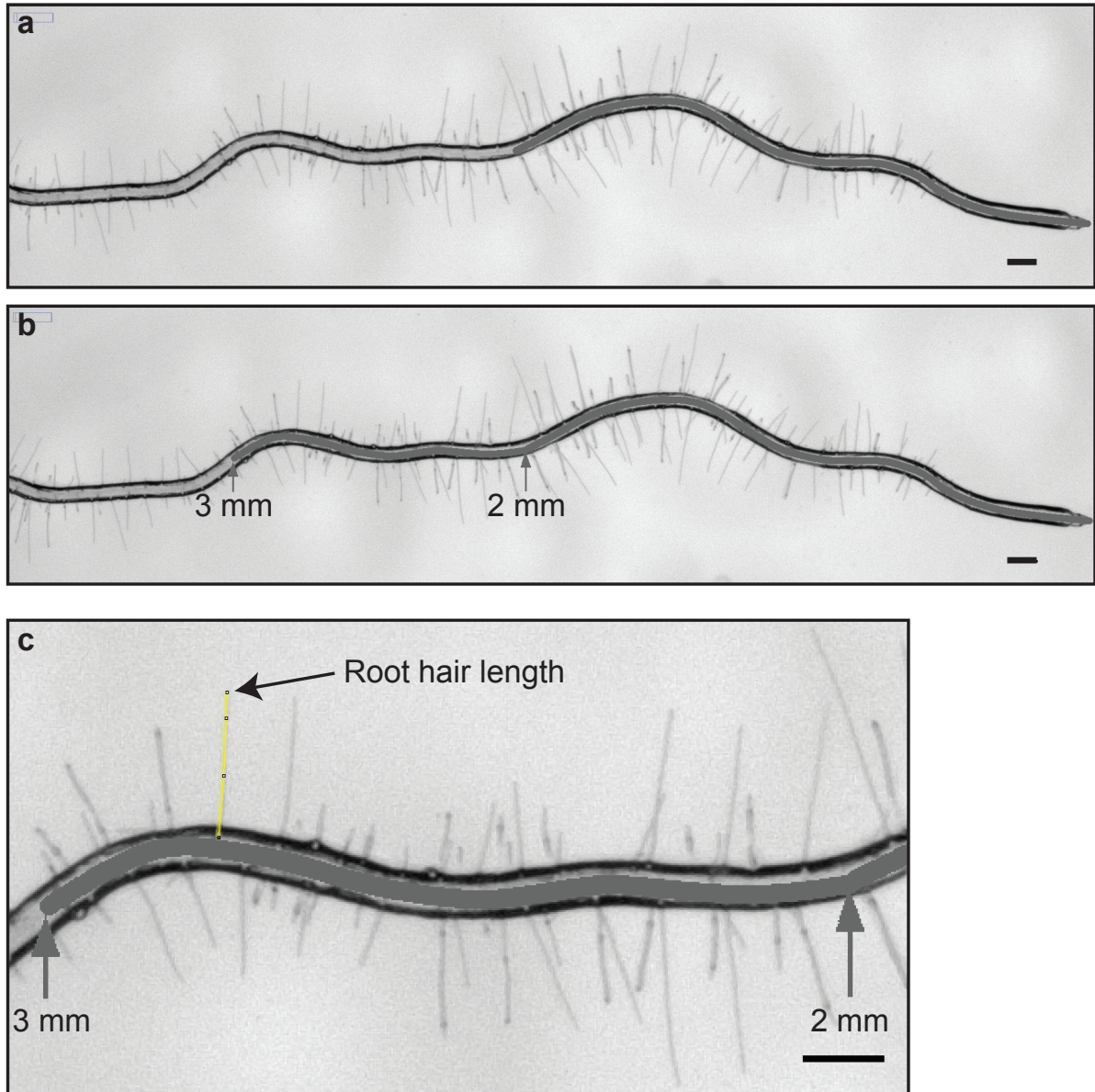


**Figure 2.** Root hair density and length quantification using Fiji. (a) Output of drawing a line between the root tip and 2 mm above the tip. (b) Output of drawing a line between 2 and 3 mm from the root tip and drawing arrows in 2 mm position and 3 mm position. (c) Output of using the segmented tool for root hair length quantification. Text has been added using Adobe Illustrator for a better explanation. Scale bar, 100 $\mu$ m.

**Manuscript I:** KL signalling regulates root hair elongation by promoting accumulation of auxin influx carrier AUX1

Reference: Villaecija-Aguilar JA., Magosch S., Hamon-Josse M., Bennett T., Gutjahr C. (2020). KL signalling regulates root hair elongation by promoting accumulation of auxin influx carrier AUX1.

## **Title:**

### **KL signalling regulates root hair elongation by promoting accumulation of auxin influx carrier AUX1**

José Antonio Villaecija-Aguilar<sup>1</sup>, Magosch S<sup>1</sup>, Maxime Hamon-Josse<sup>2</sup>, Tom Bennett<sup>2</sup>, Caroline Gutjahr<sup>1</sup>.

<sup>1</sup>Plant Genetics, School of Life Sciences Weihenstephan, Technical University of Munich (TUM), Emil Ramann Str. 4, 85354 Freising, Germany.

<sup>2</sup>School of Biology, Faculty of Biological Sciences, University of Leeds, Leeds, LS2 9JT, United Kingdom

## **Abstract:**

KARRIKIN INSENSITIVE 2 (KAI2) is the receptor of still unknown endogenous plant hormones, called KAI2-ligands (KLs), which mimic karrikins, small molecules found in germination inducing wildfire smoke. Recent genetic studies have shown that the KL signalling pathway is an essential regulator of root hair development. However, the downstream mechanisms by which KL signalling regulates root hair growth remain unknown. Here we show that KL signalling mutants attenuate the root hair elongation response to low external phosphate, which is known to be mediated by auxin transport. Our qPCR analysis and the DR5 based auxin response reporter suggested that auxin signalling and/or distribution, is altered in KL perception mutant roots. Pharmacological treatment with NAA but not fully with 2,4D rescues the root hair phenotype of *kai2*, indicating that disruption in auxin influx is the likely causes of the *kai2* root hair phenotype. In fact, auxin influx carrier *aux1* mutants are resistant to KAR treatment for induction of root hair growth. Furthermore, exogenous KAR induces the accumulation of AUX1-YFP in the epidermal cell layer above the lateral root cap. Thus, our results suggest that KL signalling regulates root hair elongation by controlling the accumulation of AUX1 and thereby auxin influx into the epidermis above the lateral root cap.

## **Introduction:**

The alpha-beta hydrolase KARRIKIN INSENSITIVE 2 (KAI2) is the receptor of karrikins, molecules produced upon wild-fire and considered to mimic unknown endogenous plant hormones, called KAI2-ligands (KLs) (Waters et al., 2012; Conn and

Nelson, 2016). Karrikin perception is similar to that of strigolactones (SLs), a group of plant hormones, which are perceived by the related alpha-beta hydrolase receptor DWARF14 (D14) (Hamiaux et al., 2012; de Saint Germain et al., 2016; Yao et al., 2016). Perception of both Karrikins and SLs requires the F-box protein MAX2 for ubiquitylation and subsequent degradation of a group of repressors, members of the SMXL protein family (Stanga et al., 2013; Soundappan et al., 2015; Wang et al., 2015; Stanga et al., 2016; Khosla et al., 2020; Wang et al., 2020). SUPPRESSOR OF MAX2 1 (SMAX1) and SMAX1-LIKE2 (SMXL2) act downstream of the KAI2-MAX2 complex to regulate the plant physiological responses to KAR/KL (Morffy et al., 2016; Stanga et al., 2016; Bhosale et al., 2018; Villaécija-Aguilar et al., 2019; Khosla et al., 2020; Wang et al., 2020). In a previous study, we demonstrated that KL signalling is a new regulator of root hair development in *Arabidopsis thaliana* (Villaécija-Aguilar et al., 2019). KL receptor mutants have lesser and shorter root hairs when compared to wild type roots. In contrast, *smx1 smx2* mutants show enhanced root hair density and length. Thus, SMAX1 and SMXL2 act as repressors of root hair development downstream of the complex KAI2-MAX2 (Villaécija-Aguilar et al., 2019).

The number and size of root hairs determine the total area/volume ratio of the whole roots, profoundly; and root hairs (RH) are critical determinants of nutrient and water uptake as well as anchorage to the soil, especially in the seedling stage (López-Bucio et al., 2005; Li et al., 2017). Root hair growth is controlled by different hormones, such as brassinosteroids, cytokinin, strigolactone, ethylene, KL and auxin (Koltai et al., 2010; Kapulnik et al., 2011b; Kapulnik et al., 2011a; Mayzlish-Gati et al., 2012; Vanstraelen and Benková, 2012; Villaécija-Aguilar et al., 2019). In particular, auxin is essential for root hair formation (Feng et al., 2017; Bhosale et al., 2018). Exogenous auxin increases root hair density and length (Pitts et al., 1998), while defects in auxin biosynthesis, signalling and/or transport reduce root hair formation (Pitts et al., 1998; Rahman et al., 2002; Swarup et al., 2004; Lee and Cho, 2008; Velasquez et al., 2016; Bhosale et al., 2018; Giri et al., 2018).

Plants adapt to variable soil conditions and especially phosphate by regulating their root hair elongation, with increased root hair growth under low phosphate and vice versa (Foehse and Jungk, 1983; Bates and Lynch, 1996; Ma et al., 2001; Williamson et al., 2001; Linkohr et al., 2002; López-Bucio et al., 2002; Müller and Schmidt, 2004;

López-Bucio et al., 2005; Nacry et al., 2005; Brown et al., 2013; López-Arredondo et al., 2014; Bhosale et al., 2018; Giri et al., 2018). Interestingly, KL perception mutants growing in ½ Murashige & Skoog medium with sufficient phosphate of 625 µM Pi phenocopy the effects of high Pi conditions in the RHL of Arabidopsis wild type seedlings (Bhosale et al., 2018; Villaécija-Aguilar et al., 2019). In concordance, previous studies suggested that MAX2 mediates the root hair responses to low Pi conditions (Mayzlish-Gati et al., 2012). Besides, the repressor double mutant *smx1 smx2* shows a RHL comparable to that of wild type under low Pi conditions (Bhosale et al., 2018; Villaécija-Aguilar et al., 2019). Recent studies have demonstrated that low phosphorus induces root hair elongation by stimulating auxin biosynthesis in the root cap and auxin transport to the root hair differentiation zone mediated by the auxin influx carrier AUX1 (Bhosale et al., 2018; Giri et al., 2018). Increased auxin levels lead to the activation of root hair specific genes mediated by the AUXIN RESPONSE FACTOR19 (ARF19). ARF19 induces the expression of the bHLH transcription factors RSL2 and RSL4 (Bhosale et al., 2018; Mangano et al., 2018). Next, RSL2 and RSL4 activate the expression of root hair specific genes (Menand et al., 2007; Yi et al., 2010). Based on these observations we hypothesized that KL signalling may regulate root hair development in an auxin-dependent manner.

Here, we demonstrate that KL signalling is required for the regulation of root hair elongation in Arabidopsis under external Pi changes. We show that the expression of the auxin reporter *DR5v2:GFP* is reduced in the root meristem of *kai2* mutants; and that external NAA but not 2,3D treatment rescued the root hair phenotype of *kai2* to the wild-type level, suggesting that import is altered in KL perception mutants. Finally, we present evidence that KL signalling regulates root hair elongation by controlling the accumulation of AUX1 in the epidermis above the lateral root cap.

## **Results:**

### **The root hair response to low phosphate requires KL signalling**

Since it was previously suggested that SL signalling regulates the root hair response to Pi mediated by MAX2 (Mayzlish-Gati et al., 2012), we first examined the effect of three different Pi concentrations, low Pi (2 µM Pi), medium Pi (625 µM) and high Pi (2 mM Pi) on KL and SL perception and signalling mutants. Consistent with previous

reports (Foehse and Jungk, 1983; Bates and Lynch, 1996; Ma et al., 2001; Williamson et al., 2001; Linkohr et al., 2002; López-Bucio et al., 2002; Müller and Schmidt, 2004; López-Bucio et al., 2005; Nacry et al., 2005; Brown et al., 2013; López-Arredondo et al., 2014; Bhosale et al., 2018; Giri et al., 2018), low Pi lead to an increase in RHL and high Pi caused a reduction in RHL in wild type relative to medium Pi (Figure 1). We observed similar RHL responses to low and high Pi in the SL receptor mutant *d14* when compared to wild type (Figure 1), indicating that SL signalling is not required for the RH response to phosphate. However, *kai2* and *max2* mutants showed a reduced root hair response to phosphate starvation with a similar RHL at medium Pi as wild type at high Pi and a similar RHL at low Pi as wild type at medium Pi. Conversely, while RHL of *smax1 smxl2* mutants was similar to wild type at high Pi, it was longer than for wild type at medium and high Pi (Figure 1). Hence, we conclude that KL signalling, but no SL signalling, is required for the root hair growth response to Pi availability.

### **SMAX1 and SMXL2 regulate root hair positioning downstream of KAI2-mediated signalling**

Because auxin is essential for the promotion of RHL upon Pi starvation (Bhosale et al., 2018; Giri et al., 2018), we hypothesised that KL signalling may regulate auxin signalling, transport and/or biosynthesis to control root hair development. Auxin is a key regulator of the planar polarity of root hair positioning (Fischer et al., 2006). Therefore, we postulated that if KL signalling converges with auxin signalling to regulate root hair development, KL signalling mutants may show an altered root hair positioning. Consistent with our hypothesis, we observed that most root hairs of *kai2* and *max2* emerge from a more intermediate position than in the wild-type (Figure 2A and B). In contrast, in *smax1 smxl2* and *max2 smax1 smxl2* mutants, a more substantial proportion of root hairs than in wild type emerges from a more basal position (rootward) (Figure 2A and B). Hence, we considered that KL signalling mutants might be perturbed in auxin biosynthesis, sensitivity or distribution.

### **KL signalling regulated auxin import in Arabidopsis root tips**

To confirm that auxin signalling is altered in KL perception mutants, we investigated the expression of *DR5v2:GFP*, an auxin-sensitive reporter (Liao et al., 2015), in the root meristem of wild type, *kai2-2* and the SL receptor mutants *d14-1*, as a control as

*d14* mutants do not show an altered root hair growth (Villaécija-Aguilar et al., 2019). Consistent with our hypothesis, we observed a significant reduction of *DR5v2:GFP* expression in the root meristem of *kai2* as compared to wild type (Figure 3A and B). This difference in *DR5v2:GFP* expression was not observed in the SL receptor mutant *d14* (Figure 3C). Taken together, these data support the hypothesis that KL signalling regulates root hair development by modulating auxin biosynthesis, signalling and/or distribution.

To examine whether this could be due to altered auxin biosynthesis or transport, we examined the expression of genes involved in these processes. Transcripts of auxin biosynthesis genes, *TAA1*, *YUC3*, *YUC6*, *DAO1*, *DAO2*, auxin transporter genes *AUX1*, *PIN2*, *PIN3*, *PIN7*, as well as the auxin receptor gene *TIR1* accumulated to similar levels as the wild type (Supplementary Figure 1), although the transcript level of the KL signalling marker gene *DLK2* was significantly reduced (Figure 6), suggesting that auxin biosynthesis and transport are not affected, at least at the transcriptional level.

We evaluated the effect of the synthetic auxins NAA and 2,4-D, on RHL in wild type and KL signalling mutant. NAA and 2,4-D have different properties. While the translocation of NAA to the cell mainly depends on efflux carrier activity, 2,4-D accumulation is controlled by an uptake carrier (Ma et al., 2018). We found that the application of 1nM NAA completely restores RHL of the KL signalling mutants to the level of wild type (Figure 4A). When treated with 2,4-D, KL signalling mutants were insensitive to 1nM 2,4-D and less sensitive to 10 nM 2,4-D than wild type (Figure 4B). Consistent with these results, *DR5v2:GFP* expression in the root meristems of *kai2-2* was also less sensitive to 2,4-D than to NAA (Figure 4C). Overall, our data suggest that *kai2* and *max2* might have decreased auxin levels in specific cell types, and that a defect in auxin import in *kai2* and *max2* mutants might reduce its sensitivity to 2,4-D treatment.

### **KL signalling regulates root hair development by modulating AUX1 abundance**

Functional characterization of the auxin-influx carrier AUX1 has shown that 2,4-D is a substrate of AUX1 (Yang et al., 2006). In addition, root hair length is severely disrupted

in *aux1* mutants (Pitts et al., 1998; Rahman et al., 2002; Swarup et al., 2004; Bhosale et al., 2018; Giri et al., 2018). In Villaecija-Aguilar et al., 2019, we demonstrated that exogenous application of KAR promotes root hair elongation. Thus, we examined the effect of KAR<sub>2</sub> treatment on RHL in wild type, and *aux1* mutants and *max2* as a negative control. Supporting our hypothesis, we observed that *max2* and *aux1* mutants are resistant to the effects of KAR treatment for RHL (Figure 5A). In Arabidopsis roots, *AUX1* is expressed in different tissues, including columella, proto-phloem, lateral root cap (LRC), and epidermal cells (Swarup et al., 2004; Péret et al., 2012). Previous studies suggested that the expression of *AUX1* in the LRC and epidermal cells contribute up to 80% of mobilized auxin required for root hair development (Jones et al., 2009; Dindas et al., 2018). We observed that exogenous application of KAR<sub>2</sub> during 2 hours induces the accumulation of AUX1-YFP in the epidermal cell layer above the LRC (Figure 5B and C). The activity of AUX1 in the epidermis is required for the root hair elongation response to external phosphate (Bhosale et al., 2018; Giri et al., 2018). Hence, we conclude that KL signalling regulates those responses by positively regulating AUX1 accumulation, likely at the post-transcriptional level (compare Supplementary Figure 1).

### **ARF7 but not ARF19 regulates root hair elongation in response to KAR treatment**

Auxin signalling requires the activation of auxin response factors (ARFs) to activate the expression of auxin-inducible genes (Zenser et al., 2001; Remington et al., 2004; Dharmasiri et al., 2005; Overvoorde et al., 2005; Tan et al., 2007; Mockaitis and Estelle, 2008; Szemenyei et al., 2008). In root hair cells, ARF7 and ARF19 are the two most abundant ARFs (Bargmann et al., 2013). In addition, *arf7* and *arf19* mutants display a reduced root hair length (Okushima et al., 2005; Bhosale et al., 2018). To investigate whether *ARF7* and *ARF19* may be involved in regulating root hair development downstream of KL signalling and AUX1 accumulation, we examined their transcript accumulation in *kai2-2* and *max2-8* mutants. Transcript levels of both genes were significantly reduced in these mutants, while this was not the case for *ARF5* and *ARF8* (Figure 6A). Furthermore, and consistent with an important role of KAI2-mediated signalling in root hair development, the expression levels of *RSL2*, *RSL4*, the expansin *EXP7* and the phosphatidylinositol transfer protein-encoding gene *COW1* were significantly reduced in *kai2-2* and *max2-8* compared to wild type (Figure 6A).

To confirm a role of ARF7 and ARF19 downstream of KL signalling in controlling RHL, we evaluated the effect of KAR<sub>2</sub> on RHL in *arf7*, *arf19* and *arf7 arf19* mutants. 1µM KAR<sub>2</sub> significantly increased RHL in wild type and *arf19* mutants (Figure 6B). In contrast, single *arf7* and double *arf7 arf19* mutants were resistant to the effect of KAR for root hair elongation (Figure 6B). Therefore, we conclude that ARF7, but not ARF19, represent a crucial regulator for KAR/KL-inducible root hair elongation.

### **Discussion:**

Changes in root hair growth are important adaptive responses to external cues. Nutrient deficiency, such as to potassium, nitrate or phosphate, promotes the elongation of root hairs presumably to increase the root surface for nutrient uptake (Bates and Lynch, 1996; Williamson et al., 2001; Høgh-Jensen and Pedersen, 2003; Brown et al., 2013; Canales et al., 2017; Klinsawang et al., 2018). The root hair responses to changes in the soil environment are controlled by several phytohormones, such as ethylene, brassinosteroids, cytokinin and auxin (Vissenberg et al., 2020). In particular, auxin biosynthesis, transport and signalling control the root hair responses to Pi deficiency in Arabidopsis and rice roots (Bhosale et al., 2018; Giri et al., 2018). Here we report that KL signalling is a new player in the mediation of root hair growth under Pi starvation and controls one of the critical components for this response, the auxin carrier AUX1.

Our study demonstrates that mutations in KL signalling attenuate the promotion of RHL by low external Pi. While low Pi significantly increases RHL, high Pi suppresses RHL in Arabidopsis wild type roots. In contrast, KL signalling mutants are at least partially resistant to those responses, with receptor mutants showing reduced RHL at low Pi and repressor mutants showing enhanced RHL at high Pi (Figure 1). It yet remains unclear, whether KL signalling is involved in the sensing of phosphate or whether it solely controls the root hair growth response.

In Arabidopsis roots, the auxin biosynthesis genes *TAA1* and *DAO1*, are upregulated under low Pi conditions (Bhosale et al., 2018). Hence, we hypothesised that KL signalling might regulate auxin biosynthesis in Arabidopsis roots. However, our qPCR-

based gene expression analysis revealed that transcript accumulation of the auxin biosynthesis genes *TAA1* and *DAO1* is unchanged in KL perception mutants roots (Supplementary Figure 1). These results suggest that KL signalling does not regulate auxin biosynthesis in the roots, at least not at the transcriptional level. However, it is unclear if KL signalling regulates auxin synthesis in the shoots and whether this would alter the total auxin content in the roots (Goldsmith, 1977; Petrášek and Friml, 2009). *Arabidopsis max2* mutants display increased auxin transport in shoots, presumably by over-accumulation of auxin efflux carriers, such as PIN1 (PIN-FORMED 1) (Crawford et al., 2010; Shinohara et al., 2013). Thus, an increase of auxin transport toward the root might increase the total auxin levels in KL signalling mutant roots. Nevertheless, pharmacological treatment with auxin increases root hair density and length (Pitts et al., 1998). Accordingly, defects in auxin signalling and/or biosynthesis reduce root hair growth (Velasquez et al., 2016). Therefore, an increase of total root auxin levels in the roots could not explain the reduction of root hair growth in the KL perception mutants. However, a reduction of auxin accumulation in the root as indicated by reduced *DR5v2:GFP* expression (Figure 3A and B) appears to explain the root hair phenotypes in KL signalling mutants.

Furthermore, we show that *ARF7*, *ARF19* expression are significantly reduced in *kai2* and *max2* mutants (Figure 6A). Our analysis of the root hair response to KAR of the single *arf7*, *arf19* and double *arf7 arf19* mutants revealed that KAR induces root hair elongation in wild-type and *arf19 single mutants*, but not in *arf7 single or arf7 arf19 double* mutants (Figure 6B). These results indicate that ARF7 is the major downstream player in KL mediation regulation of root hair elongation. This appears to be partially contradictory with a role of KL signalling on root hair response to low Pi. Bhosale et al., 2018 concluded that ARF19, rather than ARF7, is the crucial transcription factor in root hair responses to low Pi. This contradiction may be resolved by considering that in our KAR treatment assay, we used ½ MS medium containing a medium Pi concentration of 625µM. *ARF19* expression decrease at 325 µM Pi and *ARF7* at 500µM Pi (Niu et al., 2015; Bhosale et al., 2018). ARF19 and ARF7 are functionally redundant, and changes in expression level and/or pattern, rather than aminoacid sequencing, are critical determinants for the function of those two transcription factors (Li et al., 2006). Perhaps, higher expression levels and/or a different expression pattern of ARF19 under lower Pi conditions could activate an ARF19 mediated root hair elongation

response to KAR, while ARF7 may be more strongly expressed at medium to high Pi concentrations. Further investigations are needed to evaluate the roles of ARF19 and ARF7 mediating the root hair response upon KAR treatment under different Pi concentrations.

ARFs are regulated by another protein family, the Aux/IAA transcriptional repressors (Remington et al., 2004; Overvoorde et al., 2005). In the presence of auxin, the auxin receptor TIR1 F-box proteins interact with Aux/IAA proteins to mediate their ubiquitination and subsequent degradation to release transcriptional responses to auxin (Zenser et al., 2001; Dharmasiri et al., 2005; Tan et al., 2007; Mockaitis and Estelle, 2008). In contrast, at low auxin levels, Aux/IAA proteins interact with ARFs to inhibit their activity by recruiting co-repressors of the TOPLESS (TPL) family, leading to the repression of auxin-responsive genes (Szemenyei et al., 2008). To test, whether KL signalling directly regulates auxin signalling or controls auxin distribution, we treated KL perception mutants, with external auxin. Because the synthetic auxin NAA, but not 2,4-D, treatment fully rescued the root hair phenotypes of *kai2* and *max2* (Figure 5), we conclude that auxin import and distribution, rather than auxin signalling, might be altered in KL perception mutants. We next show that the auxin influx carrier AUX1 is required for the regulation of root hair elongation by KL signalling (Figure 5A). Our data further suggest that KL induces the accumulation of AUX1 in the epidermis above the lateral root cap (Figure 5B and C). The importance of AUX1 in the epidermis and lateral root cap for the regulation of root hairs has been previously reported (Jones et al., 2009; Bhosale et al., 2018). Besides, protein expression and promoter activity pattern analysis indicates that SMAX1 localises principally to the lateral root cap and columella in the roots of Arabidopsis seedlings (Soundappan et al., 2015; Khosla et al., 2020). Therefore, it is plausible that SMAX1 and SMXL2 proteins suppress root hair growth in Arabidopsis by repressing AUX1 accumulation in the epidermis above the lateral root cap.

Currently, it is unknown how SMAX1 and/or SMXL2 regulate AUX1 accumulation and/or activity. AUX1 is regulated by different plant hormones, including ethylene and cytokinin (Růžička et al., 2007; Street et al., 2016). In particular, treatment with an inhibitor of ethylene biosynthesis, AVG, reduced AUX1 accumulation in the root tip (Street et al., 2016), while treatment with the ethylene precursor enhanced it (Růžička et al., 2007), indicating a direct role of ethylene in AUX1 accumulation. Besides,

ethylene treatment induces root hair elongation in *Arabidopsis* (Pitts et al., 1998). Therefore, it is plausible that ethylene regulates root hair elongation via AUX1 accumulation. Recent studies suggested that SMAX1 inhibits ethylene biosynthesis in *Lotus japonicus* (Carbonnel et al., in revision). We may deduce that *Arabidopsis* SMAX1 and/or SMXL2 play similar roles in the control of ethylene synthesis, which may result in AUX1 accumulation and leading to changes in root hair development. Supporting this hypothesis, AVG treatment suppresses the root hair elongation response to *rac*-GR24 (one stereoisomer of which, acts through KAI2) in *Arabidopsis* (Kapulnik et al., 2011b; Kapulnik et al., 2011a). Therefore, ethylene biosynthesis is likely critical for the control of RHL by KL signalling.

In summary, our study suggests a complex interaction between the signalling pathways of different hormones. Perhaps, low Pi conditions lead to an increase in biosynthesis of the still unknown KL, inducing KL signalling. The activation of KL signalling might lead to an increase in ethylene biosynthesis, resulting in AUX1 accumulation in the epidermis above the lateral root. Changes in auxin influx mediated by AUX1 causes the accumulation of auxin in specific cell types, stimulating auxin signalling mediated by ARFs. Next, ARFs trigger the activation of the transcription factors RSL2 and RLS4, which lead to the induction of genes, such as *COW1* and *EXP7*, thus initiating the root hair elongation machinery.

## **Material and methods:**

### **Plant material**

Genotypes of *Arabidopsis thaliana* were in Columbia-0 (Col-0) or Landsberg *erecta* (Ler) parental backgrounds. The following mutants were used: Ler: *kai2-2*, *max2-8* (Nelson et al., 2011). Col-0: *d14-1*, *kai2-2* (Bennett et al., 2016), *max2-1* (Stirnberg et al., 2002), *smax1-2 smxl2-1* (Stanga et al., 2016), *aux1-7* (Pickett et al., 1990), *arf7-1*, *arf19-1* (Harper et al., 2000), *arf7-1 arf19-1* (Okushima et al., 2005), *DR5v2:GFP* (Liao et al., 2015).

### **Plant growth conditions**

For analysis of root hair length, *Arabidopsis thaliana* seeds were grown in axenic conditions on 12x12cm square plates containing 60 ml agar-solidified medium. Seed were surface sterilized by washing with 1 ml of 70% (v/v) ethanol and 0.05% (v/v) Triton X-100 with gentle mixing by inversion for 6 minutes at room temperature, followed by 1 wash with 96% ethanol and 5 washes with sterile distilled water. Seedlings were grown on plates containing 0.5X Murashige & Skoog medium, pH5.8 (½ MS) (Duchefa, Netherlands), supplemented with 1% sucrose and solidified with 1.5% agar. For root hair length experiment under different phosphate conditions, seedlings were grown on plates containing modified ½ MS medium, with low (2 µM), medium (625 µM) or high (2 mM) Pi with KH<sub>2</sub>PO<sub>4</sub>, pH 5.8, supplemented with 1% sucrose and solidified with 1.5% agar. Potassium concentrations were adjusted with KCl. Plates were stratified at 4°C for 2-3 days in the dark, and then transferred to a growth cabinet under controlled conditions at 22 °C, 16-h/8-h light/dark cycle (intensity ~120 µmol m<sup>-2</sup> s<sup>-1</sup>) with plates vertically placed.

### **Phytohormone treatments**

NAA was purchased from Sigma-Aldrich (St. Louis, United States). 2,4-D was purchased from Duchefa (Netherlands). KAR<sub>2</sub> was purchased from Olchemim (Olomouc, Czech Republic). NAA or 2,4-D were dissolved in either 2% DMSO, 70% ethanol for a 1mM stock, or 100% ethanol for the preparation of 10 mM stock solution. KAR<sub>2</sub> was purchased from Olchemim (Olomouc, Czech Republic). For treatment with KAR<sub>2</sub>, 1 mM stock solutions were prepared in 70% methanol. The volume required to reach the final concentration of these stock solutions was added to molten media prior

to pouring Petri dishes for root hair elongation experiments. In each root hair elongation experiment, an equivalent volume of solvent was added to Petri dishes for untreated controls. For confocal experiments with KAR<sub>2</sub>, the volume required to reach the final concentration of these stock solutions was added to ½ MS liquid medium. For this experiment, an equivalent volume of solvent was added to ½ MS liquid medium for untreated controls.

### **Determination of root hair length and position**

For root hair length experiments, images of a minimum of 10 roots per genotype and treatment were taken with a Zeiss Discovery V8 microscope equipped with a Zeiss Axiocam 503 camera. Root hair length was measured for 10 different root hairs per root, between 2 and 3 mm from the root tip using Fiji. For root hair position, images between 2 and 3 mm from the root tip were taken with a Leica DM6 B microscope equipped with a Leica DFC9000 GT camera. The root hair position was determined following the method described by (Masucci and Schiefelbein, 1994) for 5-15 root hairs per root and a minimum of 8 roots per genotype.

### **Confocal microscopy**

Laser-scanning confocal microscopy for *DR5v2:GFP* expression was performed using either Zeiss LSM700 or LSM880 imaging system with a 20X lens. Roots were stained with propidium iodide (10ug/ml) and mounted on slides. GFP excitation was performed using a 488 nm laser, and fluorescence was detected between 488 and 555nm. Propidium iodide excitation was performed using a 561 nm laser, and fluorescence was detected between above 610nm. The same detection settings were used for all images captured in a single experiment. GFP quantification was performed on non-saturated images, using Zeiss 'ZEN' software. For *AUX1-YFP* expression laser-scanning confocal microscopy was performed using Leica SP8 imaging system with 20X or 40X lens. YFP excitation was detected between 520 and 550nm.

### **RNA extraction and gene expression analysis**

For qRT-PCR analysis, at least 100 roots per sample was rapidly shock frozen in liquid nitrogen. RNA was extracted using NucleoSpin RNA plant and fungi kit (Macherey-Nagel). The concentration and purity of RNA were evaluated with DS-11 FX+

spectrophotometer/fluorometer (DeNovix). First-strand cDNA was produced in a 20  $\mu$ L reaction volume using the Superscript IV kit (Invitrogen).

The cDNA was diluted with water in a 1:20 ratio and 2  $\mu$ L of this solution was used for qRT-PCR in a 7  $\mu$ L reaction volume using a EvaGreen Mastermix (Metabion, UNG+/ROX+ 2x conc.) and primers shown in Supplementary Table 1. To quantify the expression of the different genes, the qPCR reaction was carried out using a CFX384 Touch<sup>TM</sup> RT-PCR detection system (Bio-Rad). Thermal cycler conditions were: 95°C 2 min, 40 cycles of 95°C 30s, 55°C 30s and 72°C 20 s, followed by dissociation curve analysis. For the calculation of the expression levels, we followed the  $\Delta\Delta$ Ct method (6). For each genotype three biological replicates were analyzed. Each sample was represented by 3 technical replicates.

### **Statistical analysis**

Statistical analyses were performed in R-studio, using one-way Analysis of Variance (ANOVA), followed by Tukey HSD post hoc test or using Student's t-test.

### **Accession numbers**

Sequence data for the genes mentioned in this article can be found in The Arabidopsis Information Resource (TAIR; <https://www.arabidopsis.org>) under the following accession numbers: *MAX3*, AT2G44990; *MAX4*, AT4G32810; *MAX1*, AT2G26170; *D14*, AT3G03990; *KAI2*, AT4G37470; *MAX2*, AT2G42620; *SMAX1*, AT5G57710; *SMXL2* AT4G30350; *SMXL6*, AT1G07200; *SMXL7*, AT2G29970; *SMXL8*, AT2G40130; *PIN1*, AT1G73590; *PIN2*, AT5G57090; *PIN3*, AT1G70940; *PIN4*, AT2G01420; *PIN7*, AT1G23080; *ARF5*, AT1G19850; *ARF7*, AT5G20730; *ARF8*, AT5G37020; *ARF19*, AT1G19220; *RSL2*, AT4G33880; *RSL4*, AT1G27740; *EXP7*, AT1G12560; *COW1*, AT4G34580; *DLK2*, AT3G24420, *TAA1*, AT1G70560; *DAO1*, AT1G14130, *DAO2*, AT1G14120; *YUC3*, AT1G04510; *YUC9*, AT1G04180; *TIR1*, AT3G62980; *AUX1*, AT2G38120; *EF1 $\alpha$* , AT5G60390.

## References:

- Bargmann, B.O., Vanneste, S., Krouk, G., Nawy, T., Efroni, I., Shani, E., Choe, G., Friml, J., Bergmann, D.C., Estelle, M., and Birnbaum, K.D.** (2013). A map of cell type-specific auxin responses. *Molecular systems biology* **9**: 688.
- Bates, T.R., and Lynch, J.P.** (1996). Stimulation of root hair elongation in *Arabidopsis thaliana* by low phosphorus availability. *Plant Cell Environ.* **19**: 529-538.
- Bennett, T., Hines, G., van Rongen, M., Waldie, T., Sawchuk, M.G., Scarpella, E., Ljung, K., and Leyser, O.** (2016). Connective auxin transport in the shoot facilitates communication between shoot apices. *PLoS Biol.* **14**: e1002446.
- Bhosale, R., Giri, J., Pandey, B.K., Giehl, R.F.H., Hartmann, A., Traini, R., Truskina, J., Leftley, N., Hanlon, M., Swarup, K., Rashed, A., Voß, U., Alonso, J., Stepanova, A., Yun, J., Ljung, K., Brown, K.M., Lynch, J.P., Dolan, L., Vernoux, T., Bishopp, A., Wells, D., von Wirén, N., Bennett, M.J., and Swarup, R.** (2018). A mechanistic framework for auxin dependent *Arabidopsis* root hair elongation to low external phosphate. *Nat. Commun.* **9**: 1409.
- Brown, L.K., George, T.S., Dupuy, L.X., and White, P.J.** (2013). A conceptual model of root hair ideotypes for future agricultural environments: what combination of traits should be targeted to cope with limited P availability? *Ann Bot* **112**: 317-330.
- Canales, J., Contreras-López, O., Álvarez, J.M., and Gutiérrez, R.A.** (2017). Nitrate induction of root hair density is mediated by TGA 1/TGA 4 and CPC transcription factors in *Arabidopsis thaliana*. *Plant J.* **92**: 305-316.
- Conn, C.E., and Nelson, D.C.** (2016). Evidence that KARRIKIN-INSENSITIVE2 (KAI2) receptors may perceive an unknown signal that is not karrikin or strigolactone. *Front. Plant Sci.* **6**: 1219.
- Crawford, S., Shinohara, N., Sieberer, T., Williamson, L., George, G., Hepworth, J., Müller, D., Domagalska, M.A., and Leyser, O.** (2010). Strigolactones enhance competition between shoot branches by dampening auxin transport. *Development* **137**: 2905-2913.
- de Saint Germain, A., Clavé, G., Badet-Denisot, M.-A., Pillot, J.-P., Cornu, D., Le Caer, J.-P., Burger, M., Pelissier, F., Retailleau, P., Turnbull, C., Sandrine, B., Joanne, C., Catherine, R., and François-Didier, B.** (2016). An histidine covalent receptor and butenolide complex mediates strigolactone perception. *Nat. Chem. Biol.* **12**: 787-794.
- Dharmasiri, N., Dharmasiri, S., and Estelle, M.** (2005). The F-box protein TIR1 is an auxin receptor. *Nature* **435**: 441.
- Dindas, J., Scherzer, S., Roelfsema, M.R.G., von Meyer, K., Müller, H.M., Al-Rasheid, K.A.S., Palme, K., Dietrich, P., Becker, D., Bennett, M.J., and Hedrich, R.** (2018). AUX1-mediated root hair auxin influx governs SCFTIR1/AFB-type Ca<sup>2+</sup> signaling. *Nat. Commun.* **9**: 1174.
- Feng, Y., Xu, P., Li, B., Li, P., Wen, X., An, F., Gong, Y., Xin, Y., Zhu, Z., Wang, Y., and Guo, H.** (2017). Ethylene promotes root hair growth through coordinated EIN3/EIL1 and RHD6/RSL1 activity in *Arabidopsis*. *Proceedings of the National Academy of Sciences of the United States of America* **114**: 13834-13839.
- Fischer, U., Ikeda, Y., Ljung, K., Serralbo, O., Singh, M., Heidstra, R., Palme, K., Scheres, B., and Grebe, M.** (2006). Vectorial information for *Arabidopsis* planar polarity is mediated by combined AUX1, EIN2, and GNOM activity. *Curr. Biol.* **16**: 2143-2149.

- Foehse, D., and Jungk, A.** (1983). Influence of phosphate and nitrate supply on root hair formation of rape, spinach and tomato plants. *Plant and Soil* **74**: 359-368.
- Giri, J., Bhosale, R., Huang, G., Pandey, B.K., Parker, H., Zappala, S., Yang, J., Dievert, A., Bureau, C., Ljung, K., Price, A., Rose, T., Larrieu, A., Mairhofer, S., Sturrock, C.J., White, P., Dupuy, L., Hawkesford, M., Perin, C., Liang, W., Peret, B., Hodgman, C.T., Lynch, J., Wissuwa, M., Zhang, D., Pridmore, T., Mooney, S.J., Guiderdoni, E., Swarup, R., and Bennett, M.J.** (2018). Rice auxin influx carrier OsAUX1 facilitates root hair elongation in response to low external phosphate. *Nat. Commun.* **9**: 1408.
- Goldsmith, M.H.M.** (1977). The Polar Transport of Auxin. *Annual Review of Plant Physiology* **28**: 439-478.
- Hamiaux, C., Drummond, R.S., Janssen, B.J., Ledger, S.E., Cooney, J.M., Newcomb, R.D., and Snowden, K.C.J.** (2012). DAD2 is an  $\alpha/\beta$  hydrolase likely to be involved in the perception of the plant branching hormone, strigolactone. *Curr. Biol.* **22**: 2032-2036.
- Harper, R.M., Stowe-Evans, E.L., Luesse, D.R., Muto, H., Tatematsu, K., Watahiki, M.K., Yamamoto, K., and Liscum, E.** (2000). The *NPH4* Locus Encodes the Auxin Response Factor ARF7, a Conditional Regulator of Differential Growth in Aerial Arabidopsis Tissue. *Plant Cell* **12**: 757-770.
- Høgh-Jensen, H., and Pedersen, M.B.** (2003). Morphological Plasticity by Crop Plants and Their Potassium Use Efficiency. *Journal of Plant Nutrition* **26**: 969-984.
- Jones, A.R., Kramer, E.M., Knox, K., Swarup, R., Bennett, M.J., Lazarus, C.M., Leyser, H.M.O., and Grierson, C.S.** (2009). Auxin transport through non-hair cells sustains root-hair development. *Nat. Cell Biol.* **11**: 78-84.
- Kapulnik, Y., Resnick, N., Mayzlish-Gati, E., Kaplan, Y., Wininger, S., Hershenhorn, J., and Koltai, H.** (2011a). Strigolactones interact with ethylene and auxin in regulating root-hair elongation in Arabidopsis. *J. Exp. Bot.* **62**: 2915-2924.
- Kapulnik, Y., Delaux, P.-M., Resnick, N., Mayzlish-Gati, E., Wininger, S., Bhattacharya, C., Séjalon-Delmas, N., Combiér, J.-P., Bécard, G., Belausov, E., Beeckman, T., Dor, E., Hershenhorn, J., and Koltai, H.** (2011b). Strigolactones affect lateral root formation and root-hair elongation in Arabidopsis. *Planta* **233**: 209-216.
- Khosla, A., Morffy, N., Li, Q., Faure, L., Chang, S.H., Yao, J., Zheng, J., Cai, M.L., Stanga, J.P., Flematti, G.R., Waters, M., and Nelson, D.C.** (2020). Structure-Function Analysis of SMAX1 Reveals Domains that Mediate its Karrikin-Induced Proteolysis and Interaction with the Receptor KAI2. *Plant Cell*: tpc.00752.02019.
- Klinsawang, S., Sumranwanich, T., Wannaro, A., and Saengwilai, P.** (2018). Effects of root hair length on potassium acquisition in rice (*Oryza sativa* L.). *APPLIED ECOLOGY AND ENVIRONMENTAL RESEARCH* **16**: 1609-1620.
- Koltai, H., Dor, E., Hershenhorn, J., Joel, D.M., Weininger, S., Lekalla, S., Shealtiel, H., Bhattacharya, C., Eliahu, E., Resnick, N., Barg, R., and Kapulnik, Y.** (2010). Strigolactones' effect on root growth and root-hair elongation may be mediated by auxin-efflux carriers. *J. Plant Growth Regul.* **29**: 129-136.
- Lee, S., and Cho, H.-T.** (2008). Auxin and root hair morphogenesis. In *Root Hairs* (Plant Cell Monographs 12) (Springer, Berlin), pp. 45-64.

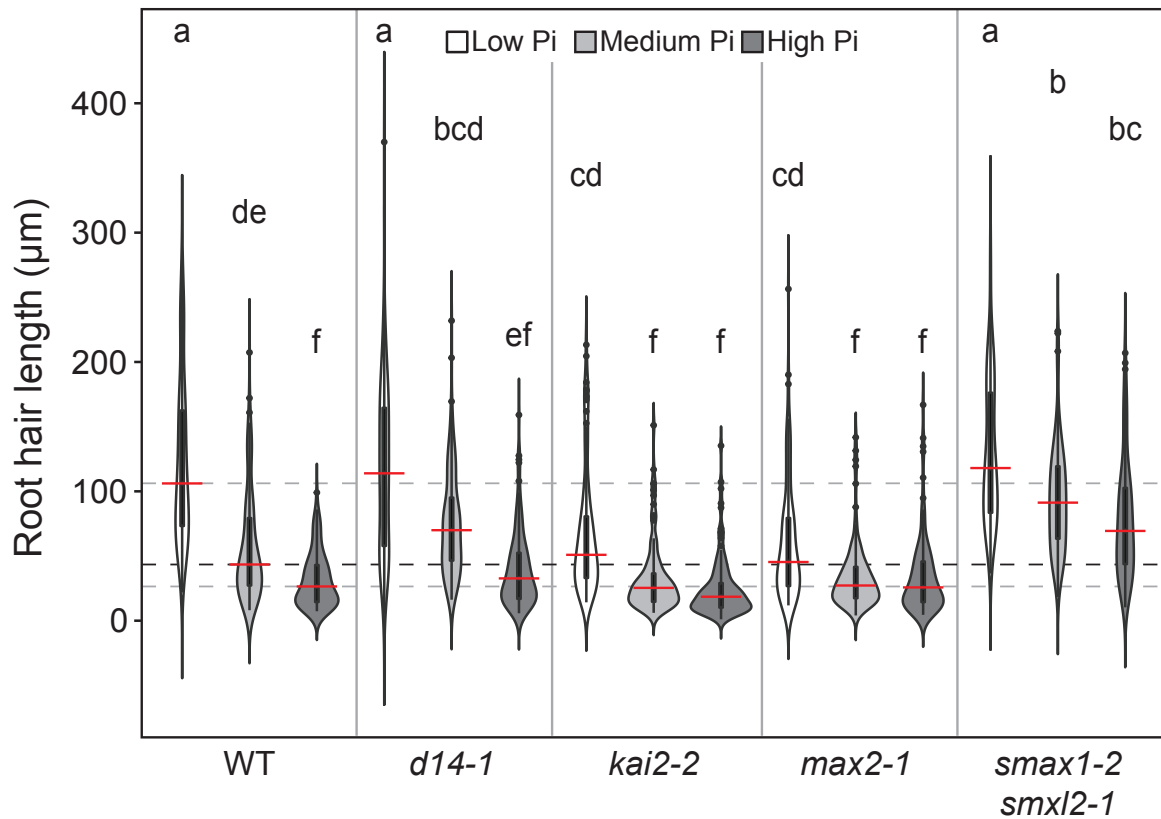
- Li, J., Dai, X., and Zhao, Y.** (2006). A Role for Auxin Response Factor 19 in Auxin and Ethylene Signaling in *Arabidopsis*. *Plant Physiol.* **140**: 899-908.
- Li, W., Nguyen, K.H., Chu, H.D., Ha, C.V., Watanabe, Y., Osakabe, Y., Leyva-González, M.A., Sato, M., Toyooka, K., Voges, L., Tanaka, M., Mostofa, M.G., Seki, M., Seo, M., Yamaguchi, S., Nelson, D.C., Tian, C., Herrera-Estrella, L., and Tran, L.-S.P.** (2017). The karrikin receptor KAI2 promotes drought resistance in *Arabidopsis thaliana*. *PLOS Genetics* **13**: e1007076.
- Liao, C.-Y., Smet, W., Brunoud, G., Yoshida, S., Vernoux, T., and Weijers, D.** (2015). Reporters for sensitive and quantitative measurement of auxin response. *Nat. Methods* **12**: 207-210.
- Linkohr, B.I., Williamson, L.C., Fitter, A.H., and Leyser, H.M.O.** (2002). Nitrate and phosphate availability and distribution have different effects on root system architecture of *Arabidopsis*. *Plant J.* **29**: 751-760.
- López-Arredondo, D.L., Leyva-González, M.A., González-Morales, S.I., López-Bucio, J., and Herrera-Estrella, L.** (2014). Phosphate nutrition: improving low-phosphate tolerance in crops. *Annu Rev Plant Biol* **65**: 95-123.
- López-Bucio, J., Hernández-Abreu, E., Sánchez-Calderón, L., Nieto-Jacobo, M.a.F., Simpson, J., and Herrera-Estrella, L.** (2002). Phosphate Availability Alters Architecture and Causes Changes in Hormone Sensitivity in the *Arabidopsis* Root System. *Plant Physiol.* **129**: 244-256.
- López-Bucio, J., Hernández-Abreu, E., Sánchez-Calderón, L., Pérez-Torres, A., Rampey, R.A., Bartel, B., and Herrera-Estrella, L.** (2005). An auxin transport independent pathway is involved in phosphate stress-induced root architectural alterations in *Arabidopsis*. Identification of BIG as a mediator of auxin in pericycle cell activation. *Plant Physiol.* **137**: 681-691.
- Ma, Q., Grones, P., and Robert, S.** (2018). Auxin signaling: a big question to be addressed by small molecules. *J Exp Bot* **69**: 313-328.
- Ma, Z., Bielenberg, D.G., Brown, K.M., and Lynch, J.P.** (2001). Regulation of root hair density by phosphorus availability in *Arabidopsis thaliana*. *Plant Cell Environ.* **24**: 459-467.
- Mangano, S., Denita-Juarez, S.P., Marzol, E., Borassi, C., and Estevez, J.M.** (2018). High Auxin and High Phosphate Impact on RSL2 Expression and ROS-Homeostasis Linked to Root Hair Growth in *Arabidopsis thaliana*. *Front. Plant Sci.* **9**: 1164-1164.
- Masucci, J.D., and Schiefelbein, J.W.** (1994). The *rhd6* mutation of *Arabidopsis thaliana* alters root-hair initiation through an auxin-and ethylene-associated process. *Plant Physiol.* **106**: 1335-1346.
- Mayzlish-Gati, E., De-Cuyper, C., Goormachtig, S., Beeckman, T., Vuylsteke, M., Brewer, P.B., Beveridge, C.A., Yermiyahu, U., Kaplan, Y., Enzer, Y., Wininger, S., Resnick, N., Cohen, M., Kapulnik, Y., and Koltai, H.** (2012). Strigolactones are involved in root response to low phosphate conditions in *Arabidopsis*. *Plant Physiol* **160**: 1329-1341.
- Menand, B., Yi, K., Jouannic, S., Hoffmann, L., Ryan, E., Linstead, P., Schaefer, D.G., and Dolan, L.** (2007). An ancient mechanism controls the development of cells with a rooting function in land plants. *Science* **316**: 1477-1480.
- Mockaitis, K., and Estelle, M.** (2008). Auxin receptors and plant development: a new signaling paradigm. *Annual review of cell and developmental biology* **24**: 55-80.
- Morffy, N., Faure, L., and Nelson, D.C.** (2016). Smoke and Hormone Mirrors: Action and Evolution of Karrikin and Strigolactone Signaling. *Trends in genetics : TIG* **32**: 176-188.

- Müller, M., and Schmidt, W.** (2004). Environmentally Induced Plasticity of Root Hair Development in *Arabidopsis*. *Plant Physiol.* **134**: 409-419.
- Nacry, P., Canivenc, G., Muller, B., Azmi, A., Van Onckelen, H., Rossignol, M., and Doumas, P.** (2005). A Role for Auxin Redistribution in the Responses of the Root System Architecture to Phosphate Starvation in *Arabidopsis*. *Plant Physiol.* **138**: 2061-2074.
- Nelson, D.C., Scaffidi, A., Dun, E.A., Waters, M.T., Flematti, G.R., Dixon, K.W., Beveridge, C.A., Ghisalberti, E.L., and Smith, S.M.** (2011). F-box protein MAX2 has dual roles in karrikin and strigolactone signaling in *Arabidopsis thaliana*. *Proc. Natl. Acad. Sci. USA.* **108**: 8897-8902.
- Niu, Y., Jin, G., Li, X., Tang, C., Zhang, Y., Liang, Y., and Yu, J.** (2015). Phosphorus and magnesium interactively modulate the elongation and directional growth of primary roots in *Arabidopsis thaliana* (L.) Heynh. *J. Exp. Bot.* **66**: 3841-3854.
- Okushima, Y., Overvoorde, P.J., Arima, K., Alonso, J.M., Chan, A., Chang, C., Ecker, J.R., Hughes, B., Lui, A., Nguyen, D., Onodera, C., Quach, H., Smith, A., Yu, G., and Theologis, A.** (2005). Functional genomic analysis of the AUXIN RESPONSE FACTOR gene family members in *Arabidopsis thaliana*: unique and overlapping functions of ARF7 and ARF19. *Plant Cell* **17**: 444-463.
- Overvoorde, P.J., Okushima, Y., Alonso, J.M., Chan, A., Chang, C., Ecker, J.R., Hughes, B., Liu, A., Onodera, C., Quach, H., Smith, A., Yu, G., and Theologis, A.** (2005). Functional Genomic Analysis of the AUXIN/INDOLE-3-ACETIC ACID Gene Family Members in *Arabidopsis thaliana*. *Plant Cell* **17**: 3282-3300.
- Péret, B., Swarup, K., Ferguson, A., Seth, M., Yang, Y., Dhondt, S., James, N., Casimiro, I., Perry, P., Syed, A., Yang, H., Reemmer, J., Venison, E., Howells, C., Perez-Amador, M.A., Yun, J., Alonso, J., Beemster, G.T.S., Laplaze, L., Murphy, A., Bennett, M.J., Nielsen, E., and Swarup, R.** (2012). AUX/LAX genes encode a family of auxin influx transporters that perform distinct function during *Arabidopsis* development. *Plant Cell* **24**: 2874.
- Petrášek, J., and Friml, J.** (2009). Auxin transport routes in plant development. *Development* **136**: 2675-2688.
- Pickett, F.B., Wilson, A.K., and Estelle, M.** (1990). The *aux1* mutation of *Arabidopsis* confers both auxin and ethylene resistance. *Plant Physiol.* **94**: 1462-1466.
- Pitts, R.J., Cernac, A., and Estelle, M.** (1998). Auxin and ethylene promote root hair elongation in *Arabidopsis*. *Plant J.* **16**: 553-560.
- Rahman, A., Hosokawa, S., Oono, Y., Amakawa, T., Goto, N., and Tsurumi, S.** (2002). Auxin and ethylene response interactions during *Arabidopsis* root hair development dissected by auxin influx modulators. *Plant Physiol* **130**: 1908-1917.
- Remington, D.L., Vision, T.J., Guilfoyle, T.J., and Reed, J.W.** (2004). Contrasting Modes of Diversification in the *Aux/IAA* and *ARF* Gene Families. *Plant Physiol.* **135**: 1738-1752.
- Růžička, K., Ljung, K., Vanneste, S., Podhorská, R., Beeckman, T., Friml, J., and Benková, E.** (2007). Ethylene Regulates Root Growth through Effects on Auxin Biosynthesis and Transport-Dependent Auxin Distribution. *Plant Cell* **19**: 2197-2212.
- Shinohara, N., Taylor, C., and Leyser, O.** (2013). Strigolactone can promote or inhibit shoot branching by triggering rapid depletion of the auxin efflux protein PIN1 from the plasma membrane. *PLoS Biol.* **11**: e1001474.

- Soundappan, I., Bennett, T., Morffy, N., Liang, Y., Stanga, J.P., Abbas, A., Leyser, O., and Nelson, D.C.** (2015). SMAX1-LIKE/D53 family members enable distinct MAX2-dependent responses to strigolactones and karrikins in *Arabidopsis*. *Plant Cell* **27**: 3143-3159.
- Stanga, J.P., Morffy, N., and Nelson, D.C.** (2016). Functional redundancy in the control of seedling growth by the karrikin signaling pathway. *Planta* **243**: 1397-1406.
- Stanga, J.P., Smith, S.M., Briggs, W.R., and Nelson, D.C.** (2013). *SUPPRESSOR OF MAX2 1* controls seed germination and seedling development in *Arabidopsis thaliana*. *Plant Physiol.* **163**: 318-330.
- Stirnberg, P., van De Sande, K., and Leyser, H.M.** (2002). MAX1 and MAX2 control shoot lateral branching in *Arabidopsis*. *Development* **129**: 1131-1141.
- Street, I.H., Mathews, D.E., Yamburkenko, M.V., Sorooshzadeh, A., John, R.T., Swarup, R., Bennett, M.J., Kieber, J.J., and Schaller, G.E.** (2016). Cytokinin acts through the auxin influx carrier AUX1 to regulate cell elongation in the root. *Development* **143**: 3982-3993.
- Swarup, R., Kargul, J., Marchant, A., Zadik, D., Rahman, A., Mills, R., Yemm, A., May, S., Williams, L., Millner, P., Tsurumi, S., Moore, I., Napier, R., Kerr, I.D., and Bennett, M.J.** (2004). Structure-Function Analysis of the Presumptive *Arabidopsis* Auxin Permease AUX1. *Plant Cell* **16**: 3069-3083.
- Szemenyei, H., Hannon, M., and Long, J.A.** (2008). TOPLESS mediates auxin-dependent transcriptional repression during *Arabidopsis* embryogenesis. *Science* **319**: 1384-1386.
- Tan, X., Calderon-Villalobos, L.I., Sharon, M., Zheng, C., Robinson, C.V., Estelle, M., and Zheng, N.** (2007). Mechanism of auxin perception by the TIR1 ubiquitin ligase. *Nature* **446**: 640-645.
- Vanstraelen, M., and Benková, E.** (2012). Hormonal interactions in the regulation of plant development. *Annual review of cell and developmental biology* **28**: 463-487.
- Velasquez, S.M., Barbez, E., Kleine-Vehn, J., and Estevez, J.M.** (2016). Auxin and Cellular Elongation. *Plant Physiol.* **170**: 1206-1215.
- Villaécija-Aguilar, J.A., Hamon-Josse, M., Carbonnel, S., Kretschmar, A., Schmidt, C., Dawid, C., Bennett, T., and Gutjahr, C.** (2019). SMAX1/SMXL2 regulate root and root hair development downstream of KAI2-mediated signalling in *Arabidopsis*. *PLOS Genetics* **15**: e1008327.
- Vissenberg, K., Claeijs, N., Balcerowicz, D., and Schoenaers, S.** (2020). Hormonal regulation of root hair growth and responses to the environment in *Arabidopsis*. *J. Exp. Bot.* **71**: 2412-2427.
- Wang, L., Wang, B., Jiang, L., Liu, X., Li, X., Lu, Z., Meng, X., Wang, Y., Smith, S.M., and Li, J.** (2015). Strigolactone signaling in *Arabidopsis* regulates shoot development by targeting D53-like SMXL repressor proteins for ubiquitination and degradation. *Plant Cell* **27**: 3128-3142.
- Wang, L., Xu, Q., Yu, H., Ma, H., Li, X., Yang, J., Chu, J., Xie, Q., Wang, Y., Smith, S.M., Li, J., Xiong, G., and Wang, B.** (2020). Strigolactone and Karrikin Signaling Pathways Elicit Ubiquitination and Proteolysis of SMXL2 to Regulate Hypocotyl Elongation in *Arabidopsis thaliana*. *Plant Cell*: tpc.00140.02020.
- Waters, M.T., Nelson, D.C., Scaffidi, A., Flematti, G.R., Sun, Y.K., Dixon, K.W., and Smith, S.M.** (2012). Specialisation within the DWARF14 protein family confers distinct responses to karrikins and strigolactones in *Arabidopsis*. *Development* **139**: 1285-1295.
- Williamson, L.C., Ribrioux, S.P.C.P., Fitter, A.H., and Leyser, H.M.O.** (2001). Phosphate Availability Regulates Root System Architecture in *Arabidopsis*. *Plant Physiol.* **126**: 875-882.

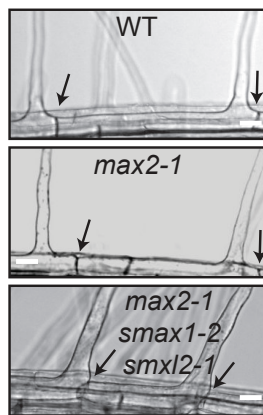
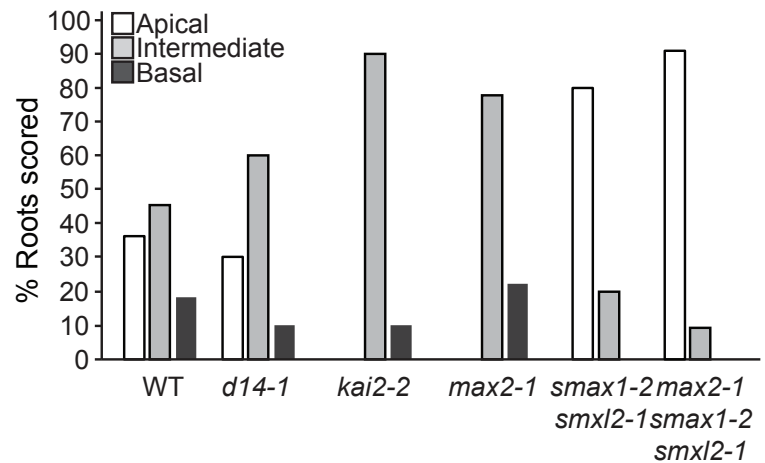
- Yang, Y., Hammes, U.Z., Taylor, C.G., Schachtman, D.P., and Nielsen, E.** (2006). High-Affinity Auxin Transport by the AUX1 Influx Carrier Protein. *Curr. Biol.* **16**: 1123-1127.
- Yao, R., Ming, Z., Yan, L., Li, S., Wang, F., Ma, S., Yu, C., Yang, M., Chen, L., Chen, L., Li, Y., Yan, C., Miao, D., Sun, Z., Yan, J., Sun, Y., Wang, L., Chu, J., Fan, S., He, W., Deng, H., Nan, F., Li, J., Rao, Z., Lou, Z., and Xie, D.** (2016). DWARF14 is a non-canonical hormone receptor for strigolactone. *Nature* **536**: 469-473.
- Yi, K., Menand, B., Bell, E., and Dolan, L.** (2010). A basic helix-loop-helix transcription factor controls cell growth and size in root hairs. *Nat Genet* **42**: 264-267.
- Zenser, N., Ellsmore, A., Leasure, C., and Callis, J.** (2001). Auxin modulates the degradation rate of Aux/IAA proteins. *Proc. Natl. Acad. Sci. USA.* **98**: 11795-11800.

**Figures:**



**Figure 1. Mutants in KL signalling attenuate the root hair elongation responses to Pi.**

Root hair length ( $\mu\text{m}$ ) of the indicated genotypes under low Pi ( $2\mu\text{M Pi}$ ), medium Pi ( $625\mu\text{M Pi}$ ) or high Pi ( $2\text{mM Pi}$ ) conditions. The black dotted line indicates the median of wild type at medium Pi. The grey dotted lines indicate the median of wild type at low and high Pi. The outline of the violin plot represents the probability of the kernel density. Black boxes represent interquartile ranges (IQR), with the red horizontal line representing the median; whiskers extend to highest and lowest data point but no more than  $\pm 1.5$  times the IQR from the box; outliers are plotted individually. Different letters indicate different statistical groups (ANOVA, posthoc Tukey,  $p \leq 0.05$ ).

**A****B**

**Figure 2. KL signalling controls root hair positioning at the epidermal cell.**

(A) Images of representative trichoblasts showing sites of root hair emergence. Arrows indicate the most apical end of the cell. (B) Frequency distribution of different root hair positions observed in the indicated genotypes.

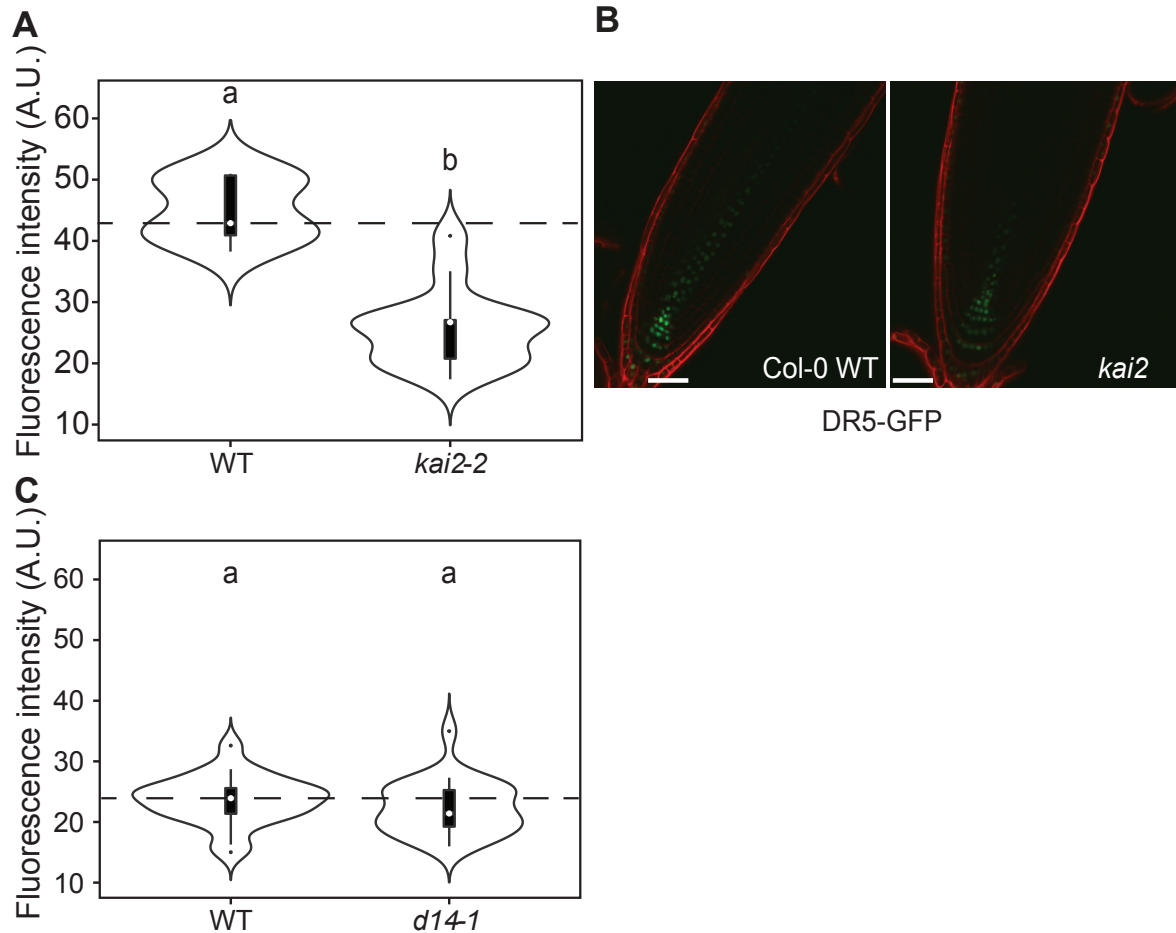


**Figure 3. KL perception mutants show reduced *DR5v2:GFP* expression in the root meristem.**

(A and C) Fluorescence intensity (arbitrary units, A.U.) of *DR5v2:GFP* of the indicated genotypes. The outline of the violin plot represents the probability of the kernel density. Black boxes represent interquartile ranges (IQR), with the red horizontal line representing the median; whiskers extend to highest and lowest data point but no more than  $\pm 1.5$  times the IQR from the box; outliers are plotted individually. Different letters indicate different statistical groups (ANOVA, posthoc Tukey,  $p \leq 0.05$ ). (B) Confocal images of representative root tips of Col-0 wild type and *kai2-2* expressing the auxin reporter *DR5v2:GFP*.

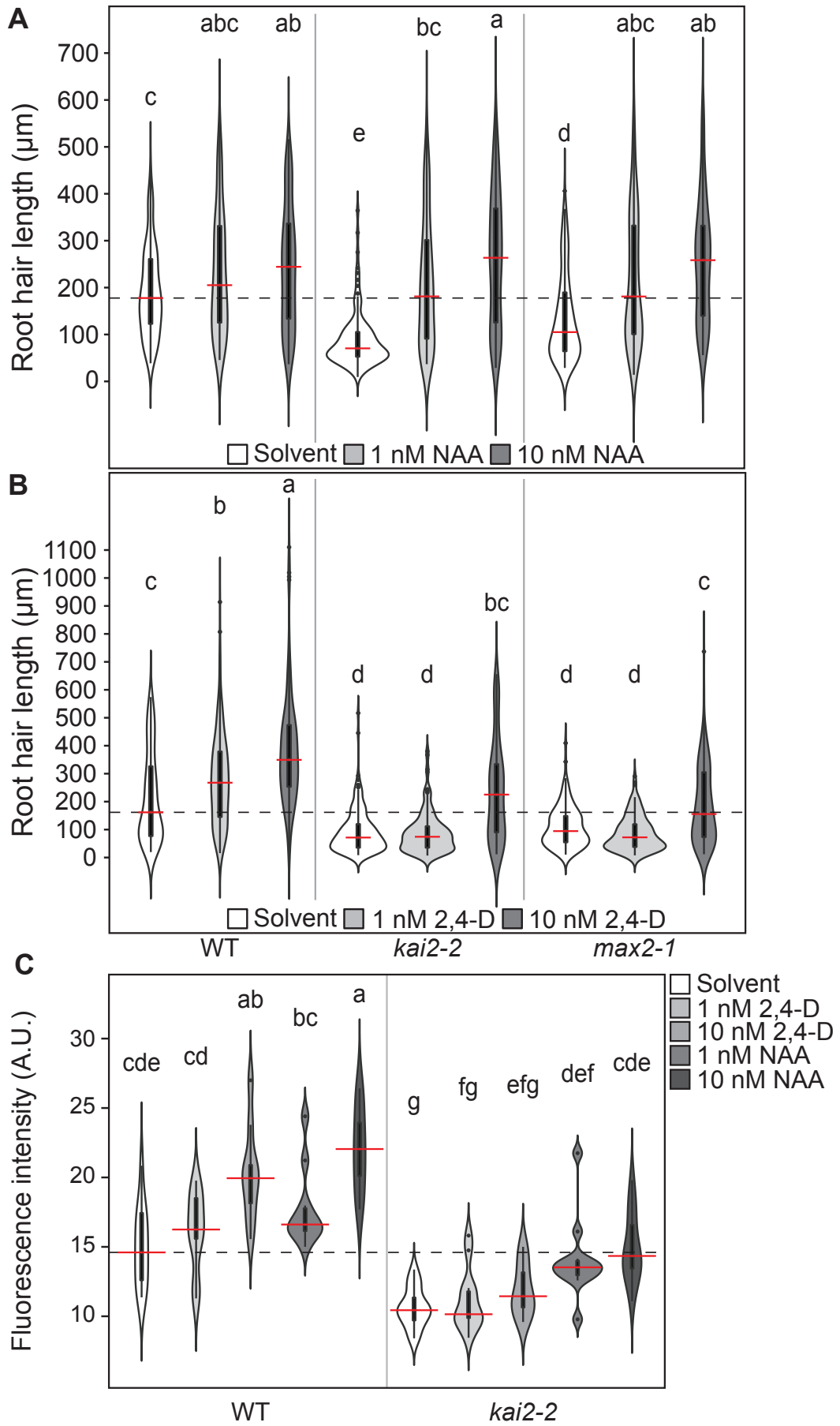


**Figure 4. KL signalling mutants show different sensitivity to NAA than to 2,4-D.**

Root hair length ( $\mu\text{m}$ ) of the indicated genotypes, treated with **(A)** solvent (96% Ethanol), 1 nM NAA or 10 nM NAA, **(B)** solvent (96% Ethanol), 1 nM 2,4-D or 10 nM 2,4-D. **(C)** Fluorescence intensity (arbitrary units, A.U.) of *DR5v2:GFP* of the Col-0 wild type and *kai2-2* genotypes, treated with solvent (96% Ethanol), 1 nM 2,4-D or 10 nM 2,4-D, 1 nM NAA or 10 nM NAA. The outline of the violin plot represents the probability of the kernel density. Black boxes represent interquartile ranges (IQR), with the red horizontal line representing the median; whiskers extend to highest and lowest data point but no more than  $\pm 1.5$  times the IQR from the box; outliers are plotted individually. Different letters indicate different statistical groups (ANOVA, posthoc Tukey,  $p \leq 0.05$ ).

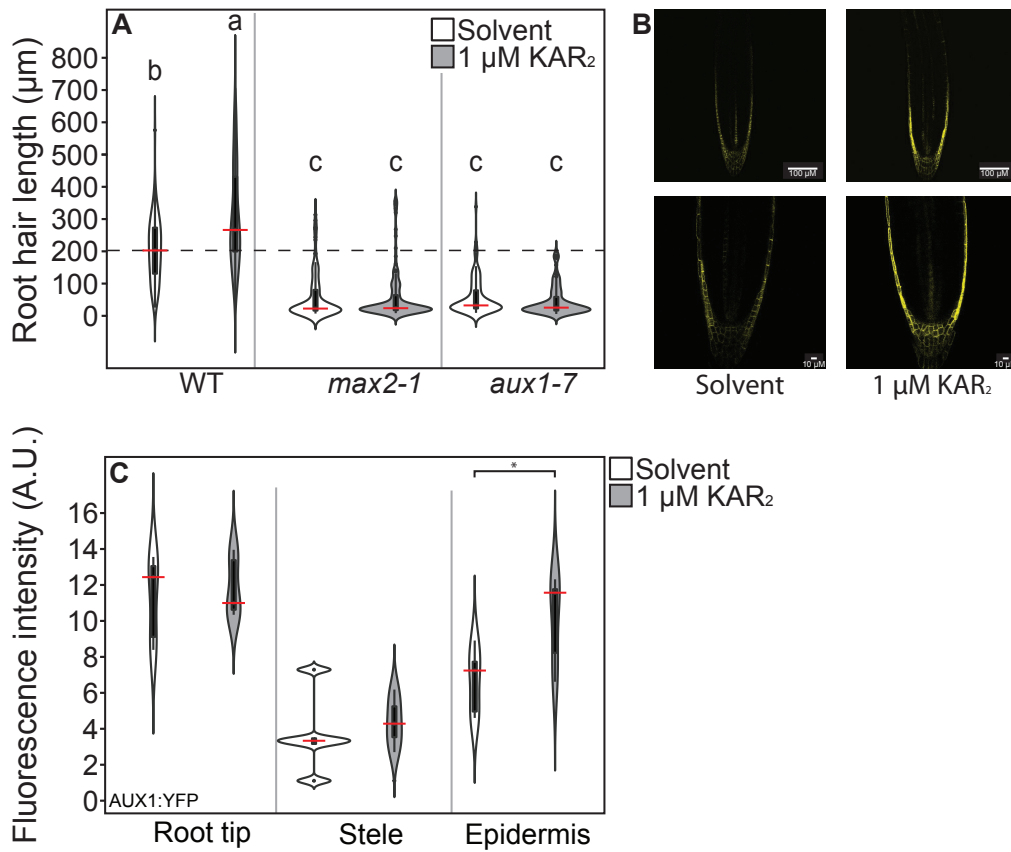


**Figure 5. KL signalling control root hair development by modulating AUX1 accumulation.**

(A) Root hair length ( $\mu\text{m}$ ) of the indicated genotypes treated with solvent (70% methanol) or 1  $\mu\text{M}$  KAR<sub>2</sub>. The outline of the violin plot represents the probability of the kernel density. Black boxes represent interquartile ranges (IQR), with the red horizontal line representing the median; whiskers extend to highest and lowest data point but no more than  $\pm 1.5$  times the IQR from the box; outliers are plotted individually. Different letters indicate different statistical groups (ANOVA, posthoc Tukey,  $p \leq 0.05$ ). (B) Confocal images of representative root tips of Col-0 wild type treated with solvent (70% methanol) or 1  $\mu\text{M}$  KAR<sub>2</sub> for 2 hours. (B) Fluorescence intensity (arbitrary units, A.U.) of AUX1:YFP of the indicated genotypes treated with solvent (70% methanol) or 1  $\mu\text{M}$  KAR<sub>2</sub> for 2 hours. Black boxes represent interquartile ranges (IQR), with the red horizontal line representing the median; whiskers extend to highest and lowest data point but no more than  $\pm 1.5$  times the IQR from the box; outliers are plotted individually. Asterisks indicate a significant difference from the solvent (Student's t-test,  $p \leq 0.05$ ).

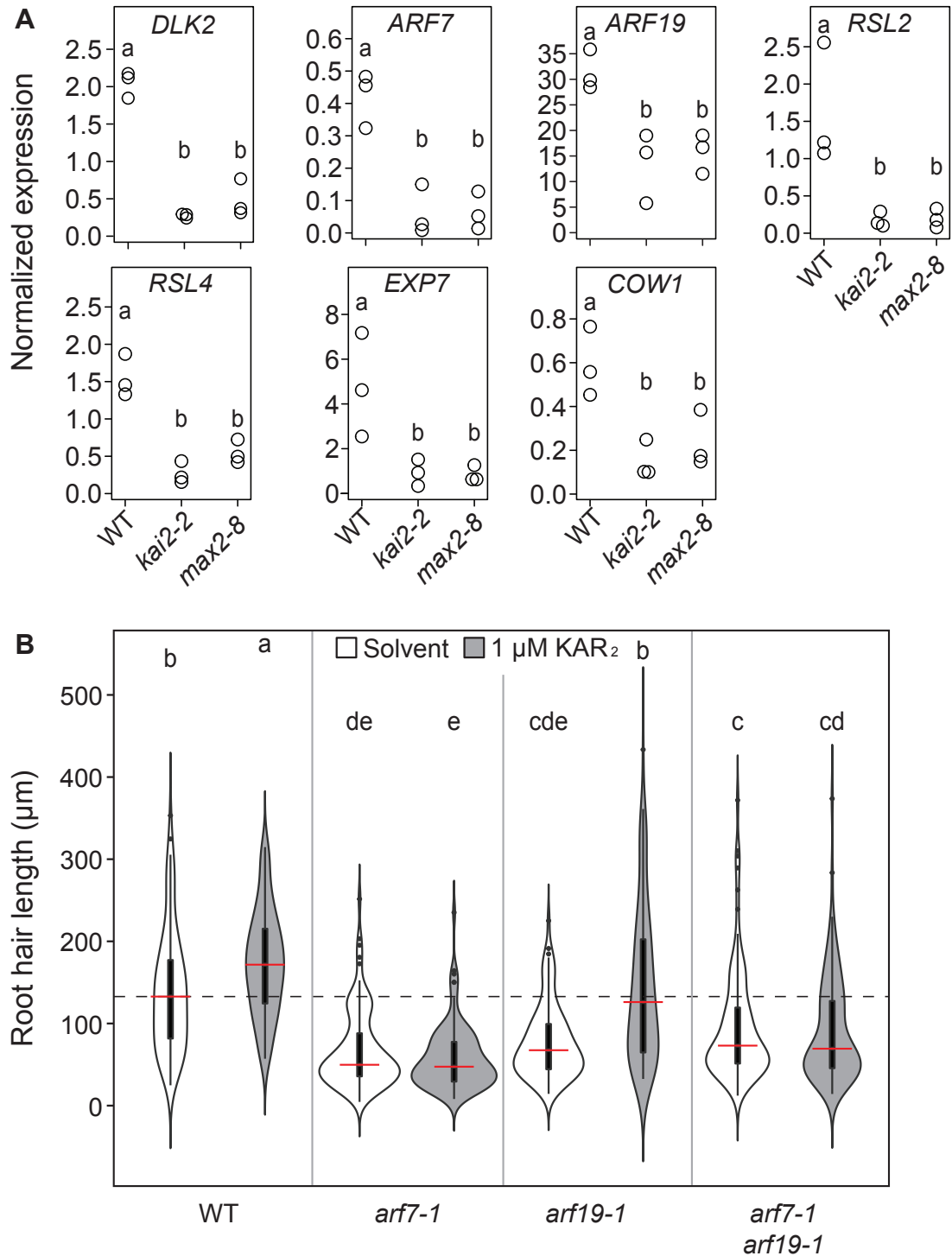
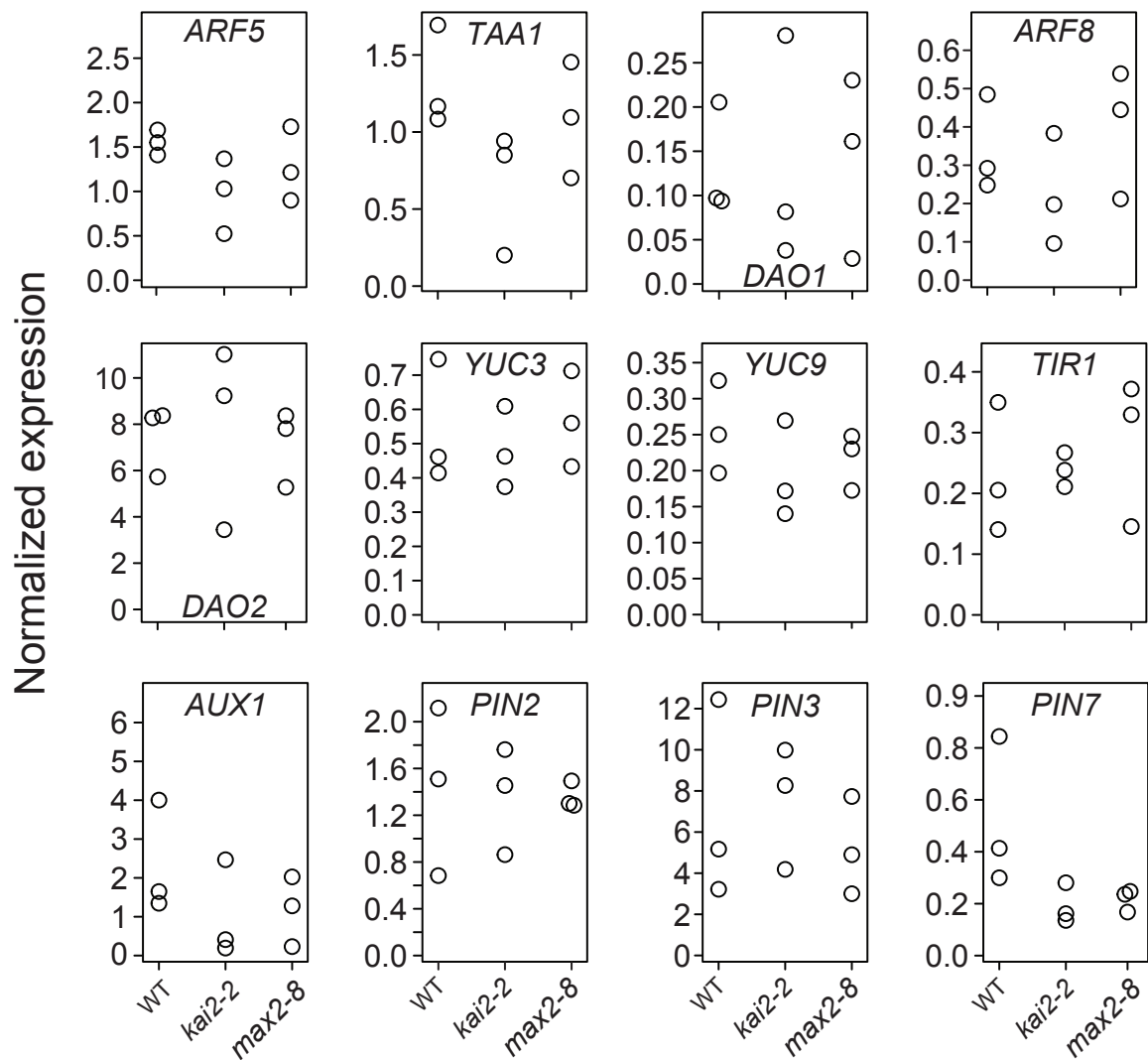


**Figure 6. ARF7 acts downstream of KL signalling in controlling root hair length.**

(A) Transcript accumulation in roots of the indicated genotypes. Expression levels of 3 biological replicates are normalized against those of *EF1 $\alpha$* . Different letters indicate different statistical groups (ANOVA, posthoc Tukey,  $p \leq 0.05$ ). (B) Root hair length ( $\mu\text{m}$ ) of the indicated genotypes treated with solvent (70% methanol) or 1  $\mu\text{M}$  KAR<sub>2</sub>. The outline of the violin plot represents the probability of the kernel density. Black boxes represent interquartile ranges (IQR), with the red horizontal line representing the median; whiskers extend to highest and lowest data point but no more than  $\pm 1.5$  times the IQR from the box; outliers are plotted individually. Different letters indicate different statistical groups (ANOVA, posthoc Tukey,  $p \leq 0.05$ ).



**Supplementary Figure 1. Auxin biosynthesis and transport gene expression.**

Transcript accumulation of *DLK2*, *TAA1*, *DAO1*, *DAO2*, *YUC3*, *YUC9*, *TIR1*, *AUX1*, *PIN2*, *PIN3* and *PIN7* in roots of the indicated genotypes. Expression levels of 3 biological replicates are normalized against those of *EF1 $\alpha$*  (ANOVA, posthoc Tukey,  $p \leq 0.05$ ).

**Supplemental Table 1.** List of primers used for qPCR analysis.

| Gene                          | Direction | Sequence                 | References                   |
|-------------------------------|-----------|--------------------------|------------------------------|
| <i>ARF5</i>                   | Forward   | TACGCCACTTAGAACCAGGCCATC |                              |
|                               | Reverse   | GTTCCCATGTACCTTCGTTTCCCG |                              |
| <i>ARF7</i>                   | Forward   | GTCATATGCATGCTCCACA      | Singh et al.,<br>2012        |
|                               | Reverse   | CAGCAGGAGCAGCCCACCT      |                              |
| <i>ARF8</i>                   | Forward   | ACATGGAGGGTTTTCTGTTCC    |                              |
|                               | Reverse   | TGGCACTGACAAAGACACTCCATC |                              |
| <i>ARF19</i>                  | Forward   | TCTTGCAGCTATCCCAACCA     |                              |
|                               | Reverse   | CGATGGCCTCGAATGATAATGTAA |                              |
| <i>RSL2</i>                   | Forward   | TCCCAATGGAACAAAGGTC      | Yi et al.,<br>2010           |
|                               | Reverse   | TCTCGGTGAGCTGAGACCAA     |                              |
| <i>RSL4</i>                   | Forward   | GTGCCAAACGGGACAAAAGT     | Yi et al.,<br>2010           |
|                               | Reverse   | TTGTGATGGAACCCCATGTC     |                              |
| <i>EXP7</i>                   | Forward   | AACCATGGGTGGTGCATG       | Zhang et al.,<br>2016        |
|                               | Reverse   | CCGCATCCGTAACCATCA       |                              |
| <i>COW1</i>                   | Forward   | CCACATGATGCTTCGATTTTTGAG | Zhang et al.,<br>2016        |
|                               | Reverse   | TAGCCTTGAGGGTAGTGC       |                              |
| <i>DLK2</i>                   | Forward   | GCTGCTTCTCCAAGGTATATAA   | Waters et al.,<br>2012       |
|                               | Reverse   | GAAATCAACCGCCCAAGCT      |                              |
| <i>TAA1</i>                   | Forward   | ATCTTACCCTGCGTTTGCGT     |                              |
|                               | Reverse   | AGCATGCTGACTCGGACATGC    |                              |
| <i>DAO1</i>                   | Forward   | CTGCAGATCAAAGGGAGATT     |                              |
|                               | Reverse   | TCTCAACCAGCCCGTAACTC     |                              |
| <i>DAO2</i>                   | Forward   | TGGTGACATGGCTACGATATG    |                              |
|                               | Reverse   | CTTCAAGATCTCTATCCACTGG   |                              |
| <i>YUC3</i>                   | Forward   | TCGTAGCGCTGTTTCATGTTT    |                              |
|                               | Reverse   | GCGAGCCAAACGGGCATATACTTC | Liu et al.,<br>2017          |
| <i>YUC9</i>                   | Forward   | AGTCCGGCGAGAAATTCAGAGG   | Liu et al.<br>2017 PNAS      |
|                               | Reverse   | AACATGAACCGAGCTTCTAACGAC |                              |
| <i>TIR1</i>                   | Forward   | GCCACTTGCAGGAATCTGAA     |                              |
|                               | Reverse   | TGAGAGACTTGAGATTGGGACA   |                              |
| <i>AUX1</i>                   | Forward   | GCTGTGCGGTGCTCTTCTTG     |                              |
|                               | Reverse   | CTTCTCCGCCGCATTCTGA      |                              |
| <i>PIN2</i>                   | Forward   | TCACGACAACCTCGCTACTAAAGC | Niu et al.,<br>2015          |
|                               | Reverse   | GTCTTGGTCCATTTCACATGCC   |                              |
| <i>PIN3</i>                   | Forward   | GAGCACCTGACAACGATCAAGG   | Niu et al.,<br>2015          |
|                               | Reverse   | GATGAGCTACAGCTTTGGTC     |                              |
| <i>PIN7</i>                   | Forward   | GGAGCCAATGAACAAGTCGG     | D'alessandro<br>et al., 2015 |
|                               | Reverse   | TCATCGGACCAGCTTTGTTT     |                              |
| <i>EF1<math>\alpha</math></i> | Forward   | GGTGGTGGCATCCATCTTGTTACA | Yi et al.,<br>2010           |
|                               | Reverse   | TGAGCACGCTCTTCTTGCTTCA   |                              |

## **IX. General discussion**

### **1. KL signalling is a major regulator of root and root hair development in *Arabidopsis thaliana***

Architecture and morphology changes of root growth and development are crucial for the adaption of plants to different soil environments. SL signalling has been assumed to control root and root hair development (Koltai et al., 2010; Kapulnik et al., 2011b; Kapulnik et al., 2011a; Ruyter-Spira et al., 2011; Mayzlish-Gati et al., 2012; Jiang et al., 2015). However, the use of mutants commonly perturbed in SL and KL signalling and the use of an unspecific strigolactone analogue in previous studies have led to incorrect attribution of phenotypes to SL signalling. This problem can be solved by studying KL and SL signalling specific mutants and thereby dissecting the function of the two pathways in the control of root and root hair development. In this thesis, I performed a detailed phenotypic analysis of different *Arabidopsis* seedling root parameters of SL synthesis and KL and SL signalling mutants.

#### **1.1 KL signalling regulates root development and root growth behaviour in *Arabidopsis thaliana***

Because of the challenges associated with the measurement of below-ground plant organs, such as roots, *Arabidopsis* plants are commonly grown on hard agar surfaces for root studies. In these conditions, the roots cannot penetrate the agar, causing changes in the root growth direction, such as skewing and waving (Vaughn and Masson, 2011). Regulation of skewing and waving includes several cellular and physiological aspects (Roy and Bassham, 2014), including different hormone signalling pathways, such as auxin in root skewing and waving (Qi and Zheng, 2013) (Soeno et al., 2010) or ethylene in root waving (Buer et al., 2003). In this thesis, I found that in addition, KL signalling is involved in the regulation of root growth direction, as KL perception mutants showed an exaggeration of root skewing and increased waving (Paper I). However, the SL receptor mutant *d14* and SL biosynthesis mutants showed similar skewing and waving as wild type. Therefore, I propose that KL and not SL signalling is an important player in the regulation of root skewing and waving under controlled conditions. Because these conclusions are based on root-agar medium interactions, the roles of KL signalling in the root growth patterns in the soil need further investigation.

Supporting our findings, a recent report (Swarbreck et al., 2019) suggested that KL signalling controls root skewing and waving. Currently, it is not possible to provide a mechanism by which KL signalling pathway regulates root skewing and waving. However, Swarbreck et al., 2019 speculated that an increased epidermal cell file rotation together with a thinner root diameter in KL perception mutants might be the cause of root skewing in *kai2*. In that study, cell file rotation was the result of measuring the total number of epidermal cells that crossed a 1 mm line. I did not find a shred of evidence that supports epidermal cell file rotation, but rather a reduction in the epidermal cell length. Besides, this reduction can also be observed in SL receptor mutants, while skewing only occurs in KL perception mutants. Hence, the reduced epidermal cell length is not likely the causes for increased skewing in KL perception mutants. Another interesting observation, is the difference in root diameter of the KL signalling mutants: in concordance with Swarbreck et al., 2019, I found that KL perception mutants but not SL perception mutants, showed thinner roots when compared to wild-type. A reduction of root diameter can account for a reduction in root surface area, which could lead to lessened friction with the medium. Considering that root skewing and waving is often explained as the result of physical interaction between the root and the growth media (Roy and Bassham, 2014), a decrease in root friction seems contradictory with the root skewing and waving phenotypes in *kai2* and *max2* mutants.

Swarbreck et al., 2019 also demonstrated that mutations in *SMAX1* or *SMXL678* suppressed the root skewing phenotype of Arabidopsis *max2* mutants. Because KL signalling, but not SL signalling, regulates root skewing (Swarbreck et al., 2019; Villaécija-Aguilar et al., 2019), these results suggest a surprising receptor target interaction between KAI2 and SMAX1 as well as SMXL678. This challenges the current KL and SL signalling model, in which D14-MAX2 interacts with SMXL6, SMXL7, and SMXL8, while KAI2-MAX2 interacts with SMAX1 and SMXL2 for the control of plant development (Morffy et al., 2016). Mutations in *SMXL6/7/8* suppress SL-related *max2* phenotypes, such as increased shoot branching and lateral root density or the reduced petiole and blade length phenotypes (Soundappan et al., 2015; Bennett et al., 2016). SMAX1 suppresses seed germination, while SMXL2 acts redundantly with SMAX1 to increase hypocotyl elongation, both mediated by KL signalling (Stanga et al., 2013; Soundappan et al., 2015; Stanga et al., 2016). Yeast

two-hybrid (Y2H) studies demonstrated that SL- or SL- analogues induce the interactions between D14 and MAX2, SMXL6 and SMXL7 (Umehara et al., 2008; Zhou et al., 2013; Wang et al., 2015; Seto et al., 2019). Besides, co-immunoprecipitation and Y2H analysis suggested the interaction between KAI2 and MAX2, SMAX1 or SMXL2 (Khosla et al., 2020; Wang et al., 2020). Nonetheless, *rac-GR24* inhibits hypocotyl elongation through KAI2 and D14, indicating that D14 can act upon SMAX1 and SMXL2 (Scaffidi et al., 2014). Accordingly, synthetic SL treatment triggers the polyubiquitination and degradation of SMXL2 via D14 and KAI2 (Wang et al., 2020). *rac-GR24* treatment also induces the interaction between SMXL6 or SMXL7 with both KAI2 and D14 (Khosla et al., 2020; Wang et al., 2020). Therefore, although most evidence favours the current model, it is possible that KAI2 interacts with SMXL6/7/8 to regulate root growth movements, such as root skewing and waving. We decided to evaluate this hypothesis in more detail by using different combinations of higher order mutants with *max2* in two different laboratories, Munich [M] and Leeds [L]. We found that single mutations in *SMAX1* or *SMXL2* suppress the root skewing phenotype of *max2*, while only a double mutation in *SMAX1* and *SMXL2* suppress the root waving of *max2*. These results indicate that root skewing and waving are controlled by the KL signalling pathway independently of each other. We next analysed the effect of a triple mutation in *SMXL6,7,8* in the root skewing and waving phenotypes of *max2*. We did not observe a suppression of the root waving phenotype of *max2* mutants, but we found a reduction in skewing in *smxl678 max2* when compared to *max2* in [M]. This was not consistent with our observations in [L], where root skewing was increased in *smxl678* relative to wild-type in [L]. Thus, I conclude that while SMAX1 and SMXL2 increase root skewing, SMXL6/7/8 suppress it. SMXLs proteins can form complex with themselves or other SMXLs in vitro (Khosla et al., 2020). Hence, it is possible that the loss of SMXL6/7/8 somehow stabilizes SMAX1 and/or SMXL2, which could explain the exaggerated root skewing in *smxl6/7/8* mutants. However, since our results vary between laboratories, those interactions might be susceptible to environmental differences. Further studies are needed to demonstrate that SMXLs can interact with each other in vivo and whether this would affect root skewing in Arabidopsis.

We next analysed the regulation of lateral root density (LRD) by MAX2, which was previously described (Kapulnik et al., 2011b; Ruyter-Spira et al., 2011; Soundappan et al., 2015). In collaboration with Dr. Tom Bennett, we demonstrated that

LRD in Arabidopsis is regulated by both KL and SL signalling pathways, by targeting the co-repressor SMAX1, SMXL2, SMXL6, SMXL7 and SMXL8 (Paper I). We observed that KL and SL biosynthesis and/or signalling mutants showed increased LRD when compared to wild type, while mutations in *SMAX1*, *SMXL2* or *SMXL678* genes suppressed the LRD phenotype of *max2*. However, it remains to be established why both KAI2 and D14 are redundant in the control of LRD. One possibility is that different external stimuli activate KL or SL signalling for the suppression of lateral root development. Apart from dissecting the role of KL and SL signalling and regulating root architectural traits, our root skewing, waving and lateral root analysis support that KL and SL signalling employ the canonical KAI2-SMAX1/SMXL2 and D14-SMXL678 receptor-target pairs.

Further work is needed to establish a mechanism that explains the roles of KAI2, D14 and MAX2 in the control root development and behaviour. Additionally, since this study has been performed using Arabidopsis, investigations in other plant species will be needed for translating research to economically important plants.

## **1.2 KL signalling regulates root hair development**

Previous reports showed decreased root hair density and length in *max2* mutants and increased root hair growth after treatment with *rac*-GR24 (Kapulnik et al., 2011b). However, it was unclear whether KL and/or SL signalling mediate the MAX2 regulation of root hair growth in Arabidopsis. KL signalling has been suggested as a critical regulator of plant survival in a post-fire environment and promotes drought resistance in Arabidopsis plants (Nelson et al., 2010; Li et al., 2017; Wang et al., 2018). Fire is an important disturbance factor in many terrestrial ecosystems, which can induce soil alterations (Kutiel and Inbar, 1993; Shakesby et al., 1993; MacDonald and Huffman, 2004; Chafer, 2008; Tessler et al., 2008; Fernández et al., 2010; Shakesby, 2011; Prats et al., 2016). Upon soil disruption, a short primary root and root hairs are the only opportunity for anchoring to the soil for young seedlings. Besides, the importance of root hair development also extends to water holding capacity of the root (Choi and Cho, 2019). Hence, it is possible that KL signalling serves as an integrator of different environmental signals, such as changes in soil and water availability, to modulate root hair development.

In this study, I evaluated the roles of both KL and SL signalling pathways in root hair density (RHD) and length (RHL) (Paper I). SL biosynthesis and *d14* mutants did not show a significant difference in root hair development when compared to wild type. Conversely, *kai2* and *max2* showed a reduction in RHD and RHL (Figure 6). Taken together, these results indicate that KL signalling, but not SL signalling, is a major regulator of root hair development in Arabidopsis. This appears to be conserved in other plant species. *Brachypodium distachyon kai2* mutants also show a reduction in root hair growth (Varshney and Gutjahr, unpublished). However, whether SLs have an influence on root hair development in other species is still unknown.

Our findings seem to be partially contradictory with the previously suggested role of the SL signalling pathway in the control of root hair growth (Koltai et al., 2010; Kapulnik et al., 2011b; Kapulnik et al., 2011a; Mayzlish-Gati et al., 2012). Here I demonstrated that external *rac*-GR24 treatments stimulate root hair density and elongation via D14- and KAI2- mediated signalling (Paper I). Thus, it is plausible that SL signalling does not play a role in root hair development in our controlled conditions, but upon exposure to different external cues, which may induce SL biosynthesis, SL signalling seems to initiate the root hair growth machinery. Indeed, the production of SLs is affected by nutrient availability (Xie et al., 2010). Phosphate starvation increases SL biosynthesis, leading to changes in root system architecture (Yoneyama et al., 2007; Kohlen et al., 2011; Ruyter-Spira et al., 2011; Yoneyama et al., 2013). In sorghum roots, nitrogen deficiency induces SL production (Yoneyama et al., 2013). Therefore, we can speculate that changes in environmental signals trigger the biosynthesis of different ligands, to either activate D14- or KAI2- mediated signalling.

Based on the KL and SL signalling model discussed above, in which D14-MAX2 interacts with SMXL6/7/8 and KAI2-MAX2 interacts with SMAX1 and SMXL2, I hypothesised that KL signalling regulates root hair growth through SMAX1 and/or SMXL2. Accordingly, mutations in *SMAX1* and *SMXL2* suppressed the root hair phenotype of *max2* mutants and have an increased RHD and RHL when compared to wild-type (Figure 6), while mutations in *SMXL6/7/8* could not suppress those phenotypes. These results indicate that RHD and RHL are indeed controlled by the repressors SMAX1 and SMXL2. Since *rac*-GR24 stimulates root hair development via

SL and KL signalling simultaneously, this opens the question of whether SL treatment induces root hair growth mediated via D14 in interaction with SMAX1/SMXL2 or SMXL6/7/8. *rac*-GR24 treatment can induce the interaction between D14 and SMAX1 or SMXL2 (Khosla et al., 2020; Wang et al., 2020). Thus, the interaction D14-SMAX1/SMXL2 in the presence of *rac*-GR24 might lead to increased root hair growth in the absence of KAI2.

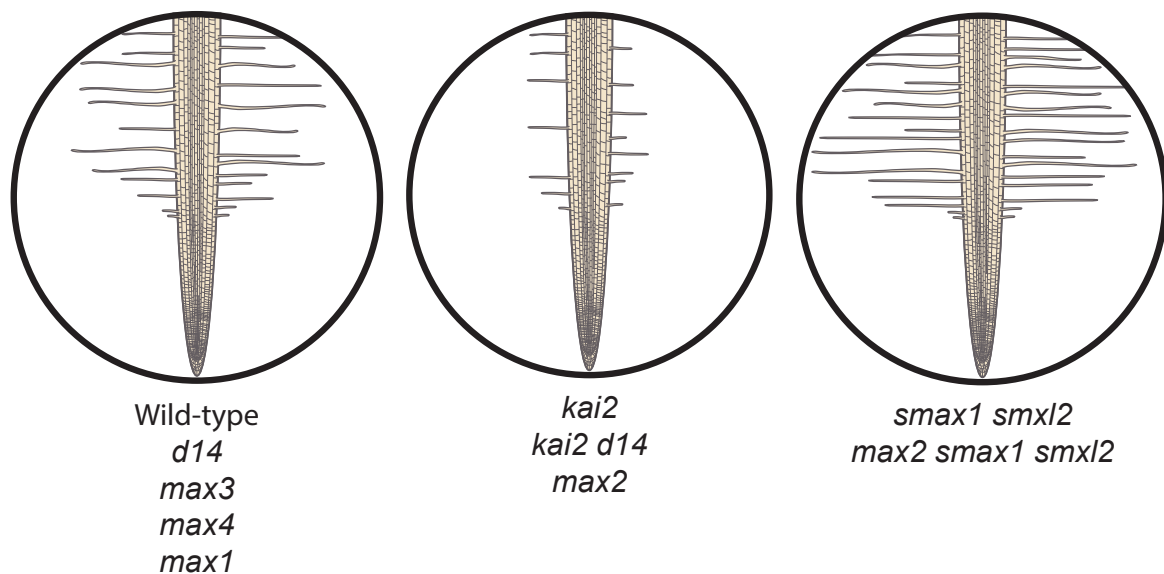


**Figure 6: Schematic representation of root hair density and length phenotype in roots of Arabidopsis KL and SL signalling mutants.**

## 2. Ligand stereo-specific of D14 and KAI2

Prior research proposed that the different stereoisomers of *rac*-GR24, GR24<sup>5DS</sup> and GR24<sup>ent5DS</sup> act specifically through D14 and KAI2, respectively (Scaffidi et al., 2014). Thus, I evaluated whether GR24<sup>5DS</sup> and GR24<sup>ent5DS</sup> incite root hair growth in a D14 or KAI2 specific manner. Surprisingly, both D14 and KAI2 responded to GR24<sup>5DS</sup> and GR24<sup>ent5DS</sup> for root hair elongation and inhibition of hypocotyl length, implying control of root hair development by both signalling pathways (Paper I). Recent reports showed that synthetic *rac*-GR24 contains a strigolactone mimic contaminant, named contalactone (de Saint Germain et al., 2019). However, we confirmed the purity of the

employed stereoisomers via NMR and CD (Villaécija-Aguilar et al., 2019), making the participation of contaminants unlikely.

The ligand binding by D14 and KAI2 has been extensively studied in the last decade (Kagiyama et al., 2013; Zhao et al., 2013; Conn et al., 2015; Waters et al., 2015; Obando et al., 2016; Xu et al., 2016; Bythell-Douglas et al., 2017; Hameed et al., 2018; Bürger et al., 2019). In most Angiosperms, KAI2 does not act as strigolactone receptor. However, in parasitic plants of the Orobanchaceae family, KAI2 has duplicated several times, diversified and some isoforms evolved to perceive SLs from the rhizosphere to promote germination (Conn et al., 2015). SLs but not KAR can act through these KAI2 versions, which contain a bigger binding pocket than the KAR receptors KAI2 (Conn et al., 2015; Conn and Nelson, 2016; Xu et al., 2016; Xu et al., 2018; Machin et al., 2020). Similarly, in Arabidopsis and rice, D14 has a larger binding pocket than KAI2 (Kagiyama et al., 2013; Zhao et al., 2013; Xu et al., 2016). Hence, the binding-specificity between D14 and KAI2 might be determined by the size of this deep binding pocket that contains a conserved catalytic triad of serine, histidine, aspartate (Kagiyama et al., 2013; Zhao et al., 2013). However, KAI2 can recognize the different stereoisomers of *rac*-GR24, which have a similar size to strigolactones (Scaffidi et al., 2014; Waters et al., 2015; Morffy et al., 2016). This suggests that the D14 pocket is bigger than necessary to bind SL, presumably for the recognition of non-canonical SLs. Likewise, the KAI2-like pocket is larger than needed to bind karrikins, and not all KAI2-like proteins bind karrikin (Machin et al., 2020), suggesting that KL is bigger than karrikin or that KAI2 might recognize a broad range of KL molecules. In conclusion, the evolutionary conservation of larger pocket sizes might have diminished the binding selectivity of KAI2 and D14, which could explain their affinity for multiple synthetic SLs, such as GR24<sup>5DS</sup> and GR24<sup>ent5DS</sup>. An essential goal in the field remains to find and produce a specific synthetic ligand of D14 for pharmacology studies of the SL signalling pathway.

### **3. Protein-protein interaction plays an important role in KL signal integration**

To better understand the KL signalling pathway, I contributed to a study on the identification of new protein interactors of KAI2 (Paper II). We found in a large-scale yeast-2-hybrid screen fifteen hormone-dependent novel interactors of KAI2, including

the GR24-dependent interactor PP2AA2. PP2AA2 represents one of the three Ser/Thr protein phosphatase 2A subunits (PP2A) in Arabidopsis (Janssens and Goris, 2001; Cho and Xu, 2007). Mutations in PP2AAs causes abnormalities in root growth, such as root agravitropism and root meristem collapse through seedling development (Zhou et al., 2004; Michniewicz et al., 2007). Hence, I hypothesised that PP2AA2 might participate in the regulation of root hair development by KAI2. Accordingly, I found a severely decreased root hair growth in Arabidopsis *pp2aa2* mutants, which phenocopied the root hair phenotypes of the KL receptor mutants (Altmann and Altmann et al., 2020). Besides, *kai2* and *pp2aa2* mutants did not respond to exogenous karrikin treatment for root hair growth, supporting that they jointly mediate KL signalling. Changes in PP2A activity lead to defects in hormone signalling (DeLong, 2006). For instance, mutations in *PP2AA2* alter auxin signalling in Arabidopsis seedlings roots, probably caused by a disruption in auxin flux (Michniewicz et al., 2007). This raised the intriguing question, whether an alteration in auxin transport and/or signalling is the cause of the root hair phenotypes in *kai2* and *pp2aa2* mutants.

#### **4. KL signalling modulates auxin influx in response to low external Pi**

Root hairs elongate to increase the root surface upon mineral nutrient deficiency, such as the deficiency of potassium, nitrate or phosphate (Bates and Lynch, 1996; Williamson et al., 2001; Høgh-Jensen and Pedersen, 2003; Brown et al., 2013; Canales et al., 2017; Klinsawang et al., 2018). The regulation of root hair development during Pi deficiency requires the activity of auxin biosynthesis, transport and transcriptional regulation of auxin signalling components in Arabidopsis and rice roots (Bhosale et al., 2018; Giri et al., 2018). Our study reveals that mutations in KL signalling perception attenuate the root hair response to low external Pi, suggesting a cross-talk of KL signalling with auxin biosynthesis or signalling (Manuscript I). Using qPCR-based gene expression analysis and the DR5 based auxin response reporter, I demonstrated that auxin signalling or distribution, but not auxin biosynthesis, is altered in the roots of KL perception mutants. Currently it is unclear whether endogenous auxin content is disrupted in KL signalling mutants roots since the alteration of auxin biosynthesis in the shoots system and/or changes in auxin transport from the shoot to the root might alter the total auxin amount in the roots (Brumos et al., 2018). In Arabidopsis roots, most of the auxin responsive gene expression is regulated by the auxin response

factors ARF7 and ARF19 (Okushima et al., 2007). Bhosale et al., 2018 showed that changes in auxin accumulation in the epidermis above the lateral root cap leads to the activation of the auxin-inducible transcription factor genes *ARF19*, which trigger the induction of the transcription factors *RSL2* and *RSL4*, which are regulators of root hair growth. In my qPCR analysis, *ARF7* and *ARF19* are less expressed in roots of the KL perception mutants as compared to wild type. Therefore, I analysed the root hair response to KAR of *arf7* and *arf19* mutants. I found that *arf7* but not *arf19* mutants are resistant to KAR with respect root hair development, indicating that ARF7 acts downstream of KL signalling to regulate root hair development positively. Since ARF19, rather than ARF7 appears to be a key transcription factor in response to low external Pi (Bhosale et al., 2018) our observations seem contradictory with a role of KL signalling in controlling the root hair response to low Pi. Perhaps, the perception of different ligands leads to the activation of *ARF7* or *ARF19*. Thus, it is possible that upon KAR treatment, KL signalling regulates root hair growth through ARF7. However, low external Pi conditions might induce the biosynthesis of unknown endogenous KL in specific cell types activating ARF19 downstream of KL signalling.

To test whether an alteration in auxin signalling is the cause of the root hair phenotypes of the KL perception mutants, we evaluated the effect of exogenous synthetic auxin on root hair growth in those mutants. Treatment with the synthetic auxin analogue NAA fully rescued the root hair phenotype of *kai2* and *max2*, indicating that impaired auxin signalling in *kai2* and *max2* is not likely the cause for the root hair phenotypes, but suggesting an alteration of auxin levels in specific cell types. To corroborate this hypothesis, I used another auxin analogue, 2,4-D. NAA and 2,4-D have differential transport characteristics. While NAA is lipophilic and can be transported by efflux carriers or taken up by diffusion through the membrane, 2,4-D is more hydrophilic and requires the activity of auxin influx carriers (Ma et al., 2018). Surprisingly, treatments with low concentrations of 2,4-D could not rescue the root hair phenotypes of the KL perception mutants, indicating that in the absence of functional KL signalling, auxin signalling is not affected *per se*, but auxin influx is disrupted. As a consequence, auxin might not be correctly distributed within the root system, leading to a reduction in root hair development.

Functional activity of the auxin influx carrier AUX1 (AUXIN RESISTANT 1) is required for auxin import and the root hair response to low external Pi in Arabidopsis (Michniewicz et al., 2007; Petrášek and Friml, 2009; Bhosale et al., 2018; Dindas et al., 2018; Giri et al., 2018). AUX1 is not detected in root hair cells, but rather in non-hair cells, indicating that hair cells do not require auxin influx to ensure auxin supply. However, auxin transport through non-hair cells might provide auxin supply to growing hair cells as the distance from the root tip increases (Jones et al., 2009). Upon Pi deficiency auxin is transported from the root tip to non-root hair cells via AUX1 to promote root hair elongation mediated by ARF19 (Bhosale et al., 2018; Giri et al., 2018). Hence, I investigated whether KL signalling affects the expression or distribution of AUX1-YFP-fusion proteins expressed under the control of the endogenous *AUX1* promoter. While *AUX1* transcript accumulation did not significantly change between wild type and *kai2* or *max2* mutants, AUX1-YFP accumulated to increased levels in the epidermis above the lateral root cap after KAR treatment. Next, I analysed the effect of KAR treatment, which increases KL mediated signalling, on root hair growth of *aux1* mutants. I demonstrated that *aux1* mutants are resistant to the effects of KAR for induction of root hair growth. These results, together with the role of SMAX1 and SMXL2 in root hair development (Villaécija-Aguilar et al., 2019), suggest that SMAX1 and SMXL2 positively influence auxin influx through promoting the accumulation of AUX1 in epidermal cells above the lateral root cap. Supporting this hypothesis, expression pattern analysis indicates that *SMAX1* promoter activity and SMAX1 localised principally to the lateral root cap and columella in the roots of Arabidopsis seedlings (Soundappan et al., 2015; Khosla et al., 2020). Further investigation will be needed to demonstrate whether and how SMAX1 and/or SMXL2 regulate AUX1 activity.

Previous studies have also suggested crosstalk between ethylene and auxin transport in Arabidopsis roots (Roman et al., 1995; Stepanova et al., 2007; Negi et al., 2008). Ethylene-based mutant screens identified that *aux1* mutants are insensitive to the inhibitory effects of ethylene on root growth (Roman et al., 1995; Stepanova et al., 2007; Negi et al., 2008). In Arabidopsis, ethylene is perceived by a family of five different ethylene receptor members, including ETR1, ERS1 (ethylene response sensor 1), ERS2, ETR2, and EIN4 (Zhao et al., 2002). In the absence of ethylene, these receptors negatively regulate downstream ethylene signalling, which culminates

in the activation of the transcription factors EIN2 and EIN3 (ETHYLENE RESPONSE FACTOR2 and(Cho et al., 2018) 3) (Bleecker and Kende, 2000; Wang et al., 2002; Guo and Ecker, 2003; Cho et al., 2018). Ethylene signalling promotes root hair growth through EIN3 activity (Feng et al., 2017). EIN3 activation indirectly triggers the expression of PSI genes (PHOSPHATE STARVATION INDUCED GENES) through the induction of the transcription factor PHR1 (PHOSPHATE STARVATION RESPONSE 1) (Nilsson et al., 2007; Nilsson et al., 2012; Liu et al., 2017). Ethylene mediates the root hair development response to Pi starvation (Song et al. 2016). Thus, ethylene-mediated stimulation of auxin transport may increase root hair formation by promoting auxin accumulation in the epidermis above the lateral root cap (Růžička et al., 2007), required for the root hair response of low external phosphate (Bhosale et al., 2018). Previous work in our group (Carbonnel et al., in revision) revealed that SMAX1 inhibits ethylene biosynthesis in *Lotus japonicus*. It is plausible that *Arabidopsis* SMAX1 and/or SMXL2 may play similar roles, and this finding may, therefore, be extrapolated to *Arabidopsis*. Hence, there is a possibility that regulation of auxin import by KL signalling is dependent on ethylene signalling. Accordingly, previous studies suggested that the ethylene signalling pathway is required for the MAX2 control of root hair development (Kapulnik et al., 2011b; Kapulnik et al., 2011a; Mayzlish-Gati et al., 2012). In conclusion, further analysis will be required to demonstrate how KL signalling controls auxin influx, but this work provides important clues for a mechanistic framework including KL signalling, ethylene and auxin signalling pathways in the regulation of root hair formation.

## X. Outlook

This doctoral work has shown the roles of SL and KL signalling in the regulation of root and root hair development in *Arabidopsis thaliana*. Members of the SMXL protein family regulate root and root hair development downstream of D14 and KAI2 in *Arabidopsis*. Although the exact function of the SMXLs remains unknown, previous research suggested that they are associated with transcriptional regulation, due to their interaction with TOPLESS (TPL) and TOPLESSRELATED (TPR) co-repressor proteins (Kagale and Rozwadowski, 2011; Zhou et al., 2013; Soundappan et al., 2015; Wang et al., 2015). Supporting this hypothesis, D53, encoded by the orthologue of *SMAXL6,7,8* in rice (*Oryza sativa*), promotes assembly of a corepressor-nucleosome complex with TPR2 (Ma et al., 2017). Currently, only one transcription factor downstream of SL signalling has been identified. D53 interacts with and suppresses the transcriptional activation activity of Ideal Plant Architecture 1 (IPA1) to regulate tiller number in rice (Song et al., 2017). The identification of new transcription factors (TFs) targeted SMAX1 and SMXL2 downstream of KL signalling will help to increase our knowledge of the KL signalling pathway and its importance in the control of plant development. One of the possible approaches to finding TFs downstream of KL signalling includes the transcriptome comparison of wild-type and *smax1 smxl2* double mutants by RNAseq in *Arabidopsis thaliana*. Because SMAX1 and SMXL2 are partially redundant for the control of seedling growth, root and root hair development (Stanga et al., 2016; Villaécija-Aguilar et al., 2019), it is possible that both repressors regulate the same plant traits in interaction with common TFs. These transcriptome analyses will help to identify common downstream targets of SMAX1 and SMXL2, which can include suppression or induction of transcriptional activity by SMAX1 and SMXL2 removal. A set of transcription factors can be predicted according to TF-binding sites in the promoters of the genes with altered expression in *smax1 smxl2* double mutants (Rhee et al., 2003; Yilmaz et al., 2011; Austin et al., 2016; Dai et al., 2016; Jayaram et al., 2016; Mele, 2016; Becker et al., 2017). Next, it would be interesting to investigate whether the predicted TFs have physical interaction with SMAX1 and/or SMXL2. Further, it will be necessary to functionally validate the selected TFs. Since mutations in SMAX1 and SMXL2 increase root hair density and length, we could hypothesise that loss of at least one of the TFs confirmed in the last step should show an alteration in root hair growth. If SMAX1 and SMXL2 repress the activity of those TFs, loss of

function of the TFs should decrease root hair density and length. However, if SMAX1 and SMXL2 activate those TFs, loss of functions of the TFs should lead to a similar *smax1 smxl2* root hair phenotype TFs can also be regulated by phosphatase proteins. For instance, PP2A positively regulates the TF BZR1, which controls brassinosteroid-responsive genes (Gendron and Wang, 2007; Tang et al., 2011). Thus, it will be interesting whether the KAI2 interactor PP2AA2 revealed in this thesis, also regulates TFs interacting with SMAX1 and/or SMXL2.

A significant finding of this work is the importance of KL signalling in root hair development. I showed that KL signalling coordinates the root hair response to low phosphate and regulates one of the critical components for this response, the auxin carrier AUX1. However, ethylene is another regulator of root hair development under phosphate starvation and of auxin influx (Nilsson et al., 2007; Negi et al., 2008; Nilsson et al., 2012) . Previous research in our group demonstrated that SMAX1 suppresses ethylene biosynthesis in *Lotus japonicus* (Carbonnel et al. in revision). Therefore, investigating whether and how KL signalling cross-talks with ethylene in the regulation of root hair development in *Arabidopsis* will be a step towards understanding how KL signalling interacts with other hormonal signalling pathways to regulate the nutritional status of the plant.

## XI. References

- Abd-Hamid, N.-A., Ahmad-Fauzi, M.-I., Zainal, Z., and Ismail, I.** (2020). Diverse and dynamic roles of F-box proteins in plant biology. *Planta* **251**: 68.
- Abe, S., Sado, A., Tanaka, K., Kisugi, T., Asami, K., Ota, S., Kim, H.I., Yoneyama, K., Xie, X., Ohnishi, T., Seto, Y., Yamaguchi, S., Akiyama, K., Yoneyama, K., and Nomura, T.** (2014). Carlactone is converted to carlactonoic acid by MAX1 in *Arabidopsis* and its methyl ester can directly interact with AtD14 in vitro. *Proc. Natl. Acad. Sci. USA.* **111**: 18084-18089.
- Akiyama, K., and Hayashi, H.** (2006). Strigolactones: chemical signals for fungal symbionts and parasitic weeds in plant roots. *Ann Bot* **97**: 925-931.
- Al-Babili, S., and Bouwmeester, H.J.** (2015). Strigolactones, a novel carotenoid-derived plant hormone. *Annu. Rev. Plant Biol.* **66**: 161-186.
- Altmann, M., Altmann, S., Rodriguez, P.A., Weller, B., Vergara, L.E., Palme, J., Marín-de la Rosa, N., Sauer, M., Wenig, M., Villaécija-Aguilar, J.A., Sales, J., Lin, C.-W., Pandiarajan, R., Young, V., Strobel, A., Gross, L., Carbonnel, S., Kugler, K.G., Garcia-Molina, A., Bassel, G.W., Falter, C., Mayer, K.F.X., Gutjahr, C., Vlot, A.C., Grill, E., and Falter-Braun, P.** (2020). Extensive signal integration by the phytohormone protein network. *Nature* *in press*.
- Arite, T., Umehara, M., Ishikawa, S., Hanada, A., Maekawa, M., Yamaguchi, S., and Kyojuka, J.** (2009). *d14*, a strigolactone-insensitive mutant of rice, shows an accelerated outgrowth of tillers. *Plant and Cell Physiology* **50**: 1416-1424.
- Austin, R.S., Hiu, S., Waese, J., Ierullo, M., Pasha, A., Wang, T.T., Fan, J., Foong, C., Breit, R., Desveaux, D., Moses, A., and Provart, N.J.** (2016). New BAR tools for mining expression data and exploring Cis-elements in *Arabidopsis thaliana*. *The Plant journal : for cell and molecular biology* **88**: 490-504.
- Bates, T.R., and Lynch, J.P.** (1996). Stimulation of root hair elongation in *Arabidopsis thaliana* by low phosphorus availability. *Plant Cell Environ.* **19**: 529-538.
- Becker, M.G., Walker, P.L., Pulgar-Vidal, N.C., and Belmonte, M.F.** (2017). SeqEnrich: A tool to predict transcription factor networks from co-expressed *Arabidopsis* and *Brassica napus* gene sets. *PLoS One* **12**: e0178256-e0178256.
- Benfey, P.N., Bennett, M., and Schiefelbein, J.** (2010). Getting to the root of plant biology: impact of the *Arabidopsis* genome sequence on root research. *Plant J.* **61**: 992-1000.
- Bennett, T., and Scheres, B.** (2010). Root development-two meristems for the price of one? *Current topics in developmental biology* **91**: 67-102.
- Bennett, T., Hines, G., van Rongen, M., Waldie, T., Sawchuk, M.G., Scarpella, E., Ljung, K., and Leyser, O.** (2016). Connective auxin transport in the shoot facilitates communication between shoot apices. *PLoS Biol.* **14**: e1002446.
- Bernhardt, C., Lee, M.M., Gonzalez, A., Zhang, F., Lloyd, A., and Schiefelbein, J.** (2003). The bHLH genes *GLABRA3* (*GL3*) and *ENHANCER OF GLABRA3* (*EGL3*) specify epidermal cell fate in the *Arabidopsis* root. *Development* **130**: 6431-6439.
- Bhosale, R., Giri, J., Pandey, B.K., Giehl, R.F.H., Hartmann, A., Traini, R., Truskina, J., Leftley, N., Hanlon, M., Swarup, K., Rashed, A., Voß, U., Alonso, J., Stepanova, A., Yun, J., Ljung, K., Brown, K.M., Lynch, J.P., Dolan, L., Vernoux, T., Bishopp, A., Wells, D., von Wirén, N.,**

- Bennett, M.J., and Swarup, R.** (2018). A mechanistic framework for auxin dependent *Arabidopsis* root hair elongation to low external phosphate. *Nat. Commun.* **9**: 1409.
- Bleecker, A.B., and Kende, H.** (2000). Ethylene: a gaseous signal molecule in plants. *Annual review of cell and developmental biology* **16**: 1-18.
- Bouwmeester, H.J., Roux, C., Lopez-Raez, J.A., and Becard, G.** (2007). Rhizosphere communication of plants, parasitic plants and AM fungi. *Trends in plant science* **12**: 224-230.
- Brewer, P.B., Koltai, H., and Beveridge, C.A.** (2013). Diverse roles of strigolactones in plant development. *Mol. Plant* **6**: 18-28.
- Brown, L.K., George, T.S., Dupuy, L.X., and White, P.J.** (2013). A conceptual model of root hair ideotypes for future agricultural environments: what combination of traits should be targeted to cope with limited P availability? *Ann Bot* **112**: 317-330.
- Bruex, A., Kainkaryam, R.M., Wieckowski, Y., Kang, Y.H., Bernhardt, C., Xia, Y., Zheng, X., Wang, J.Y., Lee, M.M., Benfey, P., Woolf, P.J., and Schiefelbein, J.** (2012). A gene regulatory network for root epidermis cell differentiation in *Arabidopsis*. *PLoS genetics* **8**: e1002446-e1002446.
- Brumos, J., Robles, L.M., Yun, J., Vu, T.C., Jackson, S., Alonso, J.M., and Stepanova, A.N.** (2018). Local auxin biosynthesis is a key regulator of plant development. *Dev. Cell* **47**: 306-318. e305.
- Buer, C.S., Wasteneys, G.O., and Masle, J.** (2003). Ethylene modulates root-wave responses in *Arabidopsis*. *Plant Physiol.* **132**: 1085-1096.
- Bürger, M., Mashiguchi, K., Lee, H.J., Nakano, M., Takemoto, K., Seto, Y., Yamaguchi, S., and Chory, J.** (2019). Structural basis of karrikin and non-natural strigolactone perception in *Physcomitrella patens*. *Cell reports* **26**: 855-865. e855.
- Butler, L.G.** (1995). Chemical communication between the parasitic weed *Striga* and its crop host: a new dimension in allelochemistry (ACS Publications).
- Bythell-Douglas, R., Rothfels, C.J., Stevenson, D.W.D., Graham, S.W., Wong, G.K.-S., Nelson, D.C., and Bennett, T.** (2017). Evolution of strigolactone receptors by gradual neo-functionalization of KAI2 paralogues. *BMC Biol.* **15**: 52.
- Canales, J., Contreras-López, O., Álvarez, J.M., and Gutiérrez, R.A.** (2017). Nitrate induction of root hair density is mediated by TGA 1/TGA 4 and CPC transcription factors in *Arabidopsis thaliana*. *Plant J.* **92**: 305-316.
- Carbonnel S., Das D., Varshney K., Kolodziej MC., Villaécija-Aguilar JA, Gutjahr C.** (2020) The karrikin signaling regulator SMAX1 controls *Lotus japonicus* root development by suppressing ethylene biosynthesis. *PNAS*. In revision.
- Causier, B., Ashworth, M., Guo, W., and Davies, B.** (2012). The TOPLESS Interactome: A Framework for Gene Repression in *Arabidopsis*. *Plant Physiol.* **158**: 423-438.
- Chafer, C.J.** (2008). A comparison of fire severity measures: an Australian example and implications for predicting major areas of soil erosion. *Catena* **74**: 235-245.
- Charnikhova, T.V., Gaus, K., Lumbroso, A., Sanders, M., Vincken, J.-P., De Mesmaeker, A., Ruyter-Spira, C.P., Screpanti, C., and Bouwmeester, H.J.** (2018). Zeapyranolactone– A novel strigolactone from maize. *Phytochemistry Letters* **24**: 172-178.

- Chiwocha, S.D.S., Dixon, K.W., Flematti, G.R., Ghisalberti, E.L., Merritt, D.J., Nelson, D.C., Riseborough, J.-A.M., Smith, S.M., and Stevens, J.C.** (2009). Karrikins: A new family of plant growth regulators in smoke. *Plant Science* **177**: 252-256.
- Cho, U.S., and Xu, W.** (2007). Crystal structure of a protein phosphatase 2A heterotrimeric holoenzyme. *Nature* **445**: 53-57.
- Cho, Y.H., Lee, S., and Yoo, S.D.** (2018). EIN 2 and EIN 3 in Ethylene Signalling. *Annual Plant Reviews* online: 169-187.
- Choi, H.-S., and Cho, H.-T.** (2019). Root hairs enhance Arabidopsis seedling survival upon soil disruption. *Scientific Reports* **9**: 11181.
- Conn, C.E., and Nelson, D.C.** (2016). Evidence that KARRIKIN-INSENSITIVE2 (KAI2) receptors may perceive an unknown signal that is not karrikin or strigolactone. *Front. Plant Sci.* **6**: 1219.
- Conn, C.E., Bythell-Douglas, R., Neumann, D., Yoshida, S., Whittington, B., Westwood, J.H., Shirasu, K., Bond, C.S., Dyer, K.A., and Nelson, D.C.** (2015). Convergent evolution of strigolactone perception enabled host detection in parasitic plants. *Science* **349**: 540-543.
- Cook, C.E., Whichard, L.P., Wall, M., Egley, G.H., Coggon, P., Luhan, P.A., and McPhail, A.T.** (1972). Germination stimulants. II. Structure of strigol, a potent seed germination stimulant for witchweed (*Striga lutea*). *Journal of the American Chemical Society* **94**: 6198-6199.
- Dai, X., Li, J., Liu, T., and Zhao, P.X.** (2016). HRGRN: A Graph Search-Empowered Integrative Database of Arabidopsis Signaling Transduction, Metabolism and Gene Regulation Networks. *Plant Cell Physiol* **57**: e12.
- Darwin, C.** (1897). *The power of movement in plants.* (Appleton).
- de Saint Germain, A., Retailleau, P., Norsikian, S., Servajean, V., Pelissier, F., Steinmetz, V., Pillot, J.-P., Rochange, S., Pouvreau, J.-B., and Boyer, F.-D.** (2019). Contalactone, a contaminant formed during chemical synthesis of the strigolactone reference GR24 is also a strigolactone mimic. *Phytochemistry* **168**: 112112.
- De Smet, I., Tetsumura, T., De Rybel, B., dit Frey, N.F., Laplaze, L., Casimiro, I., Swarup, R., Naudts, M., Vanneste, S., and Audenaert, D.** (2007). Auxin-dependent regulation of lateral root positioning in the basal meristem of Arabidopsis. *Development* **134**: 681-690.
- Delaux, P.-M., Xie, X., Timme, R.E., Puech-Pages, V., Dunand, C., Lecompte, E., Delwiche, C.F., Yoneyama, K., Bécard, G., and Séjalon-Delmas, N.** (2012). Origin of strigolactones in the green lineage. *New Phytol.* **195**: 857-871.
- DeLong, A.** (2006). Switching the flip: protein phosphatase roles in signaling pathways. *Curr. Opin. Plant Biol.* **9**: 470-477.
- Di Cristina, M., Sessa, G., Dolan, L., Linstead, P., Baima, S., Ruberti, I., and Morelli, G.** (1996). The *Arabidopsis Athb-10* (GLABRA2) is an HD-Zip protein required for regulation of root hair development. *Plant J.* **10**: 393-402.
- Dindas, J., Scherzer, S., Roelfsema, M.R.G., von Meyer, K., Müller, H.M., Al-Rasheid, K.A.S., Palme, K., Dietrich, P., Becker, D., Bennett, M.J., and Hedrich, R.** (2018). AUX1-mediated root hair auxin influx governs SCFTIR1/AFB-type Ca<sup>2+</sup> signaling. *Nat. Commun.* **9**: 1174.
- Dixon, K., Merritt, D., Flematti, G., and Ghisalberti, E.** (2009). Karrikinolide—a phytoactive compound derived from smoke with applications in horticulture, ecological restoration and agriculture. *Acta Horticulturae* **813**: 155-170.

- Duan, J., Yu, H., Yuan, K., Liao, Z., Meng, X., Jing, Y., Liu, G., Chu, J., and Li, J.** (2019). Strigolactone promotes cytokinin degradation through transcriptional activation of CYTOKININ OXIDASE/DEHYDROGENASE 9 in rice. *Proc. Natl. Acad. Sci. USA.* **116**: 14319-14324.
- Dubrovsky, J., Soukup, A., Napsucially-Mendivil, S., Jeknić, Z., and Ivanchenko, M.** (2009). The lateral root initiation index: an integrative measure of primordium formation. *Ann Bot* **103**: 807-817.
- Dubrovsky, J.G., and Forde, B.G.** (2012). Quantitative analysis of lateral root development: pitfalls and how to avoid them. *Plant Cell* **24**: 4-14.
- Feng, Y., Xu, P., Li, B., Li, P., Wen, X., An, F., Gong, Y., Xin, Y., Zhu, Z., Wang, Y., and Guo, H.** (2017). Ethylene promotes root hair growth through coordinated EIN3/EIL1 and RHD6/RSL1 activity in *Arabidopsis*. *Proceedings of the National Academy of Sciences of the United States of America* **114**: 13834-13839.
- Fernández, C., Vega, J., and Vieira, D.** (2010). Assessing soil erosion after fire and rehabilitation treatments in NW Spain: performance of RUSLE and revised Morgan–Morgan–Finney models. *Land degradation & development* **21**: 58-67.
- Flematti, G.R., Ghisalberti, E.L., Dixon, K.W., and Trengove, R.D.** (2004). A compound from smoke that promotes seed germination. *Science* **305**: 977-977.
- Flematti, G.R., Ghisalberti, E.L., Dixon, K.W., and Trengove, R.D.** (2009). Identification of Alkyl Substituted 2H-Furo[2,3-c]pyran-2-ones as Germination Stimulants Present in Smoke. *Journal of Agricultural and Food Chemistry* **57**: 9475-9480.
- Flematti, G.R., Goddard-Borger, E.D., Merritt, D.J., Ghisalberti, E.L., Dixon, K.W., and Trengove, R.D.** (2007). Preparation of 2H-furo [2, 3-c] pyran-2-one derivatives and evaluation of their germination-promoting activity. *Journal of Agricultural and Food Chemistry* **55**: 2189-2194.
- Fukaki, H., and Tasaka, M.** (2009). Hormone interactions during lateral root formation. *Plant Mol. Biol.* **69**: 437.
- Galway, M.E., Masucci, J.D., Lloyd, A.M., Walbot, V., Davis, R.W., and Schiefelbein, J.W.** (1994). The *TTG* gene is required to specify epidermal cell fate and cell patterning in the *Arabidopsis* root. *Developmental biology* **166**: 740-754.
- Ganguly, A., Lee, S.H., Cho, M., Lee, O.R., Yoo, H., and Cho, H.-T.** (2010). Differential auxin-transporting activities of PIN-FORMED proteins in *Arabidopsis* root hair cells. *Plant Physiol.* **153**: 1046-1061.
- Garbers, C., DeLong, A., Deruere, J., Bernasconi, P., and Söll, D.** (1996). A mutation in protein phosphatase 2A regulatory subunit A affects auxin transport in *Arabidopsis*. *EMBO J.* **15**: 2115-2124.
- Gendron, J.M., and Wang, Z.-Y.** (2007). Multiple mechanisms modulate brassinosteroid signaling. *Curr. Opin. Plant Biol.* **10**: 436-441.
- Giri, J., Bhosale, R., Huang, G., Pandey, B.K., Parker, H., Zappala, S., Yang, J., Dievart, A., Bureau, C., Ljung, K., Price, A., Rose, T., Larrieu, A., Mairhofer, S., Sturrock, C.J., White, P., Dupuy, L., Hawkesford, M., Perin, C., Liang, W., Peret, B., Hodgman, C.T., Lynch, J., Wissuwa, M., Zhang, D., Pridmore, T., Mooney, S.J., Guiderdoni, E., Swarup, R., and Bennett, M.J.** (2018). Rice auxin influx carrier OsAUX1 facilitates root hair elongation in response to low external phosphate. *Nat. Commun.* **9**: 1408.

- Gomez-Roldan, V., Fermas, S., Brewer, P.B., Puech-Pagès, V., Dun, E.A., Pillot, J.-P., Letisse, F., Matusova, R., Danoun, S., Portais, J.-C., Bouwmeester, H., Bécard, G., Beveridge, C.A., Rameau, C., and Rochange, S.F.** (2008). Strigolactone inhibition of shoot branching. *Nature* **455**: 189-194.
- Grierson, C., Nielsen, E., Ketelaarc, T., and Schiefelbein, J.** (2014). Root hairs. *The Arabidopsis Book/American Society of Plant Biologists* **12**.
- Guo, H., and Ecker, J.R.** (2003). Plant responses to ethylene gas are mediated by SCFEBF1/EBF2-dependent proteolysis of EIN3 transcription factor. *Cell* **115**: 667-677.
- Guo, Y., Zheng, Z., La Clair, J.J., Chory, J., and Noel, J.P.** (2013). Smoke-derived karrikin perception by the  $\alpha/\beta$ -hydrolase KAI2 from Arabidopsis. *Proc. Natl. Acad. Sci. USA*. **20**: 8284-8289.
- Gutjahr, C., Gobbato, E., Choi, J., Riemann, M., Johnston, M.G., Summers, W., Carbonnel, S., Mansfield, C., Yang, S.-Y., Nadal, M., Acosta, I., Takano, M., Jiao, W.-B., Schneeberger, K., Kelly, K.A., and Paszowski, U.** (2015). Rice perception of symbiotic arbuscular mycorrhizal fungi requires the karrikin receptor complex. *Science* **350**: 1521-1524.
- Guyomarc'h, S., Léran, S., Auzon-Cape, M., Perrine-Walker, F., Lucas, M., and Laplaze, L.** (2012). Early development and gravitropic response of lateral roots in *Arabidopsis thaliana*. *Philosophical Transactions of the Royal Society B: Biological Sciences* **367**: 1509-1516.
- Hameed, U.S., Haider, I., Jamil, M., Kountche, B.A., Guo, X., Zarban, R.A., Kim, D., Al-Babili, S., and Arold, S.T.** (2018). Structural basis for specific inhibition of the highly sensitive ShHTL7 receptor. *EMBO reports* **19**.
- Hendrix, P., Turowski, P., Mayer-Jaekel, R., Goris, J., Hofsteenge, J., Merlevede, W., and Hemmings, B.** (1993). Analysis of subunit isoforms in protein phosphatase 2A holoenzymes from rabbit and *Xenopus*. *Journal of Biological Chemistry* **268**: 7330-7337.
- Høgh-Jensen, H., and Pedersen, M.B.** (2003). Morphological Plasticity by Crop Plants and Their Potassium Use Efficiency. *Journal of Plant Nutrition* **26**: 969-984.
- Hwang, Y., Choi, H.-S., Cho, H.-M., and Cho, H.-T.** (2017). Tracheophytes Contain Conserved Orthologs of a Basic Helix-Loop-Helix Transcription Factor That Modulate *ROOT HAIR SPECIFIC* Genes. *Plant Cell* **29**: 39-53.
- Ishida, T., Kurata, T., Okada, K., and Wada, T.** (2008). A genetic regulatory network in the development of trichomes and root hairs. *Annu. Rev. Plant Biol.* **59**: 365-386.
- Ito, S., Yamagami, D., Umehara, M., Hanada, A., Yoshida, S., Sasaki, Y., Yajima, S., Kyojuka, J., Ueguchi-Tanaka, M., Matsuoka, M., Shirasu, K., Yamaguchi, S., and Asami, T.** (2017). Regulation of Strigolactone Biosynthesis by Gibberellin Signaling. *Plant Physiol.* **174**: 1250-1259.
- Ivanchenko, M.G., Muday, G.K., and Dubrovsky, J.G.** (2008). Ethylene–auxin interactions regulate lateral root initiation and emergence in *Arabidopsis thaliana*. *Plant J.* **55**: 335-347.
- Janssens, V., and Goris, J.** (2001). Protein phosphatase 2A: a highly regulated family of serine/threonine phosphatases implicated in cell growth and signalling. *The Biochemical journal* **353**: 417-439.
- Jayaram, N., Usvyat, D., and Martin, A.C.** (2016). Evaluating tools for transcription factor binding site prediction. *BMC bioinformatics*: 1.

- Jia, K.-P., Baz, L., and Al-Babili, S.** (2017). From carotenoids to strigolactones. *J. Exp. Bot.* **69**: 2189-2204.
- Jiang, L., Matthys, C., Marquez-Garcia, B., De Cuyper, C., Smet, L., De Keyser, A., Boyer, F.-D., Beeckman, T., Depuydt, S., and Goormachtig, S.** (2015). Strigolactones spatially influence lateral root development through the cytokinin signaling network. *J. Exp. Bot.* **67**: 379-389.
- Jiang, L., Liu, X., Xiong, G., Liu, H., Chen, F., Wang, L., Meng, X., Liu, G., Yu, H., Yuan, Y., Yi, W., Zhao, L., Ma, H., He, Y., Wu, Z., Melcher, K., Qian, Q., Xu, H.E., Wang, Y., and Li, J.** (2013). DWARF 53 acts as a repressor of strigolactone signalling in rice. *Nature* **504**: 401.
- Jones, A.R., Kramer, E.M., Knox, K., Swarup, R., Bennett, M.J., Lazarus, C.M., Leyser, H.M.O., and Grierson, C.S.** (2009). Auxin transport through non-hair cells sustains root-hair development. *Nat. Cell Biol.* **11**: 78-84.
- Kagale, S., and Rozwadowski, K.** (2011). EAR motif-mediated transcriptional repression in plants: an underlying mechanism for epigenetic regulation of gene expression. *Epigenetics* **6**: 141-146.
- Kagiyama, M., Hirano, Y., Mori, T., Kim, S.Y., Kyojuka, J., Seto, Y., Yamaguchi, S., and Hakoshima, T.** (2013). Structures of D 14 and D 14 L in the strigolactone and karrikin signaling pathways. *Genes to Cells* **18**: 147-160.
- Kapulnik, Y., Resnick, N., Mayzlish-Gati, E., Kaplan, Y., Wininger, S., Hershenhorn, J., and Koltai, H.** (2011a). Strigolactones interact with ethylene and auxin in regulating root-hair elongation in *Arabidopsis*. *J. Exp. Bot.* **62**: 2915-2924.
- Kapulnik, Y., Delaux, P.-M., Resnick, N., Mayzlish-Gati, E., Wininger, S., Bhattacharya, C., Séjalon-Delmas, N., Combiér, J.-P., Bécard, G., Belausov, E., Beeckman, T., Dor, E., Hershenhorn, J., and Koltai, H.** (2011b). Strigolactones affect lateral root formation and root-hair elongation in *Arabidopsis*. *Planta* **233**: 209-216.
- Khosla, A., Morffy, N., Li, Q., Faure, L., Chang, S.H., Yao, J., Zheng, J., Cai, M.L., Stanga, J.P., Flematti, G.R., Waters, M., and Nelson, D.C.** (2020). Structure-Function Analysis of SMAX1 Reveals Domains that Mediate its Karrikin-Induced Proteolysis and Interaction with the Receptor KAI2. *Plant Cell*: tpc.00752.02019.
- Kim, D.W., Lee, S.H., Choi, S.B., Won, S.K., Heo, Y.K., Cho, M., Park, Y.I., and Cho, H.T.** (2006). Functional conservation of a root hair cell-specific cis-element in angiosperms with different root hair distribution patterns. *Plant Cell* **18**: 2958-2970.
- Kim, T.-W., Guan, S., Sun, Y., Deng, Z., Tang, W., Shang, J.-X., Sun, Y., Burlingame, A.L., and Wang, Z.-Y.** (2009). Brassinosteroid signal transduction from cell-surface receptor kinases to nuclear transcription factors. *Nat. Cell Biol.* **11**: 1254-1260.
- Klinsawang, S., Sumranwanich, T., Wannaro, A., and Saengwilai, P.** (2018). Effects of root hair length on potassium acquisition in rice (*Oryza sativa* L.). *APPLIED ECOLOGY AND ENVIRONMENTAL RESEARCH* **16**: 1609-1620.
- Kohlen, W., Charnikhova, T., Liu, Q., Bours, R., Domagalska, M.A., Beguerie, S., Verstappen, F., Leyser, O., Bouwmeester, H., and Ruyter-Spira, C.** (2011). Strigolactones are transported through the xylem and play a key role in shoot architectural response to phosphate deficiency in nonarbuscular mycorrhizal host *Arabidopsis*. *Plant Physiol.* **155**: 974-987.
- Koltai, H., and Beveridge, C.A.** (2013). Strigolactones and the coordinated development of shoot and root. In *Long-Distance Systemic Signaling and Communication in Plants* (Springer), pp. 189-204.

- Koltai, H., Dor, E., Hershenhorn, J., Joel, D.M., Weininger, S., Lekalla, S., Shealtiel, H., Bhattacharya, C., Eliahu, E., Resnick, N., Barg, R., and Kapulnik, Y.** (2010). Strigolactones' effect on root growth and root-hair elongation may be mediated by auxin-efflux carriers. *J. Plant Growth Regul.* **29**: 129-136.
- Kutiel, P., and Inbar, M.** (1993). Fire impacts on soil nutrients and soil erosion in a Mediterranean pine forest plantation. *Catena* **20**: 129-139.
- Lee, M.M., and Schiefelbein, J.** (1999). WEREWOLF, a MYB-related protein in Arabidopsis, is a position-dependent regulator of epidermal cell patterning. *Cell* **99**: 473-483.
- Li, J., Dai, X., and Zhao, Y.** (2006). A Role for Auxin Response Factor 19 in Auxin and Ethylene Signaling in Arabidopsis. *Plant Physiol.* **140**: 899-908.
- Li, W., Nguyen, K.H., Chu, H.D., Ha, C.V., Watanabe, Y., Osakabe, Y., Leyva-González, M.A., Sato, M., Toyooka, K., Voges, L., Tanaka, M., Mostofa, M.G., Seki, M., Seo, M., Yamaguchi, S., Nelson, D.C., Tian, C., Herrera-Estrella, L., and Tran, L.-S.P.** (2017). The karrikin receptor KAI2 promotes drought resistance in *Arabidopsis thaliana*. *PLOS Genetics* **13**: e1007076.
- Li, Y., Wang, Y., Tan, S., Li, Z., Yuan, Z., Glanc, M., Domjan, D., Wang, K., Xuan, W., Guo, Y., Gong, Z., Friml, J., and Zhang, J.** (2020). Root Growth Adaptation is Mediated by PYLs ABA Receptor-PP2A Protein Phosphatase Complex. *Advanced Science* **7**: 1901455.
- Liang, Y., Ward, S., Li, P., Bennett, T., and Leyser, O.** (2016). SMAX1-LIKE7 signals from the nucleus to regulate shoot development in Arabidopsis via partially EAR motif-independent mechanisms. *Plant Cell* **28**: 1581-1601.
- Liu, G., Stirnemann, M., Gübeli, C., Egloff, S., Courty, P.-E., Aubry, S., Vandenbussche, M., Morel, P., Reinhardt, D., Martinoia, E., and Borghi, L.** (2019). Strigolactones Play an Important Role in Shaping Exodermal Morphology via a KAI2-Dependent Pathway. *iScience* **17**: 144-154.
- Liu, Y., Xie, Y., Wang, H., Ma, X., Yao, W., and Wang, H.** (2017). Light and Ethylene Coordinately Regulate the Phosphate Starvation Response through Transcriptional Regulation of *PHOSPHATE STARVATION RESPONSE1*. *Plant Cell* **29**: 2269-2284.
- López-Bucio, J., Hernández-Abreu, E., Sánchez-Calderón, L., Nieto-Jacobo, M.a.F., Simpson, J., and Herrera-Estrella, L.** (2002). Phosphate Availability Alters Architecture and Causes Changes in Hormone Sensitivity in the Arabidopsis Root System. *Plant Physiol.* **129**: 244-256.
- Ma, H., Duan, J., Ke, J., He, Y., Gu, X., Xu, T.-H., Yu, H., Wang, Y., Brunzelle, J.S., Jiang, Y., Rothbart, S.B., Xu, H.E., Li, J., and Melcher, K.** (2017). A D53 repression motif induces oligomerization of TOPLESS corepressors and promotes assembly of a corepressor-nucleosome complex. *Science Advances* **3**: e1601217.
- Ma, Q., Grones, P., and Robert, S.** (2018). Auxin signaling: a big question to be addressed by small molecules. *J Exp Bot* **69**: 313-328.
- MacDonald, L.H., and Huffman, E.L.** (2004). Post-fire soil water repellency. *Soil Science Society of America Journal* **68**: 1729-1734.
- Machin, D.C., Hamon-Josse, M., and Bennett, T.** (2020). Fellowship of the rings: a saga of strigolactones and other small signals. *New Phytol.* **225**: 621-636.
- Mangano, S., Denita-Juarez, S.P., Marzol, E., Borassi, C., and Estevez, J.M.** (2018). High Auxin and High Phosphate Impact on RSL2 Expression and ROS-Homeostasis Linked to Root Hair Growth in *Arabidopsis thaliana*. *Front. Plant Sci.* **9**: 1164-1164.

- Masson, P.H., Tasaka, M., Morita, M.T., Guan, C., Chen, R., and Boonsirichai, K.** (2002). *Arabidopsis thaliana*: A Model for the Study of Root and Shoot Gravitropism. *Arabidopsis Book* **1**: e0043-e0043.
- Masucci, J.D., and Schiefelbein, J.W.** (1994). The *rh6* mutation of *Arabidopsis thaliana* alters root-hair initiation through an auxin- and ethylene-associated process. *Plant Physiol.* **106**: 1335-1346.
- Masucci, J.D., and Schiefelbein, J.W.** (1996). Hormones act downstream of TTG and GL2 to promote root hair outgrowth during epidermis development in the *Arabidopsis* root. *Plant Cell* **8**: 1505-1517.
- Matusova, R., Rani, K., Verstappen, F.W., Franssen, M.C., Beale, M.H., and Bouwmeester, H.J.** (2005). The strigolactone germination stimulants of the plant-parasitic *Striga* and *Orobanch* spp. are derived from the carotenoid pathway. *Plant Physiol.* **139**: 920-934.
- Mayzlish-Gati, E., De-Cuyper, C., Goormachtig, S., Beeckman, T., Vuylsteke, M., Brewer, P.B., Beveridge, C.A., Yermiyahu, U., Kaplan, Y., Enzer, Y., Wininger, S., Resnick, N., Cohen, M., Kapulnik, Y., and Koltai, H.** (2012). Strigolactones are involved in root response to low phosphate conditions in *Arabidopsis*. *Plant Physiol* **160**: 1329-1341.
- Mele, G.** (2016). *Arabidopsis* Motif Scanner. *BMC Bioinformatics* **17**: 50.
- Menand, B., Yi, K., Jouannic, S., Hoffmann, L., Ryan, E., Linstead, P., Schaefer, D.G., and Dolan, L.** (2007). An ancient mechanism controls the development of cells with a rooting function in land plants. *Science* **316**: 1477-1480.
- Michniewicz, M., Zago, M.K., Abas, L., Weijers, D., Schweighofer, A., Meskiene, I., Heisler, M.G., Ohno, C., Zhang, J., and Huang, F.** (2007). Antagonistic regulation of PIN phosphorylation by PP2A and PINOID directs auxin flux. *Cell* **130**: 1044-1056.
- Millar, K.D., Johnson, C.M., Edelmann, R.E., and Kiss, J.Z.** (2011). An endogenous growth pattern of roots is revealed in seedlings grown in microgravity. *Astrobiology* **11**: 787-797.
- Millward, T.A., Zolnierowicz, S., and Hemmings, B.A.** (1999). Regulation of protein kinase cascades by protein phosphatase 2A. *Trends in biochemical sciences* **24**: 186-191.
- Moreno-Risueno, M.A., Van Norman, J.M., Moreno, A., Zhang, J., Ahnert, S.E., and Benfey, P.N.** (2010). Oscillating gene expression determines competence for periodic *Arabidopsis* root branching. *Science* **329**: 1306-1311.
- Morffy, N., Faure, L., and Nelson, D.C.** (2016). Smoke and Hormone Mirrors: Action and Evolution of Karrikin and Strigolactone Signaling. *Trends in genetics : TIG* **32**: 176-188.
- Moturu, T.R., Thula, S., Singh, R.K., Nodzyński, T., Vařeková, R.S., Friml, J., and Simon, S.** (2018). Molecular evolution and diversification of the SMXL gene family. *J. Exp. Bot.* **69**: 2367-2378.
- Nakamura, H., Xue, Y.-L., Miyakawa, T., Hou, F., Qin, H.-M., Fukui, K., Shi, X., Ito, E., Ito, S., Park, S.-H., Miyauchi, Y., Asano, A., Totsuka, N., Ueda, T., Tanokura, M., and Asami, T.** (2013). Molecular mechanism of strigolactone perception by DWARF14. *Nat. Commun.* **4**: 2613.
- Negi, S., Ivanchenko, M.G., and Muday, G.K.** (2008). Ethylene regulates lateral root formation and auxin transport in *Arabidopsis thaliana*. *Plant J.* **55**: 175-187.

- Nelson, D.C., Flematti, G.R., Riseborough, J.-A., Ghisalberti, E.L., Dixon, K.W., and Smith, S.M.** (2010). Karrikins enhance light responses during germination and seedling development in *Arabidopsis thaliana*. *Proc. Natl. Acad. Sci. USA*. **107**: 7095-7100.
- Nelson, D.C., Riseborough, J.-A., Flematti, G.R., Stevens, J., Ghisalberti, E.L., Dixon, K.W., and Smith, S.M.** (2009). Karrikins discovered in smoke trigger *Arabidopsis* seed germination by a mechanism requiring gibberellic acid synthesis and light. *Plant Physiol*. **149**: 863-873.
- Nelson, D.C., Scaffidi, A., Dun, E.A., Waters, M.T., Flematti, G.R., Dixon, K.W., Beveridge, C.A., Ghisalberti, E.L., and Smith, S.M.** (2011). F-box protein MAX2 has dual roles in karrikin and strigolactone signaling in *Arabidopsis thaliana*. *Proc. Natl. Acad. Sci. USA*. **108**: 8897-8902.
- Nilsson, L., Müller, R., and Nielsen, T.H.** (2007). Increased expression of the MYB-related transcription factor, *PHR1*, leads to enhanced phosphate uptake in *Arabidopsis thaliana*. *Plant Cell Environ*. **30**: 1499-1512.
- Nilsson, L., Müller, R., and Nielsen, T.H.** (2007). Increased expression of the MYB-related transcription factor, *PHR1*, leads to enhanced phosphate uptake in *Arabidopsis thaliana*. *Plant Cell Environ*. **30**: 1499-1512.
- Nilsson, L., Lundmark, M., Jensen, P.E., and Nielsen, T.H.** (2012). The *Arabidopsis* transcription factor *PHR1* is essential for adaptation to high light and retaining functional photosynthesis during phosphate starvation. *Physiol. Plant*. **144**: 35-47.
- Obando, M.L., Conn, C.E., Hoffmann, B., Bythell-Douglas, R., Nelson, D.C., Rameau, C., and Bonhomme, S.** (2016). Structural modelling and transcriptional responses highlight a clade of PpKAI2-LIKE genes as candidate receptors for strigolactones in *Physcomitrella patens*.
- Okada, K., and Shimura, Y.** (1990). Reversible root tip rotation in *Arabidopsis* seedlings induced by obstacle-touching stimulus. *Science* **250**: 274-276.
- Okushima, Y., Fukaki, H., Onoda, M., Theologis, A., and Tasaka, M.** (2007). ARF19 regulate lateral root formation via direct activation of LBD/ASL genes in *Arabidopsis*. *Plant Cell* **19**: 118.
- Omoarelojie, L., Kulkarni, M., Finnie, J., and Van Staden, J.** (2019). Strigolactones and their crosstalk with other phytohormones. *Ann Bot* **124**: 749-767.
- Pandya-Kumar, N., Shema, R., Kumar, M., Mayzlish-Gati, E., Levy, D., Zemach, H., Belausov, E., Winer, S., Abu-Abied, M., Kapulnik, Y., and Koltai, H.** (2014). Strigolactone analog GR24 triggers changes in PIN2 polarity, vesicle trafficking and actin filament architecture. *New Phytol*. **202**: 1184-1196.
- Pauwels, L., Barbero, G.F., Geerinck, J., Tilleman, S., Grunewald, W., Pérez, A.C., Chico, J.M., Bossche, R.V., Sewell, J., Gil, E., García-Casado, G., Witters, E., Inzé, D., Long, J.A., De Jaeger, G., Solano, R., and Goossens, A.** (2010). NINJA connects the co-repressor TOPLESS to jasmonate signalling. *Nature* **464**: 788-791.
- Péret, B., Swarup, K., Ferguson, A., Seth, M., Yang, Y., Dhondt, S., James, N., Casimiro, I., Perry, P., Syed, A., Yang, H., Reemmer, J., Venison, E., Howells, C., Perez-Amador, M.A., Yun, J., Alonso, J., Beemster, G.T.S., Laplaze, L., Murphy, A., Bennett, M.J., Nielsen, E., and Swarup, R.** (2012). AUX/LAX genes encode a family of auxin influx transporters that perform distinct function during *Arabidopsis* development. *Plant Cell* **24**: 2874.
- Petrášek, J., and Friml, J.** (2009). Auxin transport routes in plant development. *Development* **136**: 2675-2688.

- Pitts, R.J., Cernac, A., and Estelle, M.** (1998). Auxin and ethylene promote root hair elongation in *Arabidopsis*. *Plant J.* **16**: 553-560.
- Prats, S.A., Wagenbrenner, J.W., Martins, M.A.S., Malvar, M.C., and Keizer, J.J.** (2016). Mid-term and scaling effects of forest residue mulching on post-fire runoff and soil erosion. *Science of the Total Environment* **573**: 1242-1254.
- Proust, H., Hoffmann, B., Xie, X., Yoneyama, K., Schaefer, D.G., Yoneyama, K., Nogué, F., and Rameau, C.** (2011). Strigolactones regulate protonema branching and act as a quorum sensing-like signal in the moss *Physcomitrella patens*. *Development* **138**: 1531-1539.
- Qi, B., and Zheng, H.** (2013). Modulation of root-skewing responses by *KNAT1* in *Arabidopsis thaliana*. *Plant J.* **76**: 380-392.
- Rhee, S.Y., Beavis, W., Berardini, T.Z., Chen, G., Dixon, D., Doyle, A., Garcia-Hernandez, M., Huala, E., Lander, G., Montoya, M., Miller, N., Mueller, L.A., Mundodi, S., Reiser, L., Tacklind, J., Weems, D.C., Wu, Y., Xu, I., Yoo, D., Yoon, J., and Zhang, P.** (2003). The Arabidopsis Information Resource (TAIR): a model organism database providing a centralized, curated gateway to Arabidopsis biology, research materials and community. *Nucleic acids research* **31**: 224-228.
- Robbins, N.E., and Dinneny, J.R.** (2015). The divining root: moisture-driven responses of roots at the micro-and macro-scale. *J. Exp. Bot.* **66**: 2145-2154.
- Roche, S., Koch, J.M., and Dixon, K.W.** (1997). Smoke enhanced seed germination for mine rehabilitation in the southwest of Western Australia. *Restoration Ecology* **5**: 191-203.
- Roche, S., Dixon, K.W., and Pate, J.S.** (1998). For everything a season: smoke-induced seed germination and seedling recruitment in a Western Australian *Banksia* woodland. *Australian Journal of Ecology* **23**: 111-120.
- Roman, G., Lubarsky, B., Kieber, J.J., Rothenberg, M., and Ecker, J.R.** (1995). Genetic analysis of ethylene signal transduction in *Arabidopsis thaliana*: five novel mutant loci integrated into a stress response pathway. *Genetics* **139**: 1393-1409.
- Roy, R., and Bassham, D.C.** (2014). Root growth movements: waving and skewing. *Plant Science* **221**: 42-47.
- Ruyter-Spira, C., Kohlen, W., Charnikhova, T., van Zeijl, A., van Bezouwen, L., de Ruijter, N., Cardoso, C., Lopez-Raez, J.A., Matusova, R., Bours, R., Verstappen, F., and Bouwmeester, H.** (2011). Physiological effects of the synthetic strigolactone analog GR24 on root system architecture in *Arabidopsis*: another below-ground role for strigolactones? *Plant Physiol.* **155**: 721-734.
- Růžička, K., Ljung, K., Vanneste, S., Podhorská, R., Beeckman, T., Friml, J., and Benková, E.** (2007). Ethylene Regulates Root Growth through Effects on Auxin Biosynthesis and Transport-Dependent Auxin Distribution. *Plant Cell* **19**: 2197-2212.
- Saeed, W., Naseem, S., and Ali, Z.** (2017). Strigolactones Biosynthesis and Their Role in Abiotic Stress Resilience in Plants: A Critical Review. *Front. Plant Sci.* **8**: 1487-1487.
- Salazar-Henao, J.E., Vélez-Bermúdez, I.C., and Schmidt, W.** (2016). The regulation and plasticity of root hair patterning and morphogenesis. *Development* **143**: 1848-1858.
- Scaffidi, A., Waters, M., Sun, Y.K., Skelton, B.W., Dixon, K.W., Ghisalberti, E.L., Flematti, G., and Smith, S.** (2014). Strigolactone hormones and their stereoisomers signal through two related

- receptor proteins to induce different physiological responses in *Arabidopsis*. *Plant Physiol.* **165**: 1221-1232.
- Schellmann, S., Schnittger, A., Kirik, V., Wada, T., Okada, K., Beermann, A., Thumfahrt, J., Jürgens, G., and Hülskamp, M.** (2002). *TRIPTYCHON* and *CAPRICE* mediate lateral inhibition during trichome and root hair patterning in *Arabidopsis*. *EMBO J.* **21**: 5036-5046.
- Scheres, B., and Wolkenfelt, H.** (1998). The *Arabidopsis* root as a model to study plant development. *Plant Physiol. Biochem.* **36**: 21-32.
- Seto, Y., Yasui, R., Kameoka, H., Tamiru, M., Cao, M., Terauchi, R., Sakurada, A., Hirano, R., Kisugi, T., Hanada, A., Umehara, M., Seo, E., Akiyama, K., Burke, J., Noriko, T.-K., Li, W., Hirano, Y., Hakoshima, T., Mashiguchi, K., Noel, J.P., Kyojuka, J., and Yamaguchi, S.** (2019). Strigolactone perception and deactivation by a hydrolase receptor DWARF14. *Nat. Commun.* **10**: 191.
- Shakesby, R.** (2011). Post-wildfire soil erosion in the Mediterranean: review and future research directions. *Earth-Science Reviews* **105**: 71-100.
- Shakesby, R.A., Coelho, C., Ferreira, A.D., Terry, J.P., and Walsh, R.P.** (1993). Wildfire impacts on soil-erosion and hydrology in wet Mediterranean forest, Portugal. *International Journal of Wildland Fire* **3**: 95-110.
- Shinohara, N., Taylor, C., and Leyser, O.** (2013). Strigolactone can promote or inhibit shoot branching by triggering rapid depletion of the auxin efflux protein PIN1 from the plasma membrane. *PLoS Biol.* **11**: e1001474.
- Siame, B.A., Weerasuriya, Y., Wood, K., Ejeta, G., and Butler, L.G.** (1993). Isolation of strigol, a germination stimulant for *Striga asiatica*, from host plants. *Journal of Agricultural and Food Chemistry* **41**: 1486-1491.
- Simon, M., Lee, M.M., Lin, Y., Gish, L., and Schiefelbein, J.** (2007). Distinct and overlapping roles of single-repeat MYB genes in root epidermal patterning. *Developmental biology* **311**: 566-578.
- Skottke, K.R., Yoon, G.M., Kieber, J.J., and DeLong, A.** (2011). Protein phosphatase 2A controls ethylene biosynthesis by differentially regulating the turnover of ACC synthase isoforms. *PLoS Genetics* **7**.
- Smith, S., and De Smet, I.** (2012). Root system architecture: insights from *Arabidopsis* and cereal crops. *Philos Trans R Soc Lond B Biol Sci* **367**: 1441-1452.
- Soeno, K., Goda, H., Ishii, T., Ogura, T., Tachikawa, T., Sasaki, E., Yoshida, S., Fujioka, S., Asami, T., and Shimada, Y.** (2010). Auxin biosynthesis inhibitors, identified by a genomics-based approach, provide insights into auxin biosynthesis. *Plant and Cell Physiology* **51**: 524-536.
- Song, L., Yu, H., Dong, J., Che, X., Jiao, Y., and Liu, D.** (2016). The Molecular Mechanism of Ethylene-Mediated Root Hair Development Induced by Phosphate Starvation. *PLoS genetics* **12**: e1006194-e1006194.
- Soundappan, I., Bennett, T., Morffy, N., Liang, Y., Stanga, J.P., Abbas, A., Leyser, O., and Nelson, D.C.** (2015). SMAX1-LIKE/D53 family members enable distinct MAX2-dependent responses to strigolactones and karrikins in *Arabidopsis*. *Plant Cell* **27**: 3143-3159.
- Staden, J.V., Brown, N.A., Jäger, A.K., and Johnson, T.A.** (2000). Smoke as a germination cue. *Plant Species Biology* **15**: 167-178.
- Stanga, J.P., Morffy, N., and Nelson, D.C.** (2016). Functional redundancy in the control of seedling growth by the karrikin signaling pathway. *Planta* **243**: 1397-1406.

- Stanga, J.P., Smith, S.M., Briggs, W.R., and Nelson, D.C.** (2013). *SUPPRESSOR OF MAX2 1* controls seed germination and seedling development in *Arabidopsis thaliana*. *Plant Physiol.* **163**: 318-330.
- Stepanova, A.N., Yun, J., Likhacheva, A.V., and Alonso, J.M.** (2007). Multilevel interactions between ethylene and auxin in *Arabidopsis* roots. *Plant Cell* **19**: 2169-2185.
- Strack, S., Zaucha, J.A., Ebner, F.F., Colbran, R.J., and Wadzinski, B.E.** (1998). Brain protein phosphatase 2A: developmental regulation and distinct cellular and subcellular localization by B subunits. *Journal of Comparative Neurology* **392**: 515-527.
- Sun, C.-H., Yu, J.-Q., and Hu, D.-G.** (2017). Nitrate: a crucial signal during lateral roots development. *Front. Plant Sci.* **8**: 485.
- Sun, K., Chen, Y., Wagerle, T., Linnstaedt, D., Currie, M., Chmura, P., Song, Y., and Xu, M.** (2008). Synthesis of butenolides as seed germination stimulants. *Tetrahedron Letters* **49**: 2922-2925.
- Swarbreck, S.M., Guerringue, Y., Matthus, E., Jamieson, F.J.C., and Davies, J.M.** (2019). Impairment in karrikin but not strigolactone sensing enhances root skewing in *Arabidopsis thaliana*. *Plant J.*
- Swarup, R., Kramer, E.M., Perry, P., Knox, K., Leyser, H.M., Haseloff, J., Beemster, G.T., Bhalerao, R., and Bennett, M.J.** (2005). Root gravitropism requires lateral root cap and epidermal cells for transport and response to a mobile auxin signal. *Nat Cell Biol* **7**: 1057-1065.
- Szemenyei, H., Hannon, M., and Long, J.A.** (2008). TOPLESS mediates auxin-dependent transcriptional repression during *Arabidopsis* embryogenesis. *Science* **319**: 1384-1386.
- Tang, W., Deng, Z., and Wang, Z.-Y.** (2010). Proteomics shed light on the brassinosteroid signaling mechanisms. *Curr. Opin. Plant Biol.* **13**: 27-33.
- Tang, W., Yuan, M., Wang, R., Yang, Y., Wang, C., Oses-Prieto, J.A., Kim, T.-W., Zhou, H.-W., Deng, Z., Gampala, S.S., Gendron, J.M., Jonassen, E.M., Lillo, C., DeLong, A., Burlingame, A.L., Sun, Y., and Wang, Z.-Y.** (2011). PP2A activates brassinosteroid-responsive gene expression and plant growth by dephosphorylating BZR1. *Nat. Cell Biol.* **13**: 124-131.
- Tessler, N., Wittenberg, L., Malkinson, D., and Greenbaum, N.** (2008). Fire effects and short-term changes in soil water repellency—Mt. Carmel, Israel. *Catena* **74**: 185-191.
- Tian, H., De Smet, I., and Ding, Z.** (2014). Shaping a root system: regulating lateral versus primary root growth. *Trends in Plant Science* **19**: 426-431.
- Tian, Q., Nagpal, P., and Reed, J.W.** (2003). Regulation of *Arabidopsis* SHY2/IAA3 protein turnover. *Plant J.* **36**: 643-651.
- Toh, S., Holbrook-Smith, D., Stokes, Michael E., Tsuchiya, Y., and McCourt, P.** (2014). Detection of parasitic plant suicide germination compounds using a high-throughput *Arabidopsis* HTL/KAI2 strigolactone perception system. *Chemistry & Biology* **21**: 988-998.
- Tsuchiya, Y., Yoshimura, M., Sato, Y., Kuwata, K., Toh, S., Holbrook-Smith, D., Zhang, H., McCourt, P., Itami, K., Kinoshita, T., and Hagihara, S.** (2015). Probing strigolactone receptors in *Striga hermonthica* with fluorescence. *Science* **349**: 864-868.
- Ueno, K., Nomura, S., Muranaka, S., Mizutani, M., Takikawa, H., and Sugimoto, Y.** (2011). *Ent-2'-epi-Orobanchol* and its acetate, as germination stimulants for *Striga gesnerioides* seeds isolated from cowpea and red clover. *Journal of agricultural and food chemistry* **59**: 10485-10490.

- Ueno, K., Furumoto, T., Umeda, S., Mizutani, M., Takikawa, H., Batchvarova, R., and Sugimoto, Y.** (2014). Helioactone, a non-sesquiterpene lactone germination stimulant for root parasitic weeds from sunflower. *Phytochemistry* **108**: 122-128.
- Umehara, M., Hanada, A., Yoshida, S., Akiyama, K., Arite, T., Takeda-Kamiya, N., Magome, H., Kamiya, Y., Shirasu, K., and Yoneyama, K.** (2008). Inhibition of shoot branching by new terpenoid plant hormones. *Nature* **455**: 195.
- van Rongen, M., Bennett, T., Ticchiarelli, F., and Leyser, O.** (2019). Connective auxin transport contributes to strigolactone-mediated shoot branching control independent of the transcription factor *BRC1*. *PLOS Genetics* **15**: e1008023.
- Vanstraelen, M., and Benková, E.** (2012). Hormonal interactions in the regulation of plant development. *Annual review of cell and developmental biology* **28**: 463-487.
- Vaughn, L.M., and Masson, P.H.** (2011). A QTL study for regions contributing to *Arabidopsis thaliana* root skewing on tilted surfaces. *G3: Genes, Genomes, Genetics* **1**: 105-115.
- Velasquez, S.M., Barbez, E., Kleine-Vehn, J., and Estevez, J.M.** (2016). Auxin and Cellular Elongation. *Plant Physiol.* **170**: 1206-1215.
- Villaécija-Aguilar, J.A., Hamon-Josse, M., Carbonnel, S., Kretschmar, A., Schmidt, C., Dawid, C., Bennett, T., and Gutjahr, C.** (2019). SMAX1/SMXL2 regulate root and root hair development downstream of KAI2-mediated signalling in Arabidopsis. *PLOS Genetics* **15**: e1008327.
- Wada, T., Tachibana, T., Shimura, Y., and Okada, K.** (1997). Epidermal cell differentiation in Arabidopsis determined by a Myb homolog, CPC. *Science* **277**: 1113-1116.
- Wallner, E.S., López-Salmerón, V., Belevich, I., Poschet, G., Jung, I., Grünwald, K., Sevillem, I., Jokitalo, E., Hell, R., Helariutta, Y., Agustí, J., Lebovka, I., and Greb, T.** (2017). Strigolactone- and Karrikin-Independent SMXL Proteins Are Central Regulators of Phloem Formation. *Current biology* : CB **27**: 1241-1247.
- Wang, K.L.-C., Li, H., and Ecker, J.R.** (2002). Ethylene biosynthesis and signaling networks. *Plant Cell* **14**: S131-S151.
- Wang, L., Waters, M.T., and Smith, S.M.** (2018). Karrikin-KAI2 signalling provides Arabidopsis seeds with tolerance to abiotic stress and inhibits germination under conditions unfavourable to seedling establishment. *New Phytol.* **219**: 605-618.
- Wang, L., Wang, B., Jiang, L., Liu, X., Li, X., Lu, Z., Meng, X., Wang, Y., Smith, S.M., and Li, J.** (2015). Strigolactone signaling in Arabidopsis regulates shoot development by targeting D53-like SMXL repressor proteins for ubiquitination and degradation. *Plant Cell* **27**: 3128-3142.
- Wang, L., Xu, Q., Yu, H., Ma, H., Li, X., Yang, J., Chu, J., Xie, Q., Wang, Y., Smith, S.M., Li, J., Xiong, G., and Wang, B.** (2020). Strigolactone and Karrikin Signaling Pathways Elicit Ubiquitination and Proteolysis of SMXL2 to Regulate Hypocotyl Elongation in Arabidopsis thaliana. *Plant Cell*: tpc.00140.02020.
- Waters, M.T., Scaffidi, A., Flematti, G.R., and Smith, S.M.** (2013). The origins and mechanisms of karrikin signalling. *Curr Opin Plant Biol* **16**: 667-673.
- Waters, M.T., Scaffidi, A., Flematti, G., and Smith, S.M.** (2015). Substrate-induced degradation of the  $\alpha/\beta$ -fold hydrolase KARRIKIN INSENSITIVE2 requires a functional catalytic triad but is independent of MAX2. *Mol. Plant* **8**: 814-817.

- Waters, M.T., Gutjahr, C., Bennett, T., and Nelson, D.C.** (2017). Strigolactone signaling and evolution. *Annu. Rev. Plant Biol.* **68**: 291-322.
- Waters, M.T., Brewer, P.B., Bussell, J.D., Smith, S.M., and Beveridge, C.A.** (2012a). The Arabidopsis ortholog of rice DWARF27 acts upstream of MAX1 in control of plant development by strigolactones. *Plant Physiol.* **159**: 1073-1085.
- Waters, M.T., Nelson, D.C., Scaffidi, A., Flematti, G.R., Sun, Y.K., Dixon, K.W., and Smith, S.M.** (2012b). Specialisation within the DWARF14 protein family confers distinct responses to karrikins and strigolactones in Arabidopsis. *Development* **139**: 1285-1295.
- Williamson, L.C., Ribrioux, S.P.C.P., Fitter, A.H., and Leyser, H.M.O.** (2001). Phosphate Availability Regulates Root System Architecture in Arabidopsis. *Plant Physiol.* **126**: 875-882.
- Won, S.-K., Lee, Y.-J., Lee, H.-Y., Heo, Y.-K., Cho, M., and Cho, H.-T.** (2009). cis-Element- and Transcriptome-Based Screening of Root Hair-Specific Genes and Their Functional Characterization in Arabidopsis. *Plant Physiol.* **150**: 1459-1473.
- Xie, X., Yoneyama, K., and Yoneyama, K.** (2010). The strigolactone story. *Annu. Rev. Phytopathol.* **48**: 93-117.
- Xie, X., Yoneyama, K., Kisugi, T., Uchida, K., Ito, S., Akiyama, K., Hayashi, H., Yokota, T., Nomura, T., and Yoneyama, K.** (2013). Confirming Stereochemical Structures of Strigolactones Produced by Rice and Tobacco. *Mol. Plant* **6**: 153-163.
- Xu, Y., Miyakawa, T., Nakamura, H., Nakamura, A., Imamura, Y., Asami, T., and Tanokura, M.** (2016). Structural basis of unique ligand specificity of KAI2-like protein from parasitic weed *Striga hermonthica*. *Scientific reports* **6**: 31386.
- Xu, Y., Miyakawa, T., Nosaki, S., Nakamura, A., Lyu, Y., Nakamura, H., Ohto, U., Ishida, H., Shimizu, T., and Asami, T.** (2018). Structural analysis of HTL and D14 proteins reveals the basis for ligand selectivity in *Striga*. *Nat. Commun.* **9**: 1-11.
- Yao, R., Ming, Z., Yan, L., Li, S., Wang, F., Ma, S., Yu, C., Yang, M., Chen, L., Chen, L., Li, Y., Yan, C., Miao, D., Sun, Z., Yan, J., Sun, Y., Wang, L., Chu, J., Fan, S., He, W., Deng, H., Nan, F., Li, J., Rao, Z., Lou, Z., and Xie, D.** (2016). DWARF14 is a non-canonical hormone receptor for strigolactone. *Nature* **536**: 469-473.
- Yi, K., Menand, B., Bell, E., and Dolan, L.** (2010). A basic helix-loop-helix transcription factor controls cell growth and size in root hairs. *Nat Genet* **42**: 264-267.
- Yilmaz, A., Mejia-Guerra, M.K., Kurz, K., Liang, X., Welch, L., and Grotewold, E.** (2011). AGRIS: the Arabidopsis Gene Regulatory Information Server, an update. *Nucleic acids research* **39**: D1118-1122.
- Yokota, T., Sakai, H., Okuno, K., Yoneyama, K., and Takeuchi, Y.** (1998). Alectrol and orobanchol, germination stimulants for *Orobanche minor*, from its host red clover. *Phytochemistry* **49**: 1967-1973.
- Yoneyama, K., Awad, A.A., Xie, X., Yoneyama, K., and Takeuchi, Y.** (2010). Strigolactones as germination stimulants for root parasitic plants. *Plant Cell Physiol* **51**: 1095-1103.
- Yoneyama, K., Xie, X., Kisugi, T., Nomura, T., and Yoneyama, K.** (2013). Nitrogen and phosphorus fertilization negatively affects strigolactone production and exudation in sorghum. *Planta* **238**: 885-894.

- Yoneyama, K., Xie, X., Kusumoto, D., Sekimoto, H., Sugimoto, Y., Takeuchi, Y., and Yoneyama, K.** (2007). Nitrogen deficiency as well as phosphorus deficiency in sorghum promotes the production and exudation of 5-deoxystrigol, the host recognition signal for arbuscular mycorrhizal fungi and root parasites. *Planta* **227**: 125-132.
- Zhang, S., Huang, L., Yan, A., Liu, Y., Liu, B., Yu, C., Zhang, A., Schiefelbein, J., and Gan, Y.** (2016). Multiple phytohormones promote root hair elongation by regulating a similar set of genes in the root epidermis in Arabidopsis. *J. Exp. Bot.*: erw400.
- Zhao, L.-H., Zhou, X.E., Yi, W., Wu, Z., Liu, Y., Kang, Y., Hou, L., de Waal, P.W., Li, S., Jiang, Y., Scaffidi, A., Flematti, G.R., Smith, S.M., Lam, V.Q., Griffin, P.R., Wang, Y., Li, J., Melcher, K., and Xu, H.E.** (2015). Destabilization of strigolactone receptor DWARF14 by binding of ligand and E3-ligase signaling effector DWARF3. *Cell Res.* **25**: 1219-1236.
- Zhao, L.-H., Zhou, X.E., Wu, Z.-S., Yi, W., Xu, Y., Li, S., Xu, T.-H., Liu, Y., Chen, R.-Z., Kovach, A., Kang, Y., Hou, L., He, Y., Xie, C., Song, W., Zhong, D., Xu, Y., Wang, Y., Li, J., Zhang, C., Melcher, K., and Xu, H.E.** (2013). Crystal structures of two phytohormone signal-transducing  $\alpha/\beta$  hydrolases: karrikin-signaling KAI2 and strigolactone-signaling DWARF14. *Cell Res.* **23**: 436-439.
- Zhao, X.-C., Qu, X., Mathews, D.E., and Schaller, G.E.** (2002). Effect of Ethylene Pathway Mutations upon Expression of the Ethylene Receptor ETR1 from Arabidopsis. *Plant Physiol.* **130**: 1983-1991.
- Zhou, F., Lin, Q., Zhu, L., Ren, Y., Zhou, K., Shabek, N., Wu, F., Mao, H., Dong, W., Gan, L., Ma, W., Gao, H., Chen, J., Yang, C., Wang, D., Tan, J., Zhang, X., Guo, X., Wang, J., Jiang, L., Liu, X., Chen, W., Chu, J., Yan, C., Ueno, K., Ito, S., Asami, T., Cheng, Z., Wang, J., Lei, C., Zhai, H., Wu, C., Wang, H., Zheng, N., and Wan, J.** (2013). D14-SCFD3-dependent degradation of D53 regulates strigolactone signalling. *Nature* **504**: 406.
- Zhou, H.-W., Nussbaumer, C., Chao, Y., and DeLong, A.** (2004). Disparate roles for the regulatory A subunit isoforms in Arabidopsis protein phosphatase 2A. *Plant Cell* **16**: 709-722.

## **XII. List of Figures**

**Figure 1:** Representative structures of the karrikins (KAR<sub>1</sub> to KAR<sub>6</sub>). (p. 23)

**Figure 2:** Phylogeny of the KAI2 and D14 protein family. (p. 25)

**Figure 3.** Structures of Strigolactones (SLs). (p. 28)

**Figure 4:** Model for KAI2 and D14 signalling pathways. (p.29)

**Figure 5.** Control of root skewing and waving. (p.33)

**Figure 6:** Schematic representation of root hair density and length phenotype in roots of Arabidopsis KL and SL signalling mutants. (p.178)

### **XIII. Acknowledgments**

Over the last year, many people supported and helped me, directly or indirectly, to achieve my big goal of finishing this thesis. I would like to thank all of you.

First of all, I would like to express my deep-felt gratitude and particular thanks to my PhD supervisor, Prof. Dr Caroline Gutjahr. Caroline has guided me in all up and down that we shared during the last almost six years. I am very grateful to her for giving me the chance to join her lab, for all the freedom to work in my scientific ideas and the opportunity to participate in several international scientific conferences. I have enjoyed many aspects of my PhD thesis, but one of the most was our discussion in long meetings. To her side, I have grown not only as a scientist but as a person.

I would like to thank the members of this PhD committee, Dr. Cordelia Bolle, Prof. Dr. Wolfgang Frank, Prof. Dr. Nicolas Gompel, Dr. Macarena Marin and Prof. Dr. Andreas Klingl for contributing with their valuable time and efforts to examine my research work.

I would also like to thank the Graduate School Life Science Munich (LSM) for financial support, the organization of practical workshops and the creation of a vast network between PhD students. Especially, I would like to thank both coordinators, Nadine Hamze for her helping in administrative tasks during the last month of my PhD and Francisca Rosa Mende, a great coordinator and person. In addition, I would like to thanks to the members of my TAC committee, Dr Ulrich Hammes and Prof. Martin Parniske for contributing with great ideas for my thesis, their valuable time and efforts over the last years.

In this line, I would also like to express my appreciation to all members of the Gutjahr Lab, the Genetic department of LMU and our colleagues in TUM. All of them made a great environment and made me feel lucky to work there. In particular, I would like to thanks to our Karrikin group, with Dr Samy Carbonnel, Dr Salar Torabi, Kartikye Varshney and Philipp Chapman. I was delighted to share both funny moments and our scientific ideas with them. I would like to thanks Salar for all our discussion and support even outside the lab. I would like to thanks to Kartikye, who was always happy to discuss any crazy idea that we had in mind. I would like to thanks to Philipp 'Chappy', an excellent technician who day to day work is invaluable in the Gutjahr lab. Thanks

for all the coffees that we shared every morning. Those moments help me to start my day with a smile.

Separately, I would like to express my heartfelt thanks to two of the best lab mates than anyone can find, Dr Samy Carbonnel and Dr Priya Pimprikar. I feel fortunate to have them close when I joined the group. I had the chance to share my lab bench with Samy and my office with Priya. I will never forget our fun in the lab, and outside, both of them became true friends.

I want to dedicate a unique paragraph to my wife, Clara and her family. Her unconditional love and support help me through the last years of my PhD. Besides, I would like to thanks her for assisting in the German translation of the summary of this thesis. I would also like to thanks all the family members of Clara, Wolfgang, Christine and Ben. From the first day, they made me feel at home in Germany.

I am very grateful to all my family. I would like to express my special appreciation to my parents for their endless support and sacrifices. Without them, I would have never gone so far. I am also lucky to have the love and support of my sister Lidia, one of the big inspiration in my life. I always look after her, and my achievements are thanks to her and our parents. Muchas gracias por todo, esto no habría sido posible sin ellos.

Last but not least, I am fortunate to have many friends outside the lab who supported me through those last years. To the people from "La Peña del Real Madrid", in special to Alba and Quique. I would like to thanks to my friends Caro, Eva, Alejandro and David. In a way or another, they were always there when I needed it most. I would also like to thanks my friends from Spain, Paco, Pablo, Patri, and Juan Jose. Although with a bit of distance, they were essential to motivate me to finish this work.

## **XIV. Copyright Clearance**

### **American Society of Plant Biologists - License Terms and Conditions**

This is a License Agreement between LMU -- Jose Antonio Villaecija Aguilar ("You") and American Society of Plant Biologists ("Publisher") provided by Copyright Clearance Center ("CCC"). The license consists of your order details, the terms and conditions provided by American Society of Plant Biologists, and the CCC terms and conditions.

**Order Date**

20-Aug-2020

**Order license ID**

1056931-1

**ISSN**

1532-298X

**Type of Use**

Republish in a thesis/dissertation

**Publisher**

AMERICAN SOCIETY OF PLANT PHYSIOLOGISTS

**Portion**

Image/photo/illustration

LICENSED CONTENT

**Publication Title**

The plant cell

**Article Title**

A Selaginella moellendorffii Ortholog of KARRIKIN INSENSITIVE2 Functions in Arabidopsis Development but Cannot Mediate Responses to Karrikins or Strigolactones.

**Author/Editor**

American Society of Plant Physiologists.

**Date**

01/01/1989

**Language**

English

**Country**

United States of America

**Rightsholder**

American Society of Plant Biologists

**Publication Type**

e-Journal

**Start Page**

1925

**End Page**

1944

**Issue**

7

**Volume**

27

**URL**<http://www.pubmedcentral.nih.gov/tocrender.fcgi?journal=95>

## REQUEST DETAILS

**Portion Type**

Image/photo/illustration

**Number of images / photos / illustrations**

1

**Format (select all that apply)**

Print, Electronic

**Who will republish the content?**

Academic institution

**Duration of Use**

Life of current and all future editions

**Lifetime Unit Quantity**

Up to 499

**Rights Requested**

Main product

**Distribution**

Worldwide

**Translation**

Original language of publication

**Copies for the disabled?**

No

**Minor editing privileges?**

No

**Incidental promotional use?**

No

**Currency**

EUR

## NEW WORK DETAILS

**Title**

Mr

**Instructor name**

Jose Antonio Villaecija Aguilar

**Institution name**

LMU

**Expected presentation date**

2020-08-23

## ADDITIONAL DETAILS

**Order reference number**

N/A

**The requesting person / organization to appear on the license**

LMU

## REUSE CONTENT DETAILS

### **Title, description or numeric reference of the portion(s)**

Figure 4A

### **Editor of portion(s)**

Waters, Mark T; Scaffidi, Adrian; Moulin, Solène L Y; Sun, Yueming K; Flematti, Gavin R; Smith, Steven M

### **Volume of serial or monograph**

27

### **Page or page range of portion**

1925-1944

### **Title of the article/chapter the portion is from**

A Selaginella moellendorffii Ortholog of KARRIKIN INSENSITIVE2 Functions in Arabidopsis Development but Cannot Mediate Responses to Karrikins or Strigolactones.

### **Author of portion(s)**

Waters, Mark T; Scaffidi, Adrian; Moulin, Solène L Y; Sun, Yueming K; Flematti, Gavin R; Smith, Steven M

### **Issue, if republishing an article from a serial**

7

### **Publication date of portion**

2015-07-01

## PUBLISHER TERMS AND CONDITIONS

Permission is granted for the life of the current edition and all future editions, in all languages and in all media.

### **CCC Reproduction Terms and Conditions**

1. Description of Service; Defined Terms. This Reproduction License enables the User to obtain licenses for reproduction of one or more copyrighted works as described in detail on the relevant Order Confirmation (the "Work(s)"). Copyright Clearance Center, Inc. ("CCC") grants licenses through the Service on behalf of the rightsholder identified on the Order Confirmation (the "Rightsholder"). "Reproduction", as used herein, generally means the inclusion of a Work, in whole or in part, in a new work or works, also as described on the Order Confirmation. "User", as used herein, means the person or entity making such reproduction.
2. The terms set forth in the relevant Order Confirmation, and any terms set by the Rightsholder with respect to a particular Work, govern the terms of use of Works in connection with the Service. By using the Service, the person transacting for a reproduction license on behalf of the User represents and warrants that he/she/it (a) has been duly authorized by the User to accept, and hereby does accept, all such terms and conditions on behalf of User, and (b) shall inform User of all such terms and conditions. In the event such person is a "freelancer" or other third party independent of User and CCC, such party shall be deemed jointly a "User" for purposes of these terms and conditions. In any event, User shall be deemed to have accepted and agreed to all such terms and conditions if User republishes the Work in any fashion.
3. Scope of License; Limitations and Obligations.
  1. All Works and all rights therein, including copyright rights, remain the sole and exclusive property of the Rightsholder. The license created by the exchange of an Order Confirmation (and/or any invoice) and payment by User of the full

amount set forth on that document includes only those rights expressly set forth in the Order Confirmation and in these terms and conditions, and conveys no other rights in the Work(s) to User. All rights not expressly granted are hereby reserved.

2. General Payment Terms: You may pay by credit card or through an account with us payable at the end of the month. If you and we agree that you may establish a standing account with CCC, then the following terms apply: Remit Payment to: Copyright Clearance Center, 29118 Network Place, Chicago, IL 60673-1291. Payments Due: Invoices are payable upon their delivery to you (or upon our notice to you that they are available to you for downloading). After 30 days, outstanding amounts will be subject to a service charge of 1-1/2% per month or, if less, the maximum rate allowed by applicable law. Unless otherwise specifically set forth in the Order Confirmation or in a separate written agreement signed by CCC, invoices are due and payable on "net 30" terms. While User may exercise the rights licensed immediately upon issuance of the Order Confirmation, the license is automatically revoked and is null and void, as if it had never been issued, if complete payment for the license is not received on a timely basis either from User directly or through a payment agent, such as a credit card company.
3. Unless otherwise provided in the Order Confirmation, any grant of rights to User (i) is "one-time" (including the editions and product family specified in the license), (ii) is non-exclusive and non-transferable and (iii) is subject to any and all limitations and restrictions (such as, but not limited to, limitations on duration of use or circulation) included in the Order Confirmation or invoice and/or in these terms and conditions. Upon completion of the licensed use, User shall either secure a new permission for further use of the Work(s) or immediately cease any new use of the Work(s) and shall render inaccessible (such as by deleting or by removing or severing links or other locators) any further copies of the Work (except for copies printed on paper in accordance with this license and still in User's stock at the end of such period).
4. In the event that the material for which a republication license is sought includes third party materials (such as photographs, illustrations, graphs, inserts and similar materials) which are identified in such material as having been used by permission, User is responsible for identifying, and seeking separate licenses (under this Service or otherwise) for, any of such third party materials; without a separate license, such third party materials may not be used.
5. Use of proper copyright notice for a Work is required as a condition of any license granted under the Service. Unless otherwise provided in the Order Confirmation, a proper copyright notice will read substantially as follows: "Republished with permission of [Rightsholder's name], from [Work's title, author, volume, edition number and year of copyright]; permission conveyed through Copyright Clearance Center, Inc. " Such notice must be provided in a reasonably legible font size and must be placed either immediately adjacent to the Work as used (for example, as part of a by-line or footnote but not as a separate electronic link) or in the place where substantially all other credits or notices for the new work containing the republished Work are located. Failure to include the required notice results in loss to the Rightsholder and CCC, and the User shall be liable to pay liquidated damages for each such failure equal to twice the use fee specified in the Order Confirmation, in addition to the use fee itself and any other fees and charges specified.
6. User may only make alterations to the Work if and as expressly set forth in the Order Confirmation. No Work may be used in any way that is defamatory, violates

the rights of third parties (including such third parties' rights of copyright, privacy, publicity, or other tangible or intangible property), or is otherwise illegal, sexually explicit or obscene. In addition, User may not conjoin a Work with any other material that may result in damage to the reputation of the Rightsholder. User agrees to inform CCC if it becomes aware of any infringement of any rights in a Work and to cooperate with any reasonable request of CCC or the Rightsholder in connection therewith.

4. Indemnity. User hereby indemnifies and agrees to defend the Rightsholder and CCC, and their respective employees and directors, against all claims, liability, damages, costs and expenses, including legal fees and expenses, arising out of any use of a Work beyond the scope of the rights granted herein, or any use of a Work which has been altered in any unauthorized way by User, including claims of defamation or infringement of rights of copyright, publicity, privacy or other tangible or intangible property.
5. Limitation of Liability. UNDER NO CIRCUMSTANCES WILL CCC OR THE RIGHTSHOLDER BE LIABLE FOR ANY DIRECT, INDIRECT, CONSEQUENTIAL OR INCIDENTAL DAMAGES (INCLUDING WITHOUT LIMITATION DAMAGES FOR LOSS OF BUSINESS PROFITS OR INFORMATION, OR FOR BUSINESS INTERRUPTION) ARISING OUT OF THE USE OR INABILITY TO USE A WORK, EVEN IF ONE OF THEM HAS BEEN ADVISED OF THE POSSIBILITY OF SUCH DAMAGES. In any event, the total liability of the Rightsholder and CCC (including their respective employees and directors) shall not exceed the total amount actually paid by User for this license. User assumes full liability for the actions and omissions of its principals, employees, agents, affiliates, successors and assigns.
6. Limited Warranties. THE WORK(S) AND RIGHT(S) ARE PROVIDED "AS IS". CCC HAS THE RIGHT TO GRANT TO USER THE RIGHTS GRANTED IN THE ORDER CONFIRMATION DOCUMENT. CCC AND THE RIGHTSHOLDER DISCLAIM ALL OTHER WARRANTIES RELATING TO THE WORK(S) AND RIGHT(S), EITHER EXPRESS OR IMPLIED, INCLUDING WITHOUT LIMITATION IMPLIED WARRANTIES OF MERCHANTABILITY OR FITNESS FOR A PARTICULAR PURPOSE. ADDITIONAL RIGHTS MAY BE REQUIRED TO USE ILLUSTRATIONS, GRAPHS, PHOTOGRAPHS, ABSTRACTS, INSERTS OR OTHER PORTIONS OF THE WORK (AS OPPOSED TO THE ENTIRE WORK) IN A MANNER CONTEMPLATED BY USER; USER UNDERSTANDS AND AGREES THAT NEITHER CCC NOR THE RIGHTSHOLDER MAY HAVE SUCH ADDITIONAL RIGHTS TO GRANT.
7. Effect of Breach. Any failure by User to pay any amount when due, or any use by User of a Work beyond the scope of the license set forth in the Order Confirmation and/or these terms and conditions, shall be a material breach of the license created by the Order Confirmation and these terms and conditions. Any breach not cured within 30 days of written notice thereof shall result in immediate termination of such license without further notice. Any unauthorized (but licensable) use of a Work that is terminated immediately upon notice thereof may be liquidated by payment of the Rightsholder's ordinary license price therefor; any unauthorized (and unlicensable) use that is not terminated immediately for any reason (including, for example, because materials containing the Work cannot reasonably be recalled) will be subject to all remedies available at law or in equity, but in no event to a payment of less than three times the Rightsholder's ordinary license price for the most closely analogous licensable use plus Rightsholder's and/or CCC's costs and expenses incurred in collecting such payment.
8. Miscellaneous.

1. User acknowledges that CCC may, from time to time, make changes or additions to the Service or to these terms and conditions, and CCC reserves the right to send notice to the User by electronic mail or otherwise for the purposes of notifying User of such changes or additions; provided that any such changes or additions shall not apply to permissions already secured and paid for.
2. Use of User-related information collected through the Service is governed by CCC's privacy policy, available online here:<https://marketplace.copyright.com/rs-ui-web/mp/privacy-policy>
3. The licensing transaction described in the Order Confirmation is personal to User. Therefore, User may not assign or transfer to any other person (whether a natural person or an organization of any kind) the license created by the Order Confirmation and these terms and conditions or any rights granted hereunder; provided, however, that User may assign such license in its entirety on written notice to CCC in the event of a transfer of all or substantially all of User's rights in the new material which includes the Work(s) licensed under this Service.
4. No amendment or waiver of any terms is binding unless set forth in writing and signed by the parties. The Rightsholder and CCC hereby object to any terms contained in any writing prepared by the User or its principals, employees, agents or affiliates and purporting to govern or otherwise relate to the licensing transaction described in the Order Confirmation, which terms are in any way inconsistent with any terms set forth in the Order Confirmation and/or in these terms and conditions or CCC's standard operating procedures, whether such writing is prepared prior to, simultaneously with or subsequent to the Order Confirmation, and whether such writing appears on a copy of the Order Confirmation or in a separate instrument.
5. The licensing transaction described in the Order Confirmation document shall be governed by and construed under the law of the State of New York, USA, without regard to the principles thereof of conflicts of law. Any case, controversy, suit, action, or proceeding arising out of, in connection with, or related to such licensing transaction shall be brought, at CCC's sole discretion, in any federal or state court located in the County of New York, State of New York, USA, or in any federal or state court whose geographical jurisdiction covers the location of the Rightsholder set forth in the Order Confirmation. The parties expressly submit to the personal jurisdiction and venue of each such federal or state court. If you have any comments or questions about the Service or Copyright Clearance Center, please contact us at 978-750-8400 or send an e-mail to [support@copyright.com](mailto:support@copyright.com).

---

This Agreement between LMU -- Jose Antonio Villaecija Aguilar ("You") and Elsevier ("Elsevier") consists of your license details and the terms and conditions provided by Elsevier and Copyright Clearance Center.

|  |   |
|--|---|
| License Number                               | 4893010905724   |
| License date                                 | Aug 20, 2020  |
| Licensed Content Publisher                   | Elsevier  |
| Licensed Content Publication                 | Trends in Genetics  |
| Licensed Content Title                       | Smoke and Hormone Mirrors: Action and Evolution of Karrikin and Strigolactone Signaling |
| Licensed Content Author                      | Nicholas Morffy,Lionel Faure,David C. Nelson  |
| Licensed Content Date                        | Mar 1, 2016   |
| Licensed Content Volume                      | 32  |
| Licensed Content Issue                       | 3   |
| Licensed Content Pages                       | 13  |
| Start Page                                   | 176   |
| End Page                                     | 188   |
| Type of Use                                  | reuse in a thesis/dissertation  |
| Portion                                      | figures/tables/illustrations  |
| Number of figures/tables/illustrations       | 1   |
| Format                                       | both print and electronic   |
| Are you the author of this Elsevier article? | No  |
| Will you be translating?                     | No  |
| Title  | Mr  |
| Institution name                             | LMU   |
| Expected presentation date                   | Aug 2020  |
| Portions                                     | Figure 1  |
|  | LMU<br>Erdinger                      Strasse                      30b                   |
| Requestor Location                           | Freising,<br>Germany<br>Attn: LMU                      85356                            |

Publisher Tax ID GB 494 6272 12

Total 0.00 EUR

Terms and Conditions

## **INTRODUCTION**

1. The publisher for this copyrighted material is Elsevier. By clicking "accept" in connection with completing this licensing transaction, you agree that the following terms and conditions apply to this transaction (along with the Billing and Payment terms and conditions established by Copyright Clearance Center, Inc. ("CCC"), at the time that you opened your Rightslink account and that are available at any time at <http://myaccount.copyright.com>).

## **GENERAL TERMS**

2. Elsevier hereby grants you permission to reproduce the aforementioned material subject to the terms and conditions indicated.

3. Acknowledgement: If any part of the material to be used (for example, figures) has appeared in our publication with credit or acknowledgement to another source, permission must also be sought from that source. If such permission is not obtained then that material may not be included in your publication/copies. Suitable acknowledgement to the source must be made, either as a footnote or in a reference list at the end of your publication, as follows:

"Reprinted from Publication title, Vol /edition number, Author(s), Title of article / title of chapter, Pages No., Copyright (Year), with permission from Elsevier [OR APPLICABLE SOCIETY COPYRIGHT OWNER]." Also Lancet special credit - "Reprinted from The Lancet, Vol. number, Author(s), Title of article, Pages No., Copyright (Year), with permission from Elsevier."

4. Reproduction of this material is confined to the purpose and/or media for which permission is hereby given.

5. Altering/Modifying Material: Not Permitted. However figures and illustrations may be altered/adapted minimally to serve your work. Any other abbreviations, additions, deletions and/or any other alterations shall be made only with prior written authorization of Elsevier Ltd. (Please contact Elsevier's permissions helpdesk [here](#)). No modifications can be made to any Lancet figures/tables and they must be reproduced in full.

6. If the permission fee for the requested use of our material is waived in this instance, please be advised that your future requests for Elsevier materials may attract a fee.

7. Reservation of Rights: Publisher reserves all rights not specifically granted in the combination of (i) the license details provided by you and accepted in the course of this licensing transaction, (ii) these terms and conditions and (iii) CCC's Billing and Payment terms and conditions.

8. License Contingent Upon Payment: While you may exercise the rights licensed immediately upon issuance of the license at the end of the licensing process for the transaction, provided that you have disclosed complete and accurate details of your proposed use, no license is finally effective unless and until full payment is received from you (either by publisher or by CCC) as provided in CCC's Billing and Payment terms and conditions. If full payment is not received on a timely basis, then any license preliminarily granted shall be deemed automatically revoked and shall be void as if never granted. Further, in the event that you breach any of these terms and conditions or any of CCC's Billing and Payment terms and conditions, the license is automatically revoked and shall be void as if never granted. Use of materials as described in a revoked license, as well as any use of the materials beyond the scope of an unrevoked license, may constitute copyright infringement and publisher reserves the right to take any and all action to protect its copyright in the materials.

9. Warranties: Publisher makes no representations or warranties with respect to the licensed material.

10. Indemnity: You hereby indemnify and agree to hold harmless publisher and CCC, and their respective officers, directors, employees and agents, from and against any and all claims arising out of your use of the licensed material other than as specifically authorized pursuant to this license.

11. No Transfer of License: This license is personal to you and may not be sublicensed, assigned, or transferred by you to any other person without publisher's written permission.

12. No Amendment Except in Writing: This license may not be amended except in a writing signed by both parties (or, in the case of publisher, by CCC on publisher's behalf).

13. Objection to Contrary Terms: Publisher hereby objects to any terms contained in any purchase order, acknowledgment, check endorsement or other writing prepared by you, which terms are inconsistent with these terms and conditions or CCC's Billing and Payment terms and conditions. These terms and conditions, together with CCC's Billing and Payment terms and conditions (which are incorporated herein), comprise the entire agreement between you and publisher (and CCC) concerning this licensing transaction. In the event of any conflict between your obligations established by these terms and conditions and those established by CCC's Billing and Payment terms and conditions, these terms and conditions shall control.

14. Revocation: Elsevier or Copyright Clearance Center may deny the permissions described in this License at their sole discretion, for any reason or no reason, with a full refund payable to you. Notice of such denial will be made using the contact information provided by you. Failure to receive such notice will not alter or invalidate the denial. In no event will Elsevier or Copyright Clearance Center be responsible or liable for any costs, expenses or damage incurred by you as a result of a denial of your permission request, other than a refund of the amount(s) paid by you to Elsevier and/or Copyright Clearance Center for denied permissions.

## LIMITED LICENSE

The following terms and conditions apply only to specific license types:

**15. Translation:** This permission is granted for non-exclusive world **English** rights only unless your license was granted for translation rights. If you licensed translation rights you may only translate this content into the languages you requested. A professional translator must perform all translations and reproduce the content word for word preserving the integrity of the article.

**16. Posting licensed content on any Website:** The following terms and conditions apply as follows: Licensing material from an Elsevier journal: All content posted to the web site must maintain the copyright information line on the bottom of each image; A hyper-text must be included to the Homepage of the journal from which you are licensing at <http://www.sciencedirect.com/science/journal/xxxxx> or the Elsevier homepage for books at <http://www.elsevier.com>; Central Storage: This license does not include permission for a scanned version of the material to be stored in a central repository such as that provided by Heron/XanEdu.

Licensing material from an Elsevier book: A hyper-text link must be included to the Elsevier homepage at <http://www.elsevier.com> . All content posted to the web site must maintain the copyright information line on the bottom of each image.

**Posting licensed content on Electronic reserve:** In addition to the above the following clauses are applicable: The web site must be password-protected and made available only to bona fide students registered on a relevant course. This permission is granted for 1 year only. You may obtain a new license for future website posting.

**17. For journal authors:** the following clauses are applicable in addition to the above:

### Preprints:

A preprint is an author's own write-up of research results and analysis, it has not been peer-reviewed, nor has it had any other value added to it by a publisher (such as formatting, copyright, technical enhancement etc.).

Authors can share their preprints anywhere at any time. Preprints should not be added to or enhanced in any way in order to appear more like, or to substitute for, the final versions of articles however authors can update their preprints on arXiv or RePEc with their Accepted Author Manuscript (see below).

If accepted for publication, we encourage authors to link from the preprint to their formal publication via its DOI. Millions of researchers have access to the formal publications on ScienceDirect, and so links will help users to find, access, cite and use the best available version. Please note that Cell Press, The Lancet and some society-owned have different preprint policies. Information on these policies is available on the journal homepage.

**Accepted Author Manuscripts:** An accepted author manuscript is the manuscript of an article that has been accepted for publication and which typically includes author-incorporated changes suggested during submission, peer review and editor-author communications.

Authors can share their accepted author manuscript:

- immediately
  - via their non-commercial person homepage or blog
  - by updating a preprint in arXiv or RePEc with the accepted manuscript
  - via their research institute or institutional repository for internal institutional uses or as part of an invitation-only research collaboration work-group
  - directly by providing copies to their students or to research collaborators for their personal use
  - for private scholarly sharing as part of an invitation-only work group on commercial sites with which Elsevier has an agreement
- After the embargo period
  - via non-commercial hosting platforms such as their institutional repository
  - via commercial sites with which Elsevier has an agreement

In all cases accepted manuscripts should:

- link to the formal publication via its DOI
- bear a CC-BY-NC-ND license - this is easy to do
- if aggregated with other manuscripts, for example in a repository or other site, be shared in alignment with our hosting policy not be added to or enhanced in any way to appear more like, or to substitute for, the published journal article.

**Published journal article (JPA):** A published journal article (PJA) is the definitive final record of published research that appears or will appear in the journal and embodies all value-adding publishing activities including peer review co-ordination, copy-editing, formatting, (if relevant) pagination and online enrichment.

Policies for sharing publishing journal articles differ for subscription and gold open access articles:

**Subscription Articles:** If you are an author, please share a link to your article rather than the full-text. Millions of researchers have access to the formal publications on ScienceDirect, and so links will help your users to find, access, cite, and use the best available version.

Theses and dissertations which contain embedded PJAs as part of the formal submission can be posted publicly by the awarding institution with DOI links back to the formal publications on ScienceDirect.

If you are affiliated with a library that subscribes to ScienceDirect you have additional private sharing rights for others' research accessed under that agreement. This includes use for classroom teaching and internal training at the

institution (including use in course packs and courseware programs), and inclusion of the article for grant funding purposes.

**Gold Open Access Articles:** May be shared according to the author-selected end-user license and should contain a [CrossMark logo](#), the end user license, and a DOI link to the formal publication on ScienceDirect.

Please refer to Elsevier's [posting policy](#) for further information.

18. **For book authors** the following clauses are applicable in addition to the above: Authors are permitted to place a brief summary of their work online only. You are not allowed to download and post the published electronic version of your chapter, nor may you scan the printed edition to create an electronic version. **Posting to a repository:** Authors are permitted to post a summary of their chapter only in their institution's repository.

19. **Thesis/Dissertation:** If your license is for use in a thesis/dissertation your thesis may be submitted to your institution in either print or electronic form. Should your thesis be published commercially, please reapply for permission. These requirements include permission for the Library and Archives of Canada to supply single copies, on demand, of the complete thesis and include permission for Proquest/UMI to supply single copies, on demand, of the complete thesis. Should your thesis be published commercially, please reapply for permission. Theses and dissertations which contain embedded PJAs as part of the formal submission can be posted publicly by the awarding institution with DOI links back to the formal publications on ScienceDirect.

### **Elsevier Open Access Terms and Conditions**

You can publish open access with Elsevier in hundreds of open access journals or in nearly 2000 established subscription journals that support open access publishing. Permitted third party re-use of these open access articles is defined by the author's choice of Creative Commons user license. See our [open access license policy](#) for more information.

#### **Terms & Conditions applicable to all Open Access articles published with Elsevier:**

Any reuse of the article must not represent the author as endorsing the adaptation of the article nor should the article be modified in such a way as to damage the author's honour or reputation. If any changes have been made, such changes must be clearly indicated.

The author(s) must be appropriately credited and we ask that you include the end user license and a DOI link to the formal publication on ScienceDirect.

If any part of the material to be used (for example, figures) has appeared in our publication with credit or acknowledgement to another source it is the responsibility

of the user to ensure their reuse complies with the terms and conditions determined by the rights holder.

**Additional Terms & Conditions applicable to each Creative Commons user license:**

**CC BY:** The CC-BY license allows users to copy, to create extracts, abstracts and new works from the Article, to alter and revise the Article and to make commercial use of the Article (including reuse and/or resale of the Article by commercial entities), provided the user gives appropriate credit (with a link to the formal publication through the relevant DOI), provides a link to the license, indicates if changes were made and the licensor is not represented as endorsing the use made of the work. The full details of the license are available at <http://creativecommons.org/licenses/by/4.0>.

**CC BY NC SA:** The CC BY-NC-SA license allows users to copy, to create extracts, abstracts and new works from the Article, to alter and revise the Article, provided this is not done for commercial purposes, and that the user gives appropriate credit (with a link to the formal publication through the relevant DOI), provides a link to the license, indicates if changes were made and the licensor is not represented as endorsing the use made of the work. Further, any new works must be made available on the same conditions. The full details of the license are available at <http://creativecommons.org/licenses/by-nc-sa/4.0>.

**CC BY NC ND:** The CC BY-NC-ND license allows users to copy and distribute the Article, provided this is not done for commercial purposes and further does not permit distribution of the Article if it is changed or edited in any way, and provided the user gives appropriate credit (with a link to the formal publication through the relevant DOI), provides a link to the license, and that the licensor is not represented as endorsing the use made of the work. The full details of the license are available at <http://creativecommons.org/licenses/by-nc-nd/4.0>. Any commercial reuse of Open Access articles published with a CC BY NC SA or CC BY NC ND license requires permission from Elsevier and will be subject to a fee.

Commercial reuse includes:

- Associating advertising with the full text of the Article
- Charging fees for document delivery or access
- Article aggregation
- Systematic distribution via e-mail lists or share buttons

Posting or linking by commercial companies for use by customers of those companies.

**20. Other Conditions:**

v1.10

**Questions? [customer care@copyright.com](mailto:customer care@copyright.com) or +1-855-239-3415 (toll free in the US) or +1-978-646-2777.**

Sep 03, 2020

---

This Agreement between LMU -- Jose Antonio Villaecija Aguilar ("You") and Elsevier ("Elsevier") consists of your license details and the terms and conditions provided by Elsevier and Copyright Clearance Center.

|  |   |
|--|---|
| License Number                               | 4893001387855                             |
| License date                                 | Aug 20, 2020                              |
| Licensed Content Publisher                   | Elsevier                                  |
| Licensed Content Publication                 | Plant Science                             |
| Licensed Content Title                       | Root growth movements: Waving and skewing |
| Licensed Content Author                      | Rahul Roy,Diane C. Bassham                |
| Licensed Content Date                        | May 1, 2014                               |
| Licensed Content Volume                      | 221                                       |
| Licensed Content Issue                       | n/a                                       |
| Licensed Content Pages                       | 6   |
| Start Page                                   | 42  |
| End Page                                     | 47  |
| Type of Use                                  | reuse in a thesis/dissertation            |
| Portion                                      | figures/tables/illustrations              |
| Number of figures/tables/illustrations       | 1   |
| Format                                       | both print and electronic                 |
| Are you the author of this Elsevier article? | No  |
| Will you be translating?                     | No  |
| Title  | Mr  |
| Institution name                             | LMU                                       |
| Expected presentation date                   | Aug 2020                                  |
| Portions                                     | Figure 2                                  |
|  | LMU                                       |
|  | Erdinger                                  |
|  | Strasse                                   |
|  | 30b                                       |
| Requestor Location                           | Freising,<br>Germany<br>Attn: LMU         |
|  | 85356                                     |
| Publisher Tax ID                             | GB 494 6272 12                            |

Total 0.00 EUR

Terms and Conditions

## **INTRODUCTION**

1. The publisher for this copyrighted material is Elsevier. By clicking "accept" in connection with completing this licensing transaction, you agree that the following terms and conditions apply to this transaction (along with the Billing and Payment terms and conditions established by Copyright Clearance Center, Inc. ("CCC"), at the time that you opened your Rightslink account and that are available at any time at <http://myaccount.copyright.com>).

## **GENERAL TERMS**

2. Elsevier hereby grants you permission to reproduce the aforementioned material subject to the terms and conditions indicated.

3. Acknowledgement: If any part of the material to be used (for example, figures) has appeared in our publication with credit or acknowledgement to another source, permission must also be sought from that source. If such permission is not obtained then that material may not be included in your publication/copies. Suitable acknowledgement to the source must be made, either as a footnote or in a reference list at the end of your publication, as follows:

"Reprinted from Publication title, Vol /edition number, Author(s), Title of article / title of chapter, Pages No., Copyright (Year), with permission from Elsevier [OR APPLICABLE SOCIETY COPYRIGHT OWNER]." Also Lancet special credit - "Reprinted from The Lancet, Vol. number, Author(s), Title of article, Pages No., Copyright (Year), with permission from Elsevier."

4. Reproduction of this material is confined to the purpose and/or media for which permission is hereby given.

5. Altering/Modifying Material: Not Permitted. However figures and illustrations may be altered/adapted minimally to serve your work. Any other abbreviations, additions, deletions and/or any other alterations shall be made only with prior written authorization of Elsevier Ltd. (Please contact Elsevier's permissions helpdesk [here](#)). No modifications can be made to any Lancet figures/tables and they must be reproduced in full.

6. If the permission fee for the requested use of our material is waived in this instance, please be advised that your future requests for Elsevier materials may attract a fee.

7. Reservation of Rights: Publisher reserves all rights not specifically granted in the combination of (i) the license details provided by you and accepted in the course of this licensing transaction, (ii) these terms and conditions and (iii) CCC's Billing and Payment terms and conditions.

8. License Contingent Upon Payment: While you may exercise the rights licensed immediately upon issuance of the license at the end of the licensing process for the

transaction, provided that you have disclosed complete and accurate details of your proposed use, no license is finally effective unless and until full payment is received from you (either by publisher or by CCC) as provided in CCC's Billing and Payment terms and conditions. If full payment is not received on a timely basis, then any license preliminarily granted shall be deemed automatically revoked and shall be void as if never granted. Further, in the event that you breach any of these terms and conditions or any of CCC's Billing and Payment terms and conditions, the license is automatically revoked and shall be void as if never granted. Use of materials as described in a revoked license, as well as any use of the materials beyond the scope of an unrevoked license, may constitute copyright infringement and publisher reserves the right to take any and all action to protect its copyright in the materials.

9. Warranties: Publisher makes no representations or warranties with respect to the licensed material.

10. Indemnity: You hereby indemnify and agree to hold harmless publisher and CCC, and their respective officers, directors, employees and agents, from and against any and all claims arising out of your use of the licensed material other than as specifically authorized pursuant to this license.

11. No Transfer of License: This license is personal to you and may not be sublicensed, assigned, or transferred by you to any other person without publisher's written permission.

12. No Amendment Except in Writing: This license may not be amended except in a writing signed by both parties (or, in the case of publisher, by CCC on publisher's behalf).

13. Objection to Contrary Terms: Publisher hereby objects to any terms contained in any purchase order, acknowledgment, check endorsement or other writing prepared by you, which terms are inconsistent with these terms and conditions or CCC's Billing and Payment terms and conditions. These terms and conditions, together with CCC's Billing and Payment terms and conditions (which are incorporated herein), comprise the entire agreement between you and publisher (and CCC) concerning this licensing transaction. In the event of any conflict between your obligations established by these terms and conditions and those established by CCC's Billing and Payment terms and conditions, these terms and conditions shall control.

14. Revocation: Elsevier or Copyright Clearance Center may deny the permissions described in this License at their sole discretion, for any reason or no reason, with a full refund payable to you. Notice of such denial will be made using the contact information provided by you. Failure to receive such notice will not alter or invalidate the denial. In no event will Elsevier or Copyright Clearance Center be responsible or liable for any costs, expenses or damage incurred by you as a result of a denial of your permission request, other than a refund of the amount(s) paid by you to Elsevier and/or Copyright Clearance Center for denied permissions.

## **LIMITED LICENSE**

The following terms and conditions apply only to specific license types:

**15. Translation:** This permission is granted for non-exclusive world **English** rights only unless your license was granted for translation rights. If you licensed translation rights you may only translate this content into the languages you requested. A professional translator must perform all translations and reproduce the content word for word preserving the integrity of the article.

**16. Posting licensed content on any Website:** The following terms and conditions apply as follows: Licensing material from an Elsevier journal: All content posted to the web site must maintain the copyright information line on the bottom of each image; A hyper-text must be included to the Homepage of the journal from which you are licensing at <http://www.sciencedirect.com/science/journal/xxxxx> or the Elsevier homepage for books at <http://www.elsevier.com>; Central Storage: This license does not include permission for a scanned version of the material to be stored in a central repository such as that provided by Heron/XanEdu.

Licensing material from an Elsevier book: A hyper-text link must be included to the Elsevier homepage at <http://www.elsevier.com> . All content posted to the web site must maintain the copyright information line on the bottom of each image.

**Posting licensed content on Electronic reserve:** In addition to the above the following clauses are applicable: The web site must be password-protected and made available only to bona fide students registered on a relevant course. This permission is granted for 1 year only. You may obtain a new license for future website posting.

**17. For journal authors:** the following clauses are applicable in addition to the above:

#### **Preprints:**

A preprint is an author's own write-up of research results and analysis, it has not been peer-reviewed, nor has it had any other value added to it by a publisher (such as formatting, copyright, technical enhancement etc.).

Authors can share their preprints anywhere at any time. Preprints should not be added to or enhanced in any way in order to appear more like, or to substitute for, the final versions of articles however authors can update their preprints on arXiv or RePEc with their Accepted Author Manuscript (see below).

If accepted for publication, we encourage authors to link from the preprint to their formal publication via its DOI. Millions of researchers have access to the formal publications on ScienceDirect, and so links will help users to find, access, cite and use the best available version. Please note that Cell Press, The Lancet and some society-owned have different preprint policies. Information on these policies is available on the journal homepage.

**Accepted Author Manuscripts:** An accepted author manuscript is the manuscript of an article that has been accepted for publication and which typically includes

author-incorporated changes suggested during submission, peer review and editor-author communications.

Authors can share their accepted author manuscript:

- immediately
  - via their non-commercial person homepage or blog
  - by updating a preprint in arXiv or RePEc with the accepted manuscript
  - via their research institute or institutional repository for internal institutional uses or as part of an invitation-only research collaboration work-group
  - directly by providing copies to their students or to research collaborators for their personal use
  - for private scholarly sharing as part of an invitation-only work group on commercial sites with which Elsevier has an agreement
- After the embargo period
  - via non-commercial hosting platforms such as their institutional repository
  - via commercial sites with which Elsevier has an agreement

In all cases accepted manuscripts should:

- link to the formal publication via its DOI
- bear a CC-BY-NC-ND license - this is easy to do
- if aggregated with other manuscripts, for example in a repository or other site, be shared in alignment with our hosting policy not be added to or enhanced in any way to appear more like, or to substitute for, the published journal article.

**Published journal article (JPA):** A published journal article (PJA) is the definitive final record of published research that appears or will appear in the journal and embodies all value-adding publishing activities including peer review co-ordination, copy-editing, formatting, (if relevant) pagination and online enrichment.

Policies for sharing publishing journal articles differ for subscription and gold open access articles:

**Subscription Articles:** If you are an author, please share a link to your article rather than the full-text. Millions of researchers have access to the formal publications on ScienceDirect, and so links will help your users to find, access, cite, and use the best available version.

Theses and dissertations which contain embedded PJAs as part of the formal submission can be posted publicly by the awarding institution with DOI links back to the formal publications on ScienceDirect.

If you are affiliated with a library that subscribes to ScienceDirect you have additional private sharing rights for others' research accessed under that agreement. This includes use for classroom teaching and internal training at the

institution (including use in course packs and courseware programs), and inclusion of the article for grant funding purposes.

**Gold Open Access Articles:** May be shared according to the author-selected end-user license and should contain a [CrossMark logo](#), the end user license, and a DOI link to the formal publication on ScienceDirect.

Please refer to Elsevier's [posting policy](#) for further information.

18. **For book authors** the following clauses are applicable in addition to the above: Authors are permitted to place a brief summary of their work online only. You are not allowed to download and post the published electronic version of your chapter, nor may you scan the printed edition to create an electronic version. **Posting to a repository:** Authors are permitted to post a summary of their chapter only in their institution's repository.

19. **Thesis/Dissertation:** If your license is for use in a thesis/dissertation your thesis may be submitted to your institution in either print or electronic form. Should your thesis be published commercially, please reapply for permission. These requirements include permission for the Library and Archives of Canada to supply single copies, on demand, of the complete thesis and include permission for Proquest/UMI to supply single copies, on demand, of the complete thesis. Should your thesis be published commercially, please reapply for permission. Theses and dissertations which contain embedded PJAs as part of the formal submission can be posted publicly by the awarding institution with DOI links back to the formal publications on ScienceDirect.

### **Elsevier Open Access Terms and Conditions**

You can publish open access with Elsevier in hundreds of open access journals or in nearly 2000 established subscription journals that support open access publishing. Permitted third party re-use of these open access articles is defined by the author's choice of Creative Commons user license. See our [open access license policy](#) for more information.

#### **Terms & Conditions applicable to all Open Access articles published with Elsevier:**

Any reuse of the article must not represent the author as endorsing the adaptation of the article nor should the article be modified in such a way as to damage the author's honour or reputation. If any changes have been made, such changes must be clearly indicated.

The author(s) must be appropriately credited and we ask that you include the end user license and a DOI link to the formal publication on ScienceDirect.

If any part of the material to be used (for example, figures) has appeared in our publication with credit or acknowledgement to another source it is the responsibility

of the user to ensure their reuse complies with the terms and conditions determined by the rights holder.

**Additional Terms & Conditions applicable to each Creative Commons user license:**

**CC BY:** The CC-BY license allows users to copy, to create extracts, abstracts and new works from the Article, to alter and revise the Article and to make commercial use of the Article (including reuse and/or resale of the Article by commercial entities), provided the user gives appropriate credit (with a link to the formal publication through the relevant DOI), provides a link to the license, indicates if changes were made and the licensor is not represented as endorsing the use made of the work. The full details of the license are available at <http://creativecommons.org/licenses/by/4.0>.

**CC BY NC SA:** The CC BY-NC-SA license allows users to copy, to create extracts, abstracts and new works from the Article, to alter and revise the Article, provided this is not done for commercial purposes, and that the user gives appropriate credit (with a link to the formal publication through the relevant DOI), provides a link to the license, indicates if changes were made and the licensor is not represented as endorsing the use made of the work. Further, any new works must be made available on the same conditions. The full details of the license are available at <http://creativecommons.org/licenses/by-nc-sa/4.0>.

**CC BY NC ND:** The CC BY-NC-ND license allows users to copy and distribute the Article, provided this is not done for commercial purposes and further does not permit distribution of the Article if it is changed or edited in any way, and provided the user gives appropriate credit (with a link to the formal publication through the relevant DOI), provides a link to the license, and that the licensor is not represented as endorsing the use made of the work. The full details of the license are available at <http://creativecommons.org/licenses/by-nc-nd/4.0>. Any commercial reuse of Open Access articles published with a CC BY NC SA or CC BY NC ND license requires permission from Elsevier and will be subject to a fee.

Commercial reuse includes:

- Associating advertising with the full text of the Article
- Charging fees for document delivery or access
- Article aggregation
- Systematic distribution via e-mail lists or share buttons

Posting or linking by commercial companies for use by customers of those companies.

**20. Other Conditions:**

v1.10

**Questions? [customer@copyright.com](mailto:customer@copyright.com) or +1-855-239-3415 (toll free in the US) or +1-978-646-2777.**